Functional genomics analysis of the secretory pathway in *Aspergillus niger*

Miguel Oliveira

Thesis committee

Thesis supervisor
Prof. dr. J. van der Oost
Personal chair at the Laboratory of Microbiology
Wageningen University

Thesis co-supervisor
Dr. L. H. de Graaff
Associate professor at the Laboratory of Microbiology
Wageningen University

Other members
Prof. dr. ir. P.J.G.M. de Wit, Wageningen University
Prof. dr. I.J. van der Klei, University of Groningen
Prof. dr. H.A.B. Wösten, Utrecht University
Dr. A.F.J. Ram, Leiden University

This research was conducted under the auspices of the Graduate School VLAG

Functional genomics analysis of the secretory pathway in *Aspergillus niger*

Miguel Oliveira

Thesis

submitted in fulfilment of the requirements for the degree of doctor
at Wageningen University
by the authority of the Rector Magnificus
Prof. dr. M.J. Kropff,
in the presence of the
Thesis Committee appointed by the Academic Board
to be defended in public
on Tuesday 5 October 2010
at 1:30 p.m. in the Aula

Miguel Oliveira
Functional genomics analysis of the secretory pathway in *Aspergillus niger*,
192 pages

Thesis, Wageningen University, Wageningen, The Netherlands (2010)

With references, with summaries in English and Dutch

ISBN: 978-90-8585-769-3

TABLE OF CONTENTS

Chapter 1

General introduction

Applied Microbiol Biotechnol (modified version accepted for publication)

The proteome and its study

The proteome was defined by Wilkins (1994) as the "protein complement to a genome". The study of the proteome is generally referred to as proteomics. Although the proteomics approach was first introduced as a concept in the mid 1990s, it has deep roots in the early 1970s, as a result of important technical advances at the level of biochemistry and genetics (Figure 1). Similar to genomics and transcriptomics, proteomics has rapidly developed into a high-throughput technology, which has allowed faster analyses of larger numbers of protein samples (Lueking et al. 1999; Wolters et al. 2001). Proteomics is therefore a core part of functional genomics, as the latter relies on high-throughput approaches for determining the relation between a given genome and the corresponding phenotypes.

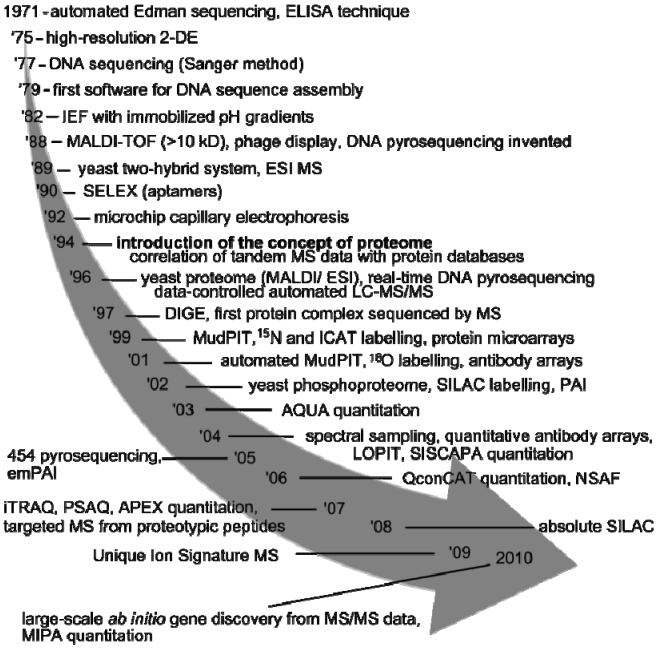

Figure 1. Timeline of major events important for the development of proteomics.

High-throughput procedures depend on rapidly increasing rates of processivity, accuracy and automation, to allow the efficient management, integration and evaluation

of rapidly expanding sets of samples and data. In the context of proteome studies, an example of a high-throughput technique is the protein array, for the quantification of individual proteins in mixtures of proteins. Like oligonucleotide arrays, protein arrays are based on analyte detection through spotted probes. These spotted probes however can be various types of specific, high-affinity molecules, ranging from proteins (antibodies) to nucleic acids (aptamers). Thus far, the most standardised protein arrays make use of spotted antibodies (Borrebaeck and Wingren 2007). In spite of the high-throughput nature of protein arrays, these also present some important limitations. Similarly to oligonucleotide arrays whose results need to be validated by quantitative techniques e.g. quantitative PCR, protein arrays also require validation by quantitative techniques such as quantitative ELISA (Zichi et al. 2008). Another important limitation is the cost and availability of the antibody reagents for this technique. In the case of filamentous fungi, only a limited number of specific antibodies is currently available for protein array detection. Last but not least, with the current protein array technology it is not possible to distinguish protein isoforms, mutated proteins or post-translational modifications.

In addition to protein arrays, other techniques exist for protein quantification, such as mass spectrometry (MS). Depending on the instrumentation used, mass spectrometers may achieve an astonishing mass accuracy below the part per million (Olsen et al. 2005). Mass spectrometry has many applications in proteomics, including (i) the analysis of protein complexes (Link et al. 1999), (ii) the detection and quantification of post-translational modifications (Jensen 2006), (iii) protein identification in complex mixtures (Eng et al. 1994; Wolters et al. 2001), (iv) protein quantification (Bantscheff et al. 2007), and (v) proteome profiling. Proteome profiling is frequently carried out to compare differences at protein level depending on genotype (wild type vs. mutant; Dong et al. 2007), on phenotype (targeted peptide quantification related to phenotype; Mallick et al. 2007), and on intracellular location (organelles; Yan et al. 2009).

Quantitative MS-based proteomics

The first systematic approaches for protein quantification in protein mixtures were based on high-resolution two-dimensional electrophoresis (2-DE). Quantification by 2-DE still presents advantages, not only due to the overall sensitivity of this technique but also because of its high resolution power as it allows for the discrimination of protein isoforms and proteins with post-translational modifications. Difference gel electrophoresis (DIGE)

further increased the potential of 2-DE as different samples could be labelled with specific dyes and analysed on the same gel. However, quantification through 2-DE also suffers from major disadvantages. The technique is still laborious, of limited reproducibility and semi-quantitative. Moreover, 2-DE shows poor quantification performance for proteins with particular features such as extremes in sizes (below 7 kDa or above 200 kDa), hydrophobicity (too high - integral membrane proteins), abundance (too low), or isoelectric point (below pH 4, above pH 10). In contrast, mass spectrometry-related technology has developed spectacularly during the past two decades to enable truly quantitative proteomics. The most standardised methods for quantitative MS-based proteomics are based on selective labelling of proteins or peptides with stable isotopes, e.g. ^{2}H, ^{13}C, ^{15}N or ^{18}O. Nowadays there are several choices for MS-based quantification in proteomics, and for this reason, only a few examples will be given in this review. Depending on the scope of the experiment, absolute or relative quantification can be used (Table 1).

Absolute quantification has a 2-log dynamic range and typically involves spiking of labelled protein or peptide standards into a sample protein or peptide mixture. Most often, absolute quantification only allows the quantification of one or few proteins from multiple biological samples. One of the largest applications of absolute quantification of proteins is the quantification of protein biomarkers, e.g. related to cells from a healthy or diseased state. The labelled molecule can be introduced at different stages of the experimental workflow, *viz.* before pre-fractionation, before tryptic digestion or after digestion. The step in which protein or peptide standards are spiked into samples is determinant for protein quantification in biological samples, since later spiking results in underestimation of protein amounts in the original unprocessed sample. In this respect, two methods give reliable estimations of protein amounts in biological samples. These methods are Protein Standard Absolute Quantification or PSAQ (Brun et al. 2007) and Stable Isotope Standards and Capture by Anti-Peptide Antibodies or SISCAPA (Anderson et al. 2004). In PSAQ, labelled protein standards are directly mixed with the sample, whereas in SISCAPA labelled peptide standards are mixed with the sample and anti-peptide antibodies are used for screening and quantification of peptides. A different approach can be used for the quantification of protein complexes, e.g. quantification using concatenated proteotypic peptides or QconCAT (Pratt et al. 2006). Proteotypic peptides are signature peptides that are unique to a protein and yield good-quality MS peaks. For this approach, an artificial gene is constructed coding for a protein of concatenated

proteotypic peptides. The gene is then expressed and the isolated standard protein is labelled. The standard protein is pooled with a sample mixture, and after tryptic digestion, each standard protein yields a distinct set of labelled peptides, each probing for a specific protein.

Table 1. Label-based quantification of proteins. +: major features; –: major limitations; A: major applications; AA: amino acids; AQUA: absolute quantification method; ICAT: isotope-coded affinity tags; ICPL: isotope-coded protein labelling; iTRAQ: isobaric tag for absolute and relative quantification; PSAQ: protein standard absolute quantification; PTM: post-translational modification; QconCAT: quantitative concatenated standard; SILAC: stable isotope labelling by amino acids in cell culture; TMT: tandem mass tags

Absolute quantification		
	PSAQ	**+** Allows extrapolation **–** Specific software A: Detection of protein isoforms; quantification of biomarkers
	SISCAPA	**+** Allows extrapolation; allows multiplexing - Depends on antibodies (expensive, difficult to implement for general use) A: Peptidomics; quantification of peptide biomarkers
	QconCAT	**+** One standard yields multiple proteins, can be obtained by expression vector **–** Underestimation; digestion not reproducible; expensive; specific software A: Quantification of protein subunits or proteins from a small pathway
	AQUA	**+** Very precise, rigorous peptide mixture quantification, detects PTMs **–** Underestimation; expensive A: Peptidomics and phosphoproteomics
Relative quantification		
in vivo or metabolic		
	^{15}N	**+** High signal for protein labelling; separation by 2-DE possible, detects PTMs **–** Only pair-wise; specific software; tissue samples not possible A: Cell culture of microorganisms, also PTMs
	SILAC	**+** Specific accurate quantification, allows multiplexing, detects PTMs **–** Labelled AA essential and not converted to other AA; growth media of controlled composition; specific software A: Cell culture; phosphoproteomics; quantifies other PTMs
in vitro		
	ICAT	**+** Sample size reduction; upstream of tryptic digestion; detects PTMs **–** Cys-lacking proteins missed; undesired side-reactions A: Cys-containing proteins in complex samples
	iTRAQ, TMT	**+** Multiplex up to 8 samples; precise co-migration in LC (iTRAQ); detects PTMs **–**MS interference; undesired side-reactions; underestimation A: Peptidomics and phosphoproteomics, medium-to-low complexity samples
	ICPL	**+** Allows extrapolation; compatible with 2-DE; PTMs **–** Trypsin does not cleave modified lysine; undesired side-reactions A: Virtually any biological sample
	^{18}O	**+** Simple setting, chemical properties not affected, no side-reactions; also PTMs **–** Requires high resolution MS (4 Da); A: Virtually any biological sample

Finally, in a method described as Absolute Quantification (AQUA) of proteins (Gerber et al. 2003) the tryptic peptides from sample digestion are mixed with labelled peptide standards. This method is very well suited for the quantification of peptides and proteins with post-translational modifications, most notably for phosphorylation. Absolute quantification given in the examples above can be applied in different contexts for the quantification of fungal proteins. QconCAT finds potential application in the simultaneous quantification of individual protein subunits of multi-subunit enzymes or in the quantification of different enzymes belonging to a common pathway, e.g. for antibiotic production. PSAQ can be applied for the quantification of specific isozymes in mixtures e.g. to determine which isozyme is responsible for a certain reaction of interest to biotechnology.

As mentioned before, label-based absolute quantification makes use of an external standard to quantify a small subset of target proteins regardless of the number of biological samples analysed. Label-based relative quantification on the other hand labels all the proteins within a single biological sample and compares these to all the unlabelled proteins of another sample. Although up to eight samples can be compared in multiplexed systems, simultaneously, this severely complicates the corresponding MS/MS analysis. The dynamic range of relative quantification is usually in the order of 1-2 logs, thus slightly lower than the 2-log dynamic range of absolute quantification. According to its nature, the labelling procedure in relative quantification can be performed in one of two ways: *in vivo*, also known as metabolic labelling, or *in vitro*. In the *in vivo* system, an organism is grown in strictly controlled defined medium supplemented with isotope-enriched nutrients. For this, two major methods exist: ^{15}N labelling (Oda et al. 1999; Krijgsveld et al. 2003) and stable isotope labelling by amino acids in cell culture or SILAC (Ong et al. 2002). The target organism is grown on either ^{15}N-containing medium (either labelled ammonium or complete cell media; ^{15}N labelling), or on medium containing one or two labelled amino acids (SILAC). The control organism is grown on normal medium. After protein extraction, the pooled light and heavy protein sets are trypsin-digested, and the obtained peptides are separated by LC-MS/MS. For these two methods of *in vivo* labelling, MS analysis usually requires specific software, capable of detecting most isotope-labelled peptides.

In the *in vitro* system, all proteins or tryptic peptides in one of the samples are labelled chemically or enzymatically. Chemical labelling in the *in vitro* system generally targets the free amino groups (including lysine side chain), cysteine residues or free carboxyl groups (including aspartate and glutamate side chains). A common problem with

chemical labelling is the occurrence of undesired side-reactions. Enzymatic labelling, also called proteolytic labelling or ^{18}O labelling, is based on tryptic digestion of protein in water containing heavy oxygen $H_2{}^{18}O$, resulting in the labelling of all tryptic peptides. A frequent problem with this approach used to be the occurrence of back-exchange of isotopes; nowadays this is prevented by incubating the tryptic peptides in $H_2{}^{18}O$. Another common problem is that high-resolution MS is required to resolve 4 Da mass differences between the two isotopic forms. Label-based relative quantification can also find applications in fungal research for the investigation of the effects on the proteome of two contrasting conditions, such as high or low temperature, oxygen, pH or specific salts. Label-based relative quantification presents a smaller dynamic range compared to absolute quantification; however, despite the lower dynamic ranges of measured protein concentration, relative quantification is able to generate proteome-wide quantification of proteins.

Nowadays, with the increasing resolution achieved by one- or multi-dimensional LC-MS instruments and due to the development of new algorithms, another group of quantification methods is becoming increasingly more standard for proteomic quantification. The approaches are collectively called label-free MS-based quantification of proteins. This type of quantification contrasts much with label-based quantification, in that it presents a lower accuracy (>30% uncertainty) compared to label-based methods. However, label-free quantification has a larger dynamic in the order of 2-3 logs of protein concentration and in general it is much cheaper and simpler compared to label-based quantification. Currently, the methods for label-free quantification of proteins are mainly based on two parameters: total ion current from chromatogram (TIC) measured prior to MS, and total spectral counts (SpC) for the tryptic peptides identified during MS/MS. TIC-based quantification is overall more accurate whereas SpC-based quantification is more sensitive and has a larger dynamic range (Zybailov et al. 2005). Another difference between the two is that TIC-based quantification requires all tryptic peptides corresponding to a protein to be detected for quantification, whereas with SpC all tryptic peptides detected can be used for protein quantification (Old et al. 2005). SpC-based quantification has recently been refined by the incorporation of other parameters such as the theoretical number of tryptic peptides per protein or the protein length in amino acids (Ishihama et al. 2005; Zybailov et al. 2006).

MS-based proteomics in filamentous fungi

Mass spectrometry-based proteomics has benefitted significantly from the many genomes sequenced in the past decade. With regard to the kingdom of fungi, genomes have become available for many species. The ascomycetes whose genomes were recently sequenced belong to all subphyla of Ascomycota, *viz,* Pezizomycotina or true ascomycetes (Machida et al. 2005; Pel et al. 2007; Espagne et al. 2008; Martínez et al. 2008; Van den Berg et al. 2008; DiGuistini et al. 2009), Saccharomycotina or true yeasts (Jones et al. 2004; Wei et al. 2007), and Taphrinomycotina i.e. dimorphic ascomycetes (Wood et al. 2002). In addition to the large group represented by the ascomycetes, also basidiomycetous genomes have been sequenced, namely from a white-rot fungus (Martínez et al. 2004), an ectomycorrhizal fungus (Martin et al. 2008) and an encapsulated yeast (Loftus et al. 2005). Full genome DNA sequencing of these fungal species has many implications, as it becomes possible to (i) predict novel open reading frames (ORFs), (ii) determine genome organisation and its relation with fungal evolution, (iii) improve gene annotation and gene function prediction by comparative analyses, (iv) unravel DNA regulatory sequences and corresponding putative regulators, and (v) provide a better understanding of fungal strain differences, including natural isolates as well as engineered laboratory strains used for instance in biotechnological processes.

Genome sequence information and systematic ORF prediction are vital to bottom-up proteomics i.e. identification of full proteins from the total corresponding tryptic peptides. For shotgun proteomics this is even more the case, as these analyses typically result in the identification of hundreds to thousands of individual proteins. Therefore, only a complete overview of all the ORFs from the genome will allow for the identification of such large numbers of proteins. Notwithstanding this dependence on genome sequence, shotgun proteomics can also validate gene models and most importantly identify protein coding regions *ab initio* (Bitton et al. 2010).

Since the past decade, several mass spectrometry-based proteomic studies were carried out in filamentous fungi. Most often, these micro-organisms have been studied for a number of practical reasons relative to either a positive or a negative impact on humans and economy. Positive impact of filamentous fungi ranges from being components of foodstuffs and participating in fermentation processes, to producing molecules of interest to biotechnological industries, namely enzymes, antibiotics, organic acids and other metabolites. Depending on the species, however, filamentous fungi may have a negative

impact varying from damage of buildings to more serious issues such as food spoilage, specific crop, animal or human diseases, and mycotoxin production.

High-resolution 2-DE has been used in a number of studies to generate fungal protein maps and in some cases even quantify proteins by DIGE. A pioneer proteomic study in *Hypocrea jecorina* (*Trichoderma reesei*) used high-resolution 2-DE and was able to identify all the subunits of the 26S proteasome, a large multi-subunit complex involved in intracellular proteolysis (Grinyer et al. 2007). Two years later, the same team processed the isolated complex by tandem anion exchange/size exclusion chromatography prior to 2-DE separation, resulting in increased operational speed and overall spot resolution (Kautto et al. 2009). Also, very recently the proteome and secretome were compared by high-resolution 2-DE for the utilisation of xylose and maltose as carbon substrates in *Aspergillus niger* (Lu et al. 2010). The intracellular proteome was in addition quantified by DIGE under the two growth conditions and conclusions were drawn for the overall effects of the two carbon sources on the proteome. Furthermore, this group also presented evidence that the proteome changes observed were larger between cultures growing in a bioreactor compared to shake flask, than the changes observed for growth on different carbon substrates within growth on bioreactor or shake flask alone. Following these major advances in 2-DE based proteomics, another group reported the use of high-resolution 2-DE to analyse protein changes during penicillin biosynthesis in three strains of *Penicillium chrysogenum* (Jami et al. 2010). The strains used were the wild-type, a strain with a small improvement for penicillin biosynthesis and a strain with a large improvement for penicillin biosynthesis. As a result of the experimental conditions used, the corresponding protein maps generated revealed an amazing number of up to a thousand distinct spots per gel, of which 950 proteins could be readily identified.

For studies of metabolic processes by proteomics it is of interest to combine proteomic analysis with metabolic measurements. The process of degradation of aromatic compounds in *Phanerochaete chrysosporium* was followed by metabolite analysis and by high-resolution 2-DE coupled to LC-MS/MS (Matsuzaki et al. 2008). Conclusions could be drawn for the process of lignin degradation based on enzyme expression values as assessed by proteomics and the amount of chemical species related to these enzymes, assessed by metabolomics. A second example of an approach combining proteomics with metabolomics comes from the analysis of the effect of lactate and starch on fumonisin B2 biosynthesis in *Aspergillus niger* (Sørensen et al. 2009). By means of an approach similar to the one adopted by Matsuzaki and co-workers, Sørensen and colleagues were able to

show a specific relation between the increase in fumonisin B2 and the enzymes affecting the intracellular levels of acetyl-CoA. From this observation Sørensen and colleagues were able to conclude that fumonisin B2 production in *A. niger* is most likely regulated by intracellular levels of acetyl-CoA.

In addition to analysis of central metabolic pathways, the study of secreted enzymes is central in filamentous fungi. Many filamentous fungi have evolved highly efficient secretion systems to export large amounts of specialised enzymes responsible e.g. for plant cell-wall degradation. For this reason these fungi are applied in various biotechnological processes. In an attempt to disclose the cellulose-degrading system in the model fungus *Neurospora crassa*, Tian and co-workers (2009) combined gene expression data with proteomic data from the secretome of this organism. By applying microarray and shotgun proteomics analysis on strains grown on different media, they were able to identify potential candidate genes involved in cellulose degradation. In addition, some of the predicted cellulolytic genes could be experimentally validated, as gene disruption resulted in growth retardation on cellulose. Another possible approach to identify a given secreted enzyme is to separate all secreted proteins, screen for a certain enzyme activity and identify the isolated protein. Following this approach in *Aspergillus fumigatus*, the secretome was separated by 2-DE and, after fluorescence assay for β-glucosidase activity, positively identified spots were analysed and the proteins identified by MS/MS (Kim et al. 2007). On the other hand, if the purpose of the analysis is to have an overview of largest number of secreted enzymes, then several media with different carbon substrates should be tested. Three such experimental approaches were carried out in aspergilli grown under varying conditions (Medina et al. 2004; Oda et al. 2006; Tsang et al. 2009). Tsang and co-workers used complex and defined media to increase the spectrum of enzymes secreted by *A. niger*. Moreover, the analysis of secreted proteins was combined with genome-wide predictions of signal-peptide containing proteins. Oda and co-workers on the other hand cultivated *Aspergillus oryzae* under solid-state or under submerged culture conditions. Following this procedure, they concluded that some enzymes were specifically secreted either on solid-state or on submerged culture conditions, regardless of medium composition. Also, proteome differences may be found between the *in vitro* and *in planta* secretomes with many proteins being expressed in only one of the two conditions as e.g. in *Fusarium graminearum* (Paper et al. 2007).

Sample preparation in fungal organelle proteomics

To date, MS-based proteomic analyses in filamentous fungi have focused on three targets: the whole cell (mycelial extract), the cytosolic proteins, and the secretome. Many important biological processes, however, occur within specific cell compartments. Most often, the production and accumulation of industrially-relevant metabolites within the cell are time- and location-dependent processes. Thus organelle proteome mapping and quantification of specific proteins across time in different cell compartments may better reveal various aspects of fungal metabolite production, e.g. penicillin production in the microbodies of *Penicillium chrysogenum* (Kiel et al. 2009).

The analysis of fungal cell organelles by proteomics is an expanding field and is expected to yield significant biotechnological advances as exemplified above for the case of penicillin production. A typical experimental setup for the proteome analysis of organelles comprises steps, such as organelle enrichment, protein separation, mass spectrometry and bioinformatics of MS data. Each of these steps can be approached differently and it is still a challenging task to combine different approaches in such a way that the final protein lists obtained are indeed unbiased representations of the organelle proteomes.

A crucial step in organelle proteomics is organelle enrichment, as downstream analysis obviously depends on good-quality organelle preparations. A typical workflow for organelle enrichment comprises three major steps, from cell disruption, and crude organelle separation to subsequent enrichment by additional separation techniques (Fig. 2). In this respect, filamentous fungi are difficult subjects for a number of reasons. First, filamentous fungi secrete proteases which enhance the commonly encountered problem of protein degradation common to other eukaryotes. Second, these micro-organisms display polarised growth supported by microtubules. These structures increase the clustering of different organelles, which makes organelle separation more difficult. Last but not least, depending on the species, filamentous fungi may possess very thick, compact cell walls. This feature complicates the cell disruption process as the latter must be gentle in order to preserve as much as possible the organelle's integrity.

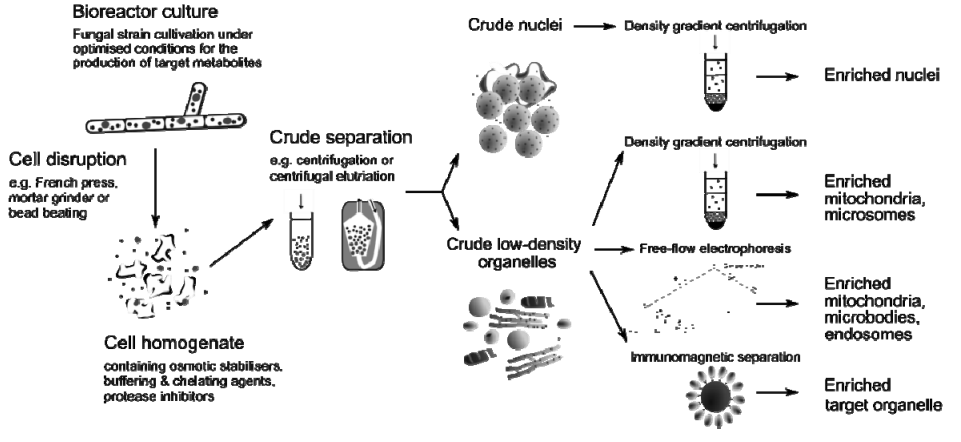

Figure 2. Proposed workflow for organelle proteomics in filamentous fungi.

Special attention must be given to the different steps of organelle proteomics in filamentous fungi. Homogenisation buffers must be isotonic, near-neutral to slightly basic, and invariably contain protease inhibitors. Ideally, the cell disruption procedures should be standardised by automation, to maintain the reproducibility of the homogenisation procedures. For this, the use of instruments such as the French pressure cell or automatic mortar grinders is recommended. It is also preferable to use less harsh conditions by using the highest biomass-to-homogenisation buffer ratio possible for feasible operation. Bead beating (bead milling) is not always recommended as it may be too harsh for large organelles such as the nucleus or vacuoles and may require extensive optimisation. Enzymatic degradation of the cell wall or protoplastation followed by gentle lysis is one of the best methods to obtain intact organelles. This method is also preferred for the enrichment of very large organelles, such as large vacuoles. Yet there are two arguments against the general use of protoplastation in fungal organelle proteomics. First and most important, protoplastation typically extends for a minimum period of 2 to 3 hours, during which fungal physiology is severely disturbed and consequently this most likely introduces an extra variable in the experiment. Second, different batches of enzyme cocktails may have very different protoplastation efficiencies, thereby decreasing overall reproducibility of this method. Another popular method with decreased reproducibility is cell disruption by manual grinding in mortar with sterile sand. Though simple and cost-effective, this is a low throughput method that is largely dependent on a number of factors, such as mortar

and buffer temperature, amount and type of sand, operator skill, time and amount of biomass used.

Following cell disruption, unbroken mycelium is removed from the homogenate suspension, for instance by suction-filtration through multiple layers of nylon gauze or miracloth, and sub-fractionation methods are used to obtain crude or enriched organelle fractions. Generally, the first step in sub-cellular fractionation is a low-speed centrifugation to allow cell debris and nuclei to be separated from lighter organelles. Although less frequently used, alternative techniques are differential detergent fractionation (Ramsby and Makowvksi 1999) and centrifugal elutriation (Lin et al. 1985). After this step, different strategies may be applied, i.e. ultracentrifugation on density gradients, immunomagnetic separation and free-flow electrophoresis. In density gradient centrifugation, linear or step density gradients can be used. Linear density gradients do not require extensive optimisation and allow organelles to migrate in such a way that after ultracentrifugation there will be a continuum of organelle distribution between different fractions, allowing for more flexibility in the choice of different fractions and therefore different organelles or organelle combinations. The use of step density gradients in general only allows the enrichment of one or few organelles. The main advantage of step gradients compared to linear gradients is that once protocols are optimised, high concentrations of the target organelle are achieved. Moreover, step preparation dispenses the need for special equipment commonly used to create linear gradients. Immunomagnetic separation (IMS) is based on the binding of specific antibodies on super-paramagnetic beads to organelle-antigens. Common bottlenecks are the often insufficient affinity or specificity of the antibody, as well as the large amount of antibodies necessary to coat the magnetic beads. IMS can be used for the enrichment of many organelles, *viz.* mitochondria (Hornig-Do et al. 2009), vacuoles (Urwyler et al. 2009), microbodies (Luers et al. 1998), endosomes (Vergés et al. 1999), secretory organelles (Kawajiri et al. 1977), and vesicles (Abe et al. 2009). Finally, a method to enrich organelles that has become more popular recently is free-flow electrophoresis (FFE). In FFE the organelle mixture moves along carrier medium between two slanted plates. Simultaneous to this, a perpendicular electrical field deflects the organelles that concentrate in specific spots at the bottom of the slanted plates. Recently, this system has been miniaturised to microchip format also known as microfluidic FFE (μ-FFE), making it attractive for the separation of minute amounts of sample coupled to very sensitive downstream MS techniques (Kohlheyer et al. 2008).

Fungal organelle proteomics in biotechnology

All methods downstream of organelle enrichment procedures are basically identical to the ones pointed earlier for general MS-based proteomic procedures. These include separation of isolated proteins by 2-DE or multidimensional LC followed by MS/MS analysis. The workflow of organelle proteomics is much dependent on the experimental aim and nature of the organelles to analyse.

Whenever the experimental aim is to study protein secretion, besides the secretome itself it is desirable to study the proteomes of secretory organelles and traffic vesicles. In a recent study, microsomal proteins from biological duplicates of *A. niger* were separated by SDS-PAGE and gel slices were processed for LC-MS/MS (de Oliveira et al. 2010). It was subsequently shown that specific microsomal proteome changes occurred after the addition of D-xylose to the culture medium. Quantification was performed based on normalised spectral abundance factors, calculated from MS spectra. Among other processes, the differentially expressed proteins were related to protein secretion and thus pointed to novel mechanisms of regulation.

Other aspects of fungal biotechnology such as bio-fuel production, organic acid metabolism or cell apoptosis are best studied from examination of the mitochondrial proteome. The first study to use enriched mitochondrial preparations in filamentous fungi was in *Trichoderma harzianum* (Grinyer et al. 2004). A crude mitochondrial pellet was obtained by differential centrifugation and a 2-DE protein map was created. Another similar study reports the characterisation of the mitochondrial proteome of *Aspergillus fumigatus* (Vödisch et al. 2009). In contrast to the previous work, crude mitochondria were further separated on a three-step density gradient for enrichment and confirmed by electron microscopy. Moreover, up to six 2-DE gels were used to construct the protein reference maps for the mycelium and the mitochondria, with a superior overall resolution.

A fungal organelle of particular industrial importance is the microbody. Microbodies in filamentous fungi can be divided into three classes: (i) peroxisomes, responsible for β-oxidation of long-chain fatty acids; (ii) glyoxisomes, which additionally participate in the glyoxylate cycle; and (iii) the Woronin body, which functions as a septal plug in case of cell injury. Microbodies have been implicated in the production of β-lactam antibiotics, most notably of penicillin. These organelles were recently analysed in *Penicillium chrysogenum*, the major penicillin producer (Kiel et al. 2009). Microbody enrichment was carried out by differential centrifugation and confirmed by electron microscopy. After SDS-PAGE

separation of proteins and processing for LC-MS/MS, 89 proteins were identified of which 79 possessed a putative microbody targeting signal, including the penicillin biosynthesis protein isopenicillin N:acyl CoA acyltransferase.

Noteworthy, due to technical advances in MS-based proteomics, the preparation of highly enriched organelle fractions (though desirable) is no longer mandatory in many situations. In the past decade, a number of studies have shown that protein profiles can be created from direct LC-MS/MS analyses of complex protein mixtures originating from separate fractions of linear gradients (Andersen et al. 2003; Dunkley et al. 2004; Dunkley et al. 2006). These profiles can be used to predict protein localisation, as assessed by labelled *in vitro* peptide standards. More recently, label-free protein profiling was achieved, increasing the power of such analyses for establishing organelle proteomes (Foster et al. 2006; Gilchrist et al. 2006; Kislinger et al. 2006; Takamori et al. 2006). Notwithstanding the simplicity of these label-free comprehensive studies, identical studies have not yet been applied to organelle proteomics of filamentous fungi.

Conclusions

This overview summarises the major aspects of quantitative proteomics in filamentous fungi, including protein quantification methods and sample preparation for organelle proteomics. Organelle proteomics in filamentous fungi still suffers from many constraints. First, in many situations, the experimental setup is not adapted to more rigorous protein quantification or to the identification of a maximal number of proteins representative of a given sample or condition. Second, reproducibility and performance of different steps, including cell disruption and sub-cellular fractionation are often neglected. Third, the potential of bioinformatics and statistics are often ignored or not efficiently exploited. For each of these common problems, potential solutions have been discussed. (1) Depending on the goal, protein quantification methods exist that are targeted to small subsets of proteins from various samples (absolute quantification) or to most proteins of two contrasting samples (relative quantification); alternatively, less expensive label-free techniques can be used as these support increased dynamic ranges and rely solely on bioinformatics of LC-MS/MS parameters. (2) Reproducibility and performance in organelle proteomics can be significantly improved by increased automation and sample processing speed, namely during the steps of homogenisation and sub-fractionation. (3) Bioinformatics is essential to organelle proteomics, not only to identify proteins and

predict their functions, but also to predict the presence of targeting sequences in proteins. Statistics also plays a major role in organelle proteomics since the analysis of complex protein samples e.g. from sub-cellular fractions requires statistical validation of protein ratios. Moreover, depending on the experimental scope, protein correlation profiling can be used to confidently identify protein candidates associated with organelles or functional complexes. Fungal organelle proteomics is still in its infancy and significant advances for the improved production of enzymes and metabolites are expected in the near future.

AIM AND OUTLINE OF THE THESIS

This thesis describes our studies on the secretory pathway of the ascomycete fungus *Aspergillus niger*. In part the project was conducted in the frame work of the fungal fermentation programme of the Kluyver Centre for Genomics of Industrial Fermentation, and as such was sponsored by the Netherlands Genomic Initiative (NGI).

In the general fungal fermentation programme, this project aimed to describe the secretory pathway of *Aspergillus niger* from a systems biology perspective through the use of functional genomics methodology. The main goal of functional genomics is to understand the dynamic relation between a given genome and a range of phenotypes. In the functional genomics area, mass spectrometry (MS)-based proteomics is a rapidly developing field. During the last decade proteomics has generated a bridge to connect genome/transcriptome with the metabolome, and more generally with certain phenotypes. In this general introduction, (**chapter 1)** a general overview of MS-based proteomics was provided, with special attention for fungal studies.

Chapter 2 describes the development of a tool for post-transcriptional gene silencing in *A. niger*. This tool allows the generation by homologous recombination of vectors that express long hairpin RNAs. Through this method, one vector was built targeting the *xlnR* gene, which codes for a major transcriptional activator of specific secreted enzymes, such as (hemi)cellulases. The expression of this activator is known to be increased in the presence of the specific inducer D-xylose. Transformed strains were screened by plate assays for extracellular enzyme activity. Silenced strains were analysed for genotype and for levels of selected transcripts on D-xylose containing medium.

In **chapter 3,** the effect of D-xylose on the transcriptome of *A. niger* was investigated by microarray analysis. The inducer D-xylose was added to *A. niger* growing on the non-

inducer sorbitol. Genes differentially expressed on D-xylose were then identified as candidate genes involved in the response to D-xylose induction. Parallel to this, statistical analysis of variance components was used to assess the individual contribution of external factors affecting the measured gene expression values. Such analysis of variance components is crucial, e.g. for reproducible sample processing for microarray analysis.

The optimised fermentation conditions that resulted from the transcriptome analysis of *A. niger* described in chapter 3 were subsequently used in an identical bioreactor culture system to generate fungal biomass for shotgun proteomics, described in **chapter 4**. *A. niger* was grown under the same conditions, i.e. using non-inducing sorbitol as a carbon source and D-xylose addition to induce secretion of extracellular (hemi)-cellulases. Mycelial cells were disrupted and microsome-enriched fractions were obtained. Microsomal proteins, representing proteins associated with secretory organelles, were then submitted to shotgun proteomics. Differential protein presence in the microsomal fractions from D-xylose induced mycelium was compared to those from non-induced sorbitol grown mycelium. From this analysis, candidate proteins were found to be involved in the response to D-xylose induction in the secretory organelles of *A. niger*.

Chapter 5 describes an extension of the proteomic study described in chapter 4 in which the inducer D-maltose was used. Additionally, total secreted proteins (secretome) were analysed. The disaccharide D-maltose is a sugar that results from starch degradation, and it induces the production of extra-cellular starch-degrading enzymes such as glucoamylase. Differential protein presence was then assessed in the secretome and in the microsomal proteins after addition of D-maltose or D-xylose relative to the addition of non-inducer D-sorbitol. This analysis showed which proteins were common to both inducers, therefore more representative of a high-secretory state, and which proteins were specifically induced on D-maltose or D-xylose.

Chapter 6 summarises the major findings of the work in this thesis and integrates previous knowledge on the transcriptional responses of *A. niger* to D-xylose or D-maltose with the findings reported on chapters 3 to 5. In addition, a model is presented on the inter-relation between mitochondria, the 20S proteasome and the ER during high-secretion conditions.

An appendix is included with all the supplementary information from chapters 3 to 5. This includes a protein sequence alignment and all the analysed results from the proteomic studies discussed in chapters 3 to 5.

Chapter 2

Efficient cloning system for construction of gene silencing vectors in *Aspergillus niger*

José Miguel Oliveira, Douwe van der Veen, Leo H. de Graaff and Ling Qin

Appl Microbiol Biotechnol (2008) **80**: 917–924

ABSTRACT

An approach based on GATEWAY recombination technology to efficiently construct silencing vectors was developed for use in the biotechnologically important fungus *Aspergillus niger*. The transcription activator of xylanolytic and cellulolytic genes XlnR of *A. niger* was chosen as target for gene silencing. Silencing was based on the expression vector pXLNRir that was constructed and used in co-transformation. From all the strains isolated (N=77), nine showed poor xylan-degrading activities in two semi-quantitative plate assays testing different activities for xylan degradation. Upon induction on D-xylose, transcript levels of *xlnR* were decreased in the *xlnR*-silenced strains, compared to a wild type background. Under these conditions, the transcript levels of *xyr*A and *xyn*B (two genes regulated by XlnR) were also decreased for these *xlnR*-silenced strains. These results indicate that the newly developed system for rapid generation of silencing vectors is an effective tool for *A. niger* and this can be used to generate strains with a tailored spectrum of enzyme activities or product formation by silencing specific genes encoding e.g. regulators such as XlnR.

INTRODUCTION

Aspergillus niger is a filamentous fungus with prominent applications in biotechnological processes. Products of the fungus have the generally recognised as safe (GRAS) status allowing them to be used as food additives. Important products that are made by fermentation of *A. niger* are organic acids such as citric acid and gluconic acid. Citric acid is used for acidification and to enhance taste and flavour in food (Ruijter et al. 2000). *A. niger* is also an important producer of enzymes that are used in food and feed applications, such as xylanases as a bread improver and pectinases in juice clarification.

Genetic and genomic tools have been developed for this fungus over the past two decades allowing specific modification and strain improvement to enhance the production of specific enzymes. The potential use of new genomic tools has increased with the publication of the genome sequence of *A. niger* (Pel et al. 2007). Recently, successful gene knock-out strategies were carried out in strains with defective pathways for non-homologous integration (Meyer et al. 2007). However, these rely on a mutant background and analysis of essential genes is still not straightforward since it is limited to heterokaryon formation in the case of *A. niger*. Moreover, as reviewed (Meyer 2008), these engineered strains are more susceptible to toxins and irradiation, probably because Ku proteins have a vital role in maintenance of telomere length and chromosome stability. Also, because this method needs a mutant background, it is not applicable toward industrial strains.

In recent years, gene silencing mediated by double-stranded (ds)RNA has opened new possibilities for the study of gene function in many organisms. Starting with pioneer studies on post-transcriptional gene silencing (PTGS) phenomena (Napoli et al. 1990; van der Krol et al. 1990; Romano and Macino 1992), many aspects of PTGS by dsRNA have been elucidated after the first study reporting the concept of dsRNA-mediated gene silencing (Fire et al. 1998).

In fungi, a number of genes involved in silencing were first described for *Neurospora crassa* (Cogoni and Macino 1997) and included QDE-1 (Cogoni and Macino 1999a), QDE-2 (Catalanotto et al. 2000), QDE-3 (Cogoni and Macino 1999b), and DCL1 (sms-3)/ DCL2 (Catalanotto et al. 2004). Since then, many vectors for RNA-mediated gene silencing in fungi have been used successfully (Goldoni et al. 2004; Fitzgerald et al. 2004; Mouyna et

al. 2004; Nakayashiki et al. 2005). Interestingly, there is indication of occurrence of siRNA-mediated mechanisms in *A. niger* (Barnes et al. 2008).

In some cases the use of RNAi technologies may be advantageous compared to other gene targeting techniques. First, for the study of essential genes since RNAi results in down-regulation of the gene function and not in loss-off-function as is the case with a knock-out strategy. Second, multiple copies of a gene or paralogous genes may be targeted with a single construct. Third, if the transformation system is based on a dominant selection marker as e.g. the *amdS* gene, a method inducing gene down-regulation can be used in industrial strains.

Functional genomics based on large-scale RNAi screens has been attempted for many organisms (Berns et al. 2004; Paddison et al. 2004; Kamath et al. 2003; Boutros et al. 2004). The application of RNAi high-throughput screens to the study of gene functions in filamentous fungi, however, is still in its initial phase.

In *A. niger* the expression of the biotechnologically important xylanase and cellulase enzymes is controlled by the Gal4-type transcription factor XlnR (van Peij et al. 1998b). XlnR controls not only the transcription of more than ten genes involved in the extracellular degradation of cellulose and hemicellulose (van Peij et al. 1998a) but also the transcription of genes that are involved in intracellular D-xylose metabolism (Hasper et al. 2000). The XlnR regulon has extensively been studied by northern blot analysis (van Peij et al. 1998a) and many aspects of XlnR-regulated expression of target genes are known. Standardised culture and induction conditions have been developed that could serve as a basis to study the effect of gene silencing in *A. niger*.

Here we describe a method for simple construction of dsRNA-expression vectors under the control of a fungal constitutive promoter. This method makes use of homologous recombination between a general destination vector and a specific entry clone to generate the corresponding dsRNA expression vector (GATEWAY). The approach has the advantage of an easy and efficient exchange of DNA fragments to produce a dsRNA expression vector. Using this approach, we were able to target for silencing the transcriptional activator XlnR in *A. niger.* We have analysed the effects of silencing of the transcriptional regulator towards the total expression of xylanases by functional assays and by measuring relative expression levels of two highly transcribed target genes encoding D-xylose reductase and endo-β-1,4-xylanase B.

RESULTS

Effect of pXLNRir on xylan-degrading activities of *A. niger*

A. niger strain NW219 was transformed by pXLNRir under the control of the constitutive *pki*A promoter and *pga*II terminator and by pGW635, and strains were screened for xylan-degrading activities. The silencing vector pXLNRir was constructed from reaction between the general destination vector pFIRD1 and an appropriate entry clone containing a portion of *xlnR* coding sequence (CDS) as depicted (Fig. 1).

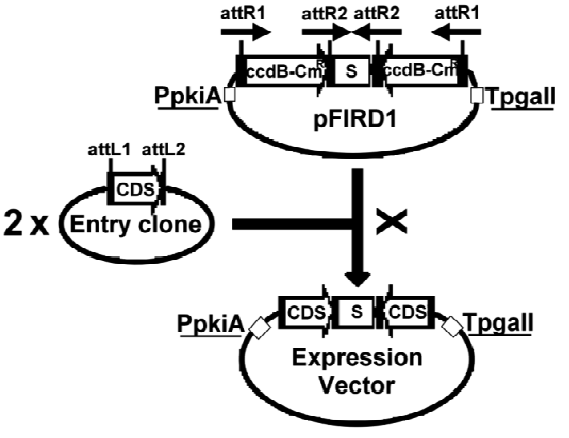

Figure 1. Construction of expression vectors for post-transcriptional gene silencing in *A. niger*. Arrow: recombination reaction of pFIRD1 destination vector with two molecules of entry clone containing a partial coding sequence;. ccdB-CmR ccdB gene plus chloramphenicol resistance gene; S spacer region.

After transformation, 77 colonies were obtained with no visible differences in morphology or growth rate on complete medium (compared to non-transformed NW219 or NW219 transformed only with pGW635). These strains and one control strain (NW219::pGW635) were isolated and analysed for endoxylanase activity and β-xylosidase/xylanase activities. Under these conditions a gradient of effects was observed in halo size and intensities of colour or fluorescence resulting from substrate degradation (Fig. 2). Compared to the control strain, nine strains (12% of 77) showed decreased activities in both assays whereas 3 different strains showed decreased endoxylanase activity but no decreased β-xylosidase/xylanase activities, and one other strain showed decreased β-xylosidase/xylanase activities but no decreased endoxylanase activity. The nine strains

that showed decreased activities in both assays were considered silenced transformant strains (either fully or partially silenced) and were further investigated, together with four non-silenced strains from co-transformation.

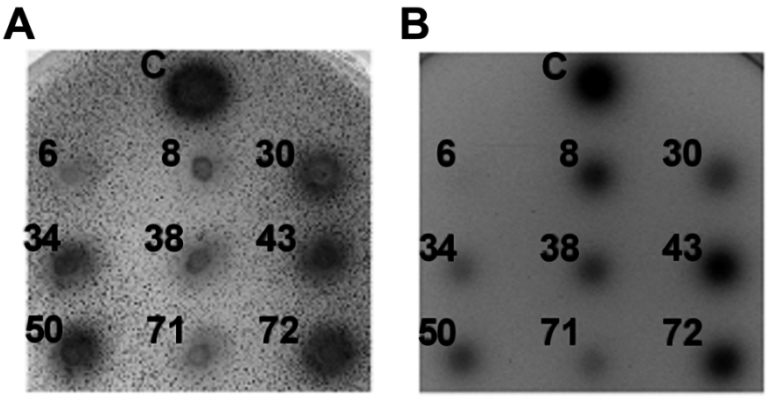

Figure 2. Semi-quantitative assays for analysis of xylan-degrading activities. (A) with AZCL xylan for detection of endoxylanase activity; (B) with MUX for detection of β-xylosidase and xylanase activities. *C:* wild type strain (NW219::pGW635); numerals designate each silenced strain (NW219::pGW635::pXLNRir).

Expression of *xlnR*, *xyr*A and *xyn*B in silenced strains

Quantitative real-time PCR was used to determine expression of *xlnR*, *xyr*A and *xyn*B in the silenced strains and in four non-silenced strains relative to the control strain (NW219::pGW635). All samples were first normalised to the added kanamycin external transcript, directly proportional to the amount of total RNA. As a second normalisation step, gene expression relative to the control strain was calculated for each strain. Strain 50 was an outlier because compared to the group of silenced strains it showed significantly higher expression for all genes tested although still lower than the control strain (Fig. 3). In all silenced strains relative gene expression was significantly decreased not only for the target gene *xlnR* but also for the regulated genes *xyr*A and *xyn*B. Moreover, for each silenced strain a moderate decrease in *xlnR* levels (to about 25-40% of wild type expression levels) was associated with a larger decrease in *xyr*A and *xyn*B expression levels (about 15% and 10% of wild type expression levels, respectively). As expected, expression levels for *xlnR*, *xyr*A, and *xyn*B in the non-silenced strains were similar to wild-type levels, within the experimental error.

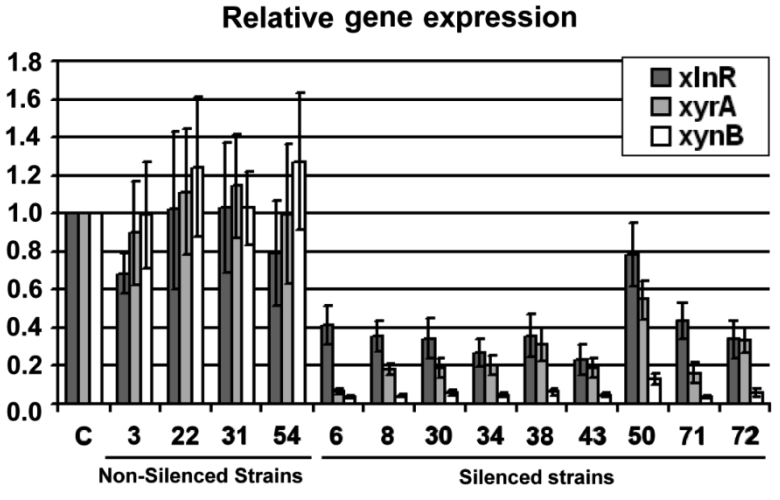

Figure 3. mRNA levels for *xlnR*, *xyr*A and *xyn*B in silenced and non-silenced strains, compared to wild type. *C:* wild type strain (NW219::pGW635). Numerals designate each strain from co-transformation (NW219:: pGW635::pXLNRir). Error bars represent 95% CI (1.962×SE).

Genome rearrangements and copy numbers of pXLNRir

Two approaches were taken for genotypic characterisation of all silenced strains: a qualitative approach based on conventional PCR and a more quantitative approach based on quantitative real-time PCR.

Through conventional PCR a fragment of about 874 bp of native *xlnR* was found in all strains using primers binding to *xlnR* but not to pXLNRir, indicating that in each case the endogenous *xlnR* locus was not affected (data not shown). Moreover, to detect genome rearrangements within integrated pXLNRir, two fragments covering the hairpin RNA expression cassette were amplified separately by PCR. Rearrangements were detected in all silenced strains (Fig. 4), although strains 6 and 30 mostly retained the two parts of the original construct according to this analysis. Strain 34 in contrast carried a truncated version of the hairpin RNA expression cassette at the 3'-region. The non-silenced strains also showed amplification of both fragments spanning the inverted repeat of pXLNRir (Fig. 4).

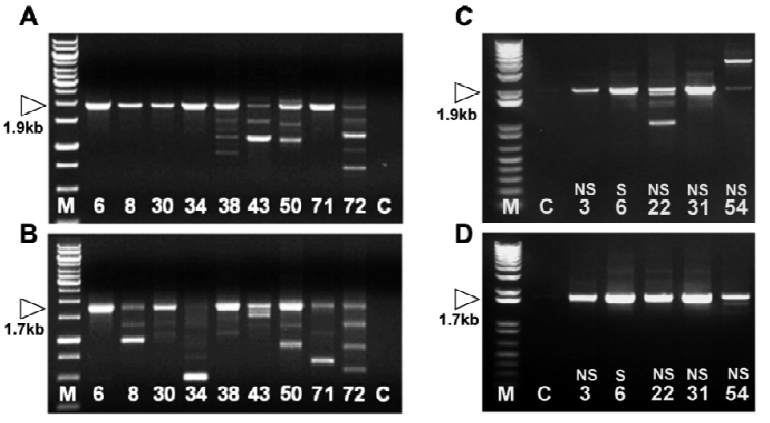

Figure 4. Genome integrity of pXLNRir. Genome integrity was assessed for both silenced (A) and (B) and non-silenced strains (C) and (D). (A) and (C) PCR-amplified 5'-region of pXLNRir. (B) and (D) PCR-amplified 3'-region of pXLNRir. M molecular weight marker. Each triangle represents the expected fragment for intact pXLNRir. Numerals designate each strain from co-transformation (NW219::pGW635::pXLNRir); *C* wild type strain (NW219::pGW635).

PCR amplification of part of the inverted repeat region of pXLNRir followed by agarose gel electrophoresis showed that within the group of silenced strains, a larger variety of fragments with stronger band intensity were produced compared to non-silenced strains (Fig. 5). Strain 6 was an outlier because an amplificaton profile more similar to that of non-silenced strains was obtained. In addition, specific amplification product was only obtained for strain 30. Furthermore, aspecific amplification was observed for the wild-type control strain (data not shown).

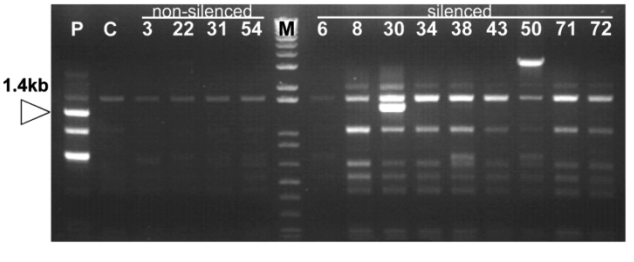

Figure 5. Inverted repeats of pXLNRir: PCR-amplified portion of inverted repeat of pXLNRir from genomic DNA of non-silenced and silenced strains. Triangle: expected fragment for intact inverted repeat region; *M*: molecular weight marker; *P*: silencing plasmid pXLNRir; *C*: wild type strain (NW219::pGW635). Numerals designate each non-silenced and silenced strain (NW219::pGW635::pXLNRir).

For quantitative analysis, a portion of *xln*R coding sequence present both in native *xln*R and in pXLNRir was amplified and detected by real-time PCR. After normalisation diverse copy numbers were obtained, indicating variable frequencies of integration of pXLNRir in the different silenced strains (Table 1).

Table 1. Copy numbers of pXLNRir in control strain. C (NW219::pGW635), non-silenced and silenced strains (NW219::pGW635::pXLNRir). Estimated copy numbers varied according to the standard deviation of measurements from three quantitative real-time-PCR runs.

Strains	Copy number of pXLNRir
Control	0
Non-silenced	
# 3	1
# 22	2, 3
# 31	10-16
# 54	0, 1
Silenced	
# 6	3, 4
# 8	1, 2
# 30	2
# 34	5, 6
# 38	5-7
# 43	1, 2
# 50	9-13
# 71	2
# 72	4-9

DISCUSSION

Phenotypic screens are widely used for strain improvement in industry. For most industrial strains a desirable phenotype such as increased or decreased enzyme production can be readily detected through simple functional assays. The system reported here relies on downstream screening of easily characterisable phenotypes. Alternatively, in the cases where a clear phenotypic difference cannot be obtained by plate screening of isolates, Reverse-Transcription PCR or Northen blot analysis may be used to confirm silencing. The GATEWAY-based technology presented in this study is based on exchange of fragments by means of two recombination reactions (BP and LR reactions). This recombination technology has the advantage that fragments originating from different genes can efficiently be inserted into an appropriate destination vector such as pFIRD1. For the construction of pXLNRir a stem length of 834 nucleotides of *xlnR* coding sequence was used, in accordance to a previous finding that stem lengths of 600 or 900 nucleotides

displayed higher silencing efficiencies in the ascomycete *Neurospora crassa* (Goldoni et al. 2004).

After transformation of *A. niger* by pXLNRir, a gradient of effects was observed on xylan-degrading activities. Although the strains with decreased xylanolytic activity obtained presented a moderately efficient silencing degree (except for strain 50, about 30% the *xlnR* expression of wild type *A. niger*), the number of silenced strains in comparison to the total number of strains obtained by co-transformation (12% of the total) was lower than expected. A number of reasons could serve as explanation for this result. First, some transformants might not be true co-transformants, even though this was not the case for the four non-silenced strains analysed. Second, some co-transformants such as non-silenced strain 54 suffered rearrangements in silencing construct. Third, silencing of *xln*R was not significant in all cases to yield an obvious decrease of xylanolytic activities, such as in the case of non-silenced strains 3 and 54.

Two confounding factors in the analysis of RNAi transformants are genome rearrangements which may occur after fungal transformation with silencing vectors and alternate silencing pathways not involving a typical Dicer-like/RISC-mediated degradation of mRNA, e.g. chromatin remodelling, DNA methylation and repeat induced mutation. In fact, non-silenced transformants often carry full silencing vectors and silenced transformants often carry only altered versions of hairpin-expression units, as previously determined (Fitzgerald et al. 2004; Moriwaki et al. 2007; Nakayashiki et al. 2005). The separate analysis of either agarose gels of amplified regions of pXLNRir from genomic DNA or of estimated copy numbers of integrated pXLNRir is not conclusive. On the one hand rearrangements may affect copy number determinations even using Southern blotting techniques which frequently miss smaller variations. On the other hand agarose gel analysis of amplified segments of genomic DNA is insufficient to provide reliable quantification. Nevertheless, combined analysis of these two methods may be used: for example copy numbers of pXLNRir do not correlate with a higher degree of silencing efficiency, a situation similar to others reported (Nicolás et al. 2003; Fitzgerald et al. 2004; Nakayashiki et al. 2005; Tanguay et al. 2006; Wälti et al. 2006; Henry et al. 2007; Yamada et al. 2007). Apart from genome instability and the occurrence of rearrangements, other factors may be responsible for a lower silencing efficiency of integrated hairpin-expression units. These factors include integration in regions of very low transcriptional activities (such as heterochromatin regions) or epigenetic modification of the inverted repeats without co-alteration of endogenous *xlnR* (possibly through RNA-induced transcriptional

silencing). Due to the high genetic diversity and genome instability of strains transformed with dsRNA-expression vectors, it may be of advantage to pre-select silenced transformants for single-locus integration of silencing vector, as these transformants would be less likely to undergo genome rearrangements in successive generations.

In spite of the fact that strains were obtained with varying genotypes for integration of pXLNRir, it was possible to obtain a clear silencing effect both on enzyme xylan-degrading activities and on transcript levels of the genes *xyr*A (encoding D-xylose reductase) and *xyn*B (also known as *xln*B, encoding endo-β-1,4-xylanase B), previously shown to be positively regulated by XlnR in *A. niger* (Hasper et al. 2000).

In conclusion, the GATEWAY-based system presented here has three noteworthy features: first, fast production of expression clones (about one week); second, use of any appropriate entry clone; and third no generation of unproductive clones. As shown for the transformation of the industrial microorganism *A. niger* with pXLNRir, it is furthermore possible to silence transcriptional regulators and screen for strains with the most desirable properties, depending on the effects of silencing on the expression of regulated genes.

MATERIALS AND METHODS

Fungal strains and media

A. niger strains used were derived from strain NW219 [*cspA1 nicA1 leuA1 pyrA6*], a derivative of CBS 120.49. Solid and liquid media were based on minimal medium (MM) (Pontecorvo et al. 1953), contained 1ml of trace elements solution (Vishniac and Santer 1957) per litre of medium and were supplemented with 16 µM nicotinic acid, 1.5 mM leucine, and 5.0 mM uridine. For strains transformed by the *pyr*A-containing plasmid pGW635 (Goosen et al. 1989), uridine was not added to the culture medium.

Construction of destination and expression vectors

Vector pIM3710 (Benen et al. 1999) was double digested with *Nsi*I and *Not*I and a 3.6 kb fragment was isolated from agarose and blunt-ended by T4 DNA polymerase. Vector pK7GWIWG2(I) (Karimi et al. 2002) was partially digested with *EcoR*V and a 4.1 kb fragment was isolated from agarose. The 4.1 kb fragment (with *ccd*B genes and homologous recombination sites in inverted repeat) was inserted by ligation into the 3.6

kb fragment of pIM3710, between the pyruvate kinase (*pkiA*) promoter and the endo-polygalacturonase II (*pgaII*) terminator from *A. niger*. *Escherichia coli* strain resistant to the toxic effects of *ccd*B gene product (One Shot® *ccd*B Survival™ T1 Phage Resistant, Invitrogen, Carlsbad, CA, USA) was used for propagation of the resulting destination vector pFIRD1. Transformation of One Shot® *ccd*B Survival™ T1 Phage-Resistant Cells with pFIRD1 was performed according to manufacturer's instructions.

The expression vector pXLNRir for silencing of *xlnR* was made as follows. A fragment of 834 bp of *xlnR* coding region (plus a total of 58bp for *att*B recombination sites) was amplified by PCR using cDNA (GenBank accession no. AJ001909) isolated from *A. niger* NW219 as template and primers attB1-xlnR and attB2-xlnR (Table 2).

Table 2. Oligonucleotide primers used for PCR in this study.

Primer name	Primer sequence (5'-3')
attB1-xlnR	*B1*-TTGAGAGCCACCATCTTAGC (*B1* = GGGGACAAGTTTGTACAAAAAAGCAGGCT)
attB2-xlnR	B2- TGACCATATTCGCCGCATAG (B2 = GGGGACCACTTTGTACAAGAAAGCTGGGT)
xlnR-borderF	GTGAACGGCACATACGACTC
xlnR-borderR	GAGCGACGCCATTGATGACC
PpkiA-spacer F	GCACAGATGCGTAAGGAGAA
PpkiA-spacer R	AGCCGTAAGAAGAGGCAAGA
spacer-TpgaIIF	TGGTCACGCTTAGTGGGTAAA
spacer-TpgaIIR	GGCTCGTATGTTGTGTGGAA
IR-spacer	AGTCGCTAGCGTGTGACCTT
xlnRir-copyF	GGACTAAGCTCCGGGTACAA
xlnRir-copyR	GAGGCGAGAGACCAAGAAAC
pki-copyF	AACTGCTCGCTACCTTTCCA
pki-copyR	CACGACCTCTCGAAACAACA
xlnR-QPCRF	GGGCAGTTTCTTGCTGCTAC
xlnR-QPCRR	GAATGTCCTCTGGTACTCCG
xyrA-QPCRF	TCGAGTTGAGTGTGCAGAATG
xyrA-QPCRR	ACTCTTGGGGATAACAGCAATC
xynB-QPCRF	CGAGTCTTACGGCGACTACA
xynB-QPCRR	ACGGACCAGTACTGAGTGAAGG
kan-QPCRF	AGCATTACGCTGACTTGACG
kan-QPCRR	AGGTGGACCAGTTGGTGATT

The following steps were performed using GATEWAY technology (Invitrogen, Carlsbad, CA, USA), according to manufacturer's instructions. Polyethylene glycol (PEG)/$MgCl_2$ purified *att*B-product and pDONR201 were mixed with BP clonase II in a 10 µl reaction mixture (BP reaction). Entry clone and destination vector pFIRD1 were mixed with LR clonase plus in a 20 µl reaction mixture (LR reaction). In both reactions, mixtures were incubated overnight at 25˚C, and treated with proteinase K. DH5α *E. coli* was

electrotransformed by DNA from the reaction mixture. After overnight incubation at 37°C on LB kanamycin (50 μg · ml^{-1}) or ampicillin (100 μg · ml^{-1}) plates, colonies were picked, cultured on liquid LB medium with the same antibiotic composition and incubated at 37˚C overnight. Entry clones and expression vectors for RNA-mediated silencing were isolated with the Wizard Plus Minipreps DNA Purification System (Promega, Madison, WI, USA).

Fungal transformation was performed as described elsewhere (Kusters-van Someren et al. 1991). In brief, enzymatic degradation of fungal cell wall was used to generate protoplasts, followed by purification by filtration and storage in isotonic sorbitol solution. For polyethylene glycol (PEG)-mediated transformation, protoplasts were incubated with 1 μg of pGW635 for selection and 30 μg of co-transforming pXLNRir for silencing of *xlnR*. Protoplasts transformed with 1 μg of pGW635 served as control for the transformation procedure. After this procedure, protoplasts were dispersed in sucrose-stabilised MM 0.6% (wt/vol) agar (0.95 M sucrose, pH6.0), and added on sucrose-stabilised MM 1.2% (wt/vol) agar with identical composition. Plates were incubated 4 days at 30˚C. After this period, spores were transferred from each strain to individual MM agar plates, containing 50 mM glucose and supplements.

Semi-quantitative assays for endoxylanase activity and β-xylosidase/xylanase activities

Spores of each isolated *A. niger* strain (transformed by pGW635 only or by pGW635 and pXLNRir) were harvested from individual MM agar plates. Saline-tween sterile solution [0.9% (wt/vol) NaCl, 0.005 % (vol/vol) Tween-80] was used for harvesting spores. For screening on endoxylanase activity and on β-xylosidase/xylanase activities, 5×10^4 and 5×10^3 spores of each strain were dotted on plate. Endoxylanase activity was assayed as described elsewhere (Hasper et al. 2004) on MM agar plates with 25 mM D-xylose and 0.1% (wt/vol) azurine-dyed and cross-linked xylan [AZCL-xylan (Megazyme, Ireland)]. β-Xylosidase/ xylanase activities were assayed on MM agar plates with 0.1% oat spelts xylan (Sigma Chemical Co., St Louis, MO, USA) and 0.5 mM 4-methylumbelliferyl-β-D-xylopyranoside [MUX (Sigma Chemical Co., St Louis, MO, USA)]. Plates assayed for β-xylosidase/ xylanase activities were incubated for 16h at 30˚C and halo formation was detected under UV light (λ=280nm).

Transfer experiments and sample quenching

For transfer experiments, cultures were made in triplicate for each strain (transformed by pGW635 only or pGW635 and pXLNRir). Spores were inoculated at a final concentration of 10^6 spores per millilitre in MM containing 0.1% (wt/vol) yeast extract, 0.1% (wt/vol) casamino acids, and 100 mM D-fructose. Cultures were grown at 30˚C in shake flasks in an orbital shaker at a constant agitation speed of 250 rpm for 18h. Mycelia were subsequently harvested, transferred as described elsewhere (van Peij et al. 1998a), and grown for 4h in MM with 50 mM D-xylose for induction. After this, mycelial samples were recovered by filtration on nylon gauze, quenched in liquid nitrogen and ground in a Mikro-dismembrator II (B. Braun, Melsungen, Germany). Frozen ground mycelial samples were stored at –80°C until further processing.

RNA isolation and cDNA synthesis

Frozen ground mycelial samples from transfer experiments were homogenised and lysed in TRIZOL Reagent (Invitrogen, Carlsbad, CA, USA). Chloroform was added and the mixtures were separated into aqueous and organic phases by phase-lock gel heavy (Eppendorf, Hamburg, Germany) according to manufacturer's instructions. The aqueous phases were transferred to an identical volume of 70% (vol/vol) ethanol, and loaded onto RNeasy Plant Mini Kit (QIAGEN, Hilden, Germany) columns for isolation and purification of RNA according to manufacturer's instructions. RNA quantity and purity was determined by spectrophotometry in a NanoDrop-1000 instrument (NanoDrop Technologies, Wilmington, DE, USA). Mixtures of 1 ng of 1.2 kb kanamycin control RNA (Promega, San Luis Obispo, CA, USA) with 1 µg of isolated RNA were treated with 0.1 $U \cdot \mu l^{-1}$ DNase I (amplification grade, Invitrogen, Carlsbad, CA, USA), incubated at 37˚C for 15 min and DNase I was subsequently heat-inactivated according to manufacturer's recommendations. The DNase-treated RNA mixtures were used as template for Reverse Transcription reactions with Omniscript RT kit (QIAGEN, Hilden, Germany), using 1.0 µM Oligo(dT)18, 0.5 mM each dNTP, RT buffer and 0.2 $U \cdot \mu l^{-1}$ Omniscript Reverse Transcriptase. The RT mixture was incubated for 1h at 37°C, the resulting cDNA mixture was diluted in DEPC-treated water (1:20) and stored at –20°C. Each cDNA sample was synthesised from each biological replicate of 3 independent cultures.

Quantitative real-time PCR

Primers for cDNA of *xlnR*, *xyr*A, *xyn*B (GenBank accession nos. AJ001909, AM269959, and AM269952) and the normaliser kanamycin external transcript (Table 2, under the label "QPCR") were designed for specific melting temperatures (60°C ±1°C), GC content (50%±5%) and amplicon sizes (139 to 150bp), using the program Primer3. Reagent preparation and sample pipetting for real-time PCR were performed in the CAS-1200 (Corbett Life Science, Sydney, Australia) automated system. Reaction mixtures for real-time PCR contained 25% (vol/vol) diluted cDNA as template (dilution 1:20), 0.15 µM each primer and ABsolute QPCR SYBR Green Mix (ABgene, Epsom, United Kingdom). Rotor-Gene 3000 (Corbett Life Science, Sydney, Australia) was used for thermal cycling and real-time detection of DNA. Thermal cycling program included enzyme heat-activation, amplification and melting steps. Two features of Rotor-Gene 6 software (Corbett Life Science, Sydney, Australia) were used: Melting Analysis and Comparative Quantitation. The Melting Analysis feature was used to determine primer-dimer formation and the Comparative Quantitation feature was used to determine take-off (TO) and amplification (A) values. The estimated values were used to calculate relative gene expression levels using the Pfaffl method (2001), normalised to the added kanamycin external transcript (proportional to total RNA used for cDNA synthesis) and to a standard condition (normalised expression of control *A. niger* NW219 transformed by pGW635 only). From each synthesised cDNA at least 3 runs were considered for analysis.

Genotyping by PCR

Frozen ground mycelial samples from transfer experiments were used for isolation of genomic DNA. Genomic DNA was isolated as described elsewhere (de Graaff et al. 1988). Starting with adequate primers (Table 2) and genomic DNA as template, PCR was used to evaluate three distinct aspects of the co-transformed strains: 1) integrity of native *xlnR*, 2) integrity of the silencing construct pXLNRir, and 3) copy numbers of pXLNRir.

Integrity of native xlnR: PCR with primers xlnR-borderF and xlnR-borderR was used to detect native *xlnR*. These primers were designed to anneal upstream and downstream of the 834 bp region of *xlnR* targeted to silencing by pXLNRir, yielding a product of 874bp.

Integrity of pXLNRir: Two regions of the silencing construct pXLNRir were targeted for PCR amplification: the upstream region spanning the *pki*A promoter and part of the spacer

sequence (primers used were PpkiA-spacer F and PpkiA-spacer R), and the downstream region spanning part of the spacer sequence and the *pgaII* terminator (primers used were Spacer-TpgaIIF and Spacer-TpgaIIR). In addition, a portion of inverted repeat of pXLNRir was targeted for amplification by single-primer PCR with primer IR-spacer.

Copy numbers of pXLNRir: Real-Time PCR was used to determine copy numbers of pXLNRir, with a primer pair specific for *xlnR* present in the inverted repeat and endogenous gene (xlnRir-copyF, xlnRir-copyR), and another pair for the normaliser gene *pkiA* (pkiA-copyF, pkiA-copyR). Reaction mixtures for real-time PCR contained about 10 ng $\cdot$ μl^{-1} genomic DNA as template, 0.15 µM each primer and ABsolute QPCR SYBR Green Mix (ABgene, Epsom, United Kingdom). Thermal cycling conditions were as mentioned above for quantitative real-time PCR. For copy number determination the Pfaffl method (2001) was used. Samples were first normalised for genomic DNA quantity using the control *pkiA* gene in order to determine the total number of copies of *xlnR* segments per genome. Afterwards, the number of *xlnR* segments was subtracted by one unit (one endogenous *xlnR* gene per genome) and divided by two (assuming that inverted repeats are integrated "en bloc" and without suffering rearrangements) to obtain the average number of inverted repeats per genome of each strain.

Acknowledgements

This research was funded by the Kluyver Centre for Genomics of Industrial Fermentation, which is supported by the Netherlands Genomics Initiative.

Chapter 3

Analysis of variance components reveals the contribution of sample processing to transcript variation

Douwe van der Veen, José Miguel Oliveira, Willy A. M. van den Berg and Leo H. de Graaff

Appl Environ Microbiol (2009) **75**: 2414–2422

ABSTRACT

The proper design of DNA microarray experiments requires knowledge of biological and technical variation of the studied biological model. For the filamentous fungus *Aspergillus niger*, a fast, quantitative real-time PCR (QPCR)-based hierarchical experimental design was used to determine this variation. Analysis of variance components determined the contribution of each processing step to total variation: 68% is due to differences in day-to-day handling and processing, while the fermentor vessel, cDNA synthesis and QPCR measurement each contributed equally to the remainder of variation. The global transcriptional response to D-xylose was analysed using Affymetrix microarrays. Twenty-four statistically differentially expressed genes were identified. These encode enzymes required to degrade and metabolise D-xylose-containing polysaccharides, as well as complementary enzymes required to metabolise complex polymers likely present in the vicinity of D-xylose-containing substrates. These results confirm previous findings that the D-xylose signal is interpreted by the fungus as the availability of a multitude of complex polysaccharides. Measurement of a limited number of transcripts in a defined experimental set-up followed by analysis of variance components is a fast and reliable method to determine biological and technical variation present in QPCR and microarray studies. This approach provides important parameters for the experimental design of batch-grown filamentous cultures and facilitates the evaluation and interpretation of microarray data.

INTRODUCTION

Culturing filamentous organisms such as *Aspergillus niger* is difficult to reproduce compared to culturing unicellular organisms. Filamentous growth is characterised by the elongation and branching of hyphae, cylindrical cells that increase in length by growth at one end. *De novo* biosynthesis and active enzyme production occur mainly at the hyphal tips. In regions of distance from the tip, the hyphae age and become biologically less active (Wösten et al. 1991). This hyphal growth is the result of adaption to the habitat of the organism, which enables it to spread over and penetrate surfaces and cross over nutrient-depleted gaps (Carlile 1995). However, under laboratory conditions, attachment of fungal mycelium to fermentor baffles and other extremities introduces heterogeneous growth that can be suppressed only to a certain extent (for instance, by cooling the fermentor headplate). The growing mycelium increases the culture broth viscosity, which reduces the mass transport of nutrients, oxygen and heat, and affects the mixing characteristics in a fermentor or shake flask over time. Physical agitation and shear stress can cause uncontrolled breakage and fragmentation of the mycelia (White et al. 2002).

Recent technologies such as global transcriptome analysis by DNA microarrays or quantitative real-time PCR (QPCR) require the use of replicate biological samples for high-quality data. Given the difficulties in culturing *A. niger*, obtaining transcript data without wasting resources requires proper experimental design. The key to designing such experiments is to determine how much replication is needed—the sample size (Wei et al. 2004). A larger amount of replicates leads to increased statistical accuracy of measurement, whereas insufficient replication impedes data analysis. The required number of independent samples depends on a variety of factors as follows: the organism under study and its biological variation, the magnitude of the expected gene response, the statistical power to detect the genuine gene response to a condition and the false discovery rate (Wei et al. 2004; Imbeaud and Auffray 2005).

Consensus is emerging on what comprises a "proper microarray experiment" (Imbeaud et al. 2005). According to this consensus, defining the experimental objectives and requirements is a necessity before actually starting an experiment (Yang and Speed 2002). During the experiment, standardised protocols and methods reduce the variability that is introduced in each process step (Salit et al. 2006). A selected experimental design makes data analysis and interpretation as simple and as powerful as possible. Finally, for publication of the microarray results and data, the minimum information about a

microarray experiment (MIAME) guidelines (Brazma et al. 2001) are adopted. Notwithstanding this consensus, Jafari and Azuaje (2006) have published an extensive review on papers describing microarray methods and applications of microarray technology and concluded that recently published gene expression data analysis studies often lack key information that is required to interpret and evaluate published data.

The goal of the present study was to minimise the variation in *A. niger* batch fermentations by optimisation of protocols and procedures. The variation between fermentations was determined with an analysis of variance components of data obtained by QPCR. This relatively inexpensive technology is used to measure transcript levels for few genes in many samples simultaneously. Furthermore, QPCR is routinely used to validate microarray results (Etienne et al. 2004; Morey et al. 2006).

The effects of the optimisation and quality control measures for our experimental set-up were assessed by examination of the global transcriptional response toward induction with D-xylose. The xylanolytic system of *A. niger* is under the control of the transcriptional activator XlnR and the genes under its control are well documented (van Peij et al. 1998a). Recently, the transcriptional response toward D-xylose was examined by microarray analysis for three *Aspergillus* species (Andersen et al. 2008). The availability of these data on the transcriptional response toward D-xylose allows for validation of the biological response observed during our studies.

RESULTS

Selection of conditions for the response system

The xylanolytic system of *A. niger* consists of enzymes that degrade cellulose and hemicellulose, is under the control of the transcriptional regulator XlnR (van Peij et al. 1998a) and can be induced by the monosaccharide D-xylose. XlnR-controlled genes are subject to carbon catabolite repression by D-xylose (de Vries et al. 1999c). To reduce this repressing effect, the D-xylose concentration that induced the xylanolytic system but had the least repressing effect on XlnR-controlled genes was determined prior to the analysis of variance components experiment. Three fermentor cultures were induced with either 0.1, 1, or 50 mM D-xylose and sampled for up to 4 h. Expression levels for two XlnR-controlled genes, *xlnB* and *xlnD*, were followed by QPCR. These genes encode endoxylanase B (Kinoshita et al. 1995) and β-xylosidase (van Peij et al. 1997), respectively.

The observed transcript levels for *xlnB* and *xlnD* are given in Fig. 1. A D-xylose concentration of 0.1 mM is able to induce both genes, with an expression ratio for *xlnD* of 190-fold at 60 min after induction. This lowest concentration of 0.1 mM D-xylose also discriminates best between non-induced and induced states: for this concentration, transcript levels increase for 60 min and return to pre-induced levels in the next hour. For both the 1-mM and 50-mM concentrations, elevated transcript levels for *xlnB* and *xlnD* could be detected up to 3 hours after induction. We decided to induce fermentor cultures with 0.1 mM D-xylose and to sample them 1 h after induction.

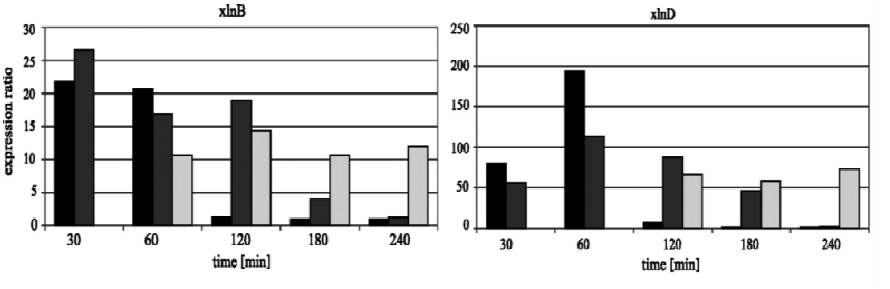

Figure 1. Expression ratios of *xlnB* and *xlnD*. The expression ratios of the *xlnB* and *xlnD* genes measured after induction with either 0.1 (black), 1 (dark grey) or 50 (light grey) mM of D-xylose. The sampling time in minutes is presented on the horizontal axis. No transcript levels were determined for the 50-mM fermentations for both genes at 30 min. At 60 min, a bad QPCR run prevented *xlnD* ratio calculation.

Experimental design

The aim of this experiment was both to minimise all variation introduced in each of the steps preceding a QPCR measurement or microarray scan and to determine their magnitude. After optimisation of the processing protocols, we investigated the variation in our experimental set-up quantitatively by QPCR. For this, a hierarchical factorial experiment was designed (Fig. 2). We performed one fermentation cycle per week for 5 weeks, using three identical fermentations per week. These cultures were induced with 0.1 mM D-xylose. A fourth culture was randomly selected as the non-induced control. Each processing step following induction was executed in duplicate, starting with the independent harvesting of mycelial samples. This led to 128 individual QPCR measurements for a single fermentation or a total of 1,920 individual measurements. Another 768 measurements originated both from non-induced cultures and from culture samples taken before induction. In total, 2,688 QPCR measurements were made.

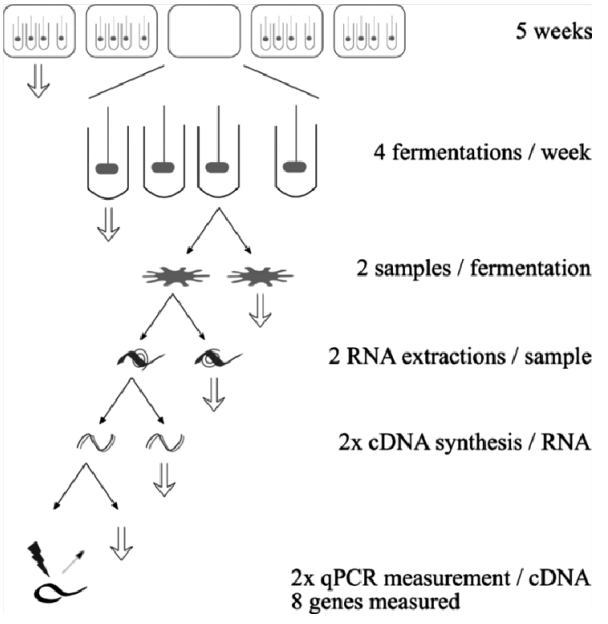

Figure 2. Experimental design. Schematic representation of hierarchical experimental design used. In a 5-week period (grey boxes), four fermentors were run. Three fermentors were induced to 0.1 mM D-xylose and the fourth fermentor was induced to 0.1 mM sorbitol. Each fermentation run was sampled twice and from each mycelial sample, total RNA was extracted twice independently. The total RNA obtained was split in two, and independent cDNA synthesis reactions were performed. Each cDNA sample that was made was used to measure eight genes in duplicate using QPCR. The grey arrow indicates an identical processing step.

In the elongation phase of a QPCR, SYBR green dye molecules intercalate with double-stranded DNA that is formed during the reaction. The dye-DNA complex absorbs blue light and emits green light (Tuma et al. 1999), which is measured and plotted against the cycle run number. The resulting sigmoid-shaped curve is used to extract the cycle threshold and amplification efficiency values. The cycle threshold value represents the amount of transcripts for a specific gene in the cDNA template upon the start of the PCR, with lower values representing more copies of a transcript present in the cDNA pool. The amplification efficiency is a primer pair-specific value that represents the efficiency of the PCR and hence is independent from the experimental conditions apart from the QPCR run itself (Tichopad et al. 2003). Insight into the variation that is introduced in all steps except the day-to-day and fermentor-to-fermentor variations is deduced from the expression ratio. This ratio expresses the relative change of a gene's transcription level compared to

that of a non-induced sample. A ratio greater than 1 indicates elevated transcription of a gene, while a ratio of 1 indicates no change. Table 1 gives descriptive statistics of the data set. Variance components were estimated for each of the three variables and were subdivided by the eight genes followed in this study (Table 2).

Table 1. Descriptive statistics. QPCR runs that did not meet quality control standards account for differences between the theoretical number of samples possible (240) and the actual number of measured samples. Ct: cycle threshold; E: amplification efficiency.

Gene or transcript	QPCR run parameters			Expression ratio	
	Measured samples	Ct ± SD	E ± SD	Measured samples	Avg ± SD
An08g05910	230	24.08 ± 1.22	1.70 ± 0.026	226	1.06 ± 0.43
An02g04120	232	21.4 ± 0.98	1.72 ± 0.044	228	1.05 ± 0.43
An14g05050	236	25.69 ± 1.47	1.68 ± 0.032	232	1.02 ± 0.42
An08g06940	236	16.49 ± 0.57	1.70 ± 0.024	232	0.88 ± 0.32
An15g01860	233	24.83 ± 1.43	1.71 ± 0.015	229	2.45 ± 1.74
Kanamycin	234	16.08 ± 0.49	1.74 ± 0.028	234	1
xlnB (*xynB*)	236	22.62 ± 1.38	1.73 ± 0.018	232	16.42 ± 9.35
xlnD	235	16.08 ± 0.82	1.73 ± 0.027	231	137.73 ± 94.90

Table 2. Relative variance components estimates. Columns indicate the terms of the random model used to describe variance and correspond to the experimental procedure outlined in Fig. 2.

Gene or transcript	Relative variance components estimates by:					
	Week	Fermentor	Biomass	RNA sample	cDNA sample	QPCR
Cycle threshold						
An08g05910	78.8	5.9	1.3	2.5	4.2	7.3
An02g04120	66.2	1.9	0.0	0.3	11.5	20.1
An14g05050	81.4	3.0	2.7	3.9	3.2	5.9
An08g06940	68.1	5.5	1.0	14.1	8.3	2.9
An15g01860	29.6	60.4	0.6	2.8	3.1	3.6
Kanamycin	67.5	0.0	0.0	18.1	10.1	4.3
xlnB (*xynB*)	69.1	10.7	0.0	4.7	9.3	6.2
xlnD	4.8	19.4	2.9	47.7	8.2	17.0
Amplification efficiency						
An08g05910	68.9	2.1	2.8	0.0	1.1	25.1
An02g04120	75.9	3.1	0.0	0.0	2.2	18.7
An14g05050	74.7	0.1	0.0	0.0	0.3	24.9
An08g06940	77.8	0.1	0.0	0.0	4.6	17.5
An15g01860	30.1	5.3	0.0	1.5	8.2	54.8
Kanamycin	71.5	0.8	0.0	7.5	2.1	18.1
xlnB (*xynB*)	31.2	6.2	7.1	0.0	11.3	44.3
xlnD	32.6	25.2	1.9	9.1	6.6	24.7
Expression ratio						
An08g05910	0.0	36.4	10.7	0.0	24.6	28.3
An02g04120	2.1	28.9	0.0	4.3	21.5	43.2
An14g05050	0.0	30.6	9.8	2.8	24.5	32.2
An08g06940	0.3	58.5	2.3	12.7	19.8	6.3
An15g01860	6.0	75.9	0.5	6.8	1.9	9.0
Kanamycin	0.0	0.0	0.0	0.0	0.0	0.0
xlnB (*xynB*)	11.7	62.0	0.0	6.0	9.4	10.9
xlnD	0.0	80.7	1.6	3.6	11.5	2.6

DNA microarray analysis results

To investigate the differences in global transcript levels between fermentations done in this study, six fermentor samples were selected for hybridisation onto DNA microarrays. These samples were selected based on differences in their distribution over the weeks and fermentor vessels used, their biomass density, and the *xlnD* expression levels observed in these samples by QPCR (Table 3).

Table 3. RNA sample properties. Coding corresponds to the data measured by QPCR. *xlnD* ratio was the average of four expression ratios calculated from the four replicate QPCR measurements.

Sample	Carbon source	Week (2-5)	Fermentor (3-5)	Biomass (1 or 2)	RNA sample	*xlnD* ratio	Dry wt ($g \cdot l^{-1}$)
A	D-Xylose	2	3	2	1	20	1.84
B		3	2	2	1	300	1.41
C		5	3	1	1	50	2.20
D		5	3	1	1	50	2.20
E		4	5	2	1	120	1.93
F	D-Sorbitol	5	5	1	1	1	1.64
G		3	4	1	1	1	1.92

To analyse technical variation that is introduced within microarray processing steps, the total RNA of one mycelial sample was split (Table 3, C and D), processed independently and hybridised onto two microarrays. RMA signal values were calculated and plotted (Fig. 3).

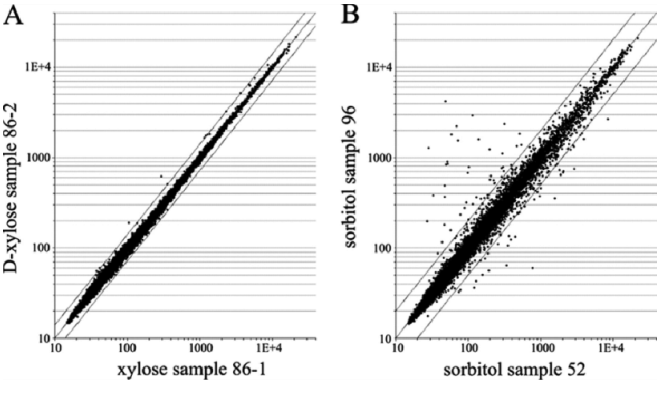

Figure 3. Technical variation between samples. Scatter plot of microarray data. (A) Two RNA samples derived from one mycelial sample (table 3, C and D) were processed independently and hybridised to two Affymetrix arrays. The RMA-normalised data of all 14,554 probe sets are plotted in a scatter plot. (B) Total RNA from two independent non-induced control fermentations (sorbitol; table 3, F and G) were hybridised, and RMA normalised-data are plotted. The lines above and below the diagonal line indicate twofold difference relative to the diagonal line.

Only the RMA signal values for 5 of 14,554 probe sets differ more than 1.5-fold but not more than 2.1-fold between the technical replicates. No mRNA sequences hybridise to these probe sets: 28S rRNA hybridises to four of five probe sets, while the fifth probe set hybridises to one of the control transcripts used in the Affymetrix array platform, the 5' region of the *Escherichia coli bioD* transcript. This result indicates that the specific microarray handling and processing steps contribute little to overall variation.

A transcriptome analysis revealed 24 genes that are significantly differentially expressed in D-xylose-induced cultures compared to sorbitol-grown cultures (Table 4).

Table 4. Differentially expressed genes on D-xylose induction. The location of the *cis*-acting motif 5'-GGNTAAA-3' is indicated in base pairs counted upstream of the ATG start codon. Values in parentheses indicate the reverse direction of this motif.

A. niger gene	Signal sequence	Description	Motif
An01g00780	Yes	*xlnB* (*xynB*); xylanase B	–216
An01g09960	Yes	*xlnD*; β-xylosidase	(–250), –147
An14g05800	Yes	*aguA*; α-glucuronidase	–277, (–183)
An09g00120	Yes	*faeA*; ferulic acid esterase A	–265, (–121)
An18g03570	Yes	*bglA*; β-glucosidase	
An14g02760	Yes	*eglA*; endoglucanase A	
An09g03300	Yes	Glycosyl hydrolase, family 31	–138
An03g00500		Glycosyl hydrolase, family 30	
An15g01500		Sugar transporter	(–417)
An11g01100		Sugar transporter	
An03g01620	Yes	Sugar transporter	–407
An06g00560		Sugar transporter	–415
An01g10920		*ladA*; L-arabitol dehydrogenase	–334
An01g03740		*xyrA*; D-xylose reductase XyrA	(–311)
An12g00030		*xdhA*; xylitol dehydrogenase	–333
An07g03140		*xkiA*; D-xylulokinase	(–672), –482
An02g03590		Galactose-1-P uridylyltransferase (similar to *S. cerevisiae* GAL7p)	(–371)
An11g10890		UDP-glucose 4-epimerase (similar to *S. cerevisiae* GAL10p)	(–577)
An07g03160		*talB*; transaldolase	–195
An08g01740		Aldehyde reductase	–765
An02g13980	Yes	Conserved hypothetical protein	–540, (+26)
An06g00830		Weak similarity to hypothetical transcription regulatory protein	
An01g11180		Hypothetical protein, FAD/FMN, containing dehydrogenase	(–329)
An11g05340	Yes	Fructosamine oxidase	

This gene list contains both *xlnB* and *xlnD*, the two genes used in the QPCR measurements to assess the induction of the xylanolytic system, as well as an additional eight enzymes that are known to be under XlnR control (van Peij et al. 1998a). The presence of four sugar transporter-encoding genes, as well as two genes encoding glycosyl hydrolases, is in accordance with the view that D-xylose initialises a response to degrade complex carbohydrates, such as hemicellulose. In addition, two genes that encode

enzymes of the Leloir pathway, the classical pathway of D-galactose catabolism, are upregulated in the induced samples. An02g03590, the ortholog of the *Saccharomyces cerevisiae* GAL7 protein, encodes the second enzyme of the Leloir pathway, while the required glucose epimerase activity is encoded by An11g10890, the ortholog of *S. cerevisiae* GAL10. The first step of this pathway, the galactokinase that phosphorylates D-galactose to D-galactose 1-phosphate, is encoded by An16g04160. This gene is induced about twofold by D-xylose, but a P value of 0.604 excludes this gene from our list of statistically differentially expressed genes. Finally, for six genes in our list of differentially expressed genes, their roles in the cellular response toward D-xylose are difficult to assess.

DISCUSSION

Experimental variation

Although, in theory, a protocol is a rigid and established code that describes all proceedings relating to an experiment, in practice, protocol steps are subject to interpretation by different experimenters. A precise description of how to handle given steps and the removal of unclear or ambiguous sentences decrease the necessity to interpret the exact meaning of a protocol phrase, which in turn leads to more-reproducible experiments. The effects of our optimisation and quantitative determination of the variation in our laboratory set-up were determined by QPCR, a cost-effective yet powerful technique to study transcript abundance.

Important parameters for high-quality QPCR measurements are the specificity of a primer pair for its target, amplification efficiency and reproducibility (Bustin 2002; Lutfalla and Uze 2006). Typically, when a newly designed primer pair is tested prior to use in quantification, a range of different annealing temperatures or primer concentrations is examined to identify conditions where only a single DNA fragment is amplified. In this study, a multitude of target genes were measured using a single PCR profile and primer concentration. The possibility that this approach affects the robustness of our QPCR measurements was assessed by the examination of the variation that is introduced in the amplification efficiency values. Within-gene variation is minimal, even when the amplification efficiency per gene varies. The most variable amplification efficiency values are for gene An02g04120, with a mean value of 1.72 and a standard deviation of 0.04 (n = 326). The reproducibility of this generalised method can be also derived from the analysis

of variance while looking at the variance component titled "QPCR" (Table 2), which includes pipetting and the actual measurement. The median relative contribution is 6.1% of the total variation (Table 2). Transcript An02g04120 again shows the highest variation, 20.1%, in this step. When this percentage is placed in its biological context, 95% of all cycle threshold values will range between 21.3 ± 0.9, which translates to 1.6-fold differences. We conclude that our standardised QPCR method is both precise and accurate.

Before the actual determination of the sources of variation in our experiment, we hypothesised that most variation is introduced by differences in the day-to-day handling and processing. The next largest variation was anticipated to be the use of the individual fermentor vessels. The results of the analysis of variance components comply with our initial hypothesis: day-to-day variation contributes to about 70% of the total variation (Table 2). This step includes the growth and harvesting of spores, the preparation of fermentation media and the assembly of fermentors. The large effect that the day-to-day variation has on the total variation can effectively be excluded by examination of the expression ratio. This ratio presents the relative change in a gene's transcript level between pre-induced and post-induced fermentation conditions. As this ratio is calculated from expression data of samples taken from the same fermentor, this result effectively cancels out the contribution of day-to-day variation. When fermentor cultures are compared by this gene expression ratio, the analysis of variance components of the ratio-derived data shows that the three steps of fermentation, cDNA synthesis and actual QPCR measurement each contribute about equally in the case of the four endogenous reference genes (Table 2).

The effect that the individual fermentation vessels have on the variation in transcript level is 60% and 80% for the two D-xylose-induced genes, *xlnB* and *xlnD*, respectively. For the malate synthase-encoding gene, the effect is 75%. Different amounts of fungal cells present in a fermentor cannot explain this effect, as only a weak correlation of cycle threshold values with the biomass concentration is found (i.e., for *xlnB*, $R^2 = 0.35$). One explanation is that small differences between fermentor headplates and vessels result in unique mixture characteristics for each fermentor. These fermentor-specific effects are reflected in small physiological differences between cultures, which may account for the observed differences in transcript levels. Since samples are taken 1 h after induction with D-xylose, such differences may affect the actual D-xylose concentration per fermentor, leading to a high reproducibility of a gene's expression within a fermentor but variation of its expression between fermentors. For example, *xlnD* induction is on average 240-fold

higher for fermentors with headplate "2" but only 100-fold higher for fermentors with headplate "4.".

D-Xylose-induced genes assessed by DNA microarray analysis

The QPCR measurements clearly showed elevated transcript levels of *xlnB* and *xlnD* after induction with D-xylose. For *xlnB*, the average increase for all 15 fermentations was by 16-fold compared to that of non-induced conditions, while for *xlnD*, the average increase was by 138-fold. For the six DNA microarrays analysed, the average increase is by 6-fold for *xlnB* and by 110-fold for *xlnD* after induction with D-xylose. The results for a gene measured by both methods are in good agreement; for instance, the Spearman rank correlation coefficient for *xlnD* measurements obtained by QPCR and microarray technologies is 0.90.

Comparison of the non-induced and D-xylose-induced samples that were hybridised onto microarrays revealed 24 genes that are statistically differentially expressed after induction with D-xylose (Table 4). Degradation of complex polysaccharide substrates starts with the uptake of signal molecules such as D-xylose that activate specific induction pathways, resulting in the expression and secretion of enzymes necessary to degrade and metabolise the polysaccharide. However, since D-xylose is rarely found by itself under natural conditions, it is likely that *A. niger* interprets the presence of D-xylose as proxy for the availability of complex carbohydrate polymers, such as (hemi)cellulose. Not only is this heterogenic response reflected in the induction of secreted enzymes but also in the activation of multiple metabolic pathways (Fig. 4). For instance, genes encoding the second step in L-arabinose metabolism and enzymes of the classical D-galactose catabolic route are significantly upregulated as well.

Five genes appear to encode enzymes that might well be related to (hemi)cellulose degradation, but of which the exact function has not been elucidated. An08g01740 encodes an aldehyde reductase. Reduction of the carboxyl group of carbohydrates by aldehyde reductases, such as the reduction of D-xylose to xylitol, is a first step in the catabolism of many monosaccharides, and the product of this gene might well play a role in the catabolism of monosaccharide substrates that are the products of (hemi)cellulose degradation. Products of D-xylose or L-arabinose catabolism are channeled into the non-oxidative branch of the pentose phosphate pathway. This pathway in turn is linked to glycolysis by the enzymes transaldolase and transketolase (Stryer 1995). While the *talB*

transaldolase is upregulated by sixfold in D-xylose-induced samples, both transketolase-encoding genes as well as the major transaldolase-encoding gene of *A. niger* have no differential expression levels under induced and non-induced conditions.

The transcriptional regulator XlnR activates the transcription of (hemi)cellulose-degrading enzymes (van Peij et al. 1998a) as well as the transcription of genes encoding metabolic enzymes (van Peij et al. 1998a; vanKuyk et al. 2001). A *cis*-acting element in the promoter region of D-xylose-induced genes, described as 5'-GGCTAAA-3' (van Peij et al. 1998a) and proposed to be generalised to 5'-GGNTAAA-3' after comparative transcriptome analysis of three *Aspergillus* species (Andersen et al. 2008), was detected in all but five significantly differentially expressed genes (Table 4), and also, the GAL1p ortholog An16g04160 has this consensus motif present 153 bp upstream in its promoter region.

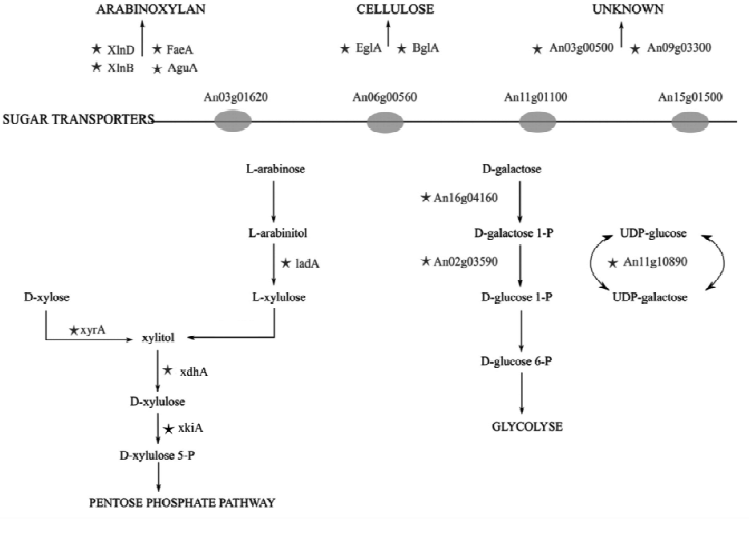

Figure 4. Enzymes induced by D-xylose. Schematic of the enzymes encoded by significantly differentially expressed genes after induction by D-xylose. (Top) Extracellular enzymes acting on complex polysaccharides, arabinoxylan, and cellulose. (Middle) Sugar transporters. (Bottom) Metabolic routes of the degradation of D-xylose, L-arabinose and D-galactose. The enzymes encoded by significantly differentially expressed genes are indicated by stars.

In this and other studies (Andersen et al. 2008), it was observed that genes non-strictly related to D-xylose metabolism have elevated transcript levels upon D-xylose

induction. The most likely explanation for this is that the fungus fine-tunes its response toward the diversity of complex substrates it encounters by coordinated action of partly overlapping regulatory systems. Expression of the XlnR-controlled ferulic acid esterase A is greater when *A. niger* is induced with both D-xylose and ferulic acid relative to induction by D-xylose or ferulic acid alone (de Vries and Visser 1999b). Aromatic compounds such as ferulic acid are not only part of arabinoxylan but are also part of pectin. No XlnR-related motif is present in the promoter region of the polysaccharide-degrading enzymes acting on cellulose, BglA and EglA, nor is that present in the promoter region of one of the uncharacterised family 30 glycosyl hydrolases. The induction of these genes in the absence of the consensus motif suggests the action of other transcriptional activators besides the xylanolytic activator XlnR. Interestingly, one of the genes of unclear function encodes a hypothetical transcription regulatory protein, and its expression patterns correlate strongly with the three genes of the Leloir pathway.

Andersen and co-workers have described a conserved set of 23 genes for which transcription is elevated on D-xylose medium (Andersen et al. 2008). Nine of these D-xylose-responsive genes are not present in our gene list, including three genes encoding sugar transporters, three glycosyl hydrolases, and three metabolic enzyme-encoding genes (encoding an aldose 1-epimerase, a short-chain dehydrogenase and an aldehyde reductase). The difference between the two gene lists can be explained by the experimental approach chosen: Andersen and co-workers have grown *A. niger* with either D-glucose or D-xylose as the sole carbon source and have sampled at D-xylose levels around 12 mM. In this study, sorbitol-grown cultures were induced with minute concentrations of D-xylose only.

In conclusion, the work presented in this study has resulted in an improved method for the generation of high-quality QPCR and microarray data from fermentations of the filamentous fungus *Aspergillus niger*. The decreased variation improves data quality and eases the use of data analysis, which is an essential prerequisite to study transcript profiling and gene regulation.

This work provides new insights into the mechanisms following D-xylose induction. The data link xylose metabolism not only to L-arabinose metabolism but also to D-galactose metabolism.

MATERIALS AND METHODS

Strain and spore preparations

A. niger 872.11 (*ΔargB pyrA6 prtF28 goxC17 cspA1*) is derived from CBS 120.49. All media were based on minimal medium (Pontecorvo et al. 1953), contained 100 mM sorbitol as the carbon source, and were supplemented with uridine and arginine. To obtain spores, 20 spores per mm^2 were plated onto complete medium plates (Pontecorvo et al. 1953), incubated for 5 days at 30°C, and allowed to mature at 4°C for 24 h. The spore suspension was washed and stored at 4°C until use.

Fermentation

Four 2.5-litre glass fermentors (Applikon) with 2.2 litres of minimal medium were kept at a constant temperature of 30 ± 0.5°C, while fermentor headplates were kept at 8°C. A total of 1.0 x 10^6 spores per millilitre were added to the fermentor. During germination, each fermentor was aerated through the headspace (50 $l \cdot h^{-1}$) and stirred at 300 rpm. When dissolved oxygen levels dropped below 60% for over 5 min, the stirrer speed was set to 750 rpm and aeration was switched to sparger inlet. This switching time point was defined as t = 0 h. Each fermentor was induced with either 0.1 mM sorbitol or D-xylose at t =14 h. Samples were snap-frozen in liquid nitrogen directly after filtration, with less than 20 s between sampling and snap-freezing.

RNA isolation

Frozen mycelium was ground for 40 s using a dismembrator (Braun Melsungen). A Trizol-chloroform extraction preceded total RNA extraction with RNeasy minicolumns (Qiagen), according to the manufacturer's protocol for yeast. RNA integrity was assessed with an Experion system (Bio-Rad) by visual inspection of the electropherograms. Graphs depicting RNA integrity categories were used as visual aids (Schröder et al. 2006). Electropherograms approximating an RNA integrity number of 8 or lower or with a 28S/18S ratio below 1.8 were discarded.

QPCR measurements

Variation in transcript levels was determined for seven *A. niger* genes and a synthetic control RNA transcript (Table 5). This synthetic control RNA transcript, a bacterial gene fused to a eukaryotic poly(A) tail (Promega), is spiked to total RNA prior to cDNA synthesis and can correct for various efficiencies of reverse transcription or PCR itself (Huggett et al. 2005). The first four genes of Table 5 were used as endogenous reference genes. These *A. niger* reference genes showed little variation in transcript levels on more than 100 microarrays that were run in our laboratory prior to this study (D. van der Veen, J. M. Oliveira, E. S. Martens-Uzunova, and L. H. de Graaff, unpublished data) and were selected using the method suggested by Lee and co-workers (2007).

Table 5. Primers used in this study. Boldface type: endogenous reference genes. F: forward primer; R: reverse primer

Gene or transcript	Description	Primers (5' to 3')
An08g06940	Histone, strong similarity to *A. nidulans* histone H4.1 (Ehinger et al. 1990)	F: ATCTTGCGTGACAACATCCA R: CACCCTCAAGGAAGGTCTTG
An08g05910	Strong similarity to *Aspergillus nidulans* SagA, which is involved in endocytosis and DNA repair (Jones et al. 1999)	F: CCAGGATGAAGAGTGGGAGA R: GCAGCTGGAGTGCTTCTTTC
An02g04120	Similarity to *S. cerevisiae* Atx2, which is a Golgi transporter involved in manganese homeostasis (Lin and Culotta 1996)	F: TTTTCAGTCTGGCTGCTCCT R: CTGTTTTCCTGCATCGTGTG
An14g05050	Strong similarity to *Schizosaccharomyces pombe* Dma1, which is a component of the spindle assembly point involved in mitotic division (Murone and Simanis 1996)	F: ACTCCAGAGGACAAGCAGGA R: GCAGACGCATGCTCTCAATA
An15g01860	Malate synthase	F: TGATTAAGACGTGTCACCGC R: GGAGTGGGCATGTAGGTGTT
An01g00780	Endoxylanase B (*xlnB/xynB*)	F: CAACTTTGTCGGTGGAAAGG R: GGGTAGCCGTGTAGATATCG
An01g09960	β-Xylosidase (*xlnD*)	F: TAATCTACGCCGGTGGTATC R: TTCTTGAGCGAAGAGGAATC
Kanamycin	Kanamycin synthetase-encoding poly(A)-tailed synthetic gene	F: AGCATTACGCTGACTTGACG R: AGGTGGACCAGTTGGTGATT

No elevated expression levels are expected for these genes (Ehringer et al. 1990; Lin and Culotta 1996; Murone and Simanis 1996; Jones et al. 1999). Expression levels for malate synthase, whose expression is not influenced by addition of D-xylose, were also measured.

Finally, the transcriptional response upon the addition of D-xylose was measured by determining the transcript levels of two genes, *xlnB* and *xlnD*. Primers were designed using the Primer3 web interface (Rozen and Skaletsky 2000) and are given in Table 5. Primer design criteria were as follows: length, 20 to 22 bp; melting temperature, 60 ± 1°C; and GC content, 50% ± 5%. Amplicons ranged from 125 to 150 bp and had a melting temperature of 80 ± 5°C.

Total isolated RNA was diluted in two steps to a concentration of 200 ng · μl^{-1}. A total of 1.00 µg of total RNA was spiked with 0.1 ng of the synthetic RNA transcript, followed by DNase I treatment. cDNA was synthesised using the Omniscript reverse transcriptase kit (Qiagen). Four units of reverse transcriptase enzyme was added to the DNase-treated total RNA at a final volume of 20 µl. The cDNA synthesis reaction was kept at 37°C and after 1 hour the synthesised cDNA was diluted 20-fold and stored at –20°C until use. For QPCR measurements, PCR primers (final concentration, 1.4 µM) and 4 µl of diluted cDNA were pipetted to 2x SYBR PCR mastermix (ABgene) using a CAS-1200 pipetting robot (Corbett Life Science).

A Rotor-Gene 3000 QPCR machine (Corbett Life Science) was used for thermocycling under the following conditions: 15 min at 95°C, followed by 40 amplification cycles (denaturation, 15 s at 95°C; annealing, 15 s at 58°C; elongation, 20 s at 72°C). For each single run, non-template control samples for every primer pair used in that run were included. After the amplification cycles, a melting step was performed. Quality control was done by inspection of the melting curve and samples with significant primer-dimer formation were not considered for analysis. The cycle threshold value and amplification efficiency were determined with the Rotor-Gene software using the comparative quantification method (the cycle threshold value corresponds to the Rotor-Gene software "take-off" value). The relative expression ratio of gene expression was calculated by following Pfaffl (2001) as follows:

$$\text{ratio} = (E_{gene})^{\Delta Ct\,(pre - post)} / (E_{kana})^{\Delta Ct\,(control - sample)}.$$

In this formula, E_{kana} denotes the amplification efficiency of the synthetic transcript and E_{gene} denotes that of the gene for which the ratio is determined. ΔCt denotes the cycle threshold difference between pre- and post-induced fermentor samples for the gene and kanamycin transcripts.

Microarray processing

cDNA and cRNA synthesis and labelling and array hybridisation were performed by following the Affymetrix users' manual (Affymetrix, Santa Clara, CA) using the one-cycle target labelling and control reagent kit and starting with 5 µg of total RNA as template material. Fifteen micrograms of fragmented and labelled cRNA was hybridised to custom-made *Aspergillus niger* arrays at 45°C for 16 h. Washing and staining were done using the hybridisation, wash, and stain kit (Affymetrix), using a GeneChip FS-450 fluidics station and an Agilent G2500A gene array scanner. Scanned images were converted into .CEL files using Microarray Suite version 5 software (Affymetrix).

Data analysis

For the 1,920 QPCR measurements obtained from the 5-week fermentor experiment, variance components were calculated by restricted maximum likelihood (REML) variance components analysis (REML sparse algorithm with average information optimisation) (Patterson and Thompson 1971) using GenStat 9.2 software (VSN International). Per gene, three REML analyses were run using each gene's cycle threshold, amplification efficiency, and expression ratio values as response variates. The following random model was applied:

$$y_{w.f.b.r.d.q.s} = \mu + \varepsilon_{week} + \varepsilon_{w.fermentor} + \varepsilon_{w.f.biomass} + \varepsilon_{w.f.b.RNA} + \varepsilon_{w.f.b.r.cDNA} + \varepsilon_{w.f.b.r.c.QPCR},$$

using w.f.b.r.c.QPCR as the residual term (subscripts are abbreviated after first usage; e.g., w.f.biomass is week.fermentor.biomass).

For microarray data analysis, .CEL files of the individual array images were imported into GeneSpring 7.3 (Agilent Technologies) using its robust multichip average (RMA) preprocessor to obtain RMA-normalised signal values for all arrays (Irizarry et al. 2003). Probe sets with an RMA-normalised signal below 37.7—three times the lowest value detected—on all arrays were discarded, leaving 9,320 probe sets (64%). In comparison, when using the Affymetrix MAS 5.1 software-derived flag calls, an average of 5,948 probe sets (41%) are called "present" per array. For the six microarrays used in this study, statistically significant differentially expressed genes were determined using the limma package (Smyth 2004). A Student's two-sample t test between the sorbitol and D-xylose arrays was executed, using empirical Bayesian statistics to moderate within-gene standard

errors, Benjamini and Hochberg's "false discovery rate" to correct for multiple testing (Benjamini and Hochberg 1995) and an adjusted P value of <0.05 to discriminate between differentially expressed genes. To check for the influence of unequal sample size bias, testing was recalculated with the inclusion of four additional sorbitol-grown samples derived from cultures grown identically (our unpublished data), giving similar results.

Microarray data accession number

Raw and RMA-normalised array data were deposited in NCBI's GEO database (Edgar et al. 2002) under series entry GSE11405.

Acknowledgements

We wold like to thank J. Thissen of the Biometris expert group of Wageningen UR for performing the variance components analysis and DSM Food Specialties for providing aid in fermentor optimisation and use of the DSM *A. niger* microarrays.

Chapter 4

Shotgun proteomics of *Aspergillus niger* microsomes upon D-xylose induction

José Miguel P. Ferreira de Oliveira, Mark W. J. van Passel,

Peter J. Schaap and Leo H. de Graaff

Appl Environ Microbiol (2010) **76**: 4421–4429

ABSTRACT

Protein secretion plays an eminent role in cell maintenance and adaptation to the extracellular environment of microorganisms. Although protein secretion is extremely efficient in filamentous fungi, the mechanisms underlying this process have remained largely uncharacterised in these organisms. In this study we analysed the effects of the D-xylose induction of cellulase and hemicellulase enzyme secretion on the protein composition of secretory organelles in *Aspergillus niger*. We aimed to systematically identify the components involved in the secretion of these enzymes via mass-spectrometry of enriched sub-cellular microsomal fractions. Under each condition, fractions enriched for secretory organelles were processed for tandem mass spectrometry, resulting in the identification of peptides that originate from 1,081 proteins, 254 of which – many of them hypothetical - were predicted to play direct roles in the secretory pathway. D-Xylose induction led to an increase in specific small GTPases known to be associated with polarised growth, exocytosis and endocytosis. Moreover, the endoplasmic-reticulum-associated degradation (ERAD) components Cdc48 and all of the fourteen 20S proteasomal subunits were recruited to the secretory organelles. In conclusion, induction of extracellular enzymes results in specific changes in the secretory sub-proteome of *A. niger* and the most prominent change found in this study is the recruitment of the 20S proteasomal subunits to the secretory organelles.

INTRODUCTION

Aspergillus niger is a soil-dwelling filamentous fungus with a high capacity for decomposing plant materials. Many of the secreted depolymerising enzymes have important biotechnological applications, e.g. to modify plant-derived food products. Homologous protein secretion in filamentous fungi may yield up to 20 g (protein) per litre of extracellular medium (Finkelstein 1987). For this reason *A. niger* has been used intensively as cell factory for enzyme production (Finkelstein 1987; Archer et al. 2008; Lubertozzi and Keasling 2009). In contrast to this, yields are much lower for heterologous protein secretion, with exceptions (Dunn-Coleman et al. 1991; Gouka et al. 1997; Ward et al. 1997; Moralejo et al. 2001).

The secretory potential of *A. niger* is not well understood, and only a limited number of functional studies have been performed to investigate the major components of the fungal secretion pathway. These studies have addressed overall transcriptional and translational responses in *A. niger*, by studying the impact of secretion-stress inducing chemicals, temperature shifts, protein overproduction or growth on carbon sources that induce changes in secretory states (Guillemette et al. 2007; Jacobs et al. 2009; Jørgensen et al. 2009).

In recent years, high-throughput shotgun proteomics has been used to study cell organelle make-up and function. Through the combined use of liquid chromatography and tandem mass spectrometry (LC-MS/MS), various studies have identified many organelle-specific proteins, including proteins related to protein secretion (Gouka et al. 1997; Wu et al. 2004; Jacobs et al. 2006; Kislinger et al. 2006; Štefanić et al. 2006). In the case of aspergilli, such studies have focused mainly on the secretome and not on the actual components of the secretory pathway (Medina et al. 2005; Oda et al. 2006; Tsang et al. 2009).

In a previous study we established defined culture conditions for the induced expression of the cellulase and hemicellulase enzyme system of *A. niger* (van der Veen et al. 2009). The expression of the corresponding genes is controlled by the dedicated transcriptional activator XlnR and its inducer D-xylose (van Peij et al. 1998a). Using identical conditions with a different strain of *A. niger*, we applied shotgun proteomics for

the analysis of enriched microsomal fractions, containing endoplasmatic reticulum (ER) membranes with associated ribosomes and Golgi membranes. The microsomal fractions were isolated either from D-xylose induced or from D-sorbitol non-induced mycelium. Following this approach, we were able to identify major protein components of the secretory organelles and to estimate their relative abundances in enriched microsomal samples.

RESULTS

Global protein analysis of the secretory machinery of *A. niger*

Shotgun proteomics was applied to analyse the secretory machinery of *A. niger* under induction of secretion, i.e., induction of cellulases and hemicellulases by D-xylose. For each of the two conditions, addition of D-xylose (induced) or D-sorbitol (non-induced), biological duplicates were taken and proteins from different pooled gradient fractions were analysed (Fig. 1) to increase the resolution similarly to previous studies (Gilchrist et al. 2006; Kislinger et al. 2006). Overall, between 32,000 and 50,000 MS/MS spectra were obtained per condition and 25 to 30% of these spectra could be assigned to proteins. In total, 1081 proteins were identified: 638 proteins were present under both conditions, 282 proteins were found only in the D-xylose-induced samples and 161 proteins exclusively in the samples from sorbitol addition. A protein database is available for *A. niger* CBS120.49, the strain used in this work (Sun et al. 2007). However, despite the improved annotation, many open reading frames (~5,672) lack a translation start resulting from errors in the genome sequence. Although not fully identical to the strain used in our laboratory the *A. niger* CBS513.88 genome-derived database was used, since from this genome an additional 3,000 proteins are predicted compared to the other high-coverage genome-sequenced strains such as *A. niger* ATCC1015 (Baker 2006). For a limited number of spectra, no proteins could be matched to the CBS513.88 proteome and the *A. niger* ATCC1015 database was used in these cases. The proteins identified in this way were included in this study (Appendix II: Supplementary Table S1, columns “XYL” and “SORB”). Upon initial curation, the total number of peptides per condition (D-xylose or D-sorbitol) could be primarily divided in the following manner:

i) related to membrane traffic and protein secretion, 26%;
ii) mitochondrial, 15%;
iii) ribosomal and translation, 13%;
iv) metabolism, 13%;
v) lipid biosynthesis and cytochrome P450 enzymes, 10%;
vi) cargo proteins, 5%;
vii) nuclear, 3%;
viii) other functions or unknown, 15%.

Proteins from non-secretory organelles, i.e., the nucleus and the mitochondrion, are given in another table (Appendix II: Supplementary Table S2).

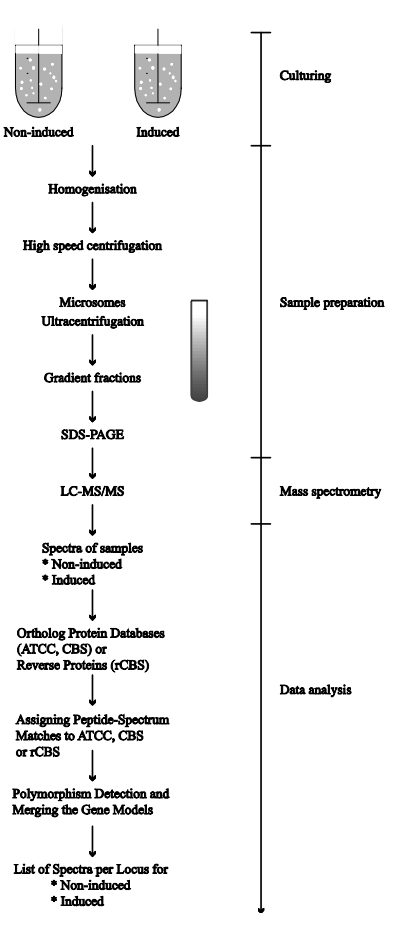

Figure 1. Workflow of the sub-cellular organelle sample preparation and data analysis.

Many secretion components in *A. niger* are highly similar to mammalian proteins. Many of the membrane traffic and secretion components identified were found to be more similar to mammalian than to yeast proteins (Appendix II: Supplementary Tables S3 to S6, boldface). These proteins (Fig 2) were predicted to be involved in:

i) N-glycan biosynthesis and transfer to asparagine in glycosylated target proteins;
ii) ER to Golgi anterograde and retrograde transport;
iii) processes mediated by Rab GTPases and interacting factors;
iv) microtubule-related processes;
v) early checkpoints of the ER associated degradation (ERAD) pathway.

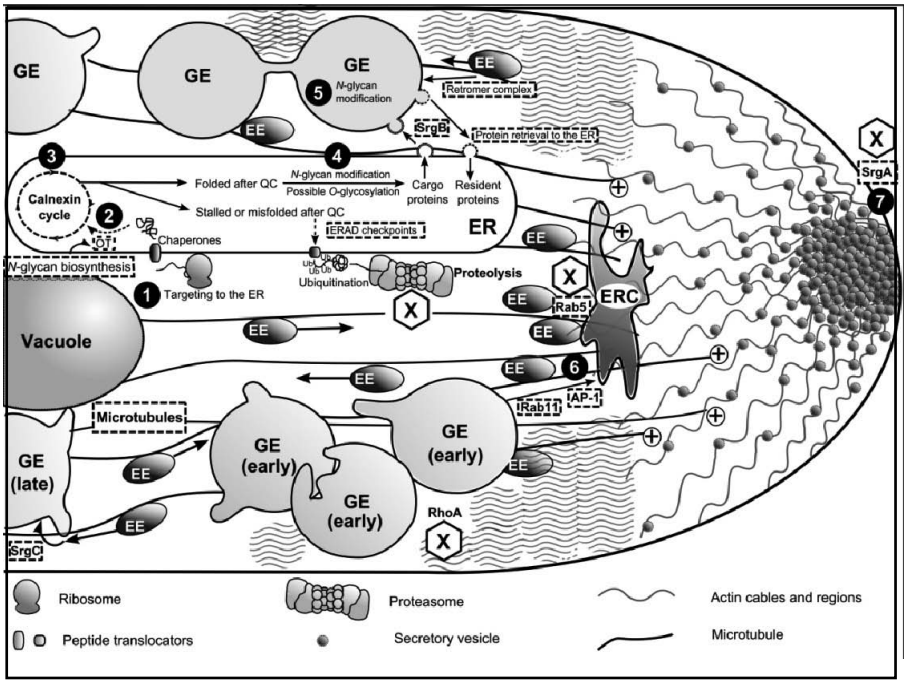

Figure 2. Secretory processes controlled by mammalian-like proteins in *A. niger*. The dashed arrows and text boxes indicate processes that are carried out by a majority of proteins more similar to human than to yeast proteins. 1: peptide biosynthesis and translocation to the ER; 2: addition of N-glycan; 3: glycoprotein folding; 4: N- and O-glycosylation: 5: N-glycosylation after transport to Golgi equivalents (GEs); 6: protein sorting and formation of secretory vesicles; 7: vesicle fusion with the plasma membrane; EE: early endosomes; ERC: endosomal recycling compartment; OT: oligosaccharyltransferase complex; QC: quality control; X: proteins abundant after D-xylose induction.

Furthermore, proteins, such as UDP-glucose:glycoprotein glucosyltransferase, were found to be much more similar to human than to yeast counterparts, particularly at the catalytic core (Appendix I: Figure S1). In addition to that, we were able to detect five secretory pathway candidate proteins from *A. niger* which lacked a corresponding yeast homologue: a protein for utilisation of Dol-P-Mannose (An04g03130), a UDP-galactose transporter (An08g10400), a tetratricopeptide repeat domain 35 protein (54765, JGI), annexin AnxC3.1 (An02g05210) and a dynamin-related Ras GTPase (An06g02180).

Secretory pathway proteins of *A. niger*

From all proteins identified in this study, 254 proteins were predicted to play a direct role in membrane traffic and protein secretion (Appendix II: Supplemental Tables S3 to S6). The secretion-related proteins with the highest abundances identified in this study were molecular chaperones (e.g., PdiA and BipA), the structural molecules actin and tubulin, oligosaccharyltransferase subunits and small GTPases (Table 1). Of the 34 high-abundance proteins identified, 11 have been previously characterised (Table 1, boldface). What is more, 21 secretory pathway proteins were differentially expressed in microsomal samples after addition of D-xylose or D-sorbitol (Table 2). The secretion-related proteins over-expressed after D-xylose induction comprised the subunits of the 20S core particle of the proteasome, the ER retrotranslocation ATPase Cdc48, Gpi12 for glycosylphophatidylinositol (GPI) anchor biosynthesis, the GTPases RhoA, SrgA and a homologue of human Rab5C protein. For the D-sorbitol condition, the cyclophilin CypA and proteins involved in targeting to the ER were found to be more abundant in the microsomal fractions.

D-Xylose induction leads to 20S proteasome recruitment to the microsomal fraction. In a previous study we analysed transcript levels resulting from D-xylose induction by microarray analysis (van der Veen et al. 2009). In this data set, no significant change was found in the transcript levels of the gene encoding the 20S core particle of the proteasome. Since the strain used in our previous study was derived from the *A. niger* CBS 120.49, we determined whether the significant increase in abundance of 20S proteasome complex proteins under the secretion-induced condition was a result of increased transcription levels. For this, we compared by QPCR the transcription levels of three

distinct types of genes: the D-xylose reductase gene (*xyrA*), which is strongly induced by D-xylose (Hasper et al. 2004); the vacuolar serine proteinase C gene (*pepC*), which is stably transcribed under a wide range of conditions (Jarai et al. 1994); and the homologues of the yeast genes *PRE7* and *CDC48*.

Table 1. Most abundant secretory pathway proteins. XYL.: D-xylose addition; SORB.: D-sorbitol addition, NSAF: normalised spectral abundance factor; ARF: ADP-ribosylation factor; Dol-P: dolichyl-phosphate; GEF: guanine nucleotide exchange factor; OT: oligosaccharyltransferase; SRP: signal recognition particle; UGPase: UDP-glucose pyrophosphorylase; boldface: characterised genes.

A. niger	Yeast	Specific Process and Function	NSAF·10^4	
			XYL	SORB
An02g14800	PDI1	Protein disulfide isomerase PdiA: disulphide bond formation	59	75.6
An07g09990	SSA4	Hsp70 protein: involved in SRP-dependent targeting to the ER	40	72.5
An11g04180	KAR2	ER ATPase BipA: protein import, protein folding, regulates the unfolded protein response (UPR) via Ire1, role in karyogamy	52.7	71.8
An07g08300	CPR1	Peptidyl-proline cis-trans isomerase CypA: cyclophilin	32.7	65.1
An17g01420	YOP1	Membrane protein: Yip1 interaction; ER tubular morphology	40	56.2
An15g00560	ACT1	Actin structural protein ActA: cell polarity, endocytosis	42.1	53.8
An07g04570	HYP2	HexA protein: assembly of Woronin body	28	50
An09g06590	HSC82	Hsp90 chaperone SspB: nearly identical to Hsp82	38.7	46.9
An01g08420	CNE1	ER chaperone calnexin ClxA: folding and QC of glycoproteins	46.4	42.4
An07g04190	WBP1	OT complex β subunit (essential)	38	42.3
An02g14560	OST1	OT complex α subunit OstA: ribophorin I (essential)	35.7	41.1
An01g04040	SAR1	ARF GTPase SarA: ER to Golgi vesicle formation	26.2	39.2
An04g02020	CPR1	ER peptidyl-prolyl cis-trans isomerase CypB: cyclophilin	41.3	37.4
An01g12810	YET3	Mutant decreases level of secreted invertase	20.7	34.6
An08g03190	TUB2	Structural protein β-tubulin TubB: forms dimers with α-tubulin	29.3	34.1
An18g05980	RHO1	Ras GTPase RhoA: Rho subfamily, involved in cell polarity	61.2	33
An18g02020	PDI1	Protein disulfide isomerase TigA: S-S bonds	25.9	33
An04g02070	CHC1	Structural molecule: clathrin heavy chain	15	31.4
An07g07760	BMH1	14-3-3 protein similar to ArtA: exocytosis, Ras/MAPK signalling	29.5	30.5
An18g06270	BMH2	1 14-3-3 protein ArtA: exocytosis, Ras/MAPK signalling	28.8	30.1
An09g05880	ROT2	ER glucosidase II α subunit: removal of 2 glucose residues	28.9	27.6
An01g04600	MPD1	Protein disulfide isomerase PrpA: N-terminus similar to Mpd1	26.2	26.6
An04g07440	SHR3	ER packaging chaperone: incorporation of amino acid permeases into COPII coated vesicles	15.5	26.4
An16g04330	DPM1	ER Dol-P β-D-mannosyltransferase: required for O-mannosylation	23.9	26
An05g00140	SRP102	SRP receptor β subunit, anchors Srp101 to the ER membrane	11.6	25.6
An01g03820	SBH2	GEF for ARFs: protein translocation to the ER	7.8	25.6
An09g06790	YPT1	Rab GTPase SrgB: ER to Golgi traffic	21.1	24
An12g00820	UGP1	UGPase: Glc-1-P + UTP <-> UDP-Glc	26.5	23.2
An01g02500	TRX1	Thioredoxin: ER-Golgi transport and vacuole inheritance	9.2	22.9
An03g04340	SEC61	ER protein targeting, P-P-bond-hydrolysis-driven transporter	12.3	22.1
An01g06060	YPT31	Rab GTPase: intra-Golgi traffic, budding of post-Golgi vesicles	24.4	21.6
An15g05740	YPT6	Rab GTPase SrgC: fusion endosomal vesicles with the late Golgi	15.1	20.5
An08g04480	SEY1	Dynamin GTPase: ER morphology	19.9	20.2
An01g13220	LHS1	ER nucleotide exchange factor for Kar2/BipA (LhsA): UPR-regulated translocation/ folding	22.1	20.2

Table 2. Relative abundance of secretion-related proteins in microsomes after addition of D-xylose or D-sorbitol. Normalised spectral abundance factors were compared by a G-test (p<0.05). SRP: signal recognition particle.

Over-represented in microsomes	Locus Tag	Description	G-Score
D-Xylose addition			
	An18g06700	Pre7 20S CP β subunit of the proteasome	26.20
	An04g09170	Cdc48 retrotranslocation ATPase	20.47
	An15g00510	Pre5 20S CP α subunit of the proteasome	16.83
	An02g10790	Pre6 20S CP α subunit of the proteasome	11.95
	An11g06720	Pre9 20S CP α subunit of the proteasome	9.91
	An05g02300	Gpi12 ER protein: GPI anchor assembly	9.47
	An02g07040	Scl1 20S CP α subunit of the proteasome	9.23
	An18g05980	RhoA Ras GTPase: cell polarity	8.56
	An18g06800	Pre10 20S CP α subunit of the proteasome	8.52
	An07g02010	Pre8 20S CP α subunit of the proteasome	8.36
	An02g03400	Pup2 20S CP α subunit of the proteasome	7.48
	An04g02470	Rab5-like GTPase: endocytosis, protein sorting	6.39
	An14g00010	SrgA Rab GTPase: exocytosis	5.70
D-Sorbitol addition			
	An07g08300	PPIase CypA: cyclophilin	10.95
	An01g03820	Shb2/Sbh1: protein translocation to the ER	9.99
	An07g09990	Ssa4/3/1/2: SRP-dependent targeting to the ER	9.49
	An07g04570	HexA protein: assembly of Woronin body	6.31
	An01g02500	Thioredoxin: ER-Golgi transport	6.05
	An04g02070	Clathrin heavy chain: structural	5.91
	An05g00140	SRP receptor β subunit: binds Srp101 to the ER	5.45
	202202 (JGI)	Sac6 actin-bundling protein	4.13

The corresponding proteins Pre7 and Cdc48 showed the largest difference in relative protein abundance in microsomes under the xylose-induced condition compared to the sorbitol control condition (Table 2). However, the transcript levels for the *A. niger* homologues of yeast *PRE7* and *CDC48* were identical under xylose-induced and sorbitol control conditions (Fig. 3). In contrast to this and as expected, the transcript levels of the xylose reductase gene were strongly increased in the presence of D-xylose, while there was no significant change in the transcript levels of *pepC*.

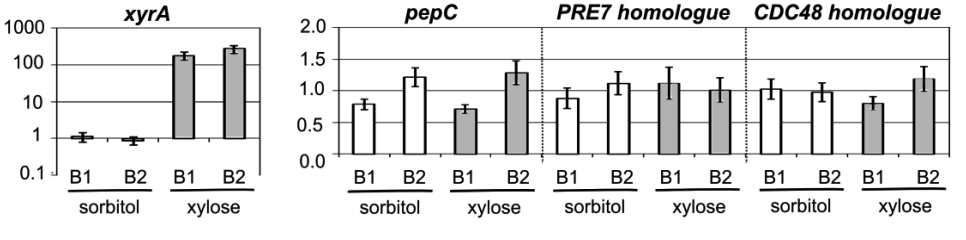

Fig. 3. Relative gene expression of the *A. niger* homologues of the yeast genes *PRE7* and *CDC48*.
B1: biological replicate 1; B2: biological replicate 2. Relative levels of *xyrA* transcripts are given in logarithmic scale. Bars represent the mean relative gene expression ± SE.

DISCUSSION

Protein secretion is a fundamental feature of filamentous fungi that is strongly related to the fungal saprophytic lifestyle. Hyphal growth requires coordination of protein secretion with cell wall synthesis, polarised growth, recycling by endocytosis, and transport of extracellular hydrolytic enzymes. Ironically, protein secretion in the kingdom *Fungi* has been best described for typically modest secretors, such as the yeast *S. cerevisiae*. Thus, compared to yeast, more sophisticated secretory mechanisms exist in the protein secretor *A. niger*. Here, we aimed to identify candidate microsomal proteins involved in intracellular membrane traffic and protein secretion upon cellulase and hemicellulase induction by D-xylose.

In order to decrease false-positive identifications of peptides, experiments have been done in duplicate and a conservative criterion was applied for peptide identification (at least 2 unique peptides in one of the biological samples and another unique peptide in the replicate), resulting in the identification of 30% of ~40,000 MS peptide spectra per condition. Organelle isolation is prone to contamination by cell components other than the target organelle as has become clear after the use of sensitive methods such as mass spectrometry (Huber et al. 2003; Lilley and Dupree 2007). Apart from technical challenges, other factors may obscure shotgun proteomic analyses, such as the multiple localisation of a given protein or the direct physical interaction of target organelles with other organelles or intracellular structures (Rusinol et al. 1994; Rizzuto et al. 1998; Mannella 2006).

Despite these limitations, we were able to identify key components of the secretory pathway of *A. niger* and to estimate their relative abundance. With regard to the relative abundance in microsomal samples, only 11 of the 34 most abundant protein components found have been previously characterised or described for *A. niger* (Table 1, boldface). Besides ranking high-abundance proteins, NSAF calculation also allows the estimation of the stoichiometry of protein subunits in protein complexes. Many protein complexes in *A. niger* were found present with the same stoichiometry as the ones observed in yeast protein complexes *in vivo* (Table 3).

Table 3. Secretory pathway and membrane traffic protein complexes identified in this study and protein subunit relative abundance. XYL.: D-xylose addition; SORB.: D-sorbitol addition, OT: oligosaccharyltransferase; n.d. not detected; *: *Saccharomyces cerevisiae* Ost4 is 36 amino acids long and therefore too small for the 10kD cutoff used in this study

Complex	Yeast	*A. niger*	NSAF · 10^4		Reference
			XYL.	SORB.	
Sec62-Sec63	Sec63	An01g13070	14.8	16.9	Feldheim et al. 1993
	Sec66	An16g08830	16.4	19.8	
	Sec62	An02g01510	9.1	14.3	
OT subcomplexes	Stt3	An16g08570	15.7	11.4	Karaoglu et al. 1997
	Ost3	An02g14930	15.3	8.2	
	Ost4*	An08g07485 (N-terminus)	n.d.	n.d.	
	Ost1	An02g14560	35.7	41.1	
	Wbp1	An07g04190	38.0	42.3	
Sec23-Sec24 heterodimer	Sec23	An01g04730	4.1	9.0	Fath et al. 2007
	Sec24	An08g10650	6.6	6.4	
p24	Emp24	An08g03590	17.3	12.2	Belden and Marlowe 1996
	Erv25	An01g08870	22.7	16.7	
Erv41-Erv46	Erv41	An03g04940	11.1	7.5	Otte et al. 2001
	Erv46	An01g04320	14.9	12.5	
AP-1 adaptor	Apl2	An16g02490	0.8	2.6	Yeung et al. 1999
	Apm1	An07g03200	1.5	2.8	
	Apl4	An01g02600	1.4	2.6	
Retromer complex inner shell	Pep8	An01g07320	4.4	9.2	Seaman et al. 1998
	Vps29	An08g01030	5.1	10.0	
	Vps35	An16g04270	9.5	11.3	
Chaperonin-containing T-complex	Tcp1	An15g06370	n.d.	n.d.	Kabir et al. 2005
	Cct2	An01g06480	1.2	1.2	
	Cct3	An02g08920	n.d.	n.d.	
	Cct4	An02g12750	1.2	2.2	
	Cct5	An11g02360	n.d.	n.d.	
	Cct6	An16g03100	n.d.	n.d.	
	Cct7	An18g05770	1.0	0.2	
	Cct8	An04g07340	n.d.	n.d.	

These protein complexes are predicted to be involved in a diversity of biological processes, namely in:

i) protein targeting to the ER by the Sec63-Sec66-Sec62 complex;

ii) addition of N-glycan to protein by the oligosaccharyltransferase complex;

iii) ER to Golgi transport by Sec23-Sec24, Emp24-Erv25 and Erv41-Erv46 complexes;

iv) Golgi protein sorting by the Apl2-Apm1-Apl4 complex;

v) endosome to Golgi transport by the Pep8-Vps29-Vps35 complex.

On the other hand, one protein complex was not completely identified in this study. This complex, termed chaperonin-containing T-complex (CCT), is required in yeast for the cytosolic assembly of actin and tubulins *in vivo*. This discrepancy could be the result of selective peptide picking during MS, incorrect gene models to identify peptides, different stoichiometry in *A. niger* or under-sampling, as the NSAF values of the identified CCT subunits were low compared to the NSAF values of the aforementioned protein complexes found with the expected stoichiometry. Moreover, we were unable to detect a few other protein complexes predicted to play a role in membrane traffic or protein secretion in *A. niger*, such as the HOPS complex for vacuole fusion and vacuole protein sorting, the GARP complex for traffic from the early endosome to the late Golgi, the ESCRT endosomal sorting complexes, and the Exocyst complex for targeting of vesicles to active sites of exocytosis. It is possible that these complexes are either rarely occurring in secretory organelles in *A. niger* or that they are more present in vesicle subpopulations that were incompletely covered during organelle enrichment procedures.

In *A. niger* specific secretory processes are carried out by proteins more similar to mammalian proteins than to yeast proteins, a phenomenon that has been reported for filamentous fungi in general (Braun et al. 1998; Kruszewska 2000). For example, most *A. niger* Rab GTPases identified here show higher similarity to mammalian than to yeast proteins. Since these proteins are involved in vesicle transport and fusion, it is very likely that this similarity to mammalian proteins would explain some fundamental differences in protein secretion of yeast and *A. niger*. Moreover, the controlled interplay between exo- and endocytosis is thought to be necessary for adequate polarised growth in filamentous fungi and this interplay must in part be determined by the primary sequence of secretory pathway proteins.

In addition to the differences in terms of protein sequence in comparison to yeast, this study also reveals important changes in the composition of the secretory pathway that may be explained by different relative protein abundances in secretory organelles. During induction of cellulase and hemicellulase secretion by D-xylose hydrolytic enzymes are efficiently synthesised and exported from the cell. These enzymes include proteins previously reported to be significantly up-regulated by D-xylose induction, namely β-xylosidase, a protein similar to bacterial xylosidase S (AxlA, An09g003300), and β-glucosidase (van der Veen et al. 2009). From the current study it becomes clear that in addition to bringing changes in the amount of cargo hydrolytic enzymes, the presence of D-xylose also promotes changes in the relative protein abundance of specific components

within the secretory organelles. Unexpectedly, proteins involved in targeting to the ER or quality control of protein glycosylation and folding were not over-represented after D-xylose induction. On the contrary, these proteins were in some cases even under-represented in comparison to the non-induced state of D-sorbitol addition. In this study it was found that D-xylose induction is associated with an increase of three GTPases that are predicted to play roles in endocytosis, exocytosis and polarised growth, and with an increase of specific components of protein degradation pathways. With regard to the three over-expressed GTPases, the RhoA and SrgA GTPases have been described as necessary for polarised growth and proper hyphal branching (Olivo et al. 2000; Punt et al. 2001; Guest et al. 2004; Asanuma et al. 2006), whereas Rab5 is known to play a role in early endocytosis in eukaryotes (Braun et al. 1998; Chen et al. 2009). This important role in endocytosis has also been investigated recently in *Aspergillus* (Abenza et al. 2009). From the study of Abenza and co-workers, it has become clear that Rab5-rich endosomes cycle rapidly along the hyphal cell in a microtubule-dependent manner. It is plausible that an increased state of protein secretion such as induction by D-xylose in *A. niger* increases the number of Rab5-rich early endosomes, thereby facilitating exchange of material with the Golgi equivalents and the hyphal tip. One observation that confirms this hypothesis is that Golgi equivalents in *Aspergillus* are relatively slow in motion and are usually found in a gradient across the hyphal cell, more concentrated near the hyphal tip but excluded from the apical body (Taheri-Talesh et al. 2008; Pantazopoulou and Peñalva 2009).

Previous microarray analyses investigated the effects of D-xylose on the transcriptome of *Aspergillus* species and linked it to metabolic pathways or cellular processes (Andersen et al. 2008; Jørgensen et al. 2009; Panagiotou et al. 2009; van der Veen et al. 2009). In our study, and in agreement with the above-mentioned transcriptome studies, at the proteome level D-xylose induction did not affect the microsomal abundance of most proteins belonging to the ERAD pathway. However, the presence of D-xylose did increase the protein microsomal abundance of Cdc48 homologue and the proteasomal 20S CP. Since there was no increase in the transcription levels of the proteasomal 20S CP both previously by microarray analysis of a daughter fungal strain (van der Veen et al. 2009) and in this study by QPCR, this strongly suggests that these proteins are recruited and that they can attach and detach from microsomes according to the cell's needs.

This study shows different strategies that *A. niger* undertakes when forced into a secretory state. Some functional routes of the cell's metabolism show differences

between induced and non-induced states via different gene expression profiles, like the cargo proteins, followed by changes in the protein abundances. In other cases, no change was found in the transcriptional status of the organism, and changes in the protein abundance in the secretory organelles can be attributed to specific recruitment of functional complexes (e.g., the proteasome). Together, this shows that secretion is a dynamic and interacting process, several aspects of which can be studied using proteomic analyses.

MATERIAL AND METHODS

Strain and culture conditions

The fungal strain used in this study was *A. niger* wild type N400 (CBS 120.49). For pre-culture, 1.0 x 10^6 spores per millilitre were inoculated into 2.5-litre fermentors (Applikon) containing 2.2 litres of minimal medium (Pontecorvo et al. 1953) with 0.05% yeast extract and 100 mM D-sorbitol at 30°C. Spore germination in bioreactors was as described previously (van der Veen et al. 2009), with headspace aeration and a stirring speed of 300 rpm; when dissolved D-oxygen levels were below 60%, the stirring speed was increased to 750 rpm and aeration was switched to the sparger inlet. This moment was defined as the actual culture starting point (t = 0 h). At 14h from the starting point, D-xylose or D-sorbitol (10 mM) was added to each culture and at t = 16 h mycelia were harvested.

Sub-cellular fractionation and marker enzyme assays

Sub-cellular fractionation was based on the work of Record and co-workers (1998) with important modifications. Mycelia were harvested by Büchner filtration on nylon gauze and were washed with sterile cold 0.25 M sucrose. From that moment until storage of the samples all procedures were conducted at 4°C. Mycelia were press dried and 6 g of mycelial sample corresponding to each of the two conditions (addition of D-xylose or D-sorbitol) was added to 80 ml of homogenisation buffer (0.25 M sucrose, 1 mM EDTA, 20 mM HEPES, pH 7.6) containing 1% (vol/vol) protease inhibitor cocktail (Sigma-Aldrich, St. Louis, MO). Cells were disrupted by French press cell homogenisation at 3,000 lb $\cdot$ in^{-2} (20.6 MPa). The resulting homogeneous suspension was filtered through two layers of

nylon gauze and the homogenate suspensions (60 ml per condition) were centrifuged at 6,500 × g for 15 min. The supernatants were centrifuged at 29,000 × g for 18 min. The mitochondrial pellets were resuspended in 2 ml of homogenisation buffer with protease inhibitors and the supernatants were centrifuged at 100,000 × g for 1 h 12 min. The microsome-enriched pellets were resuspended in 2 ml of 0.4 M sucrose, 1 mM EDTA, 20 mM HEPES, pH 7.6 in a Dounce homogeniser (10 gentle strokes with loose piston), and 200 µL of these suspensions (1 mg protein) was loaded onto each linear 9-ml buffered sucrose gradient (1 mM EDTA, 20 mM HEPES, pH 7.6; densities 1.06 to 1.17 $g \cdot ml^{-1}$) and centrifuged at 130,000 × g for 13 h 42 min at 4°C. Fractions of 360 µL were collected and samples were stored at –80°C until further processing was done. Protein concentrations were estimated using the Bradford method (Bradford 1976) with bovine serum albumin as standard. The NADPH-cytochrome c reductase assay, as a marker enzyme for microsomes, was done using a commercially available kit (Sigma-Aldrich, St. Louis, MO) according to the manufacturer's instructions.

Sample preparation for LC-MS/MS.

Enriched microsomal fractions from ultracentrifugation were pooled in two groups according to density (one of higher density and one of lower density) and loaded onto Microcon YM-10 columns (cut-off, 10 kD; Millipore, Eschborn, Germany). The concentrated enriched samples were run on 12% SDS polyacrylamide gels and the gels were stained according to the manufacturer's instruction using Colloidal Blue Staining (Invitrogen, Carlsbad, CA, USA). Each gel lane was cut into five slices; the slices were cut into smaller pieces of about 1 mm^3, washed with ultra-pure water and 50% acetonitrile in 50 mM NH_4HCO_3, pH 8.0. The gel samples were reduced with 50 mM dithiothreitol (DTT) in 50 mM NH_4HCO_3, pH 8.0, for 2 h at 60°C. Subsequently, the DTT solutions were removed and samples were alkylated with 100 mM iodoacetamide in NH_4HCO_3, pH 8.0 for 1 h at room temperature in the dark with occasional mixing. The iodoacetamide solutions were removed and samples were washed with NH_4HCO_3, pH 8.0. Gel pieces were frozen at –20°C and thawed at least three times to increase the accessible area for trypsin digestion. All gel pieces were rehydrated in 25 $ng \cdot \mu l^{-1}$ trypsin (Sequencing grade modified trypsin, Promega, Madison, WI) and digested overnight at room temperature. In order to maximise peptide extraction, all solutions from trypsin digestion were transferred to new tubes, and gel pieces were subjected to two rounds of 1 min of sonication, the first round

with 10% trifluoroacetic acid (TFA) and the second round with 5% acetonitrile, 1% TFA. After each of these two rounds, the solutions were removed and added to the original trypsin digests. Final pH was adjusted to 2.5 by addition of 10% TFA.

Liquid chromatography tandem mass spectrometric analysis

LC-MS/MS was performed at Biqualys, as described previously (van Esse et al. 2008). Briefly, samples were loaded on a pre-concentration column and peptides were eluted to an analytical column with an acetonitrile gradient and a fixed concentration of formic acid. The resulting eluent was subjected to an electrospray potential via a coupled platinum electrode. MS spectra were measured on an LTQ-Orbitrap (Thermo Electron, San Jose, CA) and MS scans of four most abundant peaks were recorded in data-dependent mode.

Mass spectrometry database searching

The resulting spectra from the MS analysis of the *A. niger* samples were submitted to a local implementation of the open mass spectrometry search algorithm (OMSSA) search engine (Geer et al. 2004). MS/MS spectra were independently searched against peptide databases derived from the predicted proteomes of *A. niger* strain CBS513.88 and strain ATCC 1015, and a decoy reverse database constructed from the reverse CBS513.88 proteome (rCBS).

All OMSSA searches used the following parameters: a precursor ion tolerance of 0.2 Da, fragment ion tolerance of 0.3 Da, a missed cleavage allowance of up to and including 2, fixed carbamide methylation, variable oxidation of methionine and deamination of glutamine and asparagine.

The E value threshold was determined iteratively from the false discovery rate (FDR) and was set to 0.01. With this setting an FDR of <5% is expected. FDR calculation was done as follows. Peptide-spectrum matches with each individual peptide database were ranked by their E values for each identified spectrum with a threshold E value < 0.01 and the top hit identified peptide sequence was selected. For FDR calculation, top hit spectral matches to peptides in the reversed database were taken and the number of false positives was divided by the number of total positives.

Functional annotation groups and sequence analysis

Proteins predicted to play a role in secretion were grouped in functional annotation groups guided by previously published functional classification schemes (Geysens et al. 2009), the Functional Catalogue (FunCat) annotation scheme and the predicted molecular function as provided with the *A. niger* CBS 531.88 genome annotation (Pel et al. 2007). Proteins considered to be involved in secretion were used for a BLAST search (NCBI) against *Saccharomyces cerevisiae* and *Homo sapiens* protein databases. Only the yeast and human reference sequence proteins which presented the lowest E values and highest percentages of positives were included in this study. Protein similarity analyses were done using the ClustalW and Jalview version 2 tools (Thompson et al. 1994; Waterhouse et al. 2009). Transmembrane domains (TMD) were assessed using the TMHMM tool (Sonnhammer et al. 1998).

Relative protein abundance and statistics

A normalised spectral abundance factor was used as a parameter to estimate relative protein abundance using the following equation (Zybailov et al. 2006):

$$(\mathrm{NSAF})_k = \frac{(\mathrm{SpC/L})_k}{\sum_{i=1}^{N} (\mathrm{SpC/L})_i}$$

where $(\mathrm{NSAF})_k$ is the normalised spectral abundance factor for a protein k, SpC is the number of spectral counts (total number of MS/MS spectra) for a given protein plus a pseudo-count factor of 0.5, and L is the protein's length. The pseudo-count was necessary to analyse differential distribution of secretion-related proteins between the two conditions (addition of xylose or sorbitol). For the proteins predicted to be involved in secretion, significant differences in NSAF values were evaluated by applying a likelihood ratio test (G-test) for independence using a null hypothesis of equal protein distribution between the two conditions.

QPCR

RNA isolation, cDNA synthesis, quantitative real-time PCR (QPCR) and data analysis were performed as described previously (Oliveira et al. 2008). In brief, total RNA was extracted, quantified and mixed with an exogenous RNA reference transcript. After enzymatic DNA degradation, oligo(dT)-mediated cDNA synthesis was performed. QPCR was performed using QPCR SYBR Green Mix (ABgene, Epsom, UK) and specific oligonucleotide primers (Table 4).

Table 4. Oligonucleotide primers used for QPCR. *xyrA*: D-xylose reductase; *pepC*: serine proteinase; *PRE7* and *CDC48* refer to the *S. cerevisiae* genes encoding the β6 subunit of the 20S proteasome and the ER retrotranslocation ATPase, respectively. The control exogenous transcript is an added RNA transcript for kanamycin/neomycin resistance.

Target gene or transcript	Forward primer (5'-3')	Reverse primer (5'-3')
xyrA (An01g03740)	TCGAGTTGAGTGTGCAGAATG	ACTCTTGGGGATAACAGCAATC
pepC (An07g03880)	TCTGGCACCATGTCTGATGT	CCCTTGAATCCCTTGACCTT
homologue of yeast *PRE7* (An18g06700)	GCTTGGACGAGGATGGTAAG	ATCCAGGAACGGCATGATAA
homologue of yeast *CDC48* (An04g09170)	TGTGCTGCCAACTTCATCTC	ATCCAGGAAAACAACGCAAG
control exogenous transcript	AGCATTACGCTGACTTGACG	AGGTGGACCAGTTGGTGATT

Two independent PCR runs were performed per cDNA sample from each biological sample (D-xylose or control D-sorbitol addition). The Pfaffl method (2001) was used to calculate relative gene expression levels double-normalised to the added exogenous RNA transcript and to the standard condition, i.e., the average normalised expression of the two biological samples from the D-sorbitol control condition.

Acknowledgements

MWJvP is funded by the Netherlands Organisation for Scientific Research (NWO) via a VENI grant.

Chapter 5

Proteomic analysis of the secretory response of *Aspergillus niger* to D-maltose and D-xylose

José Miguel de Oliveira, Mark W. J. van Passel, Peter J. Schaap and Leo H. de Graaff

Submitted for publication

ABSTRACT

Fungi utilise polysaccharide substrates through extracellular digestion catalysed by secreted enzymes. Thus far, protein secretion by the filamentous fungus *Aspergillus niger* has mainly been studied at the level of individual proteins, and by genome and transcriptome analyses. To extend these studies, a complementary proteomics approach was applied here. During growth of *A. niger* on D-sorbitol, small amounts of D-maltose or D-xylose were used as inducers of specific sets of extracellular enzymes. Upon induction, protein compositions in the extracellular medium as well as in enriched secretory organelles (microsomes) were analysed using a shotgun proteomics approach.

In total 102 secreted and 1,126 microsomal proteins were identified. Both D-maltose and D-xylose resulted in the increase of specific extracellular enzymes as well as of microsomal proteins. In addition, the induction of extracellular enzymes was confirmed at the gene expression level, e.g. glucoamylase A on D-maltose, and β-xylosidase D on D-xylose. D-Sorbitol had no effect on the expression of (hemi)cellulases or starch-degrading enzymes, compared to D-xylose or D-maltose. Furthermore, D-maltose addition caused an increase in microsomal proteins related to translation (*e.g.* Rpl15) and vesicular transport (e.g. the endosomal-cargo receptor Erv14). Finally, D-maltose increases the amount of mitochondrial proteins and the proteasome 20S core particle proteins which are associated with microsomes.

Micromolar amounts of inducers of protein secretion were sufficient to cause a direct response at the protein levels of dedicated enzymes. Furthermore, shortly after induction by D-maltose or D-xylose, the corresponding dedicated enzymes were found in microsomes and extracellularly. Finally, D-maltose induction increases the amount of microsomal proteins involved in proteasome-mediated degradation, energy production, vesicular transport including endosomal recycling and protein translation.

INTRODUCTION

Filamentous fungi are remarkable secretors of metabolites and hydrolytic enzymes, and this has granted them a prominent role in biotechnology (Archer et al. 2008). Many of the hydrolytic enzymes secreted by fungi have evolved to degrade the complex structure of plant cell wall (McCann and Carpita 2008). The most prominent enzymes that are secreted in the process of plant cell wall decomposition are hemicellulases (e.g. xylanases), cellulases, pectinases and proteases. These enzymes have been studied extensively at the biochemical and genetic level due to their economical interest. The enzymes are being applied as food and feed additives and are used in the saccharification of plant biomass for the production of bioethanol (Shimokawa et al. 2009).

In the ascomycete *Aspergillus niger* the biosynthesis of many extracellular enzymes is regulated at the transcriptional level. The transcription factors governing expression are either repressors, such as the common carbon-catabolite repressor CreA (Dowzer and Kelly 1991), or activators such as XlnR and AmyR that turn on the expression of genes encoding (hemi)cellulolytic enzymes in the presence of D-xylose (van Peij et al 1998a) and amylolytic enzymes in the presence of D-maltose (Petersen et al. 1999), respectively. Both the XlnR and the AmyR regulons are repressed by CreA in the presence of D-glucose.

Recent studies have made an effort in improving our understanding of the mechanisms via which extracellular enzymes and proteins in general are secreted in aspergilli. With the publication of the annotated genome of *A. niger* (Pel et al. 2007), many genes have been identified as genes related to protein secretion. Based on this annotation and on bioinformatics analyses, another study reports the candidate genes related to protein secretion in *A. niger*, with emphasis on the processes taking place in the endoplasmic reticulum (ER) (Geysens et al. 2009). In addition to bioinformatic *in silico* predictions of genes related to secretion, the transcriptional responses of *A. niger* were studied under a variety of conditions related to protein secretion, namely by the use of disruptors of protein glycosylation and folding in the ER (Al-Sheikh et al. 2004; Guillemette et al. 2007), or by comparison of strains overproducing specific proteins (Jacobs et al. 2009). From these studies it became clear that the unfolded protein response (UPR) together with individual proteins from the secretory pathway play an important role in secretion in *A. niger*. Moreover, the secretome of *A. niger* has been reported in two high-coverage proteomics studies. In a first study, *A. niger* was grown on different complex and defined media after which the secretome was compared with the proteins predicted to

contain a signal peptide (Tsang et al. 2009). From this work 222 secreted proteins were identified, some of them differentially present during cultivation on certain types of medium. In a second study, *A. niger* was grown either in shake-flasks or in a bioreactor, with D-xylose and D-maltose as carbon substrates, and the secretome was compared with the total proteome from cell extracts (Lu et al. 2010). From this study, it was concluded that *A. niger* responds in different ways to the utilisation of D-maltose and D-xylose and the spectrum of secreted proteins is very different between shake-flask and bioreactor cultivation. Also, the proteomic response occurs both intracellularly and at the level of secreted enzymes. Despite all the above-mentioned studies, the essential mechanisms underlying the high secretion capacity have not been fully elucidated.

We have recently initiated a proteomics approach to investigate potential differences in the secretome and the microsomal proteome of *A. niger* that are caused by low and high secretion growth conditions. Based on our previous studies (van der Veen et al. 2009; de Oliveira et al. 2010), the low secretion conditions result from fermentor-grown mycelium, using D-sorbitol as a carbon source. The high secretion conditions result from mycelial cultures to which D-xylose or D-maltose were added, thus inducing (hemi)cellulase or amylase secretion, respectively. A shotgun proteomics approach was used for the analysis of the protein fractions.

RESULTS AND DISCUSSION

Secretome and microsomal proteome of *A. niger*

Analysis of the secreted proteins from the culture filtrates of all three induction conditions using D-sorbitol, D-xylose and D-maltose resulted in the identification of 102 secretome proteins totally. Of these, 52 proteins (51%) are present in all three conditions (Fig.1A). We were not able to positively identify in the culture filtrate any of the major mycelial proteins of aspergilli described in previous studies (Lu et al. 2010; Vödisch et al. 2009). Yet, a few proteins were identified that lacked a recognisable signal sequence or were predicted to be located intracellularly. Since we did not analyse the total intracellular proteome of *A. niger* in this experiment, we cannot exclude the possibility that these proteins were released upon cell lysis and therefore they are presented in a separate table (Appendix II: Supplementary Table S7).

Analysis of the microsomal proteins after separation by SDS-PAGE and tryptic digestion in gel, resulted in the identification of 1,126 proteins, of which, 510 proteins (45%) were present in all three conditions (Fig. 1B). In *A. niger*, between 6 to 8% of the total proteins are predicted to contain a signal sequence (Tsang et al. 2009). Signal sequence predictions in our work indicated that 92% of the secreted proteins contain a signal peptide (Appendix II: Supplementary Table S8), whereas 25% of the microsomal proteins contain either a signal peptide or a signal anchor (Appendix II: Supplementary Table S1).

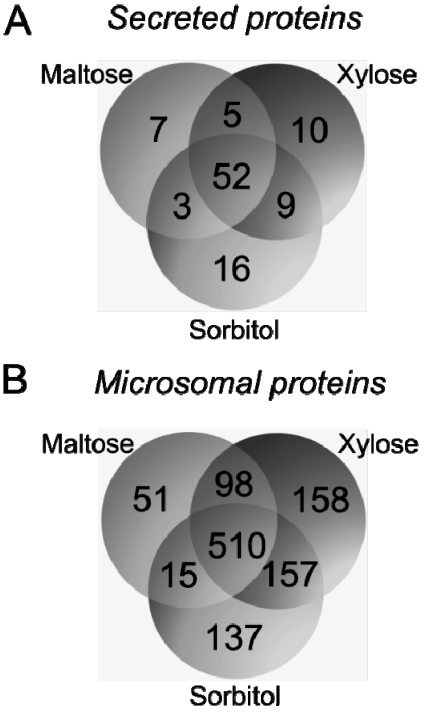

Figure 1. Venn diagrams of the identified *A. niger* proteins. (A) secreted proteins; (B) microsomal proteins. D-maltose, D-xylose, or D-sorbitol was added to *A. niger* cultivated on D-sorbitol.

Microsomal proteins were grouped in the following categories: i) membrane traffic and protein secretion, 23%; ii) mitochondrial, 13%; iii) translation, 12%; iv) metabolism and defense against reactive oxygen species, 12%; v) cargo proteins, 8%; vi) lipid biosynthesis, 8%; vii) transporters, 5%; and viii) others or unknown, 14%.

Secretome under amylolytic and (hemi)cellulolytic conditions

Proteins of the secretome were classified according to their predicted enzyme class (Appendix II: Supplementary Table S8), and the class distribution was determined for each condition. According to enzyme class, hydrolases represented about 60% of the secreted proteins, and as such this was the largest group in all three conditions (Fig. 2). Compared to the total number of proteins secreted, induction by D-xylose resulted in the highest percentage of secreted hydrolases. Growth on D-sorbitol gave rise to the highest percentage of non-enzyme secreted proteins, like an ortholog of *Schizosaccharomyces cerevisiae* cell wall protein Psu1, or a protein of unknown function (JGI37529). On the other hand, D-maltose addition was associated with the highest percentage of oxidoreductases identified in the culture filtrate. In a previous study in which *A. niger* was grown on D-maltose, it was observed that a number of oxidoreductases (e.g. catalases) were more highly expressed compared to growth on D-xylose (Lu et al. 2010). It was hypothesised that growth on D-maltose increased the amount of reactive oxygen species (ROS) formed extracellularly, compared to D-xylose, and this was accompanied by an increase in enzymes related to ROS. Our results are in line with these previously reported observations.

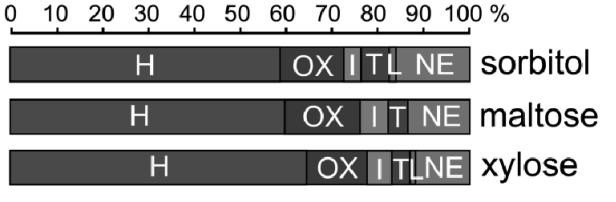

Figure 2. Enzyme class distribution of all secreted proteins. Bar size indicates percentage of enzymes of the total of secreted proteins detected for each condition. H: hydrolases; OX: oxidoreductases; I: isomerases; T: transferases; L: ligases; NE: non-enzyme proteins.

Each of the secreted proteins was also ranked according to a normalised spectral abundance factor (NSAF), which estimates the protein's relative abundance on the basis of the MS spectral counts and predicted protein length. The most abundant secreted proteins for all three experimental conditions used were the *A. niger* anti-fungal protein (ANAFP), the protease aspergillopepsin A (PepA) and the starch-degrading enzyme

glucoamylase A (GlaA). ANAFP is a homologue of *Penicillium* anti-fungal protein (PAF) from *Penicillium chrysogenum.* Like PAF, ANAFP inhibits fungal growth and is probably secreted by *A. niger* as a defense against fungal competitors (Gun Lee et al. 1999). Additional abundantly secreted proteins include: (i) β-glucanotransferases, responsible for glucan remodelling, (ii) RNase T2, also known as actibind, that can result in arrested cell growth in plants by binding to actin (Roiz et al. 2006), (iii) chloroperoxidase, has that has an important role in lignin degradation, (iv) muconate cycloisomerase that has a putative role in the degradation of aromatic compounds (Kellner et al. 2010), and (v) sulfhydryl oxidase that is most likely involved in maintaining redox balance e.g. through oxidation of reduced glutathione (de la Motte and Wagner 1987). These proteins presumably have specific functions that need to be constantly active, independently of the external carbon sources.

Following the analysis of highly abundant proteins, the enzymes responsible for starch or (hemi)cellulose degradation were investigated (Fig. 3).

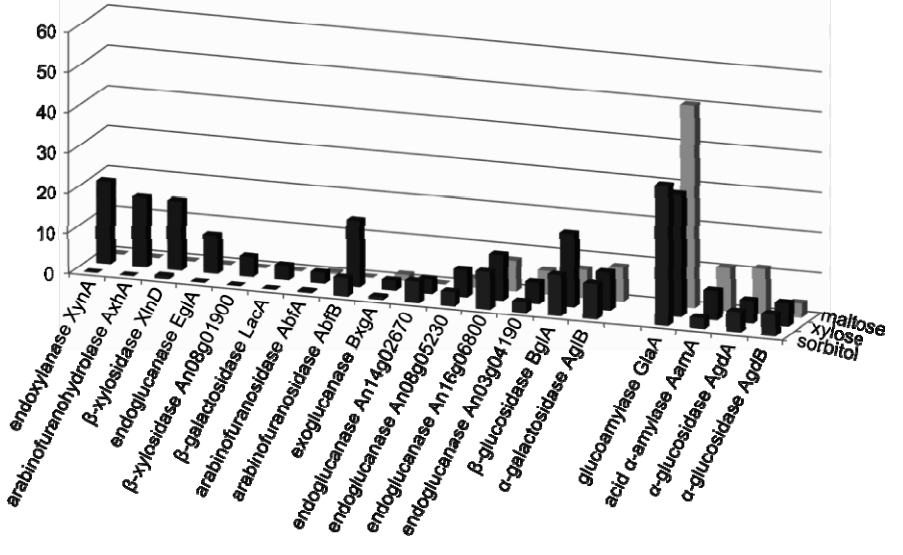

Figure 3. Relative abundance of enzymes related to (hemi)cellulose or starch degradation. The relative abundance values are given in NSAF·10^3.

The enzymes related to starch degradation were not only present upon D-maltose induction. The starch-degrading enzymes glucoamylase A, acid α-amylase (AamA), and α-glucosidase A (AgdA) were more abundant on the D-maltose condition than on D-xylose or D-sorbitol, whereas α-glucosidase B (AgdB) was found to be less abundant on D-maltose. Although counter-intuitive, this observation may reflect the fact that the expression pattern of *agd*B may differ from that of *gla*A, *aam*A and *agd*A (Yuan et al. 2008), perhaps pointing to different modes of regulation. In contrast to the amylolytic enzymes that were present even when no D-maltose was added, the enzymes involved in (hemi)cellulose degradation either were present only upon D-xylose induction, or were increased on D-xylose. With regard to D-xylose induction, β-xylosidase XlnD whose gene expression is known to be controlled by XlnR, was detected; however, also a novel putative β-xylosidase (An08g01900) was found that thus far was not reported to be regulated by XlnR. Moreover, proteins previously found to be more expressed after D-xylose induction, such as α-xylosidase AxlA, endoxylanase B, a putative xylanase (An15g04550), ferulic acid esterase FaeA, and acetyl xylan esterase AxeA, were detected after D-xylose induction, although the number of unique peptides was insufficient for statistical validation (Appendix II: Supplementary Table S9). In addition to this, a clear difference was detected on the relative abundance of different types of galactosidase. The β-galactosidase A (LacA) that is regulated at transcriptional level by XlnR, was found more abundant upon D-xylose addition (Fig. 3). On the other hand, α-galactosidase B (AglB) was only present at a very low level under the same condition. Although the two corresponding genes have previously been shown to be more expressed in the presence of xyloglucan, the *agl*B gene has been found to be also expressed on a large range of substrates (de Vries et al. 1999a), in contrast to *lacA*, which is exclusively expressed on xyloglucan-derived substrates. These data support the notion that these galactosidases perform distinct functions in the *A. niger* metabolism. As to the expression of endoglucanases, of the four putative endoglucanases found, only two - An08g05230 and An16g06800 - were more abundant on D-xylose than on the remaining conditions.

In addition to the proteomic analysis, we also investigated the relative gene expression patterns of *xln*D, *lac*A, *gla*A, *agd*A and *aam*A by QPCR analysis. Compared to the D-sorbitol non-induced condition, the *xln*D and *lac*A genes were highly expressed after D-xylose induction while *gla*A, *agd*A and *aam*A were highly expressed after D-maltose induction (Fig.4).

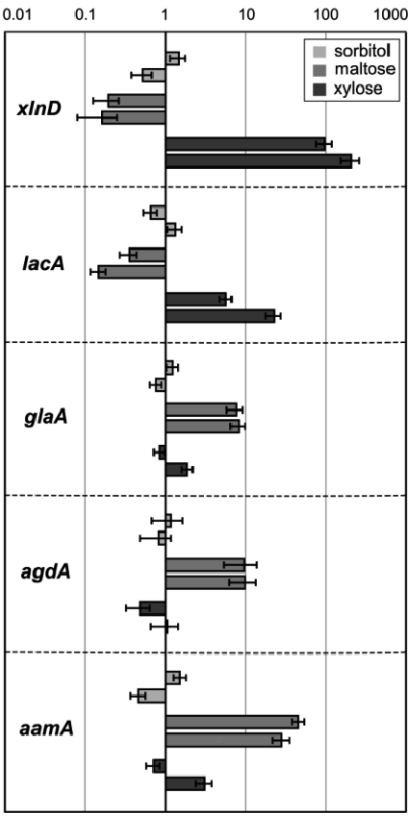

Figure 4. Relative gene expression of selected genes involved in (hemi)cellulose or starch degradation as determined by QPCR. *xlnD*: β-xylosidase D; *lacA*: β-galactosidase A; *glaA*: glucoamylase A; *agdA*: α-glucosidase A; *aamA*: acid α-amylase. Expression values were normalised to the average D-sorbitol values for each gene and are given on a logarithmic scale. Bars represent relative gene expression ± *SE*.

The combined results of the secretome and the transcription analyses confirmed that, in this experimental setting, D-maltose and D-xylose induced the expression of specific enzymes and these enzymes were secreted into the extracellular medium.

A G-test was then used to assess differential relative abundance on each condition (Table 1), on the basis of individual NSAF values.

Table 1. Proteins differentially represented in the secretome. (p): putative function, identity inferred from sequence similarity.

Protein	Locus tag	G-score D-maltose	G-score D-xylose
Abundant on D-maltose addition only			
Endo-arabinanase AbnC (p)	An02g10550	5.99	
Acid α-amylase AamA	An11g03340	5.04	
Abundant on D-xylose addition only			
Endoxylanase XynA	An03g00940		23.59
Arabinofuranohydrolase AxhA	An03g00960		19.29
β-Xylosidase XlnD	An01g09960		18.25
Endoglucanase A EglA	An14g02760		8.23
Arabinofuranosidase B AbfB	An15g02300		7.13
Cell wall protein PhiA (p)	An14g01820		5.27
β-Xylosidase (p)	An08g01900		4.97
Lower on D-maltose addition only			
Unknown hypothetical	37529	8.27	
Antifungal protein ANAFP	An07g01320	7.06	
Amidase (p)	An05g01860	4.26	
Lower on D-xylose addition only			
Guanyl-specific RNase T1 (p)	42238		8.61
Lower on D-maltose and D-xylose addition			
RNase T2 (actibind)	An01g10580	4.16	13.70
Sensor of PKC1-MPK1 Wsc1 (p)	An03g00250	4.24	5.10

In our studies, D-maltose induction differentially increased the extracellular amounts of the aforementioned acid α-amylase and of endo-arabinanase AbnC.

For the D-xylose condition, together with enzymes for (hemi)cellulose degradation, the homologue of *Aspergillus fumigatus* PhiA appeared to be over-represented. PhiA is a cell surface protein essential for phialide and conidium-spore development. These results suggest that D-xylose may have a positive effect on PhiA expression at the cell surface in *A. niger*. PhiA has been previously found to have its gene expression increased in an *xlnR*-overexpressing strain of *A. oryzae* grown on D-xylose as carbon substrate (Noguchi et al. 2009). This suggests that in *A. niger* this protein may be over-expressed on D-xylose through the action of XlnR, although the rationale of the apparent link is not obvious.

The secreted proteins that are less abundant on D-maltose, on D-xylose or both of these conditions include enzymes such as RNases, amidases, ANAFP and a homologue of yeast Wsc1 (Slg1) protein, involved in cell wall maintenance (Table 1). The reason why these secreted proteins are decreased upon D-maltose or D-xylose induction is unclear. Possibly, these proteins are not subject to regulation by carbon substrate, and their

decreased abundance relative to the total proteins secreted is a consequence of increased production of the extracellular enzymes induced by D-xylose or D-maltose.

Comparative analysis of the microsomal proteome

In one of our previous studies, the effect of induction by D-xylose on microsomal proteins of *A. niger* was investigated using the same experimental setup as was used in this study (de Oliveira et al. 2010). Here, we have studied the induction by D-maltose and made a comparison with the D-xylose induced conditions. For the comparison of the different microsomal proteins present in each condition, the same method as the one used for secretome analysis was followed, i.e. ranking of the differential relative abundance by a G-test. Since a large list of proteins was obtained (Tables 2 and 3) and for the sake of clarity, only the proteins with a G-score larger than 10 are discussed, i.e., the top 25% of the significantly increased and the top 10% of the decreased proteins upon induction.

In Table 2 the proteins overrepresented upon D-maltose or D-xylose induction are provided. In total, 27 proteins were significantly more abundant upon D-maltose or D-xylose induction as compared to the D-sorbitol control. On D-xylose 26 proteins were more abundant and on D-maltose 37 proteins. The proteins that were more abundant on the D-maltose and D-xylose conditions compared to D-sorbitol were identified as ERAD or mitochondrial proteins. In previous work we have shown that the proteasome 20S core particle is associated with the microsomal fractions by recruitment upon D-xylose induction, but this does not occur upon D-sorbitol addition (de Oliveira et al. 2010). Here, for D-maltose we find identical results. The 20S proteasome assembly is an ATP-dependent process, and the increased presence of mitochondrial proteins suggests that upon D-maltose and D-xylose induction a larger fraction of the mitochondria are associated with the ER, thereby facilitating the export of ATP and consequently the 20S proteasome assembly.

Other proteins that are highly expressed on both inducing conditions include a protein for ribosomal assembly Rpp0, a small GTPase for vesicular transport RhoA, a plasma membrane H^+-ATPase for cell polarity PmaA and the metabolic enzyme oxaloacetate acetyl hydrolase involved in oxalate formation (Ruijter et al. 1999; Han et al. 2007).

Table 2. Protein homologues of the microsomal proteins significantly increased for the D-maltose and D-xylose conditions. *Af: A. fumigatus; And: A. nidulans; Ao: A. oryzae; Ap: A. parasiticus; At: Arabidopsis thaliana; Hs: Homo sapiens; Nc: Neurospora crassa; Sc: Saccharomyces cerevisiae; Sp: Schizosaccharomyces pombe; Yl: Yarrowia lipolytica*. Values in parentheses: G-scores for differential presence.

Category	More abundant on D-maltose and D-xylose	More abundant on D-maltose only	More abundant on D-xylose only
Biosynthetic cargo	AamA (13.1/5.8), *Sc*Lap4 (4.2/4.4)	GlaA (16.8)	XlnD (17.3), AxlA (6.6)
Translation-related	*Sc*Rpp0 (11.3/4.2)	*Sc*Rpl15 (16.1), *Sp*vip1 (5.9), *Sc*Rpl31 (5.8), *Sc*Rps31 (5.8), *Sc*Rps6 (4.7), *Sc*Rpl1 (4.7), *Sc*Pth2 (4.2)	*Sp*Cdc60 (5.8)
Cytosolic chaperones		*Sc*Zuo1 (3.9)	
Translocation to the ER		*Sc*Sec11 (8.5)	
Protein anchoring			*Sc*Gpi12 (9.5)
ERAD	*Sc*Pre7 (25.0/26.2), *Sc*Pre5 (18.3/16.8), *Sc*Cdc48 (10.9/20.5), *Sc*Pre6 (8.5/11.9), *Sc*Pre9 (10.0/9.9), *Sc*Scl1 (9.8/9.2), *Sc*Pre8 (10.5/8.4), *Sc*Pup2 (10.4/7.5), *Sc*Pre10 (7.5/8.5), *Sc*Cep52 (10.4/7.5)	*Sc*Pre1 (4.7), *Sc*Pup1 (4.5)	
Vesicular transport	RhoA (16.6/8.6), SrgA (8.5/5.7), *Hs*RAB5C (5.6/6.4)	*Sc*Erv14 (20.5), *Sc*Yip1 (10.1), *Hs*ARF6 (8.0), *Sc*Vps21-like protein (5.8), *Sc*Sec17 (4.8)	
Golgi/post-Golgi sorting		*Sc*Vps68-like (4.1)	
Lipid biosynthesis and CYP450 enzymes		*Ao*PLTPAO (8.5), *Ap*OrdA (4.3)	*Af*Afu1g10100 (6.1)
Mitochondrial	*Nc*nuo14 (5.5/13.3), *Sc*Cox4 (8.0/8.4), *Nc*nuo51 (4.5/11.1), *Sp*qcr1 (4.6/11.0), *Sc*Aco1 (5.2/6.5), *Hs*SLC25A13 (4.1/7.2), *Sc*Yhm1 (4.2/6.7), *Sc*Hsp60 (4.0/4.7)	*Sc*Qcr8 (15.4), *Nc*nuo12.3 (6.8), *Nc*nuo19.3 (6.2), *Sp*SPAPJ691.03 (5.3), *Sc*Atp3 (4.2), *Sc*Pic2-like (3.9)	*Sc*Mcr1 (7.5), *Sc*Yhm2 (6.7), *Nc*CYT-1 (6.2), *Sp*rip1 (5.7), *Sc*Atp7 (5.5), *Yl*:YALI0F25135p (5.4), *Nc*nuo78 (4.8), *Hs*NAA16 (4.7), *Sc*Fcj1-like (4.5), *Sc*Phb1(4.1), *Sc*Ctp1 (4.0), *Nc*nuo21.3 (3.8)
Transporters	*And*PmaA (14.1/11.8)		
Metabolism	OahA (14.6/14.2)	*Hs*CHDH (6.9), *Sc*Eno1 (6.6), TpiA (6.3), An02g10150 (6.0), *Sc*Gln1 (4.7)	XyrA (14.6), *Sc*Dld1 (5.8), *Af*Gcy1 (4.7)
Nuclear	*Sp*Smd1 (4.0/4.5)	*Sc*Hhf1 (19.5), *Sc*Nop1 (5.0)	
Unknown and others		An04g08060 (9.6), An04g05750 (8.3), *At*NIT1 (6.5), *Sc*Env7 (4.5)	*Af*Afu3g08290 (5.4), An11g07020 (4.9), An11g00890 (4.7), *Af*Afu4g03280 (4.4), *Sc*YHR045w (4.1) , An18g01000 (4.0)

As for the remainder of the proteins, a few cargo proteins were specific for one or induced in both conditions. Glucoamylase A was found more abundant on D-maltose, β-xylosidase XlnD was only detected on D-xylose and acid α-amylase AamA was found on both but more abundant on D-maltose compared to D-xylose. D-Maltose induction also increased endosomal-cargo receptor Erv14, histone H4 and the protein component of the large subunit Rpl15.

Table 3. Protein homologues of the microsomal proteins significantly decreased for the D-maltose and D-xylose conditions. *And: A. nidulans; Ao: A. oryzae; Hs: Homo sapiens; Nc: Neurospora crassa; Sc: Saccharomyces cerevisiae; Sp: Schizosaccharomyces pombe*. Values in parentheses: G-scores for differential presence.

Category	Less abundant on D-maltose and D-xylose	Less abundant on D-maltose only	Less abundant on D-xylose only
Biosynthetic cargo		An05g02280 (4.5)	
Translation-related	*Sc*Wrs1 (7.9/5.7)	*Sc*Rps16b (8.9), *Hs*Rps24 (4.9)	*Sc*Rpl17b (7.4), *Sc*Rpl27 (7.1), *Hs*Rps18 (6.5), *Sc*Rpl28 (6.3), *Sc*Rps9 (5.1), *Sc*Rpl21A (5.1), *Sc*Rps20 (4.6), *Sc*Rpl7A (4.4), *Hs*Rpl12 (4.0), *Sc*Rpl3 (3.9)
Cytosolic chaperones	CypA (14.2/10.9)	SspB (5.0)	*Hs*HSPA8 (9.4)
Translocation to the ER			*Sc*Sbh2 (10.0), *Sc*Srp102 (5.4)
Protein glycosylation/ QC		AgdE (6.8)	
Vesicular transport	*Ao*AO090026000708 (9.0/6.0)	*Sc*Yop1 (6.5), *Sc*Sec21 (6.1)	
Golgi/post-Golgi sorting	*Hs*CLTC (9.8/5.9)		
Morphogenesis and cytoskeleton	*And*HEX1 (9.1/6.3)	*Sp*cdc4 (9.5), *Sp*SPBC31F10.16 (5.3), *And*MpkA (4.0)	*Sc*Sac6 (4.1)
Lipid biosynthesis and CYP450 enzymes	*Sc*Sec14 (4.2/10.2), *Sp*fas2 (4.7/4.2)	*Sc*Tsc10 (5.8), AclA (4.8)	
Mitochondrial		*Sc*Idh2 (4.4), *Hs*GOT2 (4.4)	*Sc*Lat1 (4.7)
Transporters		*Hs*KCNAB2 (4.0)	
Metabolism	*Sc*Gcy1 (10.5/9.0), ArgB (11.3/7.9), *Sc*Ser3 (11.1/6.3), *Sc*Hnt1 (4.1/7.5)	*Sc*Adk1 (4.7), *Sc*Aat2 (4.6), *Hs*PYCR1 (4.5), *Sc*Gph1 (4.2)	*Ao*AO090020000635 (5.2), *Sp*SPAC19G12.04 (4.3), *Sc*Cys4 (4.1)
ROS defence	An02g12940 (5.1/4.0)		
Nuclear		*Sc*Nic96 (6.5), An09g00500 (4.6), *Sc*Nup170 (4.0)	
Unknown and others	*Hs*CIRBP (5.5/9.4)	*Nc*NCU03370 (10.7), *Sp*SPCC1450.12 (3.9)	An12g05040 (7.9), An18g00950 (7.8)

Several proteins were found to be induced by D-maltose or D-xylose, however, few proteins were found to be decreased under these conditions (table 3). The microsomal proteins that were found in decreased levels upon the D-maltose and D-xylose conditions were the cytoplasmic chaperone CypA, the phosphatidylinositol-phosphatidylcholine

transfer Sec14 protein and the three metabolic enzymes glycerol dehydrogenase, 3-phosphoglycerate dehydrogenase and ornithine carbamoyltransferase, just to name the largest differences. In addition, an unknown protein from the perilipin (lipid binding) family was decreased on D-maltose.

The comparative analysis of the secretome and the microsomal proteome reveals that 29 proteins are present both in the secretory organelles as well as outside of the cell (Table 4).

Table 4. Proteins shared by the secretome and microsomal proteome. CW: cell wall; SP: signal peptide; NSAF: normalised spectral abundance factor; Mal.: D-maltose; Xyl.: D-xylose; Sorb.: D-sorbitol. Underlined values: NSAF increased compared to D-sorbitol control. Values in parentheses: NSAF decreased compared to D-sorbitol control.

Protein	Locus tag	Microsomal (NSAF.10^4)			Secreted (NSAF.10^3)		
		Mal.	Xyl.	Sorb.	Mal.	Xyl.	Sorb.
Glucoamylase GlaA	An03g06550	63.9	41.3	25.8	50.4	30.6	35.1
Acid α-amylase AamA	An11g03340	14.6	8.4	1.3	10.9	7.4	2.9
α-Glucosidase AgdA	An04g06920	5.5	3.0	1.5	11.5	5.8	5.2
β-Xylosidase XlnD	An01g09960	0.1	13.6	0.2	0.4	17.0	0.8
β-Galactosidase LacA	An01g12150	0.1	2.2	0.4	0.3	3.7	0.2
β-Glucosidase BglA/ bgl1	An18g03570	3.1	9.5	5.6	7.1	18.2	10.3
Glucanotransferase BgtB	An03g05290	3.0	4.1	4.2	25.7	35.8	23.5
Glucanotransferase GelA	An10g00400	5.4	5.7	2.0	23.5	22.2	34.7
Glucanotransferase GelD	An09g00670	2.6	3.2	4.1	9.1	7.8	9.5
Glucanotransferase	53033	3.8	6.2	2.7	10.3	10.6	8.8
CW protein CrhD	An01g11010	4.6	6.1	2.3	8.1	5.6	7.8
Serine-type carboxypeptidase I	An02g04690	0.6	1.2	0.2	7.2	5.2	9.0
Carboxypeptidase S1	An03g05200	2.5	4.6	5.7	18.0	14.5	12.7
Barrierpepsin	An18g01320	1.2	2.6	2.0	3.2	3.8	4.1
CW organisation protein EcmA	An04g01230	2.4	4.3	2.9	12.3	14.2	23.1
Catalase CatR	An01g01820	9.8	15.4	10.9	9.2	6.5	10.4
Monophenol monooxigenase	An01g09220	4.5	2.9	4.2	19.3	16.5	16.8
Muconate cycloisomerase	An01g14730	1.4	3.5	5.0	24.5	27.3	23.7
Hydroxynicotine oxidase	An07g02360	6.0	6.7	7.8	23.7	21.2	22.8
Conserved hypothetical	An04g08730	1.0	1.2	3.2	8.1	9.7	10.4
Adenosine permease	An10g00800	1.8	0.7	2.9	13.6	5.5	7.6

The cargo proteins GlaA, AamA, AgdA, XlnD, LacA and BglA showed similar trends in relative amounts according to condition in the microsomal and secreted fractions. For the other proteins these trends were not so evident, either because the amounts were too similar across conditions or because other factors may have influenced the detection of the protein in the culture filtrate. For instance, glycosylphosphatidyl-inositol (GPI)-anchored glucanotransferases and cell wall proteins might not be easily released into the culture filtrate. The comparison of protein relative amounts present in the secretome and in microsomes is also difficult because of the factor time, since, due to the experimental set up, the secreted proteins accumulated over a period of 16h. The microsomal

proteome on the other hand was the result of microsomes isolated in a defined moment in time; therefore some proteins might accumulate whereas others might be immediately secreted.

Conclusions

A proteomic approach was taken to analyse in parallel the secretome and the microsomal proteome of *A. niger* in the presence of different inducers of extracellular enzyme production. By using a semi-quantitative method based on MS spectral counts, we were able to estimate the relative amounts of secreted and secretory proteins upon induction of extracellular enzyme production. This study confirms that D-maltose and D-xylose induce the production of specific extracellular enzymes in *A. niger*. Moreover, we were able to show that induction by D-maltose also results in the association of the 20S core of the proteasome with secretory organelles, just as was recently reported for D-xylose induction. With the advent of more sophisticated proteomic techniques, a more comprehensive view of the dynamic composition of fungal organelles is expected. Future studies on complex processes such as protein secretion will clearly benefit from accurate descriptions of organelle proteomes and their inter-relations.

MATERIAL AND METHODS

Strain and culture conditions

All experiments were conducted using the *A. niger* wild type strain N400 (CBS 120.49), cultured in 2.5 litres fed-batch bioreactors (Applikon). For pre-cultures 1.0×10^6 spores per millilitre were inoculated in 2.2 litres of minimal medium (Pontecorvo et al. 1953) containing 0.05% yeast extract and 100 mM D-sorbitol, at 30°C. Spore germination was as described previously (van der Veen et al. 2009), with headspace aeration and a stirring speed of 300 rpm. When dissolved oxygen levels decreased to 60%, stirring speed was switched to 750 rpm and the sparger inlet was used for aeration. This moment was considered the actual culture starting point. After 14h from the culture starting point, D-maltose, D-xylose or D-sorbitol (10 mM) was added to each culture and 2 hours later a 100 ml sample was taken from each fermentor and filtered through nylon gauze. Part of the harvested mycelium was processed for sub-cellular fractionation and the other part was

immediately frozen in liquid nitrogen and stored at –80°C. Culture filtrate was also frozen in liquid nitrogen and stored at –80°C. All experiments were done in two biological replicates.

Sample preparation for LC-MS/MS

Microsome enrichment techniques and subsequent preparation for LC-MS/MS were as described previously (de Oliveira et al. 2010). Parallel to this, culture filtrate aliquots from each condition were loaded on Microcon YM-10 columns (cut-off 10 kDa, Millipore, Eschborn, Germany); the final concentrated sample contained at least 100 µg protein and was processed for LC-MS/MS analysis. Concentrated protein samples were reduced with DTT and alkylated with iodoacetamide. Afterwards, excess iodoacetamide was removed by addition of cysteine (70 mM final concentration). Samples were overnight digested with 10 ng · μl^{-1} trypsin (sequencing grade modified trypsin, Promega, Madison, WI, USA) at room temperature, and after this, trifluoroacetic acid was added to a final pH of 2.5.

LC-MS/MS analysis and protein identification

LC-MS/MS was performed as described previously (van Esse et al. 2008). In summary, each sample was loaded on a pre-concentration column and the respective peptides were passed through an acetonitrile gradient in an analytical column of fixed formic acid concentration. The eluent was subjected to an electrospray potential by means of a coupled platinum electrode. MS spectra were measured in an LTQ-Orbitrap instrument (Thermo Electron, San Jose, CA, USA). MS scans of the four most abundant peaks were recorded in data-dependent mode. Quantitative MS/MS spectra were searched using the Open Mass Spectrometry Search Algorithm (OMSSA) (Geer et al. 2004). The spectra were independently searched against peptide databases derived from the predicted proteomes of *A. niger* strains CBS713.88 and ATCC 1015, and a decoy reverse database constructed from the reverse proteome of strain CBS713.88. All OMSSA searches used the following parameters: a precursor ion tolerance of 0.2 Da, a fragment ion tolerance of 0.3 Da, a missed cleavage allowance of up to and including 2, fixed carbamide methylation, variable oxidation of methionine and deamination of glutamine and asparagine. The E value threshold was determined iteratively from the false discovery rate (FDR) and was set to 0.01, in which case any given FDR is expected to be below 5%. Peptide-spectrum matches

with each individual peptide database were ranked by their E-value for each identified spectrum with a threshold E-value < 0.01 and the top hit identified peptide sequence was selected. For FDR calculation, top hit spectral matches to peptides in the reversed database were taken and the number of false positives was divided by the number of total positives. Proteins were only considered present under each condition, *viz.* addition of D-maltose, D-xylose or D-sorbitol, whenever at least 2 unique peptides were identified in one of the biological replicates and 1 unique peptide was identified in the other biological replicate for the same condition.

Relative protein abundance and functional annotation

Relative abundance of each protein within the total pool of proteins was estimated by calculation of normalised spectral abundance factors (Zybailov et al. 2006):

$$(\mathrm{NSAF})_k = \frac{(\mathrm{SpC/L})_k}{\sum_{i=1}^{N} (\mathrm{SpC/L})_i}$$

in which $(NSAF)_k$ is the normalised spectral abundance factor for a protein *k*, SpC is the number of spectral counts for a given protein plus a pseudocount factor of 0.5, and L is the protein's length. The pseudocount was introduced to enable statistical analysis in the cases where a protein could not be detected in at least one of the three conditions (addition of D-maltose, D-xylose or D-sorbitol). Significant differences in NSAF values were investigated by applying the likelihood ratio G-test for independence with the null hypothesis of equal protein distribution between conditions. Transmembrane domains (TMD) were assessed using the TMHMM tool (Sonnhammer et al. 1998) and signal sequence predictions were done with a local implementation of SignalP 3.0 (Bendtsen et al. 2004). Culture filtrate proteins were identified as extracellular enzymes whenever they contained at least one conserved catalytic domain, as assessed by similarity search using blastp and conserved domain search (NCBI). Microsomal proteins predicted were grouped in functional annotation groups guided by previously published functional classification schemes (Geysens et al. 2009), the Functional Catalogue (FunCat) annotation scheme and the predicted molecular function as provided with the *A. niger* CBS 531.88 genome annotation (Pel et al. 2007).

Quantitative real-time PCR (QPCR)

All steps from RNA isolation and cDNA synthesis to QPCR and data analysis were as described elsewhere (Oliveira et al. 2008). Briefly, total RNA was extracted, mixed with an exogenous RNA reference transcript, and cDNA was synthesised using Oligo(dT) primers. QPCR SYBR Green Mix (ABgene, Epsom, UK) and specific oligonucleotide primers (Table 5) were used for QPCR. Two independent PCR runs were performed per cDNA sample from each biological replicate. The Pfaffl method (2001) was used to calculate relative gene expression levels, double-normalised to the added exogenous RNA transcript and to the standard condition, i.e. the average normalised expression of the two biological samples from the D-sorbitol control condition.

Table 5. Oligonucleotide primers used for QPCR. F: forward primer; R: reverse primer.

Target gene and locus tag	Product	Primer sequence (5'-3')
xlnD (An01g09960)	β-xylosidase D	F: TAATCTACGCCGGTGGTATC R: TTCTTGAGCGAAGAGGAATC
lacA (An01g12150)	β-galactosidase A	F: GGCGAGGACTACGAAGACAA R: AATGCCTGCCTCAGAGAGAC
glaA (An03g06550)	glucoamylase A	F: GCATCCACACCTTTGATCCT R: TCGCTGTCACTGAGACCATC
agdA (An04g06920)	α-glucosidase A	F: TCCCATTCTACCGAAACCAC R: GGCCAGGTCAAACAACGTAT
aamA (An11g03340)	acid α-amylase	F: TCGGCCTACATTACCTACGC R: CTGAGGAGCCTTTGTTGGAG
exogenous normaliser transcript	kanamycin/neomycin resistance gene	F: AGCATTACGCTGACTTGACG R: AGGTGGACCAGTTGGTGATT

Authors' contributions

JMPFO performed most of the experimentation. PJS contributed with database management, spectral assignment and targeting sequence predictions. LHdG supervised all the experimental work. All authors contributed to the experimental and analytical design. LHdG, MWJvP, and PJS critically revised the manuscript. All authors read and approved the final manuscript.

Acknowledgements

We would like to thank John van der Oost for critically revising the manuscript, and Niels Zondervan for insightful discussions on mitochondria-associated membrane. MWJvP is funded by the Netherlands Organisation for Scientific Research (NWO) via a VENI grant.

Chapter 6

General discussion

General overview

In the course of evolution, filamentous fungi have evolved sophisticated enzyme systems for the degradation of complex extracellular substrates, such as the polysaccharide components of plant cell walls. It is commonly accepted that the expression of enzyme systems for extracellular digestion is regulated and fine-tuned by external molecules that serve as signals for the presence of specific substrates. Extracellular degradation of substrates is a complex process mainly for two reasons. Firstly, since a polysaccharide substrate is usually made of various monomers connected by different chemical linkages, it is likely that one signal molecule will trigger the production of a mixture of enzymes of various activities to effectively degrade the polysaccharide. Secondly, since different polysaccharides can share some monomers although in different proportions, the fungus must fine-tune the enzymes secreted so as to degrade the correct polysaccharide. Thus, it is most likely not only the presence but both presence and concentration of different signal molecules that influence the decision of secreting certain enzymes for extracellular degradation.

In aspergilli, the best studied systems for extracellular polysaccharide degradation are the ones governed by the activators XlnR and AmyR. XlnR is an activator of several (hemi)cellulases (Stricker et al. 2008), whereas AmyR activates the expression of starch-degrading enzymes (Tsukagochi et al. 2001). The signal molecule for XlnR-mediated (hemi)cellulase degradation is D-xylose. AmyR action is dependent on starch degradation products, such as maltose or isomaltose (Tsukagochi et al. 2001). In **chapter 2** the *xlnR* gene was silenced by a vector expressing hairpin RNA directed to a portion of *xlnR* coding region. Such a hairpin RNA for gene silencing may also be targeted to other genes, such as genes playing a potential role in the secretory pathway. However, such a silencing system would still require major improvements as pointed out in **chapter 2**. These improvements would be mostly related to the prevention of genome rearrangements subsequent to transformation and a selection or reporter system for screening transformants.

In **chapter 3**, the transcriptional response to the signal molecule D-xylose was investigated. The experimental set-up was designed to allow dissection of the transcriptional response to D-xylose induction of extracellular enzymes instead of the more general transcriptome difference due to D-xylose utilisation. For that, *A. niger* was adapted to grow overnight on the non-inducer D-sorbitol, after which period a small perturbation was introduced by the addition of micromolar amounts of D-xylose. This

study confirmed that D-xylose activates enzymes related to the hydrolysis of D-xylose residues from xylan and also enzymes responsible for the hydrolysis and modification of many polysaccharide building blocks occurring e.g. on arabinoxylan or cellulose. In addition, optimised bioreactor conditions were determined to minimise the variation in gene expression data attributed to the experimental set-up.

The optimised bioreactor conditions described in **chapter 3** were then used to investigate the proteome changes occurring in the secretory pathway of *A. niger* upon induction of secretion by D-xylose, as described in **chapter 4**. Proteins from enriched microsome fractions were separated by SDS-PAGE and after in-gel digestion proteins were subjected to LC-MS/MS. A large number of proteins was identified (> 1,100) of which ~ 25% were predicted to be related to membrane traffic and protein secretion. **Chapter 4** only discusses the proteins that are potentially related to secretion, although the complete data for the other proteins are presented as well. D-xylose induction was responsible for an increase in the relative amounts of proteins playing diverse roles in protein secretion, namely small GTPases for vesicle transport and polarised growth. Most importantly, the 20S core particle of the proteasome, which is involved in the cytosolic degradation of mis-folded proteins, was only present under D-xylose induction but not when D-sorbitol control was used. These results point to a novel mode of regulation of the secretory pathway in filamentous fungi in which the proteasome is recruited to secretory organelles upon the induction of extracellular enzymes.

The proteomic analysis of induction of extracellular enzymes given in **chapter 4** is further expanded in **chapter 5** in two ways. First, the effect of D-maltose on the microsomal proteome is also studied. Second, for both induction systems i.e. D-xylose and D-maltose, analysis of the secretome is additionally included. The proteins secreted during D-xylose induction were mostly related to arabinoxylan and cellulose degradation. The proteins secreted during D-maltose induction, were mostly enzymes involved in starch degradation. Moreover, "non-classically secreted proteins"were detected, a class defined here as proteins lacking an N-terminal signal sequence for secretion (signal peptide) or signal anchor. Examples of the latter proteins include thioredoxin, hsp60, BipA and two proteins from the mitochondrial inner and outer membranes. Since these proteins have a predicted intracellular and in some cases even a membrane-embedded localisation, and because no indication exists for an extracellular localisation or function, they were considered as putative contaminants resulting from cell lysis. When globally analysed, the microsomal-associated proteins that were most abundant after induction belonged mainly

to the 20S proteasome, to the mitochondrial membranes or to the cytosolic pool of small GTPases involved in vesicular transport and endocytosis.

The large number of proteins identified in **chapters 4 and 5** is a result of digestion of different gel slices from each protein mixture. Spectral counting and normalised spectral abundance factor (NSAF) calculation allowed for estimation of protein relative amounts. The estimated amounts between different proteins may vary depending on the quality of the gene models. The gene model for strain CBS 513.88 is more suitable for this than the one from strain N400, as explained in **chapter 4**. G-test is a robust method for assessing and ranking proteins for their differential presence based on normalised spectral counts

Comparison of transcriptomics and proteomics

The expression and secretion of extracellular enzymes depends not only on the presence of inducer signal molecules but also on other external factors such as pH and more general culture conditions, such as submerged vs. solid state, or cultivation in shake-flask vs. bioreactor (MacCabe et al. 1998; Gielkens et al. 1999; Oda et al. 2006; Lu et al. 2010). In addition to this, previous work has shown that the developing mycelium of *A. niger* is highly differentiated since different genes are expressed and different proteins secreted in different regions of the mycelium (Levin et al. 2007). The studies reported in **chapters 3 to 5** were performed in bioreactor cultures and a dispersed morphology was achieved by stirring. Moreover, biological replicates were taken for each condition. As assessed in **chapter 3**, variation in gene expression data was reduced by considering the partial variation introduced on each experimental step from spore harvesting and fungal culture to signal probe detection.

The overall effect of D-xylose on gene expression has been characterised in aspergilli. Andersen and co-workers (2008) compared the gene expression of *A. niger*, *A. nidulans* and *A. oryzae* grown on D-xylose or D-glucose. Within this analysis, 22 genes were found to be up-regulated on D-xylose. These genes were identified as part of a core response to D-xylose in the three *Aspergillus* species. Similar to this, another study reports the transcriptional response of *A. niger* adapted to grow on D-xylose and D-maltose (Jørgensen et al. 2009). In contrast to these studies on the response to D-xylose in contrast to D-glucose or D-maltose, another study focused on the proteins expressed in an *xlnR* over-expressing strain in contrast to an *xlnR*-deletion mutant (Noguchi et al. 2009).

The differentially expressed genes identified in these studies (Andersen et al. 2008; Jørgensen et al. 2009; Noguchi et al. 2009) were compared to the genes identified in our study in **chapter 3**. All the differentially expressed genes were then compared to the microsomal and the secreted proteins discussed in **chapters 4 and 5**. The result of this cross-study comparison is summarised in Figure 1, which represents the transcriptome and proteome response to D-xylose in *A. niger*.

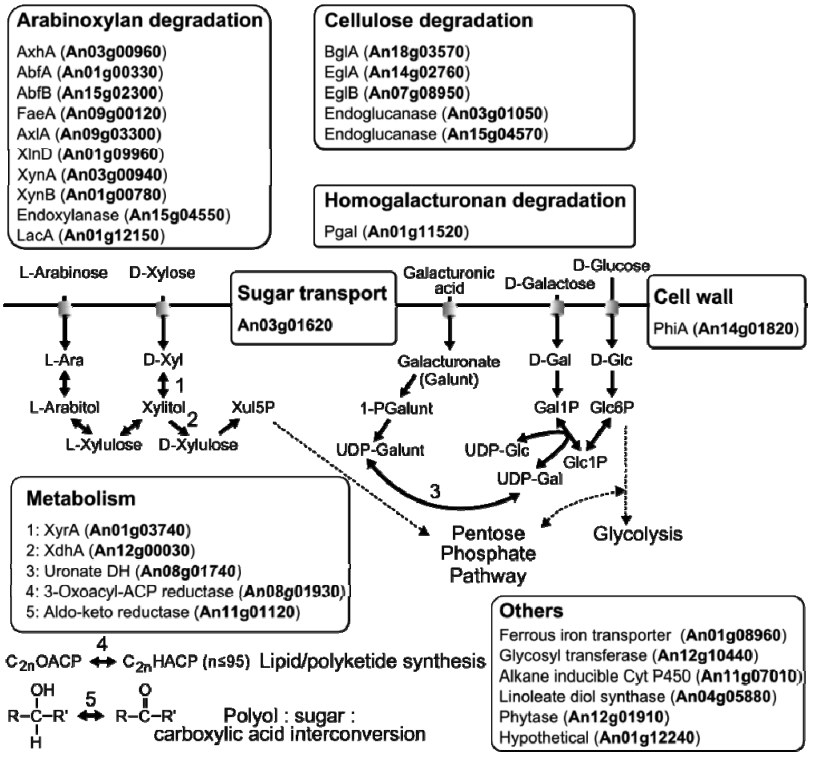

Figure 1. The core response to D-xylose induction in *A. niger*. Integrated cartoon based on previous molecular analyses, and recent proteomics and transcriptomics studies. The genes and corresponding proteins more abundant on D -xylose are depicted. ACP: acyl carrier protein; Ara: arabinose; Gal: galactose; Glc: glucose; HACP: hydroxyenoyl acyl carrier protein; OACP: oxoenoyl acyl carrier protein; Xul5P: xylulose 5-phosphate; Xyl: xylose.

Apart from the secreted enzymes, various other proteins were found more abundant on D-xylose. One major facilitator superfamily (MFS) transporter identified (An03g01620) was previously described as highly expressed on D-xylose and on D-galacturonic acid (Martens-Uzunova and Schaap Fungal Genet Biol 2008). It is thus likely that this transporter plays an important role in the uptake of substrates from pectin degradation, especially from xylogalacturonan. Moreover, a putative uronate dehydrogenase (An08g01740) may have a key function on the interconversion of UDP-galacturonate and UDP-galactose. The first two enzymes for D-xylose utilisation are NADPH-dependent D-xylose reductase (XyrA) and NADH-dependent xylitol dehydrogenase (XdhA). Both enzymes were found exclusively on D-xylose and not on D-maltose or D-sorbitol. This suggests that their main substrate is D-xylose and xylitol, respectively. Moreover, upon D-xylose induction, an aldo-keto reductase (An11g01120) was found that may be necessary for the rapid inter-conversion between polyols, sugars and carboxylic acids.

After the analysis of the conserved transcriptome and proteome response to D-xylose, the response to D-maltose was assessed. In *A. oryzae*, the MAL operon is responsible for D-maltose utilisation. In *A. niger* however, such an operon does not exist and D-maltose must be converted to D-glucose in a process mediated by the AmyR regulon (Vongsangnak 2009). Unfortunately, no transcriptome analysis was performed on D-maltose as an inducer in the course of this thesis to match the system used for the proteomic study described in **chapter 5**. However, a number of studies report the effects of D-maltose or its monomer D-glucose. Besides the above-mentioned studies (Andersen et al. 2008; Jørgensen et al. 2009), which make use of D-glucose and D-maltose respectively, another study has focused more specifically on the amylolytic system of *A. niger* (Yuan et al. 2008). In the latter, wild-type *A. niger* and an *amyR*-deletion strain are compared for global gene expression on D-maltose as a carbon substrate. In order to dissect the D-maltose response in *A. niger*, the candidate genes from these studies (Andersen et al. 2008; Jørgensen et al. 2009; Yuan et al. 2008) were compared to the proteins described in **chapter 5** which were relatively abundant upon D-maltose induction (Fig. 2).

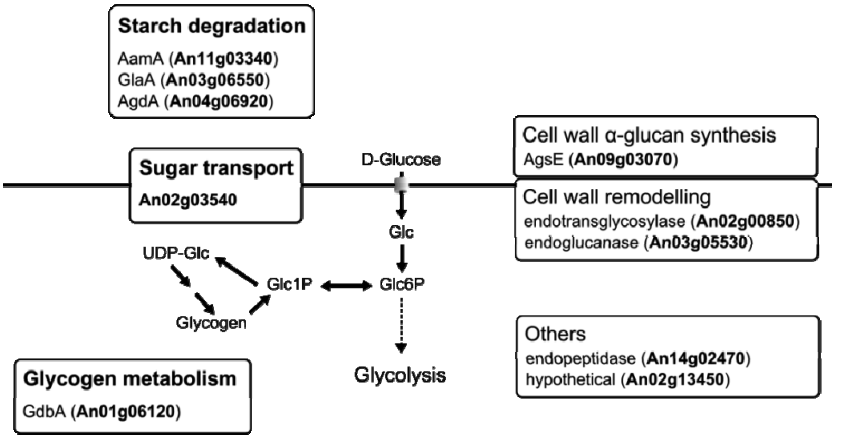

Figure 2. The core response to D-maltose induction in *A. niger*. The genes and corresponding proteins more abundant on D -maltose are depicted. Glc: glucose.

D-Maltose induction resulted in the activation of a modest number of proteins whose corresponding genes were also up-regulated on D-maltose. Besides the enzymes glucoamylase A, acid α-amylase and α-glucosidase A, D-maltose also induced a hexose transporter (An02g03540) and a putative glycogen debranching enzyme (An01g0120). Other candidates include a protein involved in α-glucan synthesis, an endopeptidase, and a putative α-1,3-mannosyltransferase (An02g13450).

Proteomic analysis of metabolic enzymes upon D-xylose or D-maltose induction

Up to 15% of the proteins in enriched microsomal fractions were identified as metabolic enzymes, 12% of which were cytosolic and 3% mitochondrial (**chapter 5**).These metabolic enzymes were present in varying relative quantities depending on the substrate added, i.e. D-xylose, D-maltose or D-sorbitol. The majority of the metabolic proteins did not fluctuate significantly under the tested conditions; one of the few exceptions includes the enzyme xylose reductase (induced only on D-xylose). Nevertheless, trends in protein

abundance can be analysed by comparison of NSAF values in the three conditions (Fig. 3). In this figure, three classes of NSAF values are depicted as differently sized circles, the colours corresponding to the supplemented substrate. According to this classification, all glycolytic enzymes were abundant on D-maltose, except the enzymes catalysing the two ATP-dependent key steps in glycolysis, i.e. phosphofructokinase (which converts fructose 6-phosphate to fructose 1,6-bisphosphate) and pyruvate kinase (which converts phosphoenolpyruvate to pyruvate). Enzymes involved in the pentose phosphate pathway were less abundant after D-maltose induction. The presence of D-xylose on the other hand, resulted in less abundance of glycolytic enzymes and more abundance of enzymes involved in the pentose phosphate pathway, which is the main pathway for D-xylose utilisation via xylulose 5-phosphate. D-Xylose and D-maltose were both associated with an increase in enzymes leading to oxalate production. One possible reason for this is that the external pH was kept constant at 3.5 in all tested cultures. At this pH, the two organic acids expected are oxalate and citrate. At pH<3 oxalate production is sharply reduced (Ruijter et al. 1999), with citrate being maximally produced at pH between 1.5 and 2.5 (Karaffa and Kubíček 2003). Gluconic acid is optimally produced at pH near 5.5 (Andersen et al. 2009) and its production was therefore not expected in the context of this work. Indeed the enzymes for gluconic acid production were not found using this experimental set up. Oxaloacetate hydrolase, the enzyme responsible for oxalate production in *A. niger*, was more abundant on D-maltose and D-xylose, compared to the D- sorbitol control. In addition to this, most mitochondrial transporters were more abundant on D-maltose and D-xylose, namely the aspartate-glutamate, the citrate-malate and the citrate-(α-ketoglutarate) antiporters.

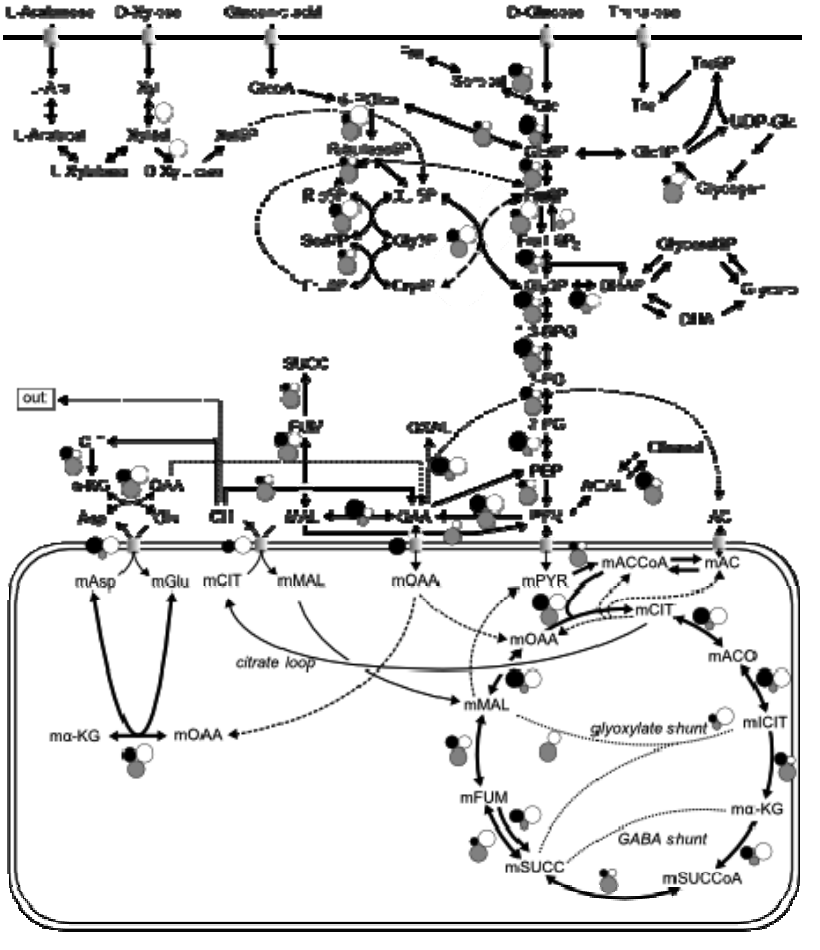

Figure 3. Metabolic enzymes found in enriched microsome samples. Black circles: D-maltose induction; white circles: D-xylose induction; grey circles: D-sorbitol control. The condition that yielded the highest NSAF value is depicted as large circles. If the NSAF value for the same protein in a different condition is at least 10% smaller compared to the largest NSAF, then a medium-sized circle is used for this condition. When the NSAF value is smaller than 20% compared to the largest NSAF, a small circle is used. The prefix "m" refers to mitochondrially localised metabolites. AC: acetate; ACAL: acetaldehyde; ACO; *cis*-aconitate; Ara: arabinose; Asp: aspartate; BPG: bisphosphoglycerate; CIT: citrate; DHA: dihydroxyacetone; Fru: fructose; FUM: fumarate; Glc: D-glucose; GlcoA: gluconic acid; Glu: glutamate; Gly: glyceraldehyde; ICIT: isocitrate; α- KG; α-ketoglutarate; MAL: malate; OAA: oxaloacetate; OXAL: oxalate; PG: phosphoglycerate; PEP: phosphoenolpyruvate; PYR: pyruvate; SUCC: succinate; SUCCoA: succinyl-CoA; Tre: trehalose.

Differentially present proteins that are not transcriptionally regulated in response to D-xylose or D-maltose

Effects of D-xylose and D-maltose on the secreted proteins

D-Xylose and D-maltose have additional effects on the proteome of *A. niger* that are not the result of differential gene expression (**chapters 4 and 5**). With regard to secreted proteins, most proteins differentially secreted on D-xylose (compared to D-glucose) were previously also found to be transcriptionally regulated, with the single exception of a putative β-xylosidase (An08g01900), as described in **chapter 5**. For D-maltose, a rather different effect was observed. Of the enzymes expected to be regulated at the transcriptional level, only acid α-amylase was found significantly more present in the culture filtrate after D-maltose induction. Secreted glucoamylase A and α-glucosidase A were found with higher NSAF values on D-maltose compared to the other conditions; however, this was insufficient for statistical validation of differential protein abundance (G-test, $p<0.05$). The result for glucoamylase A and α-glucosidase A can be explained by the fact that unlike the enzymes that are under the strict control of XlnR and that are activated only by D-xylose, the amylolytic enzymes are constitutively expressed at basal levels and further activated by D-maltose. Since the mycelium of *A. niger* was not transferred before addition of D-maltose, the positive effect of 2-hour induction on D-maltose may have been obscured by the overnight basal accumulation of these enzymes on the culture broth from cultures pre-grown on D-sorbitol. Nevertheless, glucoamylase was found significantly more abundant upon D-maltose addition in microsomes. Another difference between secretome upon addition of D-maltose versus addition of D-xylose, was that on D-maltose four of the above mentioned "non-classically secreted proteins" were found differentially more abundant extracellularly. Although rather unexpected, these proteins have been detected extracellularly in a number of studies. A few non-classically secreted proteins were detected in our study in statistically significant amounts to allow for positive protein identification. Some of these have been also identified extracellularly in previous work, such as the secretory thioredoxin TrxA (Shah et al. 2009), glucose-6-phosphate isomerase PgiA (Lu et al. 2010) or a putative dehydrogenase JGI208521 (Tsang

et al. 2009). In spite of this, both the mechanism of secretion and the extracellular function of some of these non-classically secreted proteins, especially of mitochondrial membrane proteins remain unaccountable. For this reason, we cannot exclude the possibility that these proteins became more abundant intracellularly on certain conditions (e.g. D-maltose induction) and were subsequently released after cell lysis.

Effects of D-xylose and D-maltose on the secretory organelles

In addition to secreted proteins, also proteins that have not previously been reported to be transcriptionally regulated by D-xylose or D-maltose were found in microsomes. This differential presence of proteins can be explained by protein-specific fluctuations of different post-transcriptional processes: (i) protein translation efficiencies, (ii) protein turnover rate, or (iii) efficiency of overall processing by secretory organelles. Comparative analysis of differential protein presence as assessed by a G-test indicated important differences between the non-transcriptionally related proteomic effects of D-xylose and D-maltose. The protein candidates that appear to be differentially present only upon D-maltose are distributed according to different categories as defined in **chapter 5**, e.g. translation, translocation to the ER, vesicular transport, mitochondrial-related and metabolism. However, the proteins differentially present only upon D-xylose addition belong to fewer categories. The proteins more abundant only upon D-xylose addition were mostly metabolic or mitochondrial. The proteins that were less abundant only on D-xylose were mostly related to protein translation. In addition to this difference in class distribution, fewer proteins were found on D-xylose that were very abundant (G-score > 8.0) compared to D-maltose or D-sorbitol control. Together, these results suggest that within the proteins that are not found to be transcriptionally regulated, D-maltose has a broader range of positive effects on different cellular processes compared to D-xylose. Processes that were particularly more represented only on D-maltose include protein translation and vesicular transport.

Apart from the proteins more abundant only on D-xylose or on D-maltose, several proteins were found more abundant on D-xylose and on D-maltose, relative to the non-induced D-sorbitol control (Fig 4). Some of these proteins (Fig. 4, asterisks) were not discussed on chapter 5, but their NSAF values were at least 3-fold increased under induction conditions, compared to NSAF values on D-sorbitol. Since D-xylose and D-maltose are signals for the expression of different classes of extracellular enzymes, the overlap of

secretory proteins more abundant on both conditions represents the general group of proteins necessary for protein secretion upon induction of extracellular enzymes. The proteins common to D-xylose and D-maltose were mostly 20S proteasomal core particle proteins or mitochondrial proteins. As mentioned during the discussion of the proteomic analysis of metabolic enzymes, oxaloacetate hydrolase appeared to be more abundant on D-xylose and D-maltose than on the D-sorbitol control, possibly indicating increased oxalate production under the experimental conditions used (constant external pH 3.5).

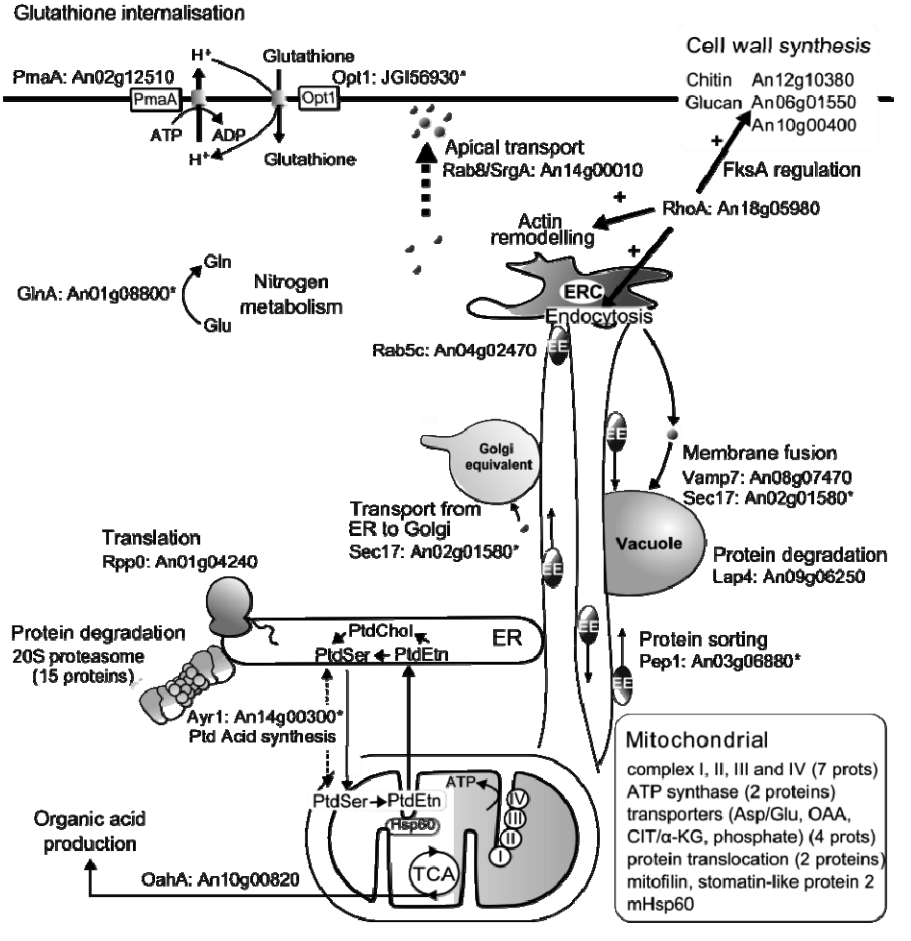

Figure 4. Major effects of D-maltose and D-xylose induction on the microsomal proteome of *A. niger*. asterisks: proteins > 3-fold increased upon induction, but statistically not found more abundant, as assessed by a G test ($p<0.05$). ERC: endocytic recycling compartment.

A glutathione uptake transport system was also more present upon induction of extracellular enzymes. This system includes the homolog of yeast Opt1, a symporter that transports protons and glutathione into the cell. It is likely that this system also involves the ATP-driven proton transporter PmaA, as this was also more abundant upon induction of secretion. Glutathione is a general antioxidant that also plays an important role in protein biosynthesis, by keeping amino acid residues in a reduced state. Another important system significantly more present under induction conditions is the one related to endocytosis, actin remodelling and polarised growth. The small GTPases Rab5c, Rab8/SrgA and RhoA best represent this system. RhoA is in addition a regulator of glucan synthesis protein FksA (An06g01550), also more abundant upon induction.

In **chapters 4 and 5** mitochondrial proteins are shown to be more abundant upon induction of secretion. The role of these proteins is still not completely clear. In eukaryotes, mitochondria and ER are inter-related (Hayashi et al. 2009). In addition, mitochondria and the proteasome form a high-order group whose disfunction is involved in neuropathologies, such as Parkinson disease (Höglinger et al. 2003; Duke et al. 2006). This inter-relation could explain why exactly the groups of the 20S proteasome and certain mitochondrial proteins are over-represented during induction of secretion. Based on this, a model is presented in which a larger fraction of mitochondria is associated to the ER in response to certain substrates (Fig. 5).

This association of mitochondria to the ER promotes the fine-tuning of mitochondrial and ER functions, e.g. for chaperone function and regulation of apoptosis, through the exchange of Ca^{2+} and ATP. If the cell is in a "high secretory state" (e.g. upon induction by D-xylose or D-maltose), mitochondria produce and export more ATP and this ATP can be locally used for the ATP-dependent assembly of the 20S proteasome at the ER surface. Simultaneously, as more proteins are produced in the ER, more mis-folded proteins will accumulate in this organelle. The mis-folded proteins can readily be degraded by the newly-assembled complete 26S proteasome.

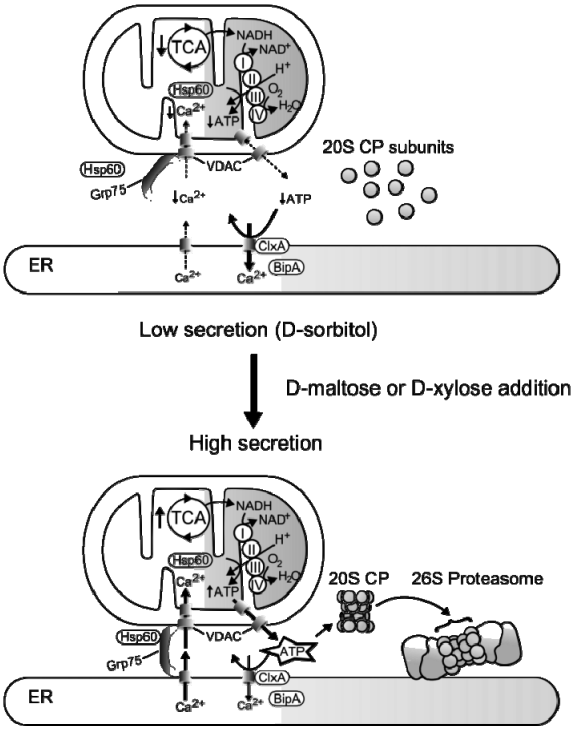

Figure 5. Model for the inter-relation of mitochondria with the ER during D-maltose and D-xylose induction. I to IV: mitochondrial complexes I to IV; Hsp60: Hsp60 chaperone (An12g04940); VDAC: porin protein (JGI 203715); Grp75: mortalin Hsp70 chaperone (An16g05090); ClxA: glycoprotein chaperone calnexin A (An01g08420); BipA: BiP ATPase for protein import and folding (An11g04180); 20S CP: proteasomal 20S core particle.

Concluding remarks

The largest paradox of protein secretion in filamentous fungi is the fact that homologous proteins are efficiently produced and secreted, whereas heterologous proteins tend to be modestly secreted, even when the corresponding genes are expressed under strong fungal promoters. This paradox is clearly not solved in by the work described in this thesis. However, the work presented here does provide some leads that could help solve this apparent contradiction. Induction of protein secretion initiates a series of important changes at various stages of protein secretion. In practice, this means that proteins in the secretory pathway must satisfy a series of requirements and this could be the basic difference between homologous and heterologous proteins. The use of strong gene

promoters to increase heterologous protein production could result in more “unfitted” proteins entering the secretory pathway, but the chances of success in completely traversing the secretory pathway would still be limited. What would be the requirements that proteins should fulfil in order to be efficiently synthesised and secreted? The list is extensive, ranging from optimal translation efficiency, targeting signals such as the presence of signal peptide, correct folding and glycosylation, and selection for export to vesicles as cargo proteins, just to mention a few. What became clear from the work presented here is that regulation by degradation plays a critical role during induction of protein secretion. In fact, because *A. niger* is such a good protein secretor, it is possible that the ER is very sensitive to mis-folded proteins and rapidly targets suspects, e.g. mis-folded proteins for proteasomal degradation. The proteasomal regulation in this model is simple. When the cell is in a "low secretory state", lower amounts of proteins are secreted. Also, less ATP is locally available, and therefore less proteasome is assembled and bound to the ER. Upon a secretion stimulus, this picture changes dramatically. Mitochondria are in closer contact to the ER and stimulate its function by interchange of Ca^{2+} and ATP. On the other hand, a local increase in ATP concentration near the ER will allow 20S assembly. Translation might also become more efficient through the action of regulators, such as Rpp0. As more extracellular enzymes enter the ER, the quality control by proteasomal degradation becomes more active. Since more proteins need to be secreted, it is expected that more secretory vesicles are created. In such case, it would be crucial to regulate the recycling of cell materials through endocytosis e.g. through Rab5c and RhoA and polarised secretion of vesicles e.g. through Rab8 and also RhoA.

To conclude, the induction of protein secretion leads to specific changes in both gene expression and protein abundance in *Aspergillus niger*. Throughout the work of this thesis, these changes have been investigated via a combination of gene expression analysis and secretory-organelle shotgun proteomics. With the advent of semi-quantitative and label-free shotgun proteomics, it has become possible to identify and quantify most of the proteins from complex protein mixtures. When applied to the analysis of organelles, shotgun proteomics has proven to be a powerful method to bridge eukaryal genomes and gene transcription to organelle-related phenotypes. In the future, the integrated analysis of the proteome is expected to reveal not only aspects of protein secretion but also many well-hidden secrets of the cell.

References

Abe N, Almenar-Queralt A, Lillo C, Shen Z, Lozach J, Briggs SP, Williams DS, Goldstein LS et al. (2009) Sunday driver interacts with two distinct classes of axonal organelles. J Biol Chem **284:** 34628-34639

Abenza JF, Pantazopoulou A, Rodríguez JM, Galindo A and Peñalva MA (2009) Long-distance movement of *Aspergillus nidulans* early endosomes on microtubule tracks. Traffic **10:** 57-75

Al-Sheikh H, Watson AJ, Lacey GA, Punt PJ, MacKenzie DA, Jeenes DJ, Pakula T, Penttila M et al. (2004) Endoplasmic reticulum stress leads to the selective transcriptional downregulation of the glucoamylase gene in *Aspergillus niger*. Mol Microbiol **53:** 1731-1742

Andersen JS, Wilkinson CJ, Mayor T, Mortensen P, Nigg EA and Mann M (2003) Proteomic characterization of the human centrosome by protein correlation profiling. Nature **426:** 570-574

Andersen MR, Lehmann L and Nielsen J (2009) Systemic analysis of the response of *Aspergillus niger* to ambient pH. Genome Biol **10:** R47

Andersen MR, Vongsangnak W, Panagiotou G, Salazar MP, Lehmann L and Nielsen J (2008) A trispecies *Aspergillus* microarray: comparative transcriptomics of three *Aspergillus* species. Proc Natl Acad Sci U S A **105:** 4387-4392

Anderson NL, Anderson NG, Haines LR, Hardie DB, Olafson RW and Pearson TW (2004) Mass spectrometric quantitation of peptides and proteins using Stable Isotope Standards and Capture by Anti-Peptide Antibodies (SISCAPA). J Proteome Res **3:** 235-244

Archer DB, Connerton IF and MacKenzie DA (2008) Filamentous fungi for production of food additives and processing aids. Adv Biochem Eng Biotechnol **111:** 99-147

Asanuma K, Yanagida-Asanuma E, Faul C, Tomino Y, Kim K and Mundel P (2006) Synaptopodin orchestrates actin organization and cell motility via regulation of RhoA signalling. Nat Cell Biol **8:** 485-491

Baker SE (2006) *Aspergillus niger* genomics: past, present and into the future. Med Mycol **44 Suppl 1:** S17-21

Bantscheff M, Schirle M, Sweetman G, Rick J and Kuster B (2007) Quantitative mass spectrometry in proteomics: a critical review. Anal Bioanal Chem **389:** 1017-1031

Barnes SE, Alcocer MJC and Archer DB (2008) siRNA as a molecular tool for use in *Aspergillus niger*. Biotechnology Letters **30:** 885-890

Belden WJ and Barlowe C (1996) Erv25p, a component of COPII-coated vesicles, forms a complex with Emp24p that is required for efficient endoplasmic reticulum to Golgi transport. J Biol Chem **271:** 26939-26946

Bendtsen JD, Nielsen H, von Heijne G and Brunak S (2004) Improved prediction of signal peptides: SignalP 3.0. J Mol Biol **340:** 783-795

Benen JA, Kester HC and Visser J (1999) Kinetic characterization of *Aspergillus niger* N400 endopolygalacturonases I, II and C. Eur J Biochem **259:** 577-585

Benjamini Y and Hochberg Y (1995) Controlling the False Discovery Rate: a Practical and Powerful Approach to Multiple testing. J R Statist Soc B **57:** 289-300

Berns K, Hijmans EM, Mullenders J, Brummelkamp TR, Velds A, Heimerikx M, Kerkhoven RM, Madiredjo M et al. (2004) A large-scale RNAi screen in human cells identifies new components of the p53 pathway. Nature **428:** 431-437

Bitton DA, Smith DL, Connolly Y, Scutt PJ and Miller CJ An integrated mass-spectrometry pipeline identifies novel protein coding-regions in the human genome. PLoS One **5:** e8949

Borrebaeck CA and Wingren C (2007) High-throughput proteomics using antibody microarrays: an update. Expert Rev Mol Diagn **7:** 673-686

Boutros M, Kiger AA, Armknecht S, Kerr K, Hild M, Koch B, Haas SA, Paro R et al. (2004) Genome-wide RNAi analysis of growth and viability in *Drosophila* cells. Science **303:** 832-835

Bradford MM (1976) A rapid and sensitive method for the quantitation of microgram quantities of protein utilizing the principle of protein-dye binding. Anal Biochem **72:** 248-254

Braun EL, Kang S, Nelson MA and Natvig DO (1998) Identification of the first fungal annexin: analysis of annexin gene duplications and implications for eukaryotic evolution. J Mol Evol **47:** 531-543

Brazma A, Hingamp P, Quackenbush J, Sherlock G, Spellman P, Stoeckert C, Aach J, Ansorge W et al. (2001) Minimum information about a microarray experiment (MIAME)-toward standards for microarray data. Nat Genet **29:** 365-371

Brun V, Dupuis A, Adrait A, Marcellin M, Thomas D, Court M, Vandenesch F and Garin J (2007) Isotope-labeled protein standards: toward absolute quantitative proteomics. Mol Cell Proteomics **6:** 2139-2149

Bustin SA (2002) Quantification of mRNA using real-time reverse transcription PCR (RT-PCR): trends and problems. J Mol Endocrinol **29:** 23-39

Carlile MJ (1995) The success of the hypha and mycelium. In *The growing fungus* (eds. N. A. R. Gow and G. M. Gad), Chapman & Hall, London.

Catalanotto C, Azzalin G, Macino G and Cogoni C (2000) Gene silencing in worms and fungi. Nature **404:** 245

Catalanotto C, Pallotta M, ReFalo P, Sachs MS, Vayssie L, Macino G and Cogoni C (2004) Redundancy of the two dicer genes in transgene-induced posttranscriptional gene silencing in *Neurospora crassa*. Mol Cell Biol **24:** 2536-2545

Chen PI, Kong C, Su X and Stahl PD (2009) Rab5 isoforms differentially regulate the trafficking and degradation of epidermal growth factor receptors. J Biol Chem **284:** 30328-30338

Cogoni C and Macino G (1997) Isolation of quelling-defective (*qde*) mutants impaired in posttranscriptional transgene-induced gene silencing in *Neurospora crassa*. Proc Natl Acad Sci U S A **94:** 10233-10238

Cogoni C and Macino G (1999) Gene silencing in *Neurospora crassa* requires a protein homologous to RNA-dependent RNA polymerase. Nature **399:** 166-169

Cogoni C and Macino G (1999) Posttranscriptional gene silencing in *Neurospora* by a RecQ DNA helicase. Science **286:** 2342-2344

de Graaff L, van den Broek H and Visser J (1988) Isolation and transformation of the pyruvate kinase gene of *Aspergillus nidulans*. Curr Genet **13:** 315-321

de Oliveira JM, van Passel MW, Schaap PJ and de Graaff LH Shotgun proteomics of *Aspergillus niger* microsomes upon D-xylose induction. Appl Environ Microbiol **76:** 4421-4429

de Vries RP, van den Broeck HC, Dekkers E, Manzanares P, de Graaff LH and Visser J (1999) Differential expression of three alpha-galactosidase genes and a single beta-galactosidase gene from *Aspergillus niger*. Appl Environ Microbiol **65:** 2453-2460

de Vries RP and Visser J (1999) Regulation of the feruloyl esterase (*faeA*) gene from *Aspergillus niger*. Appl Environ Microbiol **65:** 5500-5503

de Vries RP, Visser J and de Graaff LH (1999) CreA modulates the XlnR-induced expression on xylose of *Aspergillus niger* genes involved in xylan degradation. Res Microbiol **150:** 281-285

DiGuistini S, Liao NY, Platt D, Robertson G, Seidel M, Chan SK, Docking TR, Birol I et al. (2009) *De novo* genome sequence assembly of a filamentous fungus using Sanger, 454 and Illumina sequence data. Genome Biol **10:** R94

Dong MQ, Venable JD, Au N, Xu T, Park SK, Cociorva D, Johnson JR, Dillin A et al. (2007) Quantitative mass spectrometry identifies insulin signaling targets in *C. elegans*. Science **317:** 660-663

Dowzer CE and Kelly JM (1991) Analysis of the *creA* gene, a regulator of carbon catabolite repression in *Aspergillus nidulans*. Mol Cell Biol **11:** 5701-5709

Duke DC, Moran LB, Kalaitzakis ME, Deprez M, Dexter DT, Pearce RK and Graeber MB (2006) Transcriptome analysis reveals link between proteasomal and mitochondrial pathways in Parkinson's disease. Neurogenetics **7:** 139-148

Dunkley TP, Hester S, Shadforth IP, Runions J, Weimar T, Hanton SL, Griffin JL, Bessant C et al. (2006) Mapping the *Arabidopsis* organelle proteome. Proc Natl Acad Sci U S A **103:** 6518-6523

Dunkley TP, Watson R, Griffin JL, Dupree P and Lilley KS (2004) Localization of organelle proteins by isotope tagging (LOPIT). Mol Cell Proteomics **3:** 1128-1134

Dunn-Coleman NS, Bloebaum P, Berka RM, Bodie E, Robinson N, Armstrong G, Ward M, Przetak M et al. (1991) Commercial levels of chymosin production by *Aspergillus*. Biotechnology (N Y) **9:** 976-981

Edgar R, Domrachev M and Lash AE (2002) Gene Expression Omnibus: NCBI gene expression and hybridization array data repository. Nucleic Acids Res **30:** 207-210

Ehinger A, Denison SH and May GS (1990) Sequence, organization and expression of the core histone genes of *Aspergillus nidulans*. Mol Gen Genet **222:** 416-424

Espagne E, Lespinet O, Malagnac F, Da Silva C, Jaillon O, Porcel BM, Couloux A, Aury JM et al. (2008) The genome sequence of the model ascomycete fungus *Podospora anserina*. Genome Biol **9:** R77

Etienne W, Meyer MH, Peppers J and Meyer RA, Jr. (2004) Comparison of mRNA gene expression by RT-PCR and DNA microarray. Biotechniques **36:** 618-620, 622, 624-616

Fath S, Mancias JD, Bi X and Goldberg J (2007) Structure and organization of coat proteins in the COPII cage. Cell **129:** 1325-1336

Feldheim D, Yoshimura K, Admon A and Schekman R (1993) Structural and functional characterization of Sec66p, a new subunit of the polypeptide translocation apparatus in the yeast endoplasmic reticulum. Mol Biol Cell **4:** 931-939

Finkelstein DB (1987) Improvement of enzyme production in *Aspergillus*. Antonie Van Leeuwenhoek **53:** 349-352

Fire A, Xu S, Montgomery MK, Kostas SA, Driver SE and Mello CC (1998) Potent and specific genetic interference by double-stranded RNA in *Caenorhabditis elegans*. Nature **391:** 806-811

Fitzgerald A, Van Kan JA and Plummer KM (2004) Simultaneous silencing of multiple genes in the apple scab fungus, *Venturia inaequalis*, by expression of RNA with chimeric inverted repeats. Fungal Genet Biol **41:** 963-971

Foster LJ, de Hoog CL, Zhang Y, Zhang Y, Xie X, Mootha VK and Mann M (2006) A mammalian organelle map by protein correlation profiling. Cell **125:** 187-199

Geer LY, Markey SP, Kowalak JA, Wagner L, Xu M, Maynard DM, Yang X, Shi W et al. (2004) Open mass spectrometry search algorithm. J Proteome Res **3:** 958-964

Gerber SA, Rush J, Stemman O, Kirschner MW and Gygi SP (2003) Absolute quantification of proteins and phosphoproteins from cell lysates by tandem MS. Proc Natl Acad Sci U S A **100:** 6940-6945

Geysens S, Whyteside G and Archer DB (2009) Genomics of protein folding in the endoplasmic reticulum, secretion stress and glycosylation in the aspergilli. Fungal Genet Biol **46:** S121-S140

Gielkens M, Gonzalez-Candelas L, Sanchez-Torres P, van de Vondervoort P, de Graaff L, Visser J and Ramon D (1999) The *abf*B gene encoding the major alpha-L-arabinofuranosidase of *Aspergillus nidulans*: nucleotide sequence, regulation and construction of a disrupted strain. Microbiology **145 (Pt 3):** 735-741

Gilchrist A, Au CE, Hiding J, Bell AW, Fernández-Rodríguez J, Lesimple S, Nagaya H, Roy L et al. (2006) Quantitative proteomics analysis of the secretory pathway. Cell **127:** 1265-1281

Goldoni M, Azzalin G, Macino G and Cogoni C (2004) Efficient gene silencing by expression of double stranded RNA in *Neurospora crassa*. Fungal Genet Biol **41:** 1016-1024

Goosen T, van Engelenburg F, Debets F, Swart K, Bos K and van den Broek H (1989) Tryptophan auxotrophic mutants in *Aspergillus niger*: inactivation of the *trp*C gene by cotransformation mutagenesis. Mol Gen Genet **219:** 282-288

Gouka RJ, Punt PJ and van den Hondel CA (1997) Efficient production of secreted proteins by *Aspergillus*: progress, limitations and prospects. Appl Microbiol Biotechnol **47:** 1-11

Grinyer J, Kautto L, Traini M, Willows RD, Te'o J, Bergquist P and Nevalainen H (2007) Proteome mapping of the *Trichoderma reesei* 20S proteasome. Curr Genet **51:** 79-88

Grinyer J, McKay M, Herbert B and Nevalainen H (2004) Fungal proteomics: mapping the mitochondrial proteins of a *Trichoderma harzianum* strain applied for biological control. Curr Genet **45:** 170-175

Guest GM, Lin X and Momany M (2004) *Aspergillus nidulans* RhoA is involved in polar growth, branching, and cell wall synthesis. Fungal Genet Biol **41:** 13-22

Guillemette T, van Peij NN, Goosen T, Lanthaler K, Robson GD, van den Hondel CA, Stam H and Archer DB (2007) Genomic analysis of the secretion stress response in the enzyme-producing cell factory *Aspergillus niger*. BMC Genomics **8:** 158

Gun Lee D, Shin SY, Maeng CY, Jin ZZ, Kim KL and Hahm KS (1999) Isolation and characterization of a novel antifungal peptide from *Aspergillus niger*. Biochem Biophys Res Commun **263:** 646-651

Hasper AA, Trindade LM, van der Veen D, van Ooyen AJ and de Graaff LH (2004) Functional analysis of the transcriptional activator XlnR from *Aspergillus niger*. Microbiology **150:** 1367-1375

Hasper AA, Visser J and de Graaff LH (2000) The *Aspergillus niger* transcriptional activator XlnR, which is involved in the degradation of the polysaccharides xylan and cellulose, also regulates D-xylose reductase gene expression. Mol Microbiol **36:** 193-200

Hayashi T, Rizzuto R, Hajnoczky G and Su TP (2009) MAM: more than just a housekeeper. Trends Cell Biol **19:** 81-88

Henry C, Mouyna I and Latge JP (2007) Testing the efficacy of RNA interference constructs in *Aspergillus fumigatus*. Curr Genet **51:** 277-284

Höglinger GU, Carrard G, Michel PP, Medja F, Lombes A, Ruberg M, Friguet B and Hirsch EC (2003) Dysfunction of mitochondrial complex I and the proteasome: interactions between two biochemical deficits in a cellular model of Parkinson's disease. J Neurochem **86:** 1297-1307

Hornig-Do HT, Günther G, Bust M, Lehnartz P, Bosio A and Wiesner RJ (2009) Isolation of functional pure mitochondria by superparamagnetic microbeads. Anal Biochem **389:** 1-5

Huber LA, Pfaller K and Vietor I (2003) Organelle proteomics: implications for subcellular fractionation in proteomics. Circ Res **92:** 962-968

Huggett J, Dheda K, Bustin S and Zumla A (2005) Real-time RT-PCR normalisation; strategies and considerations. Genes Immun **6:** 279-284

Imbeaud S and Auffray C (2005) 'The 39 steps' in gene expression profiling: critical issues and proposed best practices for microarray experiments. Drug Discov Today **10:** 1175-1182

Irizarry RA, Bolstad BM, Collin F, Cope LM, Hobbs B and Speed TP (2003) Summaries of Affymetrix GeneChip probe level data. Nucleic Acids Res **31:** e15

Ishihama Y, Oda Y, Tabata T, Sato T, Nagasu T, Rappsilber J and Mann M (2005) Exponentially modified protein abundance index (emPAI) for estimation of absolute protein amount in proteomics by the number of sequenced peptides per protein. Mol Cell Proteomics **4:** 1265-1272

Jacobs DI, Olsthoorn MM, Maillet I, Akeroyd M, Breestraat S, Donkers S, van der Hoeven RA, van den Hondel CA et al. (2009) Effective lead selection for improved protein production in *Aspergillus niger* based on integrated genomics. Fungal Genet Biol **46 Suppl 1:** S141-152

Jacobs ME, DeSouza LV, Samaranayake H, Pearlman RE, Siu KW and Klobutcher LA (2006) The *Tetrahymena thermophila* phagosome proteome. Eukaryot Cell **5:** 1990-2000

Jafari P and Azuaje F (2006) An assessment of recently published gene expression data analyses: reporting experimental design and statistical factors. BMC Med Inform Decis Mak **6:** 27

Jami MS, Barreiro C, García-Estrada C and Martín JF Proteome analysis of the penicillin producer *Penicillium chrysogenum*: Characterization of protein changes during the industrial strain improvement. Mol Cell Proteomics

Jarai G, van den Hombergh H and Buxton FP (1994) Cloning and characterization of the *pepE* gene of *Aspergillus niger* encoding a new aspartic protease and regulation of *pepE* and *pepC*. Gene **145:** 171-178

Jensen ON (2006) Interpreting the protein language using proteomics. Nat Rev Mol Cell Biol **7:** 391-403

Jones GW, Hooley P, Farrington SM, Shawcross SG, Iwanejko LA and Strike P (1999) Cloning and characterisation of the *sagA* gene of *Aspergillus nidulans*: a gene which affects sensitivity to DNA-damaging agents. Mol Gen Genet **261:** 251-258

Jones T, Federspiel NA, Chibana H, Dungan J, Kalman S, Magee BB, Newport G, Thorstenson YR et al. (2004) The diploid genome sequence of *Candida albicans*. Proc Natl Acad Sci U S A **101:** 7329-7334

Jørgensen TR, Goosen T, Hondel CA, Ram AF and Iversen JJ (2009) Transcriptomic comparison of *Aspergillus niger* growing on two different sugars reveals coordinated regulation of the secretory pathway. BMC Genomics **10:** 44

Kabir MA, Kaminska J, Segel GB, Bethlendy G, Lin P, Della Seta F, Blegen C, Swiderek KM et al. (2005) Physiological effects of unassembled chaperonin Cct subunits in the yeast *Saccharomyces cerevisiae*. Yeast **22:** 219-239

Kamath RS, Fraser AG, Dong Y, Poulin G, Durbin R, Gotta M, Kanapin A, Le Bot N et al. (2003) Systematic functional analysis of the *Caenorhabditis elegans* genome using RNAi. Nature **421:** 231-237

Karaffa L and Kubíček CP (2003) *Aspergillus niger* citric acid accumulation: do we understand this well working black box? Appl Microbiol Biotechnol **61:** 189-196

Karaoglu D, Kelleher DJ and Gilmore R (1997) The highly conserved Stt3 protein is a subunit of the yeast oligosaccharyltransferase and forms a subcomplex with Ost3p and Ost4p. J Biol Chem **272:** 32513-32520

Karimi M, Inze D and Depicker A (2002) GATEWAY vectors for *Agrobacterium*-mediated plant transformation. Trends Plant Sci **7:** 193-195

Kautto L, Grinyer J, Birch D, Kapur A, Baker M, Traini M, Bergquist P and Nevalainen H (2009) Rapid purification method for the 26S proteasome from the filamentous fungus *Trichoderma reesei*. Protein Expr Purif **67:** 156-163

Kawajiri K, Ito A and Omura T (1977) Subfractionation of rat liver microsomes by immunoprecipitation and immunoadsorption methods. J Biochem **81:** 779-789

Kiel JA, van den Berg MA, Fusetti F, Poolman B, Bovenberg RA, Veenhuis M and van der Klei IJ (2009) Matching the proteome to the genome: the microbody of penicillin-producing *Penicillium chrysogenum* cells. Funct Integr Genomics **9:** 167-184

Kim KH, Brown KM, Harris PV, Langston JA and Cherry JR (2007) A proteomics strategy to discover β-glucosidases from *Aspergillus fumigatus* with two-dimensional page in-gel activity assay and tandem mass spectrometry. J Proteome Res **6:** 4749-4757

Kinoshita K, Takano M, Koseki T, Ito K and Iwano K (1995) Cloning of the *xynNB* gene encoding xylanase B from *Aspergillus niger* and its expression in *Aspergillus kawachii*. J Ferment Bioeng **79:** 422-428

Kislinger T, Cox B, Kannan A, Chung C, Hu P, Ignatchenko A, Scott MS, Gramolini AO et al. (2006) Global survey of organ and organelle protein expression in mouse: combined proteomic and transcriptomic profiling. Cell **125:** 173-186

Kohlheyer D, Eijkel JC, van den Berg A and Schasfoort RB (2008) Miniaturizing free-flow electrophoresis - a critical review. Electrophoresis **29:** 977-993

Krijgsveld J, Ketting RF, Mahmoudi T, Johansen J, Artal-Sanz M, Verrijzer CP, Plasterk RH and Heck AJ (2003) Metabolic labeling of *C. elegans* and *D. melanogaster* for quantitative proteomics. Nat Biotechnol **21:** 927-931

Kruszewska JS, Saloheimo M, Migdalski A, Orlean P, Penttilä M and Palamarczyk G (2000) Dolichol phosphate mannose synthase from the filamentous fungus *Trichoderma reesei* belongs to the human and *Schizosaccharomyces pombe* class of the enzyme. Glycobiology **10:** 983-991

Kusters-van Someren MA, Harmsen JA, Kester HC and Visser J (1991) Structure of the *Aspergillus niger pel*A gene and its expression in *Aspergillus niger* and *Aspergillus nidulans*. Curr Genet **20:** 293-299

Lee S, Jo M, Lee J, Koh SS and Kim S (2007) Identification of novel universal housekeeping genes by statistical analysis of microarray data. J Biochem Mol Biol **40:** 226-231

Leiter E, Szappanos H, Oberparleiter C, Kaiserer L, Csernoch L, Pusztahelyi T, Emri T, Pocsi I et al. (2005) Antifungal protein PAF severely affects the integrity of the plasma membrane of *Aspergillus nidulans* and induces an apoptosis-like phenotype. Antimicrob Agents Chemother **49:** 2445-2453

Levin AM, de Vries RP, Conesa A, de Bekker C, Talon M, Menke HH, van Peij NN and Wosten HA (2007) Spatial differentiation in the vegetative mycelium of *Aspergillus niger*. Eukaryot Cell **6:** 2311-2322

Lilley KS and Dupree P (2007) Plant organelle proteomics. Curr Opin Plant Biol **10:** 594-599

Lin JT, Griffith OM and Corse JW (1985) Subcellular fractionation of wheat leaf protoplasts by centrifugal elutriation. Anal Biochem **148:** 10-14

Lin SJ and Culotta VC (1996) Suppression of oxidative damage by *Saccharomyces cerevisiae* ATX2, which encodes a manganese-trafficking protein that localizes to Golgi-like vesicles. Mol Cell Biol **16:** 6303-6312

Link AJ, Eng J, Schieltz DM, Carmack E, Mize GJ, Morris DR, Garvik BM and Yates JR, 3rd (1999) Direct analysis of protein complexes using mass spectrometry. Nat Biotechnol **17:** 676-682

Loftus BJ, Fung E, Roncaglia P, Rowley D, Amedeo P, Bruno D, Vamathevan J, Miranda M et al. (2005) The genome of the basidiomycetous yeast and human pathogen *Cryptococcus neoformans*. Science **307:** 1321-1324

Lu X, Sun J, Nimtz M, Wissing J, Zeng AP and Rinas U The intra- and extracellular proteome of *Aspergillus niger* growing on defined medium with xylose or maltose as carbon substrate. Microb Cell Fact **9:** 23

Lubertozzi D and Keasling JD (2009) Developing *Aspergillus* as a host for heterologous expression. Biotechnol Adv **27:** 53-75

Lueking A, Horn M, Eickhoff H, Büssow K, Lehrach H and Walter G (1999) Protein microarrays for gene expression and antibody screening. Anal Biochem **270:** 103-111

Luers GH, Hartig R, Mohr H, Hausmann M, Fahimi HD, Cremer C and Volkl A (1998) Immuno-isolation of highly purified peroxisomes using magnetic beads and continuous immunomagnetic sorting. Electrophoresis **19:** 1205-1210

Lutfalla G and Uze G (2006) Performing quantitative reverse-transcribed polymerase chain reaction experiments. Methods Enzymol **410:** 386-400

MacCabe AP, Orejas M, Pérez-González JA and Ramón D (1998) Opposite patterns of expression of two *Aspergillus nidulans* xylanase genes with respect to ambient pH. J Bacteriol **180:** 1331-1333

Machida M, Asai K, Sano M, Tanaka T, Kumagai T, Terai G, Kusumoto K, Arima T et al. (2005) Genome sequencing and analysis of *Aspergillus oryzae*. Nature **438:** 1157-1161

Mallick P, Schirle M, Chen SS, Flory MR, Lee H, Martin D, Ranish J, Raught B et al. (2007) Computational prediction of proteotypic peptides for quantitative proteomics. Nat Biotechnol **25:** 125-131

Martens-Uzunova ES and Schaap PJ (2008) An evolutionary conserved d-galacturonic acid metabolic pathway operates across filamentous fungi capable of pectin degradation. Fungal Genet Biol **45:** 1449-1457

Martin F, Aerts A, Ahrén D, Brun A, Danchin EG, Duchaussoy F, Gibon J, Kohler A et al. (2008) The genome of *Laccaria bicolor* provides insights into mycorrhizal symbiosis. Nature **452:** 88-92

Martínez D, Berka RM, Henrissat B, Saloheimo M, Arvas M, Baker SE, Chapman J, Chertkov O et al. (2008) Genome sequencing and analysis of the biomass-degrading fungus *Trichoderma reesei* (syn. *Hypocrea jecorina*). Nat Biotechnol **26:** 553-560

Martínez D, Larrondo LF, Putnam N, Gelpke MD, Huang K, Chapman J, Helfenbein KG, Ramaiya P et al. (2004) Genome sequence of the lignocellulose degrading fungus *Phanerochaete chrysosporium* strain RP78. Nat Biotechnol **22:** 695-700

Matsuzaki F, Shimizu M and Wariishi H (2008) Proteomic and metabolomic analyses of the white-rot fungus *Phanerochaete chrysosporium* exposed to exogenous benzoic acid. J Proteome Res **7:** 2342-2350

McCann MC and Carpita NC (2008) Designing the deconstruction of plant cell walls. Curr Opin Plant Biol **11:** 314-320

Medina ML, Haynes PA, Breci L and Francisco WA (2005) Analysis of secreted proteins from *Aspergillus flavus*. Proteomics **5:** 3153-3161

Medina ML, Kiernan UA and Francisco WA (2004) Proteomic analysis of rutin-induced secreted proteins from *Aspergillus flavus*. Fungal Genet Biol **41:** 327-335

Meyer V (2008) Genetic engineering of filamentous fungi – Progress, obstacles and future trends. Biotechnol Adv **26:** 177-185

Meyer V, Arentshorst M, El-Ghezal A, Drews AC, Kooistra R, van den Hondel CA and Ram AF (2007) Highly efficient gene targeting in the *Aspergillus niger kus*A mutant. J Biotechnol **128:** 770-775

Moralejo FJ, Watson AJ, Jeenes DJ, Archer DB and Martin JF (2001) A defined level of protein disulfide isomerase expression is required for optimal secretion of thaumatin by *Aspegillus awamori*. Mol Genet Genomics **266:** 246-253

Morey JS, Ryan JC and Van Dolah FM (2006) Microarray validation: factors influencing correlation between oligonucleotide microarrays and real-time PCR. Biol Proced Online **8:** 175-193

Mouyna I, Henry C, Doering TL and Latgé JP (2004) Gene silencing with RNA interference in the human pathogenic fungus *Aspergillus fumigatus*. FEMS Microbiol Lett **237:** 317-324

Murone M and Simanis V (1996) The fission yeast *dma1* gene is a component of the spindle assembly checkpoint, required to prevent septum formation and premature exit from mitosis if spindle function is compromised. Embo J **15:** 6605-6616

Nakayashiki H, Hanada S, Nguyen BQ, Kadotani N, Tosa Y and Mayama S (2005) RNA silencing as a tool for exploring gene function in ascomycete fungi. Fungal Genet Biol **42:** 275-283

Napoli C, Lemieux C and Jorgensen R (1990) Introduction of a chimeric chalcone synthase gene into petunia results in reversible co-suppression of homologous genes *in trans*. Plant Cell **2:** 279-289

Nicolás FE, Torres-Martínez S and Ruiz-Vázquez RM (2003) Two classes of small antisense RNAs in fungal RNA silencing triggered by non-integrative transgenes. Embo J **22:** 3983-3991

Noguchi Y, Sano M, Kanamaru K, Ko T, Takeuchi M, Kato M and Kobayashi T (2009) Genes regulated by AoXlnR, the xylanolytic and cellulolytic transcriptional regulator, in *Aspergillus oryzae*. Appl Microbiol Biotechnol **85:** 141-154

Oda K, Kakizono D, Yamada O, Iefuji H, Akita O and Iwashita K (2006) Proteomic analysis of extracellular proteins from *Aspergillus oryzae* grown under submerged and solid-state culture conditions. Appl Environ Microbiol **72:** 3448-3457

Oda Y, Huang K, Cross FR, Cowburn D and Chait BT (1999) Accurate quantitation of protein expression and site-specific phosphorylation. Proc Natl Acad Sci U S A **96:** 6591-6596

Old WM, Meyer-Arendt K, Aveline-Wolf L, Pierce KG, Mendoza A, Sevinsky JR, Resing KA and Ahn NG (2005) Comparison of label-free methods for quantifying human proteins by shotgun proteomics. Mol Cell Proteomics **4:** 1487-1502

Oliveira JM, van der Veen D, de Graaff LH and Qin L (2008) Efficient cloning system for construction of gene silencing vectors in *Aspergillus niger*. Appl Microbiol Biotechnol **80:** 917-924

Olivo C, Vanni C, Mancini P, Silengo L, Torrisi MR, Tarone G, Defilippi P and Eva A (2000) Distinct involvement of cdc42 and RhoA GTPases in actin organization and cell shape in untransformed and Dbl oncogene transformed NIH3T3 cells. Oncogene **19:** 1428-1436

Olsen JV, de Godoy LM, Li G, Macek B, Mortensen P, Pesch R, Makarov A, Lange O et al. (2005) Parts per million mass accuracy on an Orbitrap mass spectrometer via lock mass injection into a C-trap. Mol Cell Proteomics **4:** 2010-2021

Ong SE, Blagoev B, Kratchmarova I, Kristensen DB, Steen H, Pandey A and Mann M (2002) Stable isotope labeling by amino acids in cell culture, SILAC, as a simple and accurate approach to expression proteomics. Mol Cell Proteomics **1:** 376-386

Otte S, Belden WJ, Heidtman M, Liu J, Jensen ON and Barlowe C (2001) Erv41p and Erv46p: new components of COPII vesicles involved in transport between the ER and Golgi complex. J Cell Biol **152:** 503-518

Paddison PJ, Silva JM, Conklin DS, Schlabach M, Li M, Aruleba S, Balija V, O'Shaughnessy A et al. (2004) A resource for large-scale RNA-interference-based screens in mammals. Nature **428:** 427-431

Panagiotou G, Andersen MR, Grotkjaer T, Regueira TB, Nielsen J and Olsson L (2009) Studies of the production of fungal polyketides in *Aspergillus nidulans* by using systems biology tools. Appl Environ Microbiol **75:** 2212-2220

Pantazopoulou A and Peñalva MA (2009) Organization and dynamics of the *Aspergillus nidulans* Golgi during apical extension and mitosis. Mol Biol Cell **20:** 4335-4347

Paper JM, Scott-Craig JS, Adhikari ND, Cuomo CA and Walton JD (2007) Comparative proteomics of extracellular proteins *in vitro* and *in planta* from the pathogenic fungus *Fusarium graminearum*. Proteomics **7:** 3171-3183

Patterson HD and Thompson R (1971) Recovery of inter-block information when block sizes are unequal. Biometrika **58:** 545-554

Pel HJ, de Winde JH, Archer DB, Dyer PS, Hofmann G, Schaap PJ, Turner G, de Vries RP et al. (2007) Genome sequencing and analysis of the versatile cell factory *Aspergillus niger* CBS 513.88. Nat Biotechnol **25:** 221-231

Petersen KL, Lehmbeck J and Christensen T (1999) A new transcriptional activator for amylase genes in *Aspergillus*. Mol Gen Genet **262:** 668-676

Pfaffl MW (2001) A new mathematical model for relative quantification in real-time RT-PCR. Nucleic Acids Res **29:** e45

Pontecorvo G, Roper JA, Hemmons LM, Macdonald KD and Bufton AW (1953) The genetics of *Aspergillus nidulans*. Adv Genet **5:** 141-238

Pratt JM, Simpson DM, Doherty MK, Rivers J, Gaskell SJ and Beynon RJ (2006) Multiplexed absolute quantification for proteomics using concatenated signature peptides encoded by QconCAT genes. Nat Protoc **1:** 1029-1043

Punt PJ, Seiboth B, Weenink XO, van Zeijl C, Lenders M, Konetschny C, Ram AF, Montijn R et al. (2001) Identification and characterization of a family of secretion-related small GTPase-encoding genes from the filamentous fungus *Aspergillus niger*: a putative *SEC4* homologue is not essential for growth. Mol Microbiol **41:** 513-525

Ramsby ML and Makowski GS (1999) Differential detergent fractionation of eukaryotic cells. Analysis by two-dimensional gel electrophoresis. Methods Mol Biol **112:** 53-66

Record E, Asther M, Moukha S, Marion D, Burlat V, Ruel K and Asther M (1998) Localization of a phosphatidylglycerol/phosphatidylinositol transfer protein in *Aspergillus oryzae*. Can J Microbiol **44:** 945-953

Rizzuto R, Pinton P, Carrington W, Fay FS, Fogarty KE, Lifshitz LM, Tuft RA and Pozzan T (1998) Close contacts with the endoplasmic reticulum as determinants of mitochondrial Ca2+ responses. Science **280:** 1763-1766

Roiz L, Smirnoff P, Bar-Eli M, Schwartz B and Shoseyov O (2006) ACTIBIND, an actin-binding fungal T2-RNase with antiangiogenic and anticarcinogenic characteristics. Cancer **106:** 2295-2308

Romano N and Macino G (1992) Quelling: transient inactivation of gene expression in *Neurospora crassa* by transformation with homologous sequences. Mol Microbiol **6:** 3343-3353

Rozen S and Skaletsky H (2000) Primer3 on the WWW for general users and for biologist programmers. Methods Mol Biol **132:** 365-386

Ruijter GJ, Panneman H, Xu D and Visser J (2000) Properties of *Aspergillus niger* citrate synthase and effects of *cit*A overexpression on citric acid production. FEMS Microbiol Lett **184:** 35-40

Ruijter GJ, van de Vondervoort PJ and Visser J (1999) Oxalic acid production by *Aspergillus niger*: an oxalate-non-producing mutant produces citric acid at pH 5 and in the presence of manganese. Microbiology **145 (Pt 9):** 2569-2576

Rusinol AE, Cui Z, Chen MH and Vance JE (1994) A unique mitochondria-associated membrane fraction from rat liver has a high capacity for lipid synthesis and contains pre-Golgi secretory proteins including nascent lipoproteins. J Biol Chem **269:** 27494-27502

Salit M (2006) Standards in gene expression microarray experiments. Methods Enzymol **411:** 63-78

Schröder A, Müller O, Stocker S, Salowsky R, Leiber M, Gassmann M, Lightfoot S, Menzel W et al. (2006) The RIN: an RNA integrity number for assigning integrity values to RNA measurements. BMC Mol Biol **7:** 3

Seaman MN, McCaffery JM and Emr SD (1998) A membrane coat complex essential for endosome-to-Golgi retrograde transport in yeast. J Cell Biol **142:** 665-681

Shah P, Atwood JA, Orlando R, El Mubarek H, Podila GK and Davis MR (2009) Comparative proteomic analysis of *Botrytis cinerea* secretome. J Proteome Res **8:** 1123-1130

Smyth GK (2004) Linear models and empirical bayes methods for assessing differential expression in microarray experiments. Stat Appl Genet Mol Biol **3:** Article3

Sonnhammer EL, von Heijne G and Krogh A (1998) A hidden Markov model for predicting transmembrane helices in protein sequences. Proc Int Conf Intell Syst Mol Biol **6:** 175-182

Sørensen LM, Lametsch R, Andersen MR, Nielsen PV and Frisvad JC (2009) Proteome analysis of *Aspergillus niger*: lactate added in starch-containing medium can increase production of the mycotoxin fumonisin B2 by modifying acetyl-CoA metabolism. BMC Microbiol **9:** 255

Štefanić S, Palm D, Svärd SG and Hehl AB (2006) Organelle proteomics reveals cargo maturation mechanisms associated with Golgi-like encystation vesicles in the early-diverged protozoan *Giardia lamblia*. J Biol Chem **281:** 7595-7604

Stricker AR, Mach RL and de Graaff LH (2008) Regulation of transcription of cellulases- and hemicellulases-encoding genes in *Aspergillus niger* and *Hypocrea jecorina* (*Trichoderma reesei*). Appl Microbiol Biotechnol **78:** 211-220

Stryer L (1995) Biochemistry. 4th ed., W H Freeman and Company, New York.

Sun J, Lu X, Rinas U and Zeng AP (2007) Metabolic peculiarities of *Aspergillus niger* disclosed by comparative metabolic genomics. Genome Biol **8:** R182

Taheri-Talesh N, Horio T, Araujo-Bazán L, Dou X, Espeso EA, Peñalva MA, Osmani SA and Oakley BR (2008) The tip growth apparatus of *Aspergillus nidulans*. Mol Biol Cell **19:** 1439-1449

Takamori S, Holt M, Stenius K, Lemke EA, Grønborg M, Riedel D, Urlaub H, Schenck S et al. (2006) Molecular anatomy of a trafficking organelle. Cell **127:** 831-846

Tanguay P, Bozza S and Breuil C (2006) Assessing RNAi frequency and efficiency in *Ophiostoma floccosum* and *O. piceae*. Fungal Genet Biol **43:** 804-812

Thompson JD, Higgins DG and Gibson TJ (1994) CLUSTAL W: improving the sensitivity of progressive multiple sequence alignment through sequence weighting, position-specific gap penalties and weight matrix choice. Nucleic Acids Res **22:** 4673-4680

Tian C, Beeson WT, Iavarone AT, Sun J, Marletta MA, Cate JH and Glass NL (2009) Systems analysis of plant cell wall degradation by the model filamentous fungus *Neurospora crassa*. Proc Natl Acad Sci U S A **106:** 22157-22162

Tichopad A, Dilger M, Schwarz G and Pfaffl MW (2003) Standardized determination of real-time PCR efficiency from a single reaction set-up. Nucleic Acids Res **31:** e122

Tsang A, Butler G, Powlowski J, Panisko EA and Baker SE (2009) Analytical and computational approaches to define the *Aspergillus niger* secretome. Fungal Genet Biol **46 Suppl 1:** S153-S160

Tsukagoshi N, Kobayashi T and Kato M (2001) Regulation of the amylolytic and (hemi-)cellulolytic genes in aspergilli. J Gen Appl Microbiol **47:** 1-19

Tuma RS, Beaudet MP, Jin X, Jones LJ, Cheung CY, Yue S and Singer VL (1999) Characterization of SYBR Gold nucleic acid gel stain: a dye optimized for use with 300-nm ultraviolet transilluminators. Anal Biochem **268:** 278-288

Urwyler S, Nyfeler Y, Ragaz C, Lee H, Müller LN, Aebersold R and Hilbi H (2009) Proteome analysis of *Legionella* vacuoles purified by magnetic immunoseparation reveals secretory and endosomal GTPases. Traffic **10:** 76-87

van den Berg MA, Albang R, Albermann K, Badger JH, Daran JM, Driessen AJ, García-Estrada C, Fedorova ND et al. (2008) Genome sequencing and analysis of the filamentous fungus *Penicillium chrysogenum*. Nat Biotechnol **26:** 1161-1168

van der Krol AR, Mur LA, Beld M, Mol JN and Stuitje AR (1990) Flavonoid genes in petunia: addition of a limited number of gene copies may lead to a suppression of gene expression. Plant Cell **2:** 291-299

van der Veen D, Oliveira JM, van den Berg WA and de Graaff LH (2009) Analysis of variance components reveals the contribution of sample processing to transcript variation. Appl Environ Microbiol **75:** 2414-2422

van Esse HP, Van't Klooster JW, Bolton MD, Yadeta KA, van Baarlen P, Boeren S, Vervoort J, de Wit PJ et al. (2008) The *Cladosporium fulvum* virulence protein Avr2 inhibits host proteases required for basal defense. Plant Cell **20:** 1948-1963

van Peij NN, Brinkmann J, Vrsanska M, Visser J and de Graaff LH (1997) β-Xylosidase activity, encoded by *xlnD*, is essential for complete hydrolysis of xylan by *Aspergillus niger* but not for induction of the xylanolytic enzyme spectrum. Eur J Biochem **245:** 164-173

van Peij NN, Gielkens MM, de Vries RP, Visser J and de Graaff LH (1998a) The transcriptional activator XlnR regulates both xylanolytic and endoglucanase gene expression in *Aspergillus niger*. Appl Environ Microbiol **64:** 3615-3619

van Peij NN, Visser J and de Graaff LH (1998b) Isolation and analysis of *xlnR*, encoding a transcriptional activator co-ordinating xylanolytic expression in *Aspergillus niger*. Mol Microbiol **27:** 131-142

vanKuyk PA, de Groot MJ, Ruijter GJ, de Vries RP and Visser J (2001) The *Aspergillus niger* D-xylulose kinase gene is co-expressed with genes encoding arabinan degrading enzymes, and is essential for growth on D-xylose and L-arabinose. Eur J Biochem **268:** 5414-5423

Vergés M, Havel RJ and Mostov KE (1999) A tubular endosomal fraction from rat liver: biochemical evidence of receptor sorting by default. Proc Natl Acad Sci U S A **96:** 10146-10151

Vishniac W and Santer M (1957) The thiobacilli. Bacteriol Rev **21:** 195-213

Vödisch M, Albrecht D, Leßing F, Schmidt AD, Winkler R, Guthke R, Brakhage AA and Kniemeyer O (2009) Two-dimensional proteome reference maps for the human pathogenic filamentous fungus *Aspergillus fumigatus*. Proteomics **9:** 1407-1415

Vongsangnak W, Salazar M, Hansen K and Nielsen J (2009) Genome-wide analysis of maltose utilization and regulation in aspergilli. Microbiology **155:** 3893-3902

Wälti MA, Villalba C, Buser RM, Grunler A, Aebi M and Kunzler M (2006) Targeted gene silencing in the model mushroom *Coprinopsis cinerea* (*Coprinus cinereus*) by expression of homologous hairpin RNAs. Eukaryot Cell **5:** 732-744

Ward PP, Chu H, Zhou X and Conneely OM (1997) Expression and characterization of recombinant murine lactoferrin. Gene **204:** 171-176

Waterhouse AM, Procter JB, Martin DM, Clamp M and Barton GJ (2009) Jalview Version 2--a multiple sequence alignment editor and analysis workbench. Bioinformatics **25:** 1189-1191

Wei C, Li J and Bumgarner RE (2004) Sample size for detecting differentially expressed genes in microarray experiments. BMC Genomics **5:** 87

Wei W, McCusker JH, Hyman RW, Jones T, Ning Y, Cao Z, Gu Z, Bruno D et al. (2007) Genome sequencing and comparative analysis of *Saccharomyces cerevisiae* strain YJM789. Proc Natl Acad Sci U S A **104:** 12825-12830

White S, McIntyre M, Berry DR and McNeil B (2002) The autolysis of industrial filamentous fungi. Crit Rev Biotechnol **22:** 1-14

Wilkins MR (1995) 2D Electrophoresis: From Protein Maps to Genomes. Proceedings of the International Meeting. Siena, Italy, September 5-7, 1994. Electrophoresis **16:** 1077-1322

Wolters DA, Washburn MP and Yates JR, 3rd (2001) An automated multidimensional protein identification technology for shotgun proteomics. Anal Chem **73:** 5683-5690

Wood V, Gwilliam R, Rajandream MA, Lyne M, Lyne R, Stewart A, Sgouros J, Peat N et al. (2002) The genome sequence of *Schizosaccharomyces pombe*. Nature **415:** 871-880

Wösten HA, Moukha SM, Sietsma JH and Wessels JG (1991) Localization of growth and secretion of proteins in *Aspergillus niger*. J Gen Microbiol **137:** 2017-2023

Wu CC, MacCoss MJ, Mardones G, Finnigan C, Mogelsvang S, Yates JR, 3rd and Howell KE (2004) Organellar proteomics reveals Golgi arginine dimethylation. Mol Biol Cell **15:** 2907-2919

Yamada O, Ikeda R, Ohkita Y, Hayashi R, Sakamoto K and Akita O (2007) Gene silencing by RNA interference in the koji mold *Aspergillus oryzae*. Biosci Biotechnol Biochem **71:** 138-144

Yan W, Aebersold R and Raines EW (2009) Evolution of organelle-associated protein profiling. J Proteomics **72:** 4-11

Yang YH and Speed T (2002) Design issues for cDNA microarray experiments. Nat Rev Genet **3:** 579-588

Yeung BG, Phan HL and Payne GS (1999) Adaptor complex-independent clathrin function in yeast. Mol Biol Cell **10:** 3643-3659

Yin QY, de Groot PW, de Koster CG and Klis FM (2008) Mass spectrometry-based proteomics of fungal wall glycoproteins. Trends Microbiol **16:** 20-26

Yuan XL, van der Kaaij RM, van den Hondel CA, Punt PJ, van der Maarel MJ, Dijkhuizen L and Ram AF (2008) *Aspergillus niger* genome-wide analysis reveals a large number of novel alpha-glucan acting enzymes with unexpected expression profiles. Mol Genet Genomics **279:** 545-561

Zichi D, Eaton B, Singer B and Gold L (2008) Proteomics and diagnostics: Let's Get Specific, again. Curr Opin Chem Biol **12:** 78-85

Zybailov B, Coleman MK, Florens L and Washburn MP (2005) Correlation of relative abundance ratios derived from peptide ion chromatograms and spectrum counting for quantitative proteomic analysis using stable isotope labeling. Anal Chem **77:** 6218-6224

Zybailov B, Mosley AL, Sardiu ME, Coleman MK, Florens L and Washburn MP (2006) Statistical analysis of membrane proteome expression changes in *Saccharomyces cerevisiae*. J Proteome Res **5:** 2339-2347

Appendix I

Supplementary figures

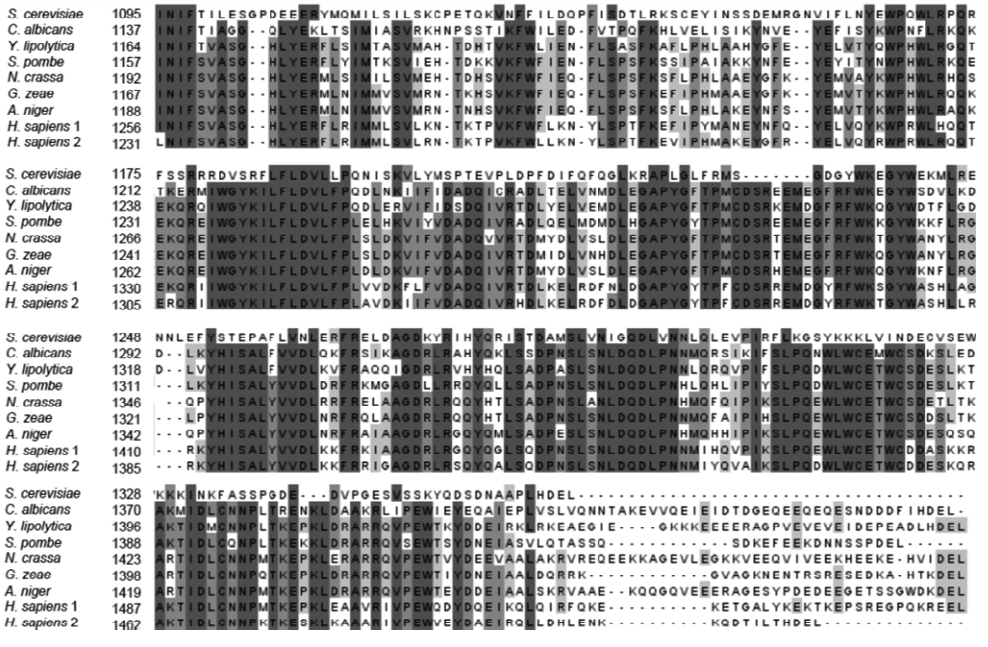

Figure S1. Sequence similarity comparison of the C-terminal portion of homologues of UDP-glucose: glycoprotein glucosyltransferase (UGGT). *S. cerevisiae*: *Saccharomyces cerevisiae*; *C. albicans: Candida albicans*; *Y. lipolytica*: *Yarrowia lipolytica*; *S. pombe*: *Schizosaccharomyces pombe*; *N. crassa*: *Neurospora crassa*; *G. zeae*: *Giberella zeae*; *A. niger*: *Aspergillus niger*; *H. sapiens* 1: *Homo sapiens* UGGT1; *H. sapiens* 2: *Homo sapiens* UGGT2.

Appendix II

Supplementary tables

Supplementary Table S1. Proteins identified from enriched microsomes. Proteins are listed according to functional annotation groups and according to relative protein abundance. Black box: significantly more abundant on D-maltose; grey box: significantly more abundant on D-xylose; white box: significantly less abundant on D-maltose or D-xylose compared to D-sorbitol; BR: biological replicate; NSAF: normalised spectral abundance factor; SS: signal sequence; ERRS: ER retention sequence; PL: protein length; M.: D-maltose addition; X.: D-xylose addition; S.: D-sorbitol addition.

Functional annotation	Protein description	Locus tag	SS	ERRS	PL	NSAF·10^4			G-score	G-score
						M.	X.	S.	M.	X.
BIOSYNTHETIC CARGO	glucan 1,4-α-glucosidase (glucoamylase) GlaA, *A. niger*	An03g06550	SP		640	63.9	41.3	25.8	16.76	3.61
BIOSYNTHETIC CARGO	similarity to hypothetical protein AAG27909.1, *A. thaliana*	An12g08720	SP		521	19.1	29.2	17.7	0.05	2.86
BIOSYNTHETIC CARGO	hypothetical protein SPBC1539.04, *S. pombe*	An07g02820	SP		287	23.5	26.1	25.8	0.11	0.00
BIOSYNTHETIC CARGO	catalase/peroxidase cpeB, *Streptomyces reticuli*	An01g01830			762	16.7	23.1	23.4	1.12	0.00
BIOSYNTHETIC CARGO	hypothetical protein B13I18.120, *N. crassa*	An09g06750	SP		277	9.6	18.5	13.6	0.68	0.76
BIOSYNTHETIC CARGO	hypothetical protein SPAC25H1.07, *S. pombe*	An07g03740	SP		946	12.5	16.7	17.7	0.89	0.03
BIOSYNTHETIC CARGO	similarity to estradiol 17-β-dehydrogenase HSD17B1, *Rattus norvegicus*	An09g00620	SP		283	11.7	15.6	13.3	0.10	0.18
BIOSYNTHETIC CARGO	catalase R CatR, *A. niger*	An01g01820	SP		730	9.8	15.4	10.9	0.05	0.80
BIOSYNTHETIC CARGO	acid α-amylase AamA, *A. niger*	An11g03340	SP		505	14.6	8.4	1.3	13.09	5.83
BIOSYNTHETIC CARGO	β-xylosidase XlnD, *A. niger*	An01g09960	SP		804	0.1	13.6	0.2	0.00	17.27
BIOSYNTHETIC CARGO	aspartic protease PepE, *A. niger*	An02g07210	SP		398	9.9	11.1	13.4	0.51	0.21
BIOSYNTHETIC CARGO	similarity to hypothetical protein YHR045w, *S. cerevisiae*	An07g03440	SA		564	9.3	13.3	4.8	1.42	4.08
BIOSYNTHETIC CARGO	hypothetical protein encoded by gene B18D24.80, *N. crassa*	An09g05630	SP		130	12.3	10.4	5.0	3.20	1.94
BIOSYNTHETIC CARGO	glucan synthase FKS, *Paracoccidioides brasiliensis*	An06g01550			1897	10.5	11.8	4.6	2.40	3.31
BIOSYNTHETIC CARGO	hypothetical protein CAE47902.1, *A. fumigatus*	An08g03970	SP		396	6.2	5.2	11.5	1.60	2.39
BIOSYNTHETIC CARGO	5-aminoimidazole-4-carboxamide ribotide transformylase Ade17, *S. cerevisiae*	An04g02060	SP		646	10.1	7.4	11.1	0.04	0.73
BIOSYNTHETIC CARGO	vacuolar alkaline phosphatase Pho8, *S. cerevisiae*	An07g07520	SA		595	5.9	11.1	7.2	0.12	0.82
BIOSYNTHETIC CARGO	hypothetical protein CAB91735.2, *N. crassa*	An04g06310	SP		257	7.1	10.2	10.6	0.72	0.01
BIOSYNTHETIC CARGO	similarity to hypothetical protein CAE76201.1, *N. crassa*	An11g09880			235	10.5	7.3	7.2	0.61	0.00
BIOSYNTHETIC CARGO	similarity to hypothetical proteinase encoded by 2SC3B6.04c, *Streptomyces coelicolor*	An03g02525	SP		199	7.0	10.4	9.8	0.47	0.02
BIOSYNTHETIC CARGO	β-glucosidase BglA/ bgl1, *A. niger*	An18g03570	SP		860	3.1	9.5	5.6	0.72	1.04
BIOSYNTHETIC CARGO	hypothetical protein CAD21051.1, *N. crassa*	An04g05430	SA		588	4.9	9.4	3.8	0.15	2.47
BIOSYNTHETIC CARGO	hypothetical protein AN1161.2, *A. nidulans*	An08g03493	SP		108	8.9	7.5	8.4	0.01	0.05
BIOSYNTHETIC CARGO	catalase cat1, *A. fumigatus*	An01g01550	SP		727	5.4	7.6	8.8	0.78	0.09
BIOSYNTHETIC CARGO	weak similarity to immunoglobulin κ light chain, *Mus musculus*	An11g01180	SP		282	5.7	8.6	3.2	0.69	2.56
BIOSYNTHETIC CARGO	similarity to β-1,3-glucanosyltransferase bgt1, *A. fumigatus*	An16g07040			423	6.8	8.3	2.8	1.77	2.91
BIOSYNTHETIC CARGO	similarity to 6-hydroxy-D-nicotine oxidase 6-HDNO, *Arthrobacter oxidans*	An07g02360	SP		551	6.0	6.7	7.8	0.23	0.08
BIOSYNTHETIC CARGO	hypothetical protein Afu3g10780, *A. fumigatus*	An02g06450	SA		351	5.2	3.9	7.8	0.52	1.35
BIOSYNTHETIC CARGO	hypothetical protein AN1817.2, *A. nidulans*	An04g08430	SP		92	5.8	6.9	7.1	0.12	0.00
BIOSYNTHETIC CARGO	capsule-associated protein CAP59, *Cryptococcus neoformans*	An18g00730	SA		430	5.2	4.8	6.3	0.11	0.21
BIOSYNTHETIC CARGO	1,3-β-glucanosyltransferase, putative, *Neosartorya fischeri* NRRL 181	53033	SP		537	3.8	6.2	2.7	0.20	1.46
BIOSYNTHETIC CARGO	cell wall protein Crh1, *S. cerevisiae*	An01g11010	SP		396	4.6	6.1	2.3	0.78	1.82
BIOSYNTHETIC CARGO	hypothetical cDNA MGC:7080, *Mus musculus*	An16g07380	SA		283	3.4	6.1	1.4	0.88	3.17
BIOSYNTHETIC CARGO	vacuolar aminopeptidase Ysci, *S. cerevisiae*	An09g06250			516	5.6	5.8	0.8	4.17	4.36
BIOSYNTHETIC CARGO	α-xylosidase AxlA strongly similar to α-xylosidase XylS, *Sulfolobus solfataricus*	An09g03300	SP		736	0.1	5.8	0.2	0.00	6.64

Functional annotation	Protein description	Locus tag	SS	ERRS	PL	NSAF·10^4			G-score	G-score
						M.	X.	S.	M.	X.
BIOSYNTHETIC CARGO	carboxypeptidase S1, *Penicillium janthinellum*	An03g05200	SP		566	2.5	4.6	5.7	1.35	0.12
BIOSYNTHETIC CARGO	1,3-β-glucanosyltransferase GelA strongly similar to gel1, *A. fumigatus*	An10g00400	SP		458	5.4	5.7	2.0	1.61	1.88
BIOSYNTHETIC CARGO	similarity to hypothetical protein B24H17.110, *N. crassa*	An14g00150	SP		207	4.6	2.2	5.6	0.10	1.59
BIOSYNTHETIC CARGO	extracellular α-glucosidase AgdA, *A. niger*	An04g06920	SP		985	5.5	3.0	1.5	2.54	0.56
BIOSYNTHETIC CARGO	hypothetical protein AAN52526.1, *Pichia angusta*	An12g03980	SP		176	4.2	3.6	5.2	0.09	0.29
BIOSYNTHETIC CARGO	similarity to cis cis-muconate lactonizing enzyme I TcMLE, Trichosporon cutaneum	An01g14730	SP		391	1.4	3.5	5.0	2.19	0.28
BIOSYNTHETIC CARGO	similarity to X-Pro dipeptidyl-peptidase IV, Xanthomonas maltophilia-	An04g02850			663	4.7	3.1	2.9	0.40	0.01
BIOSYNTHETIC CARGO	hypothetical protein 9G6.250, *N. crassa*	An18g03780	SA		986	2.3	4.7	1.4	0.18	1.78
BIOSYNTHETIC CARGO	chitin synthase C chsC, *A. fumigatus*	An09g04010			914	4.6	1.5	2.1	0.90	0.12
BIOSYNTHETIC CARGO	serine proteinase PepC, *A. niger*	An07g03880	SP		497	3.7	4.5	3.9	0.01	0.04
BIOSYNTHETIC CARGO	similarity to esterase from patent WO9802556-A2, *Alcaligenes* sp.	An05g02280	SP		375	0.3	2.6	4.5	4.48	0.49
BIOSYNTHETIC CARGO	hypothetical protein Afu4g03090, *A. fumigatus*	An14g02280	SA		342	2.8	4.5	2.7	0.00	0.47
BIOSYNTHETIC CARGO	weak similarity to tyrosinase melC2, Streptomyces lincolnensis-	An01g09220	SP		406	4.5	2.9	4.2	0.01	0.23
BIOSYNTHETIC CARGO	carboxypeptidase Y CpyA from patent WO9609397-A1, *A. niger*	An08g08750	SP		557	2.5	4.0	4.4	0.55	0.02
BIOSYNTHETIC CARGO	EcmA strongly similar to GPI-anchored cell wall organization protein ECM33, *S. pombe*	An04g01230	SP		401	2.4	4.3	2.9	0.05	0.26
BIOSYNTHETIC CARGO	BgtB similar to glucan 1,3-β-glucosidase Bgl2, *S. cerevisiae*	An03g05290	SP		464	3.0	4.1	4.2	0.20	0.00
BIOSYNTHETIC CARGO	lysophospholipase phospholipase B, *Penicillium notatum*	An02g13220	SP		640	3.2	4.1	1.8	0.37	0.88
BIOSYNTHETIC CARGO	1,3-β-glucanosyltransferase GelD strongly similar to gel3, *A. fumigatus*	An09g00670	SP		541	2.6	3.2	4.1	0.35	0.12
BIOSYNTHETIC CARGO	similarity to protein fragment SEQ ID NO:5981 from patent EP1108790-A2, Corynebacterium glutamicum	An09g06330	SP		679	0.8	2.0	4.0	2.38	0.70
BIOSYNTHETIC CARGO	similarity to human secreted protein fragment from patent WO9909155-A1, *H. sapiens*	An02g13670	SP		492	2.4	3.1	4.0	0.39	0.10
BIOSYNTHETIC CARGO	hypothetical protein Afu6g14120, *A. fumigatus*	An06g01030			500	3.6	3.8	1.3	1.15	1.27
BIOSYNTHETIC CARGO	chitin synthase C chsC, *A. fumigatus*	An12g10380			884	3.7	3.2	0.4	2.99	2.32
BIOSYNTHETIC CARGO	chitin synthase with a myosin motor-like domain csmA, *A. nidulans*	An02g02340			1760	3.3	3.6	3.0	0.02	0.06
BIOSYNTHETIC CARGO	hypothetical protein Afu6g14020, *A. fumigatus*	An05g01770	SP		438	1.7	3.5	1.5	0.02	0.84
BIOSYNTHETIC CARGO	hypothetical protein AAM96660.1, *Sphingobium chlorophenolicum*	An07g04850	SP		346	3.4	2.3	1.1	1.19	0.44
BIOSYNTHETIC CARGO	putative α-glucan synthase AgsE strongly similar to mok1p, *S. pombe*	An09g03070	SP		2426	3.3	2.6	2.0	0.33	0.07
BIOSYNTHETIC CARGO	hypothetical conserved protein SPAC12B10.16c, *S. pombe*	An04g08730	SP		536	1.0	1.2	3.2	1.18	0.93
BIOSYNTHETIC CARGO	chitin synthase C chsC, *A. fumigatus*	An03g06360			873	3.1	0.5	0.4	2.19	0.01
BIOSYNTHETIC CARGO	similarity to acid phosphatase precursor rPAP, *Rattus norvegicus*	An16g01730	SP		476	2.0	2.5	3.0	0.19	0.05
BIOSYNTHETIC CARGO	similarity to bladder tumour EST encoded protein 16 from patent DE19818619-A1, *H. sapiens*	An04g02540	SA		491	1.1	0.9	2.9	0.86	1.09
BIOSYNTHETIC CARGO	similarity to hypothetical protein CAD21295.1, *N. crassa*	An12g10210			289	1.8	2.8	0.4	0.91	1.90
BIOSYNTHETIC CARGO	extracellular protease precursor Bar1, *S. cerevisiae*	An18g01320	SP		456	1.2	2.6	2.0	0.22	0.07
BIOSYNTHETIC CARGO	proteinase SlpE, Streptomyces lividans	An12g08560	SP		624	1.9	2.5	1.5	0.05	0.26
BIOSYNTHETIC CARGO	similarity to glucanase ZmGnsN4 from patent WO200073470-A2, *Zea mays*	An04g03680			281	1.9	2.2	1.4	0.08	0.20
BIOSYNTHETIC CARGO	β-galactosidase LacA, *A. niger*	An01g12150	SP		1007	0.1	2.2	0.4	0.17	1.44
BIOSYNTHETIC CARGO	similarity to hypothetical protein CAD21056.1, *N. crassa*	An01g10460			544	1.0	0.8	2.1	0.45	0.61
BIOSYNTHETIC CARGO	chitin synthase chs1, *A. nidulans*	An07g05570			915	2.0	1.7	1.3	0.15	0.05

Functional annotation	Protein description	Locus tag	SS	ERRS	PL	NSAF·10^4			G-score	G-score
						M.	X.	S.	M.	X.
BIOSYNTHETIC CARGO	phospholipase B, *Penicillium notatum*	An09g01240	SP		638	1.8	1.6	1.4	0.05	0.01
BIOSYNTHETIC CARGO	Gly-X carboxypeptidase precursor Yscs, *S. cerevisiae*	An02g13740	SP		578	1.7	1.7	1.6	0.00	0.01
BIOSYNTHETIC CARGO	similarity to hypothetical protein ID880, Bradyrhizobium japonicum	An02g13300	SP		907	0.1	1.7	0.1	0.00	1.54
BIOSYNTHETIC CARGO	triacylglycerol lipase lipI, Geotrichum candidum	An09g02270	SP		592	1.3	1.7	1.5	0.03	0.01
BIOSYNTHETIC CARGO	similarity to carboxypeptidase D, *Penicillium janthinellum*	An06g00310	SP		605	1.2	1.6	1.5	0.03	0.01
BIOSYNTHETIC CARGO	hypothetical protein	An02g09290	SA		608	1.6	0.7	1.5	0.00	0.26
BIOSYNTHETIC CARGO	similarity to hypothetical protein KIAA1715, *H. sapiens*	An14g02990	SA		430	0.2	1.5	1.5	1.01	0.00
BIOSYNTHETIC CARGO	chitin synthase with a myosin motor-like domain csmA- *A. nidulans*	An02g02360			1855	1.4	1.3	0.1	1.53	1.36
BIOSYNTHETIC CARGO	putative α-glucan synthase AgsA strongly similar to ags1p, *S. pombe*	An04g09890	SP		2397	1.4	1.2	0.5	0.45	0.34
BIOSYNTHETIC CARGO	dipeptidyl aminopeptidase type IV DapB, *A. niger*	An02g11420			901	0.8	1.3	0.1	0.53	1.06
BIOSYNTHETIC CARGO	precursor of carboxypeptidase Kex1, *S. cerevisiae*	An08g00430	SP		612	1.2	1.0	0.2	0.79	0.59
BIOSYNTHETIC CARGO	α-galactosidase AglC, *A. niger*	An09g00260	SP		748	1.0	1.1	1.2	0.02	0.01
BIOSYNTHETIC CARGO	serine-type carboxypeptidase I cdpS, A. saitoi	An02g04690	SP		524	0.6	1.2	0.2	0.16	0.69
BIOSYNTHETIC CARGO	capsular associated protein CAP10, Filobasidiella neoformans	An01g04570	SP		997	0.8	0.8	0.1	0.48	0.55
CYTOSOLIC CHAPERONES	heat shock protein 70 hsp70, *Ajellomyces capsulatus*	An07g09990			637	53.5	40.0	72.4	2.84	9.44
CYTOSOLIC CHAPERONES	cyclophilin-like peptidyl prolyl cis-trans isomerase CypA, *A. niger*	An07g08300			174	28.9	32.6	64.9	14.25	10.91
CYTOSOLIC CHAPERONES	heat shock protein SspB, *A. niger*	An09g06590			702	27.5	38.6	46.8	5.05	0.78
CYTOSOLIC CHAPERONES	dnaK-type molecular chaperone Ssb2, *S. cerevisiae*	An16g09260			614	14.8	11.3	11.2	0.49	0.00
CYTOSOLIC CHAPERONES	heat shock protein Hsp70 ss1p, *S. pombe*	An08g05300			712	10.1	12.3	6.4	0.83	1.89
CYTOSOLIC CHAPERONES	transcription activator Adr1, *S. cerevisiae*	An04g05270			327	5.6	4.7	8.3	0.56	1.04
CYTOSOLIC CHAPERONES	zuotin Zuo1, *S. cerevisiae*	An14g01560			447	6.9	3.8	1.5	3.89	1.11
CYTOSOLIC CHAPERONES	estrogen receptor-binding cyclophilin cypD, Bos primigenius taurus	An07g05920			372	6.6	3.6	6.6	0.00	0.89
CYTOSOLIC CHAPERONES	similarity to hypothetical mold-specific protein MS8, *Ajellomyces capsulatus*	An12g02120			353	1.5	2.3	4.8	1.78	0.89
CYTOSOLIC CHAPERONES	hypothetical phosphate/PEP translocator protein At2g25520, *A. thaliana*	An02g08670			399	4.0	3.4	2.9	0.17	0.03
CYTOSOLIC CHAPERONES	small glutamine-rich tetratricopeptide protein SGT, *H. sapiens*	An08g01640			341	1.6	0.8	2.7	0.29	1.07
CYTOSOLIC CHAPERONES	stress-induced protein Sti1, *S. cerevisiae*	An12g00790			629	2.2	1.9	2.3	0.00	0.04
ERAD/UPR	cytoplasmic ubiquitin/ribosomal protein Cep52 *S. cerevisiae*	An01g02880			128	25.9	12.0	7.1	11.35	1.26

Functional annotation	Protein description	Locus tag	SS	ERRS	PL	NSAF·10^4			G-score	G-score
						M.	X.	S.	M.	X.
ERAD/UPR	proteasome 20S subunit Pre7, *S. cerevisiae*	An18g06700			260	21.0	21.8	0.5	25.00	26.18
ERAD/UPR	valosin-containing protein like AAA-ATPase Cdc48, *S. cerevisiae*	An04g09170			820	13.2	21.0	1.4	10.88	20.46
ERAD/UPR	proteasome 20S subunit Pre8, *S. cerevisiae*	An07g02010			279	17.2	15.2	3.3	10.45	8.36
ERAD/UPR	proteasome 20S subunit C2, *Rattus norvegicus*	An15g00510			262	15.9	14.8	0.5	18.29	16.82
ERAD/UPR	proteasome 20S subunit Pre10, *S. cerevisiae*	An18g06800			274	14.4	15.5	3.3	7.50	8.52
ERAD/UPR	proteasome 20S subunit Scl1, *S. cerevisiae*	An02g07040			244	12.7	12.2	1.6	9.81	9.23
ERAD/UPR	26S proteasome subunit 9, *H. sapiens*	An18g05070			424	6.8	7.0	11.3	1.14	1.03
ERAD/UPR	proteasome 20S subunit Pre6, *S. cerevisiae*	An02g10790			270	8.3	11.0	0.5	8.46	11.94
ERAD/UPR	proteasome 20S subunit Pre3, *S. cerevisiae*	An13g01210			199	8.1	10.4	4.6	0.97	2.34
ERAD/UPR	proteasome 20S subunit Pup2, *S. cerevisiae*	An02g03400			246	10.0	7.7	0.5	10.39	7.48
ERAD/UPR	proteasome 20S subunit Pre9, *S. cerevisiae*	An11g06720			255	9.6	9.5	0.5	10.02	9.90
ERAD/UPR	similarity to DnaJ protein SIS1, Cryptococcus curvatus	An04g01720			355	6.9	8.4	7.0	0.00	0.13
ERAD/UPR	proteasome 19S regulatory particle subunit Rpn5, *S. cerevisiae*	An11g09690			488	7.7	5.0	8.3	0.02	0.81
ERAD/UPR	26S proteasome regulatory subunit S2, *H. sapiens*	An18g03010			906	5.1	7.3	7.9	0.62	0.03
ERAD/UPR	26S proteasome regulatory chain 12 rpn12, *H. sapiens*	An07g10110	SP		356	6.9	5.3	4.0	0.77	0.18
ERAD/UPR	proteasome 19S regulatory particle subunit Rpt6, *S. cerevisiae*	An14g00180			389	6.9	3.0	2.3	2.33	0.09
ERAD/UPR	proteasome 20S subunit Pup3, *S. cerevisiae*	An04g01800			206	3.6	6.6	3.2	0.03	1.22
ERAD/UPR	interferon-induced double-stranded RNA-activated PK inhibitor P58, *H. sapiens*	An11g11250	SP		507	6.5	5.2	5.9	0.03	0.05
ERAD/UPR	proteasome 20S subunit Pre4, *S. cerevisiae*	An18g06680			260	6.2	5.9	2.5	1.60	1.41
ERAD/UPR	similarity to hypothetical eIF-3 p110 subunit, *C. elegans*	An17g02180	SP		255	2.1	6.0	3.6	0.39	0.63
ERAD/UPR	proteasome 20S subunit Pre2, *S. cerevisiae*	An11g01760			379	5.9	4.5	1.0	3.81	2.37
ERAD/UPR	proteasome 20S subunit Pre1, *S. cerevisiae*	An04g01870			203	5.8	4.9	0.6	4.75	3.70
ERAD/UPR	similarity to hypothetical cell growth regulator OS-9, *H. sapiens*	An16g08470	SP		509	2.3	3.4	5.4	1.25	0.46
ERAD/UPR	similarity to hypothetical protein SPCC285.11, *S. pombe*	An01g12370			525	3.5	5.3	5.2	0.35	0.00
ERAD/UPR	ubiquitin activating protein Uba1, *S. cerevisiae*	An15g06020			1034	2.8	5.1	3.6	0.11	0.26
ERAD/UPR	proteasome 19S regulatory particle subunit Rpn12, *S. cerevisiae*	An16g02210			278	2.7	2.9	5.1	0.78	0.62
ERAD/UPR	proteasome 20S subunit Pup1, *S. cerevisiae*	An11g04620			272	5.1	3.6	0.5	4.48	2.76
ERAD/UPR	similarity to hypothetical AAA family ATPase SCD8A.32c, *Streptomyces coelicolor*	An11g03970			596	4.1	4.1	5.0	0.09	0.10
ERAD/UPR	proteasome 19S regulatory particle subunit Rpn9, *S. cerevisiae*	An08g10710			381	4.8	2.1	3.8	0.12	0.45
ERAD/UPR	ubiquitin fusion degradation protein Ufd2, *S. cerevisiae*	An04g01730			1073	0.9	1.8	4.5	2.61	1.22
ERAD/UPR	hypothetical v-snare binding protein SPAC56F8.08, *S. pombe*	An07g01470			324	1.0	0.8	4.4	2.34	2.67
ERAD/UPR	proteasome 19S regulatory particle subunit Rpt5, *S. cerevisiae*	An18g05230			464	4.4	2.1	2.5	0.51	0.03
ERAD/UPR	protein phosphatase type 2C Ptc2, *S. cerevisiae*	An08g00830			424	4.3	2.8	2.1	0.73	0.08
ERAD/UPR	dnaJ protein homolog Ydj1, *S. cerevisiae*	An01g04280			413	3.4	2.8	4.1	0.07	0.23
ERAD/UPR	ubiquitin specific protease HAUSP, *H. sapiens*	An09g05480			1155	2.7	3.7	3.5	0.11	0.00
ERAD/UPR	proteasome 19S regulatory particle subunit Rpt4, *S. cerevisiae*	An18g06230			393	1.4	2.5	3.6	1.08	0.20
ERAD/UPR	similarity to tumour suppressor protein TSA305 from patent WO9928457-A1, *H. sapiens*	An01g12720	SP		689	2.3	2.2	3.2	0.14	0.18
ERAD/UPR	26S proteasome regulatory subunit rpn3p, *S. pombe*	An11g10380			645	0.8	1.3	3.0	1.33	0.75
ERAD/UPR	hypothetical protein TEMO, *Rattus norvegicus*	An04g05320			1963	2.9	1.8	0.5	1.95	0.83

Functional annotation	Protein description	Locus tag	SS	ERRS	PL	NSAF·10^4			G-score	G-score
						M.	X.	S.	M.	X.
ERAD/UPR	proteasome 19S regulatory particle subunit Rpn2, *S. cerevisiae*	An04g03270	SP		1147	0.8	2.3	1.5	0.18	0.17
ERAD/UPR	hypothetical protein YLR361c, *S. cerevisiae*	An03g02770	SA		551	1.7	1.8	1.7	0.00	0.01
ERAD/UPR	ERAD component similar to autocrine motility factor receptor Amfr, *Mus musculus*	An16g07970	SP		712	1.4	0.1	0.2	1.01	0.01
ERAD/UPR	similarity to naaladase II, *H. sapiens*	An02g06300			888	0.8	0.9	0.1	0.54	0.62
QC ER,GOLGI	protein disulfide isomerase A PdiA, *A. niger*	An02g14800	SP	HDEL	515	63.7	59.0	75.4	0.99	2.02
QC ER,GOLGI	dnaK-type molecular chaperone BipA, *A. niger*	An11g04180	SP	HDEL	672	64.1	52.7	71.7	0.43	2.91
QC ER,GOLGI	cyclophilin cypB, *A. nidulans*	An04g02020	SP	HEEL	212	49.9	41.2	37.4	1.80	0.19
QC ER,GOLGI	calcium-binding protein precursor cnx1p, *S. pombe*	An01g08420	SP		562	42.8	46.3	42.3	0.00	0.19
QC ER,GOLGI	dolichyl-diphosphooligosaccharide transferase 48kD chain DDOST, Gallus gallus	An07g04190	SP		458	29.6	38.0	42.3	2.23	0.23
QC ER,GOLGI	oligosaccharyltransferase α subunit OstA, *A. niger*	An02g14560	SP		503	26.6	35.7	41.1	3.14	0.38
QC ER,GOLGI	disulfide isomerase TigA, *A. niger*	An18g02020	SP	KDEL	359	20.5	25.9	32.9	2.90	0.85
QC ER,GOLGI	α-glucosidase AgdE strongly similar to ModA, *Dictyostelium discoideum*	An09g05880	SP		957	11.5	28.9	27.6	6.80	0.03
QC ER,GOLGI	protein disulfide-isomerase pdi1, *C. elegans*	An02g05890	SP		731	25.6	28.5	17.6	1.49	2.60
QC ER,GOLGI	PDI related protein A PrpA, *A. niger*	An01g04600	SP	HDEL	464	19.6	26.2	26.6	1.07	0.00
QC ER,GOLGI	UTP-glucose-1-phosphate uridylyltransferase Ugp1, *S. cerevisiae*	An12g00820			521	21.1	26.5	23.2	0.10	0.22
QC ER,GOLGI	similarity to ER membrane protein Shr3, *S. cerevisiae*	An04g07440			192	15.0	15.5	26.4	3.16	2.87
QC ER,GOLGI	mannose phospho-dolichol synthase dpm1, Hypocrea jecorina	An16g04330			245	23.1	23.9	26.0	0.17	0.09
QC ER,GOLGI	dnaK-type molecular chaperone LhsA, *A. niger*	An01g13220	SP	KDEL	1000	18.7	22.1	20.1	0.05	0.09
QC ER,GOLGI	golgi α-1 6 mannosyltransferase subunit Anp1, *S. cerevisiae*	An04g01260	SP		411	16.4	21.7	15.5	0.02	1.05
QC ER,GOLGI	similarity to oligosaccharyltransferase δ subunit Swp1, *S. cerevisiae*	An04g03495	SP		287	14.5	21.7	16.7	0.16	0.63
QC ER,GOLGI	glucosidase I Cwh41, *S. cerevisiae*	An15g01420	SP	HDEL	822	9.5	20.9	13.7	0.79	1.50
QC ER,GOLGI	glucosidase II β subunit strongly similar to 80K protein H precursor G19P1, *H. sapiens*	An13g00620	SP	KDEL	568	15.6	12.9	16.7	0.04	0.50
QC ER,GOLGI	mannosyltransferase Ktr5, *S. cerevisiae*	An18g02170	SA		502	10.0	16.3	8.0	0.22	2.90
QC ER,GOLGI	translation initiation factor 3 47 kDa subunit stt3p, *S. pombe*	An16g08570	SA		741	12.5	15.7	11.4	0.06	0.68
QC ER,GOLGI	dolichyl-diphosphooligosaccharide-protein transferase γ chain Ost3- *S. cerevisiae*	An02g14930	SP		335	9.9	15.3	8.1	0.17	2.24
QC ER,GOLGI	α-1,6-mannosyltransferase Ktr1, *S. cerevisiae*	An02g09940	SA		398	11.5	13.4	12.1	0.01	0.06
QC ER,GOLGI	similarity to hypothetical guanosine-diphosphatase, *S. pombe*	An08g04450			561	9.7	13.3	9.0	0.02	0.83
QC ER,GOLGI	glutamine-fructose-6-phosphate transaminase Gfa1, *S. cerevisiae*	An18g06820			694	8.8	7.4	12.9	0.79	1.51
QC ER,GOLGI	protein O-mannosyl transferase PmtA, *A. niger*	An07g10350			741	9.4	12.5	9.3	0.00	0.48
QC ER,GOLGI	α-1,6-mannosyltransferase kre2, C. albicans	An14g03910	SP		392	8.4	11.7	10.9	0.32	0.03
QC ER,GOLGI	class I α-mannosidase AAB62720.1, Spodoptera frugiperda	An06g01510	SP		869	6.8	10.3	5.5	0.12	1.44
QC ER,GOLGI	glycoprotein glucosyltransferase gpt1p, *S. pombe*	An07g06430	SP	KDEL	1495	6.9	9.9	9.1	0.30	0.04
QC ER,GOLGI	UDP-glucose 4-epimerase Gal10, *S. cerevisiae*	An14g03820			371	9.5	9.5	9.5	0.00	0.00
QC ER,GOLGI	dnaJ protein homolog Scj1, *S. cerevisiae*	An05g00880	SP	KDEL	416	5.4	7.6	9.1	0.94	0.13
QC ER,GOLGI	mannosyltransferase 1 PMT1, C. albicans	An11g09890			944	3.5	4.9	7.6	1.52	0.59
QC ER,GOLGI	peptidyl-prolyl isomerase FKBP-21, *N. crassa*	An01g06670	SP	KDEL	135	7.1	4.7	4.8	0.45	0.00
QC ER,GOLGI	weak similarity to heat shock protein dnaJ, Brucella ovis	An12g00580	SP		364	2.6	3.2	6.8	1.88	1.30
QC ER,GOLGI	tetratricopeptide repeat domain protein, *Neosartorya fischeri* NRRL 181	54765			300	6.8	5.7	6.5	0.01	0.05
QC ER,GOLGI	DnaJ-like protein MTJ1, *Mus musculus*	An18g06470	SP		397	3.5	2.5	6.2	0.77	1.64

Functional annotation	Protein description	Locus tag	SS	ERRS	PL	NSAF·10^4			G-score	G-score
						M.	X.	S.	M.	X.
QC ER,GOLGI	dolichyl-phosphate-D-mannose--protein O-mannosyltransferase Pmt4, *S. cerevisiae*	An16g08490	SA		771	3.2	6.0	4.9	0.36	0.11
QC ER,GOLGI	similarity to phosphoacetylglucosamine mutase AGM1, C. albicans	An18g05170			552	5.6	2.8	3.1	0.76	0.01
QC ER,GOLGI	endoplasmatic reticulum oxidising protein EroA, *A. niger*	An16g07620	SP	HEEL	600	5.5	5.6	5.0	0.03	0.03
QC ER,GOLGI	similarity to α-1,6-mannosyltransferase from patent JP09003097-A, Pichia pastoris	An05g02320	SP		406	3.4	5.5	1.6	0.68	2.31
QC ER,GOLGI	α-1,6-mannosyltransferase Hoc1, *S. cerevisiae*	An12g07020			421	2.8	4.9	2.2	0.08	1.11
QC ER,GOLGI	cell wall biosynthesis protein MNN9, C. albicans	An03g05010	SP		392	1.4	4.8	4.3	1.61	0.03
QC ER,GOLGI	mannosylation protein Lec35, Cricetulus griseus	An04g03130			299	1.8	4.5	2.2	0.04	0.84
QC ER,GOLGI	αN-acetylglucosamine transferase, K. lactis	An11g10260	SP		345	0.9	4.4	2.6	0.85	0.47
QC ER,GOLGI	aminonitrophenyl propanediol resistance protein Anp1, *S. cerevisiae*	An15g06230	SA		491	2.0	4.2	3.4	0.41	0.08
QC ER,GOLGI	protein influencing Itr1 expression Die2, *S. cerevisiae*	An02g02980	SP		566	1.3	2.1	3.9	1.33	0.57
QC ER,GOLGI	similarity to mannosyl transferase Alg9, *S. cerevisiae*	An08g07020	SA		602	2.7	2.8	3.7	0.16	0.10
QC ER,GOLGI	α-mannosidase Mns1, *S. cerevisiae*	An18g06220	SA		663	1.5	3.4	2.9	0.51	0.03
QC ER,GOLGI	similarity to α-1,6-mannosyltransferase Hoc1, *S. cerevisiae*	An03g01090	SP		413	1.8	3.3	2.2	0.04	0.21
QC ER,GOLGI	mannose-1-phosphate guanyltransferase MPG1, T. reesei	An04g04990	SP		364	2.1	1.7	3.2	0.26	0.45
QC ER,GOLGI	α-1,6-mannosyltransferase Hoc1, *S. cerevisiae*	An07g04940	SP		362	1.5	2.7	1.1	0.06	0.75
QC ER,GOLGI	glutamine-fructose-6-phosphate transaminase Gfa1, *S. cerevisiae*	An03g05940			702	2.6	0.1	0.2	2.48	0.01
QC ER,GOLGI	similarity to αN-acetylglucosamine transferase GNT1, K. lactis	An03g02990	SA		410	0.8	2.4	1.0	0.02	0.66
QC ER,GOLGI	hypothetical protein EAU36877, a novel DnaK-type chaperone, A. terreus	An12g10590	SP	HDEL	489	0.7	2.4	2.4	1.05	0.00
QC ER,GOLGI	hypothetical glycosyl transferase SPCC330.08, *S. pombe*	An18g05910	SP		545	0.6	1.8	1.2	0.21	0.13
QC ER,GOLGI	glucosyltransferase Alg8, *S. cerevisiae*	An04g08820	SP		580	1.3	1.7	0.7	0.20	0.47
QC ER,GOLGI	α-mannosidase msd2, *A. nidulans*	An02g11720			1089	0.5	1.2	1.1	0.22	0.01
(POST)GOLGI SORTING	clathrin heavy chain, Bos taurus	An04g02070			1711	11.3	15.0	31.4	9.81	5.88
(POST)GOLGI SORTING	vacuolar protein sorting-associated protein Vps35, *S. cerevisiae*	An16g04270			866	4.8	9.5	11.2	2.65	0.15
(POST)GOLGI SORTING	hypothetical polyphosphate synthase Vtc3, *S. cerevisiae*	An07g09800			794	5.8	9.2	10.3	1.29	0.06
(POST)GOLGI SORTING	vacuolar protein sorting protein Vps29, *S. cerevisiae*	An08g01030			195	3.8	5.1	10.0	2.84	1.63
(POST)GOLGI SORTING	embryogenesis protein H β 58, *Mus musculus*	An01g07320			352	2.7	4.4	9.2	3.72	1.79
(POST)GOLGI SORTING	carboxypeptidase Y-sorting protein Pep1, *S. cerevisiae*	An03g06880	SP		1472	6.2	7.9	2.6	1.54	2.86
(POST)GOLGI SORTING	similarity to negative regulator of Cdc Fourty two Vtc1, *S. cerevisiae*	An12g04710			808	4.4	6.8	7.9	1.02	0.08
(POST)GOLGI SORTING	protein involved in vacuolar protein sorting Mvp1, *S. cerevisiae*	An04g09250			558	1.7	7.6	2.6	0.16	2.61
(POST)GOLGI SORTING	hypothetical protein B13O20.120, similar to Vps68, *N. crassa*	An15g00540	SA		173	5.6	0.5	0.8	4.14	0.04
(POST)GOLGI SORTING	ergosterol biosynthesis protein Kes1, *S. cerevisiae*	An02g07570			415	1.8	2.0	4.1	0.90	0.76
(POST)GOLGI SORTING	hypothetical protein YKR088c, *S. cerevisiae*	An01g08590	SP		340	2.2	3.4	2.7	0.05	0.10
(POST)GOLGI SORTING	armadillo repeat-containing protein Vac8, *S. cerevisiae*	An14g05020			576	2.8	2.3	3.4	0.06	0.19
(POST)GOLGI SORTING	similarity to hypothetical protein CAD21062.1, *N. crassa*	An01g13390	SP		374	1.4	3.1	0.3	0.71	2.56
(POST)GOLGI SORTING	sorting nexin-1-like protein Vps5, *S. cerevisiae*	An01g08400			567	0.6	0.5	2.5	1.34	1.53
(POST)GOLGI SORTING	similarity to cation-dependent mannose 6-phosphate receptor precursor CD-MPR-Bos taurus	An18g03490	SP		324	1.6	2.5	2.0	0.03	0.06
(POST)GOLGI SORTING	clathrin associated epsin 2A, *H. sapiens*	An07g08220			525	0.6	0.5	2.2	0.98	1.15
(POST)GOLGI SORTING	glutamate carboxypeptidase II, *Rattus norvegicus*-	An18g03980	SA		765	0.1	1.8	1.5	1.35	0.02

Functional annotation	Protein description	Locus tag	SS	ERRS	PL	NSAF·10^4			G-score	G-score
						M.	X.	S.	M.	X.
(POST)GOLGI SORTING	P-type ATPase Drs2, *S. cerevisiae*	An15g01510			1193	1.7	1.7	0.5	0.63	0.66
(POST)GOLGI SORTING	transport ATPase Drs2, *S. cerevisiae*	An12g04500			1358	1.5	0.7	0.1	1.48	0.55
(POST)GOLGI SORTING	synexin (annexin VII), *Mus musculus*	An02g05210			449	0.7	1.4	1.4	0.25	0.00
LIPID, CYP450 ENZYMES	cytoplasmic ATP citrate lyase AclA strongly similar to ATP citrate lyase, *H. sapiens*	An11g00530			485	28.9	33.6	47.9	4.79	2.52
LIPID, CYP450 ENZYMES	cytochrome P450 oxidoreductase, *A. fumigatus* Af293	211877			541	35.3	36.2	47.3	1.73	1.49
LIPID, CYP450 ENZYMES	mitochondrial ATP citrate lyase strongly similar to ATP citrate lyase ACL1, Sordaria macrospora	An11g00510			656	40.2	41.1	43.4	0.12	0.06
LIPID, CYP450 ENZYMES	fatty acid synthase α subunit fas2p, *S. pombe*	An01g00060			1862	22.4	23.3	39.4	4.72	4.20
LIPID, CYP450 ENZYMES	cholesterol 24-hydroxylase, *Mus musculus*	An12g05360	SP		569	24.2	23.3	37.7	2.94	3.43
LIPID, CYP450 ENZYMES	similarity to fatty-acyl-CoA synthase β chain Fas1, *S. cerevisiae*	An01g00050			1464	25.8	23.6	35.8	1.63	2.52
LIPID, CYP450 ENZYMES	myo-inositol-1-phosphate synthase INO1, *A. thaliana*	An10g00530			533	28.7	32.6	33.9	0.43	0.02
LIPID, CYP450 ENZYMES	NADPH cytochrome P450 oxidoreductase CprA, *A. niger*	An08g07840	SP		695	22.6	30.0	26.7	0.35	0.18
LIPID, CYP450 ENZYMES	sterol transmethylase ERG6, C. albicans	An14g01590			377	29.2	28.9	22.4	0.90	0.83
LIPID, CYP450 ENZYMES	squalene synthase ERG9, Candida utilis	An12g01890		KQEL	472	18.3	28.5	25.6	1.20	0.15
LIPID, CYP450 ENZYMES	stearoyl-CoA desaturase P-ole1, *Pichia angusta*	An07g01960			456	15.7	20.4	25.9	2.54	0.67
LIPID, CYP450 ENZYMES	cytochrome P450 monooxygenase avnA, A. parasiticus	An18g02680	SP		493	15.8	18.8	25.6	2.31	1.02
LIPID, CYP450 ENZYMES	membrane steroid hormone-binding protein MSBP, Bos taurus	An16g04430	SA		169	13.3	15.5	23.8	3.04	1.79
LIPID, CYP450 ENZYMES	cytochrome b5, Mortierella alpina	An11g04370			138	17.8	22.9	21.6	0.37	0.03
LIPID, CYP450 ENZYMES	similarity to cyclopropane-fatty-acyl-phospholipid synthase, Escherichia coli	An13g00740			517	21.3	22.5	20.4	0.02	0.11
LIPID, CYP450 ENZYMES	C-8 sterol isomerase erg-1, *N. crassa*	An01g03350	SP		215	17.4	18.0	22.4	0.62	0.46
LIPID, CYP450 ENZYMES	membrane protein YBR159w, *S. cerevisiae*	An02g03570	SA		346	18.2	16.9	20.6	0.15	0.37
LIPID, CYP450 ENZYMES	squalene monooxygenase, *Rattus norvegicus*	An03g03770	SP		512	14.4	15.3	16.5	0.14	0.04
LIPID, CYP450 ENZYMES	oleate δ-12 desaturase odeA, *A. nidulans*	An08g05160			466	8.9	14.1	14.2	1.21	0.00
LIPID, CYP450 ENZYMES	similarity to hypothetical fatty acid elongation protein Sur4, *S. cerevisiae*	An01g10340			543	8.9	11.5	13.2	0.85	0.12
LIPID, CYP450 ENZYMES	PtdIns-PtdCho transfer protein Sec14, *S. cerevisiae*	An16g03590			322	4.3	1.4	12.5	4.16	10.20
LIPID, CYP450 ENZYMES	cytochrome P450 sterol δ22-desaturase Erg5, *S. cerevisiae*	An11g03230			534	10.2	12.0	11.4	0.07	0.01
LIPID, CYP450 ENZYMES	similarity to hypothetical protein YJL145w, *S. cerevisiae*	An09g06480			477	6.5	5.9	11.7	1.51	1.99
LIPID, CYP450 ENZYMES	eburicol 14 α-demethylase cyp51, Uncinula necator	An13g00090	SA		556	9.4	10.9	8.6	0.03	0.25
LIPID, CYP450 ENZYMES	C-3 sterol dehydrogenase/C-4 decarboxylase ERG26, C. albicans	An15g03090	SA		412	10.6	5.5	4.1	3.00	0.20
LIPID, CYP450 ENZYMES	phosphatidylethanolamine methyltransferase cho2p, *S. pombe*	An15g06310			1077	6.2	7.3	10.5	1.09	0.58
LIPID, CYP450 ENZYMES	similarity to protein involved in regulation of the inositol biosythesis Scs2, *S. cerevisiae*	An04g01310			286	6.4	6.0	10.4	1.01	1.22
LIPID, CYP450 ENZYMES	cytochrome P450 monooxygenase avnA, A. parasiticus	An18g00260	SP		513	6.5	4.0	9.9	0.72	2.52
LIPID, CYP450 ENZYMES	acyltransferase ataA, *A. nidulans*	An12g03960	SP		293	6.9	8.3	9.3	0.35	0.06
LIPID, CYP450 ENZYMES	hypothetical Ptd-glycerol/PtdIns transfer protein pltpao, A. oryzae	An02g03310	SP		174	9.2	0.5	0.7	8.50	0.04
LIPID, CYP450 ENZYMES	C-4 methyl sterol oxidase Erg25, *A. fumigatus* Af293	53706			298	8.2	8.2	9.2	0.05	0.06
LIPID, CYP450 ENZYMES	similarity to cytochrome P-450 cyp509A1, Cunninghamella elegans	An18g02700	SA		529	5.5	9.0	5.6	0.00	0.79
LIPID, CYP450 ENZYMES	cytochrome P450 monooxygenase stcS, *A. nidulans*	An12g02080			510	4.4	9.0	6.9	0.55	0.29
LIPID, CYP450 ENZYMES	cyclopropane-fatty-acyl-phospholipid synthase, Escherichia coli	An02g04530			510	6.9	9.0	7.4	0.02	0.16
LIPID, CYP450 ENZYMES	3-Hydroxy-3-methylglutaryl-CoA reductase HMGR, Gibberella fujikuroi	An07g08280	SA		1114	4.5	6.9	8.0	1.01	0.09

annotation	Protein description	Locus tag	SS	ERRS	PL	NSAF·10^4			G-score	G-score
						M.	X.	S.	M.	X.
LIPID, CYP450 ENZYMES	similarity to cytochrome P450 3A13, *Mus musculus*	An11g05680	SA		539	5.4	5.2	8.0	0.51	0.59
LIPID, CYP450 ENZYMES	lanosterol 14 α-demethylase (P450(14DM)) CYP51, Penicillium italicum	An11g02230	SP		512	4.4	7.9	3.8	0.04	1.48
LIPID, CYP450 ENZYMES	acetyl-CoA carboxylase SPAC56E4.04c, *S. pombe*	An12g04020			2283	7.9	6.9	7.1	0.04	0.00
LIPID, CYP450 ENZYMES	lipid metabolism protein YER044c from patent WO200058521-A2, *S. cerevisiae*	An02g03580	SP		149	6.5	6.7	7.8	0.14	0.10
LIPID, CYP450 ENZYMES	3-ketosphinganine reductase Tsc10, *S. cerevisiae*	An08g03450			322	1.0	2.5	7.7	5.83	2.72
LIPID, CYP450 ENZYMES	fatty acid elongase Fen1, *S. cerevisiae*	An02g09910			342	5.9	7.6	7.2	0.12	0.01
LIPID, CYP450 ENZYMES	hypothetical cytochrome P450 protein 2E4.050, *N. crassa*	An12g01360	SA		592	6.7	7.2	6.4	0.01	0.05
LIPID, CYP450 ENZYMES	phosphatidate cytidylyltransferase Cds1, *S. cerevisiae*	An07g09570			453	5.0	7.0	4.3	0.05	0.64
LIPID, CYP450 ENZYMES	similarity to cytochrome P450 3A7, *H. sapiens*	An18g02740	SP		590	6.7	6.9	5.9	0.05	0.07
LIPID, CYP450 ENZYMES	alkane-inducible cytochrome P450 alk2, Candida tropicalis	An11g07010	SP		502	4.0	6.6	3.4	0.06	1.09
LIPID, CYP450 ENZYMES	similarity to precursor of 3-oxoacyl-(acyl-carrier-protein) reductase, Cuphea lanceolata	An08g01930			338	0.3	6.1	0.4	0.01	6.11
LIPID, CYP450 ENZYMES	choline-transport mutant SCT1 supressor protein, *S. cerevisiae*	An14g03360	SA		711	5.3	4.9	6.0	0.05	0.11
LIPID, CYP450 ENZYMES	oxide squalene cyclising enzyme from patent JP08308568-A, Rattus rattus	An09g06490			735	2.2	6.0	2.3	0.00	1.72
LIPID, CYP450 ENZYMES	farnesyl-pyrophosphate synthase FPPS, Gibberella fujikuroi	An02g10350			346	5.9	4.9	4.9	0.09	0.00
LIPID, CYP450 ENZYMES	fatty acid hydroxylase Scs7, *S. cerevisiae*	An01g14200			372	3.2	5.6	5.2	0.52	0.01
LIPID, CYP450 ENZYMES	dihydrosphingosine/sphingosine phosphate lyase Dpl1, *S. cerevisiae*	An04g06200			636	1.5	4.1	5.5	2.42	0.21
LIPID, CYP450 ENZYMES	1-acyldihydroxyacetone-phosphate reductase Ayr1, *S. cerevisiae*	An14g00300			295	4.0	5.2	1.3	1.40	2.46
LIPID, CYP450 ENZYMES	very long chain fatty acid synthase Tsc13, *S. cerevisiae*	An04g05930			309	5.2	5.0	3.8	0.22	0.16
LIPID, CYP450 ENZYMES	diphosphomevalonate decarboxylase Erg19, *S. cerevisiae*	An04g01540			404	2.9	1.1	4.8	0.48	2.49
LIPID, CYP450 ENZYMES	cholesterol 7α-hydroxylase CYP7, Sus scrofa	An16g05910	SP		499	3.6	4.5	3.4	0.01	0.16
LIPID, CYP450 ENZYMES	hypothetical protein YOR311c, *S. cerevisiae*	An02g09160			384	3.1	3.5	4.4	0.24	0.10
LIPID, CYP450 ENZYMES	serine C-palmitoyltransferase chain Lcb1, *S. cerevisiae*	An06g01540			504	3.2	3.4	4.4	0.19	0.12
LIPID, CYP450 ENZYMES	O-methylsterigmatocystin oxidoreductase ordA, A. parasiticus	An10g00110	SP		537	4.2	0.2	0.2	4.25	0.01
LIPID, CYP450 ENZYMES	alkane-hydroxylating cytochrome P-450 CYP52A3-A, Candida maltosa	An02g10700	SP		506	4.0	1.6	2.3	0.46	0.13
LIPID, CYP450 ENZYMES	dihydrosphingosine-1-phosphate phosphatase Ysr3, *S. cerevisiae*	An14g05510			533	3.0	3.2	3.7	0.06	0.03
LIPID, CYP450 ENZYMES	phosphatidylserine synthase pS232, Triticum aestivum	An01g09480			236	2.3	3.4	1.7	0.10	0.64
LIPID, CYP450 ENZYMES	fatty acid ω-hydroxylase CYP505, *Fusarium oxysporum*	An16g02820			1104	0.9	2.0	3.4	1.61	0.35
LIPID, CYP450 ENZYMES	isotrichodermin C-15 hydroxylase Tri11, Fusarium sporotrichioides	An08g09230	SP		500	1.5	2.3	3.4	0.75	0.19
LIPID, CYP450 ENZYMES	similarity to hypoxia-induced protein #21 from patent WO200246465-A2, *H. sapiens*	An04g02050			348	0.3	1.3	3.4	2.97	0.95
LIPID, CYP450 ENZYMES	similarity to hypothetical membrane protein YPL087w, *S. cerevisiae*	An01g07640			299	2.5	3.3	3.0	0.05	0.01
LIPID, CYP450 ENZYMES	hypothetical protein involved in ergosterol biosynthesis SPBC646.08c, *S. pombe*	An11g11120			422	3.3	0.2	0.3	2.89	0.02
LIPID, CYP450 ENZYMES	cytochrome P450 52A4, Candida maltosa	An11g01550	SA		521	1.0	2.9	3.2	1.21	0.01
LIPID, CYP450 ENZYMES	Niemann-Pick C1 protein, *H. sapiens*	An11g05000	SP		1277	2.8	3.2	1.9	0.15	0.31
LIPID, CYP450 ENZYMES	diacylglycerol acyltransferase DAGAT, *A. thaliana*	An12g03600			456	1.6	2.6	3.1	0.48	0.06
LIPID, CYP450 ENZYMES	serine palmitoyltransferase 2 Lcb2, *S. cerevisiae*	An08g04100			676	2.1	3.1	2.1	0.00	0.18
LIPID, CYP450 ENZYMES	aminoalcoholphosphotransferase AAPT1, Glycine max-	An16g07870	SP		387	3.0	0.2	0.3	2.49	0.02
LIPID, CYP450 ENZYMES	hypothetical protein AN80 from patent WO9924580-A2, *A. nidulans*	An04g05000			420	0.8	1.9	2.8	1.22	0.15
LIPID, CYP450 ENZYMES	cytochrome P450 monooxygenase TRI4, Myrothecium roridum	An10g00150	SP		508	2.7	2.0	1.3	0.54	0.14
LIPID, CYP450 ENZYMES	very long-chain fatty acyl-CoA synthase Fat1, *S. cerevisiae*	An07g09190	SP		655	1.5	1.2	2.6	0.31	0.48

Functional annotation	Protein description	Locus tag	SS	ERRS	PL	NSAF·10^4			G-score	G-score
						M.	X.	S.	M.	X.
LIPID, CYP450 ENZYMES	weak similarity to phosphatidic acid phosphatase ATPAP2 from patent WO200005385-A1- *A. thaliana*	An04g03870	SP		298	2.5	0.3	0.4	1.61	0.02
LIPID, CYP450 ENZYMES	similarity to hypothetical protein BAC11036.1, *H. sapiens*	An01g01000	SA		410	0.8	2.4	1.0	0.02	0.66
LIPID, CYP450 ENZYMES	sterol δ14 15-reductase erg-3, *N. crassa*	An18g03480	SA		497	0.6	2.4	0.8	0.01	0.82
LIPID, CYP450 ENZYMES	phenylacetate hydroxylase pahA, P. chrysogenum	An16g01030	SP		516	0.6	2.3	2.3	1.00	0.00
LIPID, CYP450 ENZYMES	O-methylsterigmatocystin oxidoreductase ord1, A. flavus	An18g01200	SA		527	0.2	2.2	0.7	0.32	0.78
LIPID, CYP450 ENZYMES	cyclopropane-fatty-acyl-phospholipid synthase, Escherichia coli-	An03g02040			428	0.7	1.5	2.1	0.69	0.12
LIPID, CYP450 ENZYMES	hydroxymethylglutaryl-coenzyme A reductase hmg1p, *S. pombe*	An04g00610			674	2.1	0.1	0.2	1.81	0.01
LIPID, CYP450 ENZYMES	cytochrome P450 monooxygenase TRI4, Myrothecium roridum	An14g03110	SP		521	1.8	1.9	1.7	0.00	0.01
LIPID, CYP450 ENZYMES	cytochrome P450 sterol δ22-desaturase Erg5, *S. cerevisiae*	An01g02810			531	1.0	1.9	0.7	0.04	0.51
LIPID, CYP450 ENZYMES	similarity to phospholipase C type Isc2, *S. cerevisiae*	An11g01640			477	0.2	1.7	0.3	0.00	1.15
LIPID, CYP450 ENZYMES	linoleate diol synthase, Gaeumannomyces graminis	An12g01320	SP		1181	0.8	1.6	1.2	0.08	0.06
LIPID, CYP450 ENZYMES	CTP synthase Ura7, *S. cerevisiae*	An03g01310			579	0.2	0.2	1.6	1.25	1.35
LIPID, CYP450 ENZYMES	similarity to phosphatidylcholine-sterol O-acyltransferase Lcat, *Mus musculus*	An16g03640	SA		628	0.5	1.0	1.4	0.47	0.08
LIPID, CYP450 ENZYMES	benzoate 4-monooxygenase cytochrome P450 53 BphA, *A. niger*	An09g03500	SA		517	1.4	0.2	0.3	0.93	0.01
LIPID, CYP450 ENZYMES	lovastatin nonaketide synthase lovB, A. terreus	An02g08290			3907	0.8	0.0	0.0	0.94	0.00
LIPID, CYP450 ENZYMES	hypothetical protein of the UPF0028 family, *S. pombe*	An14g03050			1482	0.4	0.8	0.3	0.02	0.28
LIPID, CYP450 ENZYMES	fatty acid synthase α subunit fasA, *A. nidulans*	An09g02010			1617	0.7	0.1	0.1	0.60	0.00
METABOLISM	oxaloacetate acetyl hydrolase OahA, *A. niger*	An10g00820			299	89.7	88.9	45.6	14.62	14.19
METABOLISM	NADP-dependent glutamate dehydrogenase GdhA from patent WO9951756-A, *A. niger*	An04g00990			460	68.5	83.7	61.3	0.40	3.47
METABOLISM	5-methyltetrahydropteroyltriglutamate--homocysteine S-methyltransferase Met6, *S. cerevisiae*	An04g01750			774	46.2	52.3	61.3	2.10	0.71
METABOLISM	phosphogluconate dehydrogenase Gnd1, *S. cerevisiae*	An11g02040			508	44.4	53.0	58.6	1.96	0.27
METABOLISM	glutamine synthase Gln1, *S. cerevisiae*	An01g08800			375	43.0	41.1	25.3	4.66	3.80
METABOLISM	transaldolase Tal1, *S. cerevisiae*	An07g03850			324	26.7	25.9	40.5	2.85	3.25
METABOLISM	adenosylhomocysteinase, *H. sapiens*	An08g01960			449	34.5	35.9	27.5	0.80	1.13
METABOLISM	sorbitol dehydrogenase strongly similar to xylitol dehydrogenase xdh, Galactocandida mastotermitis	An07g01290			369	30.4	17.8	34.1	0.22	5.21
METABOLISM	mitochondrial aspartate aminotransferase mAspAT, *Mus musculus*	An04g06380			429	17.7	24.2	32.4	4.39	1.20
METABOLISM	transketolase Tkl1, *S. cerevisiae*	An08g06570			684	26.4	29.1	31.3	0.42	0.08
METABOLISM	adenylate kinase Adk1, *S. cerevisiae*	An07g10100			258	15.3	31.1	29.7	4.68	0.03
METABOLISM	glucose-6-phosphate isomerase PgiA strongly similar to Pgi1, *S. cerevisiae*	An16g05420			553	26.1	23.0	29.8	0.25	0.89
METABOLISM	cytoplasmic serine hydroxymethyltransferase Shm2, *S. cerevisiae*	An16g02970			471	27.0	27.4	24.5	0.12	0.15
METABOLISM	glyceraldehyde-3-phosphate dehydrogenase GpdA, *A. niger*	An16g01830			336	23.8	14.8	23.6	0.00	2.05
METABOLISM	aldehyde dehydrogenase AldA, *A. niger*	An08g07290			497	23.0	20.9	17.5	0.75	0.29
METABOLISM	phosphopyruvate hydratase ENO1, C. albicans	An18g06250			438	21.7	12.1	8.0	6.56	0.85
METABOLISM	malate dehydrogenase precursor MDH, *Mus musculus*	An15g00070			330	21.0	16.1	15.4	0.89	0.02
METABOLISM	phosphoglycerate dehydrogenase serA, Escherichia coli	An17g02330			480	4.7	7.7	20.8	11.07	6.28
METABOLISM	fructose-bisphosphate aldolase Fba1, *S. cerevisiae*	An02g07470			360	19.9	10.8	11.2	2.47	0.01

Functional annotation	Protein description	Locus tag	SS	ERRS	PL	NSAF·10^4			G-score	G-score
						M.	X.	S.	M.	X.
METABOLISM	S-adenosylmethionine synthase eth-1, *N. crassa*	An08g02700			387	15.7	13.3	19.8	0.47	1.30
METABOLISM	pyruvate carboxylase PycA, *A. niger*	An04g02090			1192	18.9	19.6	19.7	0.02	0.00
METABOLISM	IMP dehydrogenase IMH3, C. albicans	An07g08170			533	19.4	14.4	11.9	1.81	0.23
METABOLISM	D-arabinose dehydrogenase Ara1, *S. cerevisiae*	An01g06970			325	19.4	11.4	10.8	2.49	0.02
METABOLISM	sulfate adenylyltransferase sC, *A. nidulans*	An11g09790			574	18.4	12.1	14.3	0.53	0.18
METABOLISM	triose-phosphate-isomerase TpiA from patent WO8704464-A, *A. niger*	An14g04920			249	17.6	9.0	5.7	6.31	0.75
METABOLISM	aldo/keto reductase Gcy1, *S. cerevisiae*	An16g04770			319	3.0	3.7	16.7	10.46	9.01
METABOLISM	ornithine carbamoyltransferase ArgB, *A. niger*	An14g03400			371	2.6	4.1	16.5	11.25	7.90
METABOLISM	hypothetical sulphite reductase SPAC4C5.05c, *S. pombe*	An15g05770			1472	10.1	9.4	15.4	1.13	1.50
METABOLISM	argininosuccinate lyase ASAL, C. albicans	An01g06560			464	14.5	13.8	14.8	0.00	0.04
METABOLISM	phosphoglycerate kinase pgkA, *A. nidulans*	An08g02260			417	13.6	8.4	14.6	0.04	1.69
METABOLISM	acetate-inducible gene aciA, *A. nidulans*	An15g00410			360	14.5	11.3	13.4	0.05	0.18
METABOLISM	acetate--CoA ligase facA, *A. nidulans*	An04g05620			670	13.2	8.7	14.5	0.06	1.46
METABOLISM	glucose-6-phosphate 1-dehydrogenase GsdA, *A. niger*	An02g12140			510	8.6	10.1	14.5	1.54	0.81
METABOLISM	similarity to adenosine 5'-monophosphoramidase Hnt1, *S. cerevisiae*	An06g01890			135	5.5	3.3	14.4	4.10	7.47
METABOLISM	aspartate transaminase, Sus scrofa	An16g05570			419	4.8	9.7	14.0	4.60	0.78
METABOLISM	acetamidase amdS, *A. nidulans*	An12g01020			579	7.6	13.2	10.5	0.49	0.30
METABOLISM	hypothetical protein EAA59446.1, *A. nidulans*	An16g05930			300	13.2	12.3	12.6	0.01	0.00
METABOLISM	isocitrate lyase acuD, *A. nidulans*	An01g09270			538	9.7	12.9	7.0	0.45	1.77
METABOLISM	D-xylose reductase XyrA, *A. niger*	An01g03740			319	0.3	12.7	0.4	0.01	14.56
METABOLISM	adenosine kinase, Cricetulus griseus	An17g01330			353	11.8	7.4	5.5	2.33	0.28
METABOLISM	arginine-specific carbamoyl-phosphate synthase subunit Cpa2, *S. cerevisiae*	An16g04970			1173	5.4	6.7	11.6	2.36	1.35
METABOLISM	pyruvate kinase PkiA, *A. niger*	An07g08990			526	6.3	7.7	11.6	1.60	0.79
METABOLISM	phosphoglycerate mutase pgm, Bacillus subtilis	An16g02990			520	7.2	5.4	11.2	0.90	2.12
METABOLISM	argininosuccinate synthase Arg1, *S. cerevisiae*	An15g02340			417	11.0	8.4	6.5	1.15	0.24
METABOLISM	glucokinase GlkA, *A. niger*	An12g08610			495	11.0	6.0	8.7	0.28	0.48
METABOLISM	aldose 1-epimerase family protein, putative, A. clavatus NRRL 1	211875			398	5.6	10.6	10.8	1.63	0.00
METABOLISM	fumarate hydratase fumR, Rhizopus oryzae	An12g07850	SP		533	7.4	8.6	10.5	0.53	0.18
METABOLISM	ATP phosphoribosyltransferase his1p, *S. pombe*	An13g01080			307	10.1	5.0	3.8	2.95	0.16
METABOLISM	glycogen phosphorylase Gph1, *S. cerevisiae*	An08g05790			881	2.8	8.5	9.9	4.21	0.10
METABOLISM	NADPH-dependent aldehyde reductase, Sporobolomyces salmonicolor	An11g01120			381	7.6	9.7	6.5	0.09	0.65
METABOLISM	copper amine oxidase AO-I, *A. niger*	An13g00710			688	2.6	8.5	7.4	2.32	0.08
METABOLISM	hexokinase HxkA, *A. niger*	An02g14380			490	8.5	5.3	6.6	0.23	0.14
METABOLISM	methylmalonate-semialdehyde dehydrogenase MMSDH, *Rattus norvegicus*	An01g08430	SP		600	2.7	5.0	8.4	3.15	0.92
METABOLISM	phosphoglucomutase pgmB, *A. nidulans*	An02g07650			555	7.1	2.8	8.2	0.07	2.82
METABOLISM	sorbitol utilization protein sou2, C. albicans	An07g03570			293	7.7	4.6	4.0	1.17	0.05
METABOLISM	threonine synthase Thr4, *S. cerevisiae*	An16g02520			520	7.6	3.3	6.7	0.05	1.21
METABOLISM	orotidine-5-monophosphate pyrophosphorylase- *Ajellomyces capsulatus*	An04g08330			191	6.2	4.2	7.5	0.13	0.90
METABOLISM	soluble cytoplasmic fumarate reductase YEL047c, *S. cerevisiae*	An16g07150	SP		629	1.9	2.7	7.2	3.37	2.12

Functional annotation	Protein description	Locus tag	SS	ERRS	PL	NSAF·10^4			G-score	G-score
						M.	X.	S.	M.	X.
METABOLISM	orotate reductase pyrE, *A. nidulans*	An02g02910			544	4.1	7.1	3.1	0.14	1.62
METABOLISM	aldehyde dehydrogenase (NADP+), *H. sapiens*	An01g09260	SP		500	4.5	7.0	4.9	0.02	0.37
METABOLISM	pyrroline-5-carboxylate reductase ProC, Pseudomonas aeruginosa	An04g02800	SP		286	1.1	5.4	6.8	4.54	0.17
METABOLISM	similarity to succinate-semialdehyde dehydrogenase NAD(P)+ gabD, Escherichia coli	An15g01740	SA		650	5.1	6.0	6.6	0.19	0.03
METABOLISM	saccharopine dehydrogenase LYS1, C. albicans	An02g07500			377	6.5	3.1	4.5	0.38	0.25
METABOLISM	hypothetical agmatinase, Escherichia coli	An02g14210	SP	KDEL	422	2.3	6.2	4.0	0.48	0.48
METABOLISM	FAD-dependent L-sorbose dehydrogenase SDH, Gluconobacter oxydans-	An03g00130			535	6.2	0.2	0.2	6.85	0.01
METABOLISM	ribose 5-phosphate isomerase RPI, *Mus musculus*	An11g00470			273	2.7	2.3	6.2	1.37	1.83
METABOLISM	mannitol dehydrogenase mtlD, Pseudomonas fluorescens	An03g02430			488	2.4	1.3	6.1	1.67	3.42
METABOLISM	α-aminoadipate reductase large subunit lys2, P. chrysogenum	An04g05420			1430	3.4	5.7	2.1	0.30	1.77
METABOLISM	glutamate decarboxylase GAD1, *A. thaliana*	An08g08840			515	5.6	5.4	5.3	0.01	0.00
METABOLISM	uridine-monophosphate kinase Ura6, *S. cerevisiae*	An13g00440			212	5.5	2.1	4.3	0.16	0.74
METABOLISM	similarity to hypothetical dehydratase/racemase, Rhodococcus erythropolis	An02g10150			563	5.5	0.2	0.2	6.01	0.01
METABOLISM	alanine transaminase ALA2, Hordeum vulgare-	An11g02620			567	5.5	2.1	3.4	0.47	0.34
METABOLISM	aldehyde dehydrogenase AldA, *A. niger*	An04g03400			502	5.3	3.8	5.4	0.00	0.30
METABOLISM	nonribosomal peptide synthase MxaA, Stigmatella aurantiaca	An02g00210			1276	3.9	5.2	5.4	0.23	0.01
METABOLISM	D-lactate dehydrogenase dld, K. lactis	An12g00020			601	2.3	5.2	0.2	2.03	5.76
METABOLISM	uronate dehydrogenase from patent DE19604798-A1, *S. cerevisiae*	An08g01740			298	2.5	5.1	0.4	1.61	4.67
METABOLISM	α subunit of assimilatory sulfite reductase Met10, *S. cerevisiae*	An11g06670	SP		1045	4.2	2.3	5.1	0.09	1.06
METABOLISM	histidinol dehydrogenase his-3, *N. crassa*	An01g12570			866	2.1	4.7	2.8	0.11	0.45
METABOLISM	phosphoribosylaminoimidazolesuccinocarboxamide synthase Ade1, *S. cerevisiae*	An11g10150			300	4.6	1.5	3.9	0.06	1.10
METABOLISM	α-isopropylmalate synthase Leu4, *S. cerevisiae*	An01g13160			626	4.6	1.9	2.7	0.51	0.15
METABOLISM	similarity to hypothetical ureidoglycolate hydrolase SPAC19G12.04, *S. pombe*	An16g08100			254	1.3	0.4	4.6	2.02	4.32
METABOLISM	adenylosuccinate synthase ade2p, *S. pombe*	An01g13920			424	4.3	4.0	4.6	0.01	0.04
METABOLISM	hypothetical protein YMR099c, *S. cerevisiae*	An04g03750			320	3.7	2.0	4.5	0.08	0.99
METABOLISM	4-aminobutyrate transaminase gatA, *A. nidulans*	An17g00910			498	1.1	2.7	4.4	2.20	0.42
METABOLISM	morphine dehydrogenase, Pseudomonas putida	An03g04560			283	4.2	2.9	4.1	0.00	0.23
METABOLISM	tryptophan synthase Trp5, *S. cerevisiae*	An02g02170			723	4.0	1.6	4.1	0.00	1.13
METABOLISM	homocitrate synthase lys1, P. chrysogenum	An04g06210			465	3.9	1.0	3.1	0.10	1.15
METABOLISM	branched-chain-amino-acid aminotransferase Bat2, *S. cerevisiae*	An04g00430	SP		412	3.9	3.3	3.5	0.02	0.01
METABOLISM	galactokinase Gal1, *S. cerevisiae*	An16g04160			524	3.9	1.9	3.2	0.06	0.35
METABOLISM	D-amino-acid oxidase DAO, Fusarium solani-	An01g02430	SP		363	3.8	2.2	3.2	0.05	0.18
METABOLISM	cystathionine β-synthase Cys4, *S. cerevisiae*	An05g00160			587	0.5	0.2	3.8	2.70	4.13
METABOLISM	aspartate transaminase aspC, Methanobacterium thermoformicicum	An08g01000			386	2.5	3.5	3.0	0.05	0.03
METABOLISM	phosphoserine transaminase Ser1, *S. cerevisiae*	An02g00890			424	1.8	1.5	3.4	0.51	0.75
METABOLISM	formamidase fmdS, *A. nidulans*	An07g05830			413	3.4	2.8	2.8	0.05	0.00
METABOLISM	multifunctional pyrimidine biosynthesis enzyme pyrABCN, *A. nidulans*	An08g07420			2277	2.7	3.2	1.7	0.24	0.50
METABOLISM	prolidase, Aureobacterium esteraromaticum	An14g02080			480	2.4	3.2	3.0	0.05	0.01
METABOLISM	glycogen debranching protein GdbA strongly similar to Gdb1, *S. cerevisiae*	An01g06120			1539	3.0	1.8	2.4	0.05	0.09

Functional annotation	Protein description	Locus tag	SS	ERRS	PL	NSAF·10^4			G-score	G-score
						M.	X.	S.	M.	X.
METABOLISM	thiamin-phosphate pyrophosphorylase/hydroxyethylthiazole kinase Thi6, *S. cerevisiae*	An12g04660			519	2.7	3.0	1.3	0.53	0.71
METABOLISM	copper amine oxidase AO-I from patent JP08070872-A, *A. niger*	An03g00730			668	0.5	1.8	2.9	1.94	0.29
METABOLISM	6-phosphofructokinase PfkA, *A. niger*	An18g01670			783	1.0	2.9	2.2	0.48	0.10
METABOLISM	NADPH-dependent carbonyl reductase S1, Candida magnoliae-	An15g05450			266	2.8	0.3	0.5	1.81	0.03
METABOLISM	methionine adenosyltransferase regulatory β subunit MAT II, *H. sapiens*	An02g10660			324	0.3	0.8	2.8	2.24	1.13
METABOLISM	bifunctional purine synthase ade1p, *S. pombe*	An15g00570			808	0.7	2.8	2.7	1.36	0.00
METABOLISM	L-iditol 2-dehydrogenase Sor1, *S. cerevisiae*	An12g00030			358	0.3	2.8	0.4	0.01	2.10
METABOLISM	3-isopropylmalate dehydratase LEU2, Phycomyces blakesleeanus	An02g03250			772	1.8	2.7	1.9	0.00	0.15
METABOLISM	saccharopine reductase LYS3, Magnaporthe grisea	An04g05260			448	1.7	2.6	0.9	0.26	0.92
METABOLISM	proclavaminic acid amidino hydrolase pah, Streptomyces clavuligerus	An03g05070	SP		382	1.4	2.6	1.7	0.03	0.19
METABOLISM	adenylosuccinate lyase ADSL, *H. sapiens*	An02g04020			483	0.7	0.2	2.4	1.06	2.27
METABOLISM	NADP-dependent malate dehydrogenase mdh, *H. sapiens*	An05g00930			596	0.2	0.5	2.4	2.27	1.45
METABOLISM	pentafunctional enzyme aroM, *A. nidulans*	An08g06810			1587	1.1	2.2	0.4	0.36	1.37
METABOLISM	ribonucleotide reductase from patent JP10014582-A, *H. sapiens*	An04g01080			865	1.9	2.2	0.8	0.48	0.73
METABOLISM	malate synthase acuE, *A. nidulans*	An15g01860			542	0.2	1.8	2.2	1.91	0.03
METABOLISM	salicylaldehyde dehydrogenase doxF, Pseudomonas sp.	An15g04100			478	0.2	0.2	1.9	1.52	1.63
METABOLISM	methylenetetrahydrofolate reductase Met13, *S. cerevisiae*	An02g03270			626	0.9	0.1	1.9	0.39	1.75
METABOLISM	fructose-1,6-bisphosphatase fbpA, A. oryzae	An04g05300			355	0.3	1.8	1.1	0.48	0.16
METABOLISM	glycogen branching enzyme GbeA strongly similar Glc3, *S. cerevisiae*	An14g04190			692	1.1	1.2	1.7	0.13	0.09
METABOLISM	glycogen synthase, *N. crassa*	An02g10310			713	0.1	0.9	1.6	1.45	0.23
METABOLISM	urease URE1, *Cryptococcus neoformans*	An01g03550			831	0.9	1.6	1.1	0.02	0.10
METABOLISM	dihydroxy-acid dehydratase Ilv3, *S. cerevisiae*	An14g03280			615	1.6	1.6	1.5	0.00	0.01
METABOLISM	trifunctional C1-tetrahydrofolate synthase Ade3, *S. cerevisiae*	An02g12420			930	0.3	0.9	0.7	0.12	0.02
METABOLISM	serine O-acetyltransferase cysA, *A. nidulans*	An09g02800			1779	0.5	0.4	0.8	0.05	0.18
METABOLISM	β-glucosidase precursor bgl2, Coccidioides immitis	An15g01890			936	0.6	0.7	0.1	0.28	0.38
MITOCHONDRIAL	mitochondrial ADP/ATP carrier anc1p, *S. pombe*	An18g04220			319	103.5	117.3	93.2	0.53	2.74
MITOCHONDRIAL	H+-transporting ATP synthase β chain, *N. crassa*	An14g04180			417	111.5	94.9	88.2	2.73	0.25
MITOCHONDRIAL	mitochondrial phosphate transport protein Mir1, *S. cerevisiae*	An01g13600	SP		314	58.9	66.9	46.7	1.39	3.59
MITOCHONDRIAL	core protein II of ubiquinol--cytochrome c reductase CAA42214.1, Bos primigenius taurus	An09g06650			458	33.4	40.7	45.7	1.92	0.28
MITOCHONDRIAL	mitochondrial F1-ATPase α-subunit Atp1, *S. cerevisiae*	An16g07410	SP		556	45.5	44.3	32.0	2.37	1.98
MITOCHONDRIAL	cytochrome-c peroxidase precursor Ccp1, *S. cerevisiae*	An04g04060			364	34.9	33.4	45.3	1.35	1.80
MITOCHONDRIAL	mitochondrial heat shock protein Hsp60, *S. cerevisiae*	An12g04940			587	43.5	45.0	26.8	4.02	4.67
MITOCHONDRIAL	F1Fo-ATP synthase subunit 7 ATP7, K. lactis	An15g01710			173	29.0	40.1	21.8	1.04	5.52
MITOCHONDRIAL	outer mitochondrial membrane protein porin, A. clavatus NRRL 1	203715			350	27.8	39.4	30.8	0.16	1.06
MITOCHONDRIAL	mitochondrial-processing peptidase subunit β strongly similar to β-MPP, *N. crassa*	An01g12210			479	27.4	37.1	13.8	4.57	11.01
MITOCHONDRIAL	cytochrome c1 of ubiquinol--cytochrome c reductase CYT-1, *N. crassa*	An01g06180	SP		316	23.3	36.8	18.5	0.56	6.17
MITOCHONDRIAL	cytochrome-b5 reductase Mcr1, *S. cerevisiae*	An01g03570	SA		322	26.9	36.1	16.5	2.48	7.45
MITOCHONDRIAL	succinate dehydrogenase Sdh1, *S. cerevisiae*	An02g12770			646	30.6	34.5	21.9	1.44	2.81
MITOCHONDRIAL	precursor of dihydrolipoamide dehydrogenase Lpd1, *S. cerevisiae*	An07g06840	SP		514	26.0	29.6	34.1	1.10	0.32

Functional annotation	Protein description	Locus tag	SS	ERRS	PL	NSAF·10^4			G-score	G-score
						M.	X.	S.	M.	X.
MITOCHONDRIAL	iron-sulfur subunit of ubiquinol--cytochrome c reductase rip1p, *S. pombe*	An14g04080	SP		238	24.7	33.7	16.9	1.46	5.67
MITOCHONDRIAL	78 kD subunit of NADH:ubiquinone reductase NDUFS1, Bos taurus	An09g06850			737	27.1	32.4	17.1	2.29	4.81
MITOCHONDRIAL	nucleoside-diphosphate kinase NDK-1, *N. crassa*	An09g05870			153	25.8	30.0	31.4	0.54	0.03
MITOCHONDRIAL	cytochrome c CycA, *A. niger*	An02g01830			112	23.8	26.6	31.3	1.01	0.39
MITOCHONDRIAL	dihydrolipoamide acetyltransferase Lat1, *S. cerevisiae*	An07g02180			675	17.6	15.6	30.2	3.39	4.73
MITOCHONDRIAL	F1Fo-ATP synthase subunit 4 ATP4, K. lactis	An16g07290	SP		244	20.6	29.9	18.6	0.10	2.65
MITOCHONDRIAL	mitochondrial malate dehydrogenase Mdh1, *S. cerevisiae*	An07g02160			340	29.9	29.4	21.8	1.27	1.15
MITOCHONDRIAL	ATP synthase coupling factor (F0) subunit e Tim11, *S. cerevisiae*	An16g08550			92	29.0	22.5	18.4	2.43	0.43
MITOCHONDRIAL	21 kD subunit of NADH:ubiquinone reductase nuo-21, *N. crassa*	An11g09390	SP		219	14.1	27.6	17.2	0.30	2.43
MITOCHONDRIAL	subunit IV of cytochrome c oxidase Cox4, *S. cerevisiae*	An07g07390			194	27.0	27.4	10.0	8.05	8.37
MITOCHONDRIAL	40 kD subunit of NADH-ubiquinone reductase NUO-40, *N. crassa*	An08g10690			372	20.4	26.4	15.0	0.82	3.17
MITOCHONDRIAL	similarity to mitochondrial pyruvate dehydrogenase complex protein Pdx1, *S. cerevisiae*	An02g11910			289	13.7	14.0	25.6	3.69	3.43
MITOCHONDRIAL	mitochondrial aspartate-glutamate carrier protein strongly similar to ARALAR2, *H. sapiens*	An07g03070			695	20.4	25.0	9.5	4.07	7.20
MITOCHONDRIAL	mitochondrial proton-pumping NADH:ubiquinone reductase nuo51, *A. niger*	An04g05640	SP		496	16.6	24.5	6.5	4.50	11.08
MITOCHONDRIAL	21.3 kD subunit of NADH:ubiquinone reductase, *N. crassa*	An06g01390			195	23.6	24.5	12.7	3.33	3.84
MITOCHONDRIAL	succinate dehydrogenase iron-sulfur protein subunit Sdh2, *S. cerevisiae*	An14g04400			300	17.5	24.3	23.8	0.99	0.01
MITOCHONDRIAL	mitochondrial import receptor MOM38, *N. crassa*	An15g00190			354	16.0	24.2	16.5	0.01	1.46
MITOCHONDRIAL	cytochrome c oxidase subunit V cox5, *A. niger*	An14g04170			198	18.9	24.1	13.8	0.80	2.86
MITOCHONDRIAL	antiproliferative protein prohibitin Phb1, *S. cerevisiae*	An08g06540	SP		279	14.2	23.6	11.6	0.25	4.13
MITOCHONDRIAL	pyruvate dehydrogenase β chain precursor Pdb1, *S. cerevisiae*	An01g00100	SP		374	15.1	15.7	22.6	1.48	1.26
MITOCHONDRIAL	citrate synthase CitA, *A. niger*	An09g06680			474	22.3	21.9	21.1	0.03	0.01
MITOCHONDRIAL	mitochondrial carrier protein Yhm1, *S. cerevisiae*	An07g10010			309	18.3	21.9	8.0	4.17	6.72
MITOCHONDRIAL	49 kD subunit of NADH:ubiquinone reductase, *N. crassa*	An02g05470			476	13.7	21.4	14.5	0.02	1.35
MITOCHONDRIAL	glycerol-3-phosphate dehydrogenase gdm1, *Mus musculus*	An08g00210	SP		704	12.9	21.1	14.9	0.15	1.06
MITOCHONDRIAL	mitochondrial import receptor TOM20, *N. crassa*	An08g07360	SP		167	17.3	16.7	21.0	0.36	0.48
MITOCHONDRIAL	ketol-acid reductoisomerase ilv-2, *N. crassa*	An09g03940	SP		401	20.5	20.9	20.4	0.00	0.01
MITOCHONDRIAL	NADH dehydrogenase [ubiquinone] 1 α subcomplex subunit 13 similar to GRIM19, *Mus musculus*	An16g02130			109	12.7	20.7	3.6	5.46	13.33
MITOCHONDRIAL	subunit VI of cytochrome c oxidase Cox6, *S. cerevisiae*	An02g09930			158	15.6	18.8	20.6	0.69	0.08
MITOCHONDRIAL	14.8 kD subunit of NADH:ubiquinone reductase, *N. crassa*	An15g00690			123	20.0	16.9	13.7	1.17	0.32
MITOCHONDRIAL	prohibitin Phb2, *S. cerevisiae*	An12g04750	SA		306	11.5	19.7	10.6	0.04	2.78
MITOCHONDRIAL	31 kD subunit of NADH:ubiquinone reductase, *N. crassa*	An11g06200			280	17.9	19.6	11.6	1.37	2.09
MITOCHONDRIAL	29.9 kD subunit of NADH:ubiquinone reductase, *N. crassa*	An02g05880			237	14.0	19.4	11.5	0.24	2.03
MITOCHONDRIAL	20.9 kD subunit of NADH:ubiquinone reductase, *N. crassa*	An14g00060			188	16.5	18.7	10.4	1.41	2.42
MITOCHONDRIAL	mitochondrial outer membrane protein Tom70, P. anserina	An03g04790	SA		629	14.8	18.2	8.9	1.49	3.27
MITOCHONDRIAL	subunit VIa of cytochrome c oxidase Cox13, *S. cerevisiae*	An11g10200			141	17.4	17.3	15.7	0.09	0.08
MITOCHONDRIAL	mitochondrial citrate-oxoglutarate carrier Yhm2, *S. cerevisiae*	An09g06670			316	12.5	17.4	5.3	2.96	6.73
MITOCHONDRIAL	H+-transporting ATP synthase δ chain precursor Atp5, *S. cerevisiae*	An02g04520			228	17.3	16.2	9.7	2.20	1.66

Functional annotation	Protein description	Locus tag	SS	ERRS	PL	NSAF·10^4			G-score	G-score
						M.	X.	S.	M.	X.
MITOCHONDRIAL	heart muscle protein mitofilin HMP, *H. sapiens*	An04g02460			631	12.0	17.0	6.8	1.47	4.52
MITOCHONDRIAL	similarity to F1F0-ATP synthase subunit g homolog Atp20, *S. cerevisiae*	An01g10880			198	15.6	16.8	8.5	2.13	2.78
MITOCHONDRIAL	subunit VIII of ubiquinol--cytochrome c reductase, *S. cerevisiae*	An08g06550			96	16.7	0.9	1.4	15.41	0.08
MITOCHONDRIAL	sorbitol dehydrogenase gutB, Bacillus subtilis	An01g03480			340	16.7	9.8	9.6	1.95	0.00
MITOCHONDRIAL	similarity to hypothetical protein AA57718.1, *A. nidulans*	An02g05900			124	16.4	13.8	13.6	0.25	0.00
MITOCHONDRIAL	hypothetical protein SPAC17C9.06, *S. pombe*	An14g00220			514	12.7	15.6	13.4	0.02	0.17
MITOCHONDRIAL	Oxodicarboxylate carrier Odc2, *S. cerevisiae*	An08g01370			305	10.9	14.5	7.2	0.73	2.46
MITOCHONDRIAL	mitochondrial receptor complex chain MOM22, *N. crassa*	An08g04070			153	9.1	10.0	14.4	1.23	0.80
MITOCHONDRIAL	hypothetical protein AN0630.2, *A. nidulans*	An01g09840	SA		74	7.2	13.4	5.3	0.31	3.66
MITOCHONDRIAL	precursor of isocitrate dehydrogenase (NAD+) chain Idh2, *S. cerevisiae*	An08g05580			438	4.6	9.3	13.3	4.40	0.74
MITOCHONDRIAL	γ chain precursor of the H+-transporting ATP synthase Atp3, *S. cerevisiae*	An01g04630			297	13.3	8.8	4.8	4.15	1.19
MITOCHONDRIAL	mitochondrial aconitate hydratase Aco1, *S. cerevisiae*	An08g10530			777	11.7	13.1	3.2	5.18	6.50
MITOCHONDRIAL	24 kD subunit of NADH:ubiquinone reductase Nuo24, *N. crassa*	An12g04780			269	10.7	12.4	7.2	0.68	1.37
MITOCHONDRIAL	oxoglutarate dehydrogenase (lipoamide) Kgd1, *S. cerevisiae*	An04g04750			1055	9.0	12.2	6.0	0.59	2.14
MITOCHONDRIAL	endonuclease SceI 75 kDa subunit Ens1, *S. cerevisiae*	An16g05090			666	10.1	10.7	11.9	0.15	0.06
MITOCHONDRIAL	hypothetical protein EAA61911.1, *A. nidulans*	An12g00220			154	11.8	7.6	9.3	0.30	0.17
MITOCHONDRIAL	23 kD subunit of NADH:ubiquinone reductase, Bos taurus	An18g05670			224	8.1	11.7	5.2	0.63	2.53
MITOCHONDRIAL	similarity to hypothetical membrane protein YGR235c, *S. cerevisiae*	An11g05700	SP		252	11.4	8.2	4.6	2.97	1.01
MITOCHONDRIAL	21/29 kD subunit of NADH:ubiquinone reductase, *N. crassa*	An04g00110			280	6.5	11.3	5.1	0.17	2.38
MITOCHONDRIAL	α subunit E1 of the pyruvate dehydrogenase complex Pda1, *S. cerevisiae*	An07g09530			404	10.8	6.5	11.3	0.01	1.31
MITOCHONDRIAL	alternative NADH:ubiquinone reductase NDH2, Y. lipolytica	An08g04240			567	7.7	10.7	2.5	2.77	5.40
MITOCHONDRIAL	subunit 6 of ubiquinol--cytochrome-c reductase Qcr6, *S. cerevisiae*	An04g05220			167	8.3	10.3	10.1	0.18	0.00
MITOCHONDRIAL	hypothetical protein CAD27304.1, *A. fumigatus*	An08g04880			263	10.2	6.5	3.5	3.44	0.95
MITOCHONDRIAL	similarity to membrane associated protein SLP-2, *H. sapiens*	An08g01590			436	8.6	10.1	3.9	1.82	2.90
MITOCHONDRIAL	19.3 kD subunit of NADH:ubiquinone reductase, *N. crassa*	An04g00060			232	9.7	5.1	1.7	6.22	1.77
MITOCHONDRIAL	similarity to single-stranded DNA-binding protein Rim1, *S. cerevisiae*	An03g03900			148	6.5	6.7	9.7	0.62	0.54
MITOCHONDRIAL	14 kD subunit of ubiquinol--cytochrome c reductase Qcr7, *S. cerevisiae*	An04g01200			122	9.6	8.1	3.2	3.38	2.22
MITOCHONDRIAL	mitochondrial sulfide dehydrogenase (coenzyme Q2) SPBC2G5.06c, *S. pombe*	An03g03640	SP		527	7.1	9.4	5.7	0.16	0.94
MITOCHONDRIAL	carnitine/acyl carnitine carrier acuH, *A. nidulans*	An03g03360			325	4.3	9.2	3.6	0.06	2.50
MITOCHONDRIAL	hypothetical protein NUO-12.3, *N. crassa*	An15g03340			106	9.1	0.9	1.2	6.76	0.07
MITOCHONDRIAL	mitochondrial elongation factor Tu, *A. thaliana*	An08g04470			440	6.1	6.8	8.6	0.43	0.21
MITOCHONDRIAL	NADH-dependent glutamate synthase NADH-GOGAT, Medicago sativa	An07g09920			2126	8.4	6.5	6.2	0.34	0.01
MITOCHONDRIAL	17.2 kD subunit of NADH:ubiquinone reductase b17.2, Bos taurus	An17g01110			140	5.3	8.4	8.4	0.67	0.00
MITOCHONDRIAL	hypothetical protein SPAPJ691.03, *S. pombe*	An08g06220	SA		90	8.3	1.0	1.4	5.34	0.08
MITOCHONDRIAL	succinyl coenzyme A synthase α subunit SYRTSA, *Rattus norvegicus*	An17g01670			332	6.8	5.2	8.2	0.14	0.71
MITOCHONDRIAL	chaperone involved in mitochondrial protein import Mge1, *S. cerevisiae*	An02g01750			240	6.7	7.9	2.7	1.73	2.65
MITOCHONDRIAL	17.8 kD subunit of NADH:ubiquinone reductase Nuo-17.8, *N. crassa*	An16g08740	SA		172	4.3	7.9	2.3	0.67	3.27
MITOCHONDRIAL	precursor of mitochondrial nuclease Nuc1, *S. cerevisiae*	An12g04110			334	2.2	7.8	3.5	0.28	1.69
MITOCHONDRIAL	flavocytochrome b2 L-lactate dehydrogenase CYB2, Pichia anomala	An14g02250			500	4.1	3.1	7.5	1.06	1.95

Functional annotation	Protein description	Locus tag	SS	ERRS	PL	NSAF·10^4			G-score	G-score
						M.	X.	S.	M.	X.
MITOCHONDRIAL	dihydrolipoamide succinyltransferase kgd2, *A. fumigatus*	An11g11280			469	5.2	7.5	4.7	0.03	0.64
MITOCHONDRIAL	carnitine O-acetyltransferase cat2, Candida tropicalis	An18g01590			643	2.2	2.9	7.5	3.10	2.04
MITOCHONDRIAL	similarity to pyruvate dehydrogenase phosphatase isoenzyme 1 PDP1, *Rattus norvegicus*	An18g05890	SP		602	3.4	7.3	6.7	1.11	0.03
MITOCHONDRIAL	2-methylcitrate dehydratase PrpD, Salmonella typhimurium	An15g01780			502	5.7	3.4	7.0	0.12	1.25
MITOCHONDRIAL	similarity to ORFX ORF2689 SEQ ID NO:5378 from patent WO200058473-A2, *H. sapiens*	An07g07880			517	6.8	4.4	2.8	1.77	0.36
MITOCHONDRIAL	Yta11, *S. cerevisiae*	An04g04970			803	6.8	6.4	1.5	3.74	3.36
MITOCHONDRIAL	mitochondrial m-AAA protease subunit Yta12, *S. cerevisiae*	An07g07000			898	6.8	5.5	2.5	2.10	1.21
MITOCHONDRIAL	mitochondrial protein Mia1, *S. cerevisiae*	An13g00670			135	2.4	3.3	6.7	2.18	1.17
MITOCHONDRIAL	hypothetical protein YNR020c, *S. cerevisiae*	An05g00110			237	3.2	6.5	1.6	0.48	3.06
MITOCHONDRIAL	22 kD subunit NADH:ubiquinone reductase, *N. crassa*	An08g04910			159	6.0	6.2	5.7	0.01	0.02
MITOCHONDRIAL	similarity to succinate dehydrogenase, *S. cerevisiae*	An01g13930	SP		220	5.3	6.1	1.8	1.88	2.56
MITOCHONDRIAL	precursor of mitochondrial isocitrate dehydrogenase IcdA, *A. niger*	An02g12430			413	5.4	4.6	6.0	0.03	0.18
MITOCHONDRIAL	methylcitrate synthase mcsA, *A. nidulans*	An15g01920			465	2.1	2.5	5.9	1.90	1.37
MITOCHONDRIAL	weak similarity to hypothetical protein YGR165w, *S. cerevisiae*	An03g04660			387	3.6	5.4	5.0	0.24	0.01
MITOCHONDRIAL	succinate dehydrogenase Sdh1, *S. cerevisiae*	An02g07600			656	5.0	3.2	3.8	0.19	0.05
MITOCHONDRIAL	AU-specific RNA-binding protein / enoyl-CoA hydratase AUH, *H. sapiens*	An02g07320			302	1.1	2.1	4.7	2.51	1.05
MITOCHONDRIAL	mitochondrial succinate-fumarate transporter Sfc1, *S. cerevisiae*	An04g09030			325	1.6	4.7	2.0	0.03	1.13
MITOCHONDRIAL	similarity to mitochondrial ribosomal protein Mrp20, *S. cerevisiae*	An18g02990			196	1.6	3.2	4.6	1.50	0.26
MITOCHONDRIAL	similarity to 13 kD subunit of NADH:ubiquinone reductase, Bos taurus	An02g11200			292	2.6	4.6	3.1	0.05	0.30
MITOCHONDRIAL	citrate transport protein Ctp1, *S. cerevisiae*	An11g11230			296	2.5	4.6	0.4	1.62	3.97
MITOCHONDRIAL	mitochondrial ribosomal protein of the large subunit Yml3, *S. cerevisiae*	An08g05500			371	4.3	2.7	3.9	0.03	0.21
MITOCHONDRIAL	mRNA processing protein of cytochrome c oxidase Mss51, *S. cerevisiae*	An12g00130			524	4.3	2.2	1.7	1.11	0.06
MITOCHONDRIAL	mitochondrial cytochrome b2, putative, A. flavus NRRL3357	53140			477	4.3	1.7	1.9	0.92	0.01
MITOCHONDRIAL	mitochondrial phosphate transport protein G7, Glycine max	An02g12070			379	4.2	3.6	0.3	3.90	3.10
MITOCHONDRIAL	similarity to hypothetical membrane protein YML030w, *S. cerevisiae*	An04g02570			177	4.2	0.5	0.7	2.72	0.04
MITOCHONDRIAL	similarity to N-acetylglucosaminyltransferase chain p110, *Rattus norvegicus*	An01g07200			833	2.7	4.2	0.2	2.74	4.72
MITOCHONDRIAL	acetyl-CoA hydrolase Ach1, *S. cerevisiae*	An16g07110			525	1.8	3.3	4.2	0.96	0.12
MITOCHONDRIAL	hypothetical protein YKR065c, *S. cerevisiae*	An01g06370			248	2.2	4.0	1.6	0.09	1.09
MITOCHONDRIAL	mitochondrial cation transporter Mmt1, *S. cerevisiae*	An07g03130			486	1.5	3.9	1.3	0.01	1.31
MITOCHONDRIAL	mitochondrial carrier protein Ymc1, *S. cerevisiae*	An18g05590			304	3.9	3.9	1.3	1.36	1.35
MITOCHONDRIAL	hypothetical protein YKL195w, *S. cerevisiae*	An07g02770			270	2.0	3.7	2.4	0.04	0.27
MITOCHONDRIAL	similarity to mitochondrial tricarboxylate carrier, Rattus sp.	An01g10190	SP		370	3.2	3.7	1.1	1.12	1.52
MITOCHONDRIAL	methionine-N-acetyltransferase Nat2, *S. cerevisiae*	An04g00220			288	3.3	2.8	2.3	0.21	0.06
MITOCHONDRIAL	hypothetical protein Afu3g06270, *A. fumigatus*	An11g10070			323	3.0	3.1	1.2	0.77	0.84
MITOCHONDRIAL	NAD(+)-isocitrate dehydrogenase subunit I idh1, *Ajellomyces capsulatus*	An18g06760			385	2.5	2.1	3.0	0.05	0.17
MITOCHONDRIAL	protein required for dispersion of mitochondria cluA, *Dictyostelium discoideum*	An02g06530			1249	2.0	3.0	2.0	0.00	0.20
MITOCHONDRIAL	long-chain-acyl-CoA dehydrogenase precursor LCAD, *Rattus norvegicus*	An13g03940			415	2.8	2.4	2.8	0.00	0.04
MITOCHONDRIAL	similarity to ribosomal protein of the small subunit Rsm7, *S. cerevisiae*	An01g03110			422	0.8	0.6	2.8	1.22	1.43
MITOCHONDRIAL	alcohol-dehydrogenase AdhA from patent WO8704464-A, *A. niger*	An17g01530			350	2.7	0.8	2.6	0.00	1.04

Functional annotation	Protein description	Locus tag	SS	ERRS	PL	NSAF·10^4			G-score	G-score
						M.	X.	S.	M.	X.
MITOCHONDRIAL	hypothetical cardionlipin synthase SPAC22A12.08c, *S. pombe*	An01g06960			364	2.1	2.7	0.4	1.32	2.06
MITOCHONDRIAL	mtRNA splice defect-suppressing mitochondrial carrier Mrs3, *S. cerevisiae*	An06g01730			319	1.7	2.5	2.0	0.04	0.06
MITOCHONDRIAL	mitochondrial NADH dehydrogenase ndh64, *N. crassa*	An11g09350			700	2.0	2.4	0.9	0.39	0.71
MITOCHONDRIAL	peptide ABC transporter protein Mdl1, *S. cerevisiae*	An04g07060	SP		787	2.3	1.5	0.5	1.27	0.52
MITOCHONDRIAL	similarity to NADH oxidase, Thermoanaerobacter brockii	An15g04420			417	2.3	0.2	0.3	1.72	0.02
MITOCHONDRIAL	mitochondrial ribosomal protein Nam9, *S. cerevisiae*	An07g09550			436	0.7	2.3	2.1	0.67	0.01
MITOCHONDRIAL	oxaloacetate transporter Oac1, *S. cerevisiae*	An14g06860			406	1.8	0.2	0.3	1.18	0.02
MITOCHONDRIAL	hypothetical protein EAA61688.1, *A. nidulans*	An14g00810			343	0.9	1.8	0.4	0.24	1.05
MITOCHONDRIAL	similarity to monooxygenase VioC, Chromobacterium violaceum	An07g09110	SP		499	1.5	1.6	1.8	0.03	0.01
MITOCHONDRIAL	similarity to 3-isopropylmalate dehydrogenase leuB, Sulfolobus sp.	An15g02490			361	0.3	1.7	0.4	0.01	1.00
MITOCHONDRIAL	acetolactate synthase protein from patent EP257993-A, *S. cerevisiae*	An16g04170			690	1.1	1.4	1.7	0.14	0.02
MITOCHONDRIAL	maintaining mitochondrial morphology protein MMM1, *N. crassa*	An15g00980	SA		484	0.2	1.7	1.3	0.89	0.04
MITOCHONDRIAL	dynamin-related protein msp1p, *S. pombe*	An08g04250	SP		919	1.5	1.5	1.3	0.02	0.01
MITOCHONDRIAL	mitochondrial carrier Leu5, *S. cerevisiae*	An04g08800			435	0.2	1.5	0.9	0.39	0.13
MITOCHONDRIAL	pyruvate dehydrogenase kinase isoform 2, *Zea mays*	An02g04000			438	0.2	1.4	0.9	0.39	0.13
MITOCHONDRIAL	component of the translocase of mitochondrial inner membrane Tim54, *S. cerevisiae*	An01g07190	SA		447	0.7	1.4	0.3	0.19	0.80
MITOCHONDRIAL	acetylglutamate kinase/N-acetyl-γ-glutamyl-P reductase precursor arg-6, *N. crassa*	An12g07580	SP		903	0.8	1.1	1.0	0.02	0.00
POLARISED GROWTH	actin γ, *A. nidulans*	An15g00560			375	52.1	42.1	53.7	0.02	1.42
POLARISED GROWTH	hex1, *A. nidulans*	An07g04570			216	24.2	28.0	49.9	9.08	6.28
POLARISED GROWTH	tubulin β chain β-tubulin, A. flavus	An08g03190			447	39.0	29.2	34.0	0.34	0.36
POLARISED GROWTH	DNA damage checkpoint protein rad24p, *S. pombe*	An07g07760			260	34.1	29.5	30.5	0.20	0.02
POLARISED GROWTH	14-3-3 protein homolog artA, *A. nidulans*	An18g06270			272	31.8	28.8	30.1	0.05	0.03
POLARISED GROWTH	tubulin α-1 chain tubA, *A. nidulans*	An01g05650			448	22.2	15.5	18.8	0.27	0.33
POLARISED GROWTH	actin-bundling protein Sac6, putative, *Neosartorya fischeri* NRRL 181	202202			644	7.5	5.5	14.3	2.19	4.12
POLARISED GROWTH	inositol hexakis-/heptakis-phosphate kinase strongly similar to protein vip1p, *S. pombe*	An16g05020			257	11.2	6.7	2.5	5.94	1.93
POLARISED GROWTH	chromosome segregation protein mal3p, *S. pombe*	An02g07690			246	7.4	7.7	10.0	0.40	0.31
POLARISED GROWTH	calmodulin 6 CaM6, *A. thaliana*	An07g01640			143	0.7	3.2	10.0	9.46	3.74
POLARISED GROWTH	septin aspD, *A. nidulans*	An08g00310			346	7.7	9.1	7.1	0.02	0.24
POLARISED GROWTH	septin aspA, *A. nidulans*	An07g05110	SP		379	5.9	7.8	4.5	0.21	0.95
POLARISED GROWTH	protein Rvs161, *S. cerevisiae*	An17g01945			261	4.5	3.8	7.5	0.74	1.22
POLARISED GROWTH	GABA-A receptor ε-like subunit, *H. sapiens*	An01g05510			320	7.0	5.9	5.3	0.25	0.04
POLARISED GROWTH	hypothetical suppressor of bem1/bud5 bem46p, *S. pombe*	An13g01220			292	3.3	5.9	6.7	1.17	0.05
POLARISED GROWTH	cell division control protein Cdc12, *S. cerevisiae*	An09g05260			383	6.4	4.0	3.1	1.22	0.13
POLARISED GROWTH	Arp2/3 complex 21kDa subunit ARC21, *H. sapiens*	An16g01570			188	6.3	6.2	6.2	0.00	0.00
POLARISED GROWTH	cofilin Cof1, *S. cerevisiae*	An14g04160			155	6.2	2.9	5.9	0.01	1.02
POLARISED GROWTH	hypothetical protein SPBC31F10.16, *S. pombe*	An02g08820			708	0.5	1.7	5.7	5.28	2.34
POLARISED GROWTH	actin like protein act2p, *S. pombe*	An18g03200			439	5.1	3.9	4.4	0.05	0.03
POLARISED GROWTH	hypothetical protein SPAC824.01, *S. pombe*	An02g02230			741	2.5	5.0	1.6	0.19	1.86
POLARISED GROWTH	cell division cycle protein Cdc50, *S. cerevisiae*	An07g10420	SA		402	4.5	4.7	2.9	0.35	0.43

Functional annotation	Protein description	Locus tag	SS	ERRS	PL	NSAF·10^4			G-score	G-score
						M.	X.	S.	M.	X.
POLARISED GROWTH	GTP-binding regulatory protein α chain fadA, *A. nidulans*	An08g06130			353	2.7	4.3	1.1	0.71	2.06
POLARISED GROWTH	mitogen-activated protein kinase mPKA, *A. nidulans*	An01g09520			421	0.3	2.8	4.0	3.99	0.22
POLARISED GROWTH	phospholipase D Spo14, *S. cerevisiae*	An15g07040			1214	1.1	1.3	2.7	0.63	0.52
POLARISED GROWTH	endosomal protein Emp70, *S. cerevisiae*	An06g01200	SP		645	2.2	2.7	0.6	0.92	1.39
POLARISED GROWTH	casein kinase i homolog cki1p, *S. pombe*	An18g06050			567	2.4	2.4	2.1	0.03	0.02
POLARISED GROWTH	similarity to hypothetical DEC1 protein homolog, *S. pombe*	An04g01830			937	1.0	2.4	1.2	0.02	0.37
POLARISED GROWTH	actin-related protein arp2p, *S. pombe*	An08g06400			341	0.3	2.4	1.1	0.50	0.44
POLARISED GROWTH	cytoskeleton assembly control protein homolog Sla2, *S. cerevisiae*	An11g10320			1015	1.4	2.2	1.2	0.02	0.34
POLARISED GROWTH	cytoskeleton specific chaperonin subunit Cct4, *S. cerevisiae*	An02g12750			536	1.0	1.2	2.2	0.45	0.30
POLARISED GROWTH	TCP1 complex β chain TCP1 β, *S. cerevisiae*	An01g06480			531	0.6	1.2	1.2	0.21	0.00
POLARISED GROWTH	component of chaperonin-containing T-complex Cct7, *S. cerevisiae*	An18g05770			631	0.5	1.0	0.2	0.13	0.57
POLARISED GROWTH	spindle pole body-associated protein dis1p, *S. pombe*	An08g10490			935	0.3	0.9	0.4	0.01	0.16
POLARISED GROWTH	myosin Myo2, *S. cerevisiae*	An17g02290			1572	0.1	0.5	0.4	0.28	0.01
NUCLEAR	similarity to heterogeneous nuclear ribonucleoprotein (hnRNP) Tom34, *S. cerevisiae*	An06g01440			336	12.4	14.8	22.8	3.12	1.74
NUCLEAR	weak similarity to myosin-like protein Mlp1, *S. cerevisiae*	An03g06670			2080	16.2	21.5	15.3	0.02	1.06
NUCLEAR	histone 4 from patent WO9919502-A1, *H. sapiens*	An02g05240			103	19.7	0.9	1.3	19.53	0.07
NUCLEAR	histone H2B, *A. nidulans*	An11g11310			141	11.4	14.7	17.5	1.31	0.24
NUCLEAR	nucleolar protein Nop1, *S. cerevisiae*	An01g12230			313	15.4	10.7	5.4	4.99	1.76
NUCLEAR	small G-protein Gsp1, C. albicans	An08g10060			214	13.5	8.8	7.9	1.48	0.05
NUCLEAR	hypothetical transmembrane protein usgS, *A. nidulans*	An07g05820			366	8.5	13.1	10.3	0.18	0.33
NUCLEAR	similarity to RNA-binding protein AUF1, *H. sapiens*	An07g02990			315	10.5	7.7	6.2	1.14	0.17
NUCLEAR	karyopherin α Srp1, *S. cerevisiae*	An15g06440			549	6.0	5.7	10.2	1.07	1.25
NUCLEAR	mRNA turnover 4 protein Mrt4, *S. cerevisiae*	An14g04940			234	9.6	6.5	6.1	0.78	0.02
NUCLEAR	mRNA cleavage factor I 25 kDa subunit CFIM25, *H. sapiens*	An16g01870			277	5.0	4.9	8.0	0.68	0.75
NUCLEAR	protein kinase skp1p, *S. pombe*	An15g00170			394	7.3	5.3	7.6	0.00	0.42
NUCLEAR	nuclear pore membrane protein Pom152, *S. cerevisiae*	An11g11140			1255	4.5	7.0	5.9	0.19	0.09
NUCLEAR	ribonucleoprotein autoantigen Sm-D, *H. sapiens*	An11g04870			121	6.2	6.7	1.1	3.97	4.54
NUCLEAR	histone H4.1, *A. nidulans*	An08g06940			103	5.2	6.1	6.3	0.11	0.00
NUCLEAR	pre-mRNA splicing factor (Srp1), putative, *Neosartorya fischeri* NRRL 181	56745			222	6.3	6.1	5.3	0.09	0.06
NUCLEAR	transcription factor btf3p, *S. pombe*	An12g07790			155	2.1	2.9	5.9	1.90	1.02
NUCLEAR	NADH oxidoreductase complex I subunit Sub2, *S. cerevisiae*	An12g08030			440	2.7	5.1	5.6	1.07	0.02
NUCLEAR	U2 snRNA-specific protein A, *H. sapiens*	An14g02360			253	5.5	3.2	4.6	0.07	0.26
NUCLEAR	similarity to hypothetical regulational protein PBK1, *H. sapiens*	An07g02690			407	2.9	2.0	5.4	0.79	1.65
NUCLEAR	nucleoporin-interacting protein Nic96, *S. cerevisiae*	An14g00100	SP		993	0.1	1.9	5.4	6.53	1.71
NUCLEAR	RNA binding protein 47 RBP47, Nicotiana plumbaginifolia	An12g00410			402	5.0	2.9	4.8	0.00	0.49
NUCLEAR	nucleoporin Nup170, *S. cerevisiae*	An07g01520			1350	0.6	1.5	4.9	3.99	1.86
NUCLEAR	hypothetical membrane protein YOL077c, *S. cerevisiae*	An01g06040			358	2.7	3.3	4.7	0.56	0.26
NUCLEAR	centromere/microtubule-binding protein Cbf5, *S. cerevisiae*	An17g02170			485	4.6	4.3	2.9	0.38	0.25
NUCLEAR	karyopherin β Kap95, *S. cerevisiae*	An01g14070			880	2.5	4.0	4.6	0.58	0.04

Functional annotation	Protein description	Locus tag	SS	ERRS	PL	NSAF·10^4			G-score	G-score
						M.	X.	S.	M.	X.
NUCLEAR	protein required for accurate mitotic chromosome segregation Cse1, *S. cerevisiae*	An15g01240			962	2.8	4.4	1.2	0.63	1.92
NUCLEAR	similarity to nuclear envelope protein cut11p, *S. pombe*	An04g01520			565	2.5	2.1	4.4	0.54	0.84
NUCLEAR	translin-like protein TRAX, Gallus gallus-	An02g08100			235	4.1	1.9	3.9	0.01	0.67
NUCLEAR	weak similarity to transcription factor Arg81, *S. cerevisiae*	An09g00500	SP		874	0.1	3.4	4.0	4.63	0.05
NUCLEAR	protein sonA, *A. nidulans*	An08g00520	SP		359	3.9	2.3	3.3	0.05	0.18
NUCLEAR	nucleolar protein Nop5, *S. cerevisiae*	An02g09260			580	3.5	3.6	3.8	0.01	0.01
NUCLEAR	similarity to transcription repressor Tup1, *S. cerevisiae*	An15g00140			583	2.7	1.4	3.8	0.17	1.15
NUCLEAR	nucleolar rRNA processing protein Gar1, *S. cerevisiae*	An01g09490			199	3.8	0.5	0.7	2.42	0.04
NUCLEAR	transcription regulator CaGCR3, C. albicans	An15g00160			849	2.1	3.7	2.6	0.05	0.20
NUCLEAR	similarity to U1 and U2 snRNPs component SmB, *H. sapiens*	An04g02130			220	2.4	3.7	1.8	0.10	0.69
NUCLEAR	nuclear protein Enp1, *S. cerevisiae*	An01g00150			493	3.7	2.0	1.3	1.17	0.15
NUCLEAR	small nucleolar RNP component Nop56, *S. cerevisiae*	An16g03090			519	3.5	3.3	3.3	0.01	0.00
NUCLEAR	hypothetical protein CAD70902.1, *N. crassa*	An07g03430			294	2.5	2.8	3.1	0.05	0.02
NUCLEAR	protein pescadillo, *H. sapiens*	An04g02640			673	3.0	3.1	0.6	1.81	1.88
NUCLEAR	RNA-binding protein 30, Nicotiana plumbaginifolia-	An02g12640			538	3.0	2.5	2.2	0.13	0.02
NUCLEAR	similarity to insertion and deletion mismatch repair protein Mlh3, *S. cerevisiae*	An04g00870			969	3.0	0.1	0.1	3.21	0.01
NUCLEAR	G proteinbinding protein CRFG, *H. sapiens*	An02g03520			655	1.8	2.6	1.4	0.05	0.38
NUCLEAR	hypothetical protein B1D1.160, *N. crassa*	An02g03860			1265	0.1	1.4	2.6	2.93	0.38
NUCLEAR	cut3p, *S. pombe*	An07g06730			1309	1.2	0.5	2.5	0.43	1.48
NUCLEAR	similarity to the protein involved in sister chromatid segregation Src1, *S. cerevisiae*	An11g01510			733	0.4	0.9	2.3	1.39	0.68
NUCLEAR	hypothetical protein encoded by B19C19.110, *N. crassa*	An07g09830			517	2.3	1.9	2.3	0.00	0.03
NUCLEAR	poly(ADP-ribose) polymerase NAP protein from patent WO200004173-A1, *Zea mays*	An18g01170			650	0.2	0.1	2.2	2.08	2.19
NUCLEAR	spliceosomal protein SAP130, *H. sapiens*	An08g09010			1209	1.5	2.2	2.0	0.08	0.00
NUCLEAR	glucose repression mediator protein Ssn6, *S. cerevisiae*	An02g03940			858	0.4	0.3	2.0	1.19	1.33
NUCLEAR	actin-related protein, *H. sapiens*	An02g14750			472	0.2	1.3	1.9	1.54	0.11
NUCLEAR	similarity to importin RanBP7, *H. sapiens*	An16g05050			1045	0.5	1.1	1.9	0.82	0.19
NUCLEAR	U5 snRNP-specific protein U5-116kD, *Mus musculus*	An16g09200			990	1.0	1.7	1.2	0.02	0.10
NUCLEAR	ribosomal RNA processing protein Rrp5, *S. cerevisiae*	An15g06390			1822	1.5	1.3	0.5	0.50	0.40
NUCLEAR	189 kD subunit of DNA-directed RNA polymerase I rpa190p, *S. pombe*	An08g07050			1680	1.3	1.1	1.3	0.00	0.01
NUCLEAR	135 kD subunit of DNA-directed RNA polymerase I, *N. crassa*	An11g01770			1213	1.0	1.3	0.1	0.79	1.15
NUCLEAR	splicing factor PRP8, *H. sapiens*	An07g07420			2407	1.0	1.2	1.1	0.01	0.00
NUCLEAR	DNA repair protein XAB2, *H. sapiens*	An18g02480			822	0.4	0.3	1.1	0.36	0.44
NUCLEAR	similarity to RecQ helicase musN, *A. nidulans*	An02g02680			1154	1.0	0.1	0.1	0.83	0.01
NUCLEAR	cell division control protein Cdc68, *S. cerevisiae*	An07g10400			1020	0.1	1.0	0.4	0.17	0.27
NUCLEAR	146D nuclear protein, Xenopus laevis	An02g05400			1206	0.8	0.8	0.8	0.00	0.00
NUCLEAR	similarity to nucleoporin Nup192, *S. cerevisiae*	An14g06530			1786	0.1	0.4	0.8	0.76	0.18
NUCLEAR	E3 ubiquitin ligase Tom1, *S. cerevisiae*	An04g05870			4068	0.6	0.8	0.7	0.03	0.00
NUCLEAR	similarity to nuclear pore complex subunit Nup100, *S. cerevisiae*	An04g05630			1949	0.3	0.1	0.7	0.22	0.44
NUCLEAR	138 kD subunit of DNA-dependent RNA polymerase II rpb2p, *S. pombe*	An12g00720			1256	0.6	0.6	0.1	0.38	0.44

Functional annotation	Protein description	Locus tag	SS	ERRS	PL	NSAF·10^4			G-score	G-score
						M.	X.	S.	M.	X.
NUCLEAR	similarity to nucleoporin nup184p, *S. pombe*	An08g06090			1832	0.3	0.6	0.2	0.01	0.22
NUCLEAR	similarity to suppressor of S.cerevisiae sin4 mutation Rlr1, *S. cerevisiae*	An17g00540			2274	0.3	0.4	0.1	0.21	0.33
NUCLEAR	regulator protein Sin3, *S. cerevisiae*	An16g07120	SP		1531	0.2	0.4	0.1	0.05	0.23
NUCLEAR	protein TRRAP, *H. sapiens*	An02g10200			3911	0.4	0.2	0.2	0.03	0.00
PROTEIN ANCHORING	similarity to secreted protein SEQ ID NO:127 from patent WO200061779-A1, *H. sapiens*	An05g02300	SP		290	7.0	14.0	2.2	2.57	9.47
PROTEIN ANCHORING	sensor/transporter protein involved in maintenance of cell wall integrity Cwh43, *S. cerevisiae*	An16g03370			911	6.7	8.4	9.6	0.51	0.07
PROTEIN ANCHORING	ankyrin repeat-containing protein Akr1, *S. cerevisiae*	An05g00200			731	9.2	7.5	4.8	1.41	0.61
PROTEIN ANCHORING	glycylpeptide N-tetradecanoyltransferase Nmt, *Ajellomyces capsulatus*	An04g02500			491	4.1	2.4	2.4	0.48	0.00
PROTEIN ANCHORING	glycosylphosphatidylinositol anchor synthesis protein Mcd4, *S. cerevisiae*	An14g00900	SP		996	1.4	2.1	4.0	1.35	0.64
PROTEIN ANCHORING	hypothetical membrane protein YCR044c, *S. cerevisiae*	An18g05180			374	2.0	2.7	1.7	0.02	0.19
PROTEIN ANCHORING	hypothetical protein Afu2g14370, *A. fumigatus*	An03g03570	SP		513	1.5	2.6	0.3	0.94	2.29
PROTEIN ANCHORING	similarity to hypothetical GPI-anchor biosynthesis protein PIG-F related protein CAD70892.1, *N. crassa*	An10g00480			259	0.4	2.4	2.5	1.67	0.00
PROTEIN ANCHORING	similarity to protease B processing protein Pbn1, *S. cerevisiae*	An17g00780			503	0.2	2.3	1.8	1.44	0.07
PROTEIN ANCHORING	protein involved in the attachment of GPI-anchors to proteins Gpi8, *S. cerevisiae*	An01g13530	SP		402	0.8	0.7	2.3	0.73	0.91
PROTEIN ANCHORING	skin cell protein from patent WO9955865-A1, Rattus sp.	An11g06770	SP		593	1.3	1.7	2.0	0.16	0.02
PROTEIN ANCHORING	hypothetical protein SPAC1F12.09, *S. pombe*	An07g09270			812	0.7	1.4	1.1	0.12	0.04
TRANSLATION	translation elongation factor 1 α, P. anserina	An18g04840			460	81.1	76.6	81.0	0.00	0.12
TRANSLATION	cytoplasmic ribosomal protein of the large subunit L7, *S. pombe*	An08g10480			263	67.0	47.6	57.8	0.69	0.98
TRANSLATION	cytoplasmic ribosomal protein of the large subunit L10a, *Rattus norvegicus*	An08g03910			217	66.5	54.4	50.9	2.08	0.12
TRANSLATION	cytoplasmic ribosomal protein of the small subunit S18, *H. sapiens*	An08g08740			155	62.7	40.1	66.2	0.09	6.46
TRANSLATION	cytoplasmic ribosomal protein of the large subunit L10, *S. cerevisiae*	An12g04870			223	62.8	46.5	53.0	0.82	0.43
TRANSLATION	cytoplasmic ribosomal protein of the small subunit S9, *H. sapiens*	An02g13840			193	54.8	38.8	61.2	0.36	5.10
TRANSLATION	cytoplasmic ribosomal protein of the large subunit L17, *Rattus norvegicus*	An01g12420			184	45.9	32.8	58.6	1.55	7.37
TRANSLATION	cytoplasmic ribosomal protein of the small subunit S4.e, *S. cerevisiae*	An11g09500			258	45.1	36.7	54.9	0.95	3.64
TRANSLATION	cytoplasmic ribosomal protein of the large subunit L6, *S. cerevisiae*	An08g03430			202	49.2	39.7	54.7	0.29	2.38
TRANSLATION	cytoplasmic acidic ribosomal protein P0, *S. cerevisiae*	An01g04240			312	50.3	37.8	22.1	11.34	4.20
TRANSLATION	cytoplasmic ribosomal protein of the large subunit L4, *S. cerevisiae*	An09g05180			372	46.2	25.9	40.2	0.43	3.09
TRANSLATION	cytoplasmic ribosomal protein of the small subunit S4, *S. cerevisiae*	An12g01350			259	45.0	40.0	33.6	1.65	0.56
TRANSLATION	cytoplasmic ribosomal protein of the large subunit L7, *S. cerevisiae*	An14g01010			273	34.8	26.7	44.2	1.12	4.36
TRANSLATION	cytoplasmic ribosomal protein of the large subunit Rpl27, *S. cerevisiae*	An18g05020			135	30.9	22.0	43.3	2.09	7.05
TRANSLATION	cytoplasmic ribosomal protein of the small subunit S5.e, *S. cerevisiae*	An01g13190			215	38.3	30.6	41.7	0.15	1.71
TRANSLATION	translation elongation factor eEF-2, Cricetulus griseus	An02g05700			844	41.1	36.6	36.8	0.24	0.00
TRANSLATION	cytoplasmic ribosomal protein of the large subunit L15 rpl15, *A. niger*	An01g03460			203	40.5	23.5	12.2	16.12	3.69
TRANSLATION	cytoplasmic ribosomal protein of the small subunit Ys24, *S. cerevisiae*	An01g14080			130	40.3	29.8	39.0	0.02	1.22
TRANSLATION	cytoplasmic ribosomal protein of the large subunit L18a Rpl20, *S. cerevisiae*	An01g03580			198	35.1	32.3	40.0	0.33	0.82
TRANSLATION	cytoplasmic ribosomal protein of the small subunit Rp10b, *S. cerevisiae*	An17g02390			256	39.6	29.2	36.0	0.17	0.71
TRANSLATION	cytoplasmic ribosomal protein of the small subunit Rp30, *S. cerevisiae*	An02g06390			200	32.6	29.3	38.3	0.46	1.21

Functional annotation	Protein description	Locus tag	SS	ERRS	PL	NSAF·10^4			G-score	G-score
						M.	X.	S.	M.	X.
TRANSLATION	cytoplasmic ribosomal protein of the large subunit L3, *S. cerevisiae*	An02g03950			392	36.8	22.8	38.1	0.02	3.91
TRANSLATION	cytoplasmic ribosomal protein of the small subunit S14.e, *N. crassa*	An02g06130			150	23.5	24.6	37.2	3.13	2.58
TRANSLATION	cytoplasmic ribosomal protein of the small subunit S3, *S. cerevisiae*	An18g03310			266	36.6	26.8	25.9	1.83	0.01
TRANSLATION	cytoplasmic ribosomal protein of the large subunit L28, *S. cerevisiae*	An11g11030			149	23.7	17.5	35.7	2.47	6.34
TRANSLATION	translation elongation factor eEF-1 γ chain, Artemia sp.	An15g00760			412	25.2	23.4	35.6	1.81	2.55
TRANSLATION	cytoplasmic ribosomal protein of the large subunit L9.b, *S. cerevisiae*	An08g00610			192	33.9	23.9	34.5	0.00	1.92
TRANSLATION	translational factor CaYST1, C. albicans	An02g09200			298	32.6	22.1	30.1	0.10	1.23
TRANSLATION	cytoplasmic ribosomal protein of the small subunit S24.e, S.cerevisiae	An12g00510			133	16.9	26.4	32.2	4.89	0.57
TRANSLATION	cytoplasmic ribosomal protein of the small subunit rps6p, *S. pombe*	An04g05850			237	32.0	18.6	17.0	4.68	0.08
TRANSLATION	cytoplasmic ribosomal protein of the large subunit L14.a, *S. cerevisiae*	An15g01690			149	29.4	27.2	30.5	0.02	0.19
TRANSLATION	ribosomal protein of the large subunit L12, *Mus musculus*	An01g04740			165	30.4	15.8	29.1	0.03	3.99
TRANSLATION	cytoplasmic ribosomal protein of the small subunit S16.e, *S. cerevisiae*	An02g06050			143	11.2	22.1	30.0	8.88	1.21
TRANSLATION	cytoplasmic ribosomal protein of the large subunit L32, Drosophila subobscura	An15g06740			179	29.2	18.6	23.9	0.53	0.67
TRANSLATION	cytoplasmic ribosomal protein of the large subunit L13, *Rattus norvegicus*	An14g00370			225	29.0	15.6	21.4	1.15	0.89
TRANSLATION	Gβ like protein cpcB, *A. nidulans*	An01g08850			316	28.1	15.1	16.0	3.32	0.03
TRANSLATION	cytoplasmic ribosomal protein of the large subunit L16, *S. cerevisiae*	An04g02120			176	23.7	18.9	27.3	0.26	1.52
TRANSLATION	cytoplasmic ribosomal protein of the small subunit S10, *S. cerevisiae*	An06g01870			154	27.1	13.5	21.1	0.74	1.70
TRANSLATION	cytoplasmic ribosomal protein of the large subunit L22, Xenopus laevis	An02g08080			124	21.5	24.0	26.2	0.45	0.10
TRANSLATION	cytoplasmic ribosomal protein of the large subunit L26, *S. cerevisiae*	An11g09120			134	24.7	19.5	26.2	0.04	0.98
TRANSLATION	translation initiation factor eIF-4A, *S. pombe*	An02g11680			398	23.9	14.7	25.8	0.07	3.06
TRANSLATION	translation elongation factor 3 Yef3, *S. cerevisiae*	An07g02650			1064	22.8	24.3	25.3	0.13	0.02
TRANSLATION	cytoplasmic ribosomal protein of the large subunit L19, *S. cerevisiae*	An05g00540			201	25.0	21.1	22.6	0.12	0.05
TRANSLATION	cytoplasmic ribosomal protein of the small subunit S13.e, S.s cerevisiae	An07g02960			151	24.8	20.9	19.8	0.56	0.03
TRANSLATION	cytoplasmic ribosomal protein of the large subunit L13a, *S. cerevisiae*	An18g03810			202	21.7	22.8	21.2	0.01	0.05
TRANSLATION	cytoplasmic ribosomal protein of the large subunit S8, *Rattus norvegicus*	An01g03160			200	17.6	17.6	22.7	0.65	0.66
TRANSLATION	cytoplasmic ribosomal protein of the small subunit S12, Sus scrofa	An18g04310			150	16.4	22.2	11.3	0.96	3.66
TRANSLATION	cytoplasmic ribosomal protein of the large subunit L30, *S. cerevisiae*	An12g04860			106	13.1	16.2	20.8	1.78	0.59
TRANSLATION	cytoplasmic ribosomal protein of the large subunit Urp1, *S. cerevisiae*	An02g13850			158	11.5	8.6	20.6	2.59	5.09
TRANSLATION	viral integration site protein int-6/EIF-3 P48, *Mus musculus*	An02g07120			452	9.2	14.6	18.1	2.94	0.39
TRANSLATION	similarity to polyadenylate-binding protein Pabp, *S. cerevisiae*	An01g03050			731	14.2	10.5	17.6	0.37	1.82
TRANSLATION	cytoplasmic ribosomal protein of the small subunit S27, *H. sapiens*	An11g09670			82	16.9	14.3	11.1	1.23	0.40
TRANSLATION	hypothetical mold-specific protein MS8, *Ajellomyces capsulatus*	An18g05640			198	9.2	16.8	9.8	0.02	1.86
TRANSLATION	translation initiation factor eIF-3 subunit, *H. sapiens*	An14g01030			505	11.6	16.6	13.6	0.16	0.29
TRANSLATION	hypothetical protein HSPC021, *H. sapiens*	An16g04580			476	11.0	13.8	15.6	0.79	0.10
TRANSLATION	cytoplasmic ribosomal protein of the large subunit L30, K. lactis	An12g07830			159	7.4	7.4	15.5	2.95	2.97
TRANSLATION	similarity to elongation factor 1 β EF-1, Oryctolagus cuniculus	An08g03490			302	15.2	6.3	8.2	2.15	0.25
TRANSLATION	cytoplasmic ribosomal protein of the small subunit Rps11b, *S. cerevisiae*	An07g08850			160	12.7	15.2	7.3	1.47	2.83
TRANSLATION	hypothetical branched-chain α-ketoacid dehydrogenase E1 β subunit, *H. sapiens*	An08g00880			375	12.8	12.3	14.9	0.16	0.26
TRANSLATION	ATP-dependent RNA helicase Ded1, *S. cerevisiae*	An04g02030			678	14.7	14.5	14.8	0.00	0.00

Functional annotation	Protein description	Locus tag	SS	ERRS	PL	NSAF·10^4			G-score	G-score
						M.	X.	S.	M.	X.
TRANSLATION	cytoplasmic ribosomal protein of the large subunit L37.b, *S. cerevisiae*	An11g09570			95	14.6	10.4	6.8	2.89	0.76
TRANSLATION	ATP-dependent RNA helicase p68, *H. sapiens*	An02g02530			565	13.4	6.9	14.5	0.04	2.78
TRANSLATION	cytoplasmic ribosomal protein of the small subunit S12 AS1, P. anserina	An16g04940			153	10.5	12.4	14.4	0.63	0.16
TRANSLATION	hypothetical protein SPAC19A8.14, *S. pombe*	An04g06320	SA		215	14.4	4.6	5.4	4.21	0.07
TRANSLATION	cytoplasmic ribosomal protein of the small subunit S26, *H. sapiens*	An18g05810			119	11.7	14.4	9.8	0.16	0.87
TRANSLATION	cytoplasmic ribosomal protein of the large subunit L35, *Rattus norvegicus*	An08g02470			121	13.2	14.2	14.0	0.02	0.00
TRANSLATION	cytoplasmic ribosomal protein of the large subunit L1, *S. cerevisiae*	An08g05730			300	13.9	6.9	4.8	4.66	0.40
TRANSLATION	cytoplasmic ribosomal protein of the large subunit Rpl37b, *S. cerevisiae*	An02g12120			109	12.7	10.7	13.1	0.01	0.23
TRANSLATION	cytoplasmic ribosomal protein of the large subunit L8.e Pl2b, *S. cerevisiae*	An17g01360			254	13.0	4.6	8.7	0.87	1.27
TRANSLATION	translation initiation factor Eif-5a.2, *S. cerevisiae*	An01g02900			160	12.7	7.3	10.6	0.20	0.59
TRANSLATION	cytosolic serine--tRNA ligase Ses1, *S. cerevisiae*	An17g02340			474	12.4	5.1	7.9	0.98	0.61
TRANSLATION	cytoplasmic ribosomal protein of the small subunit S20, *S. cerevisiae*	An07g06760			116	12.0	3.9	12.3	0.00	4.61
TRANSLATION	translation initiation factor eIF-3, *S. pombe*	An01g04430			1052	9.4	12.1	7.8	0.16	0.94
TRANSLATION	translation initiation factor 3 subunit eIF3 β, *H. sapiens*	An01g06230			740	9.4	11.6	6.1	0.68	1.69
TRANSLATION	cytoplasmic ribosomal protein of the large subunit L43a, *S. cerevisiae*	An04g08980			92	10.5	10.8	7.1	0.66	0.78
TRANSLATION	similarity to pre-induction sporulation gene acoB, *A. nidulans*	An13g00430			375	7.7	9.9	10.0	0.31	0.00
TRANSLATION	cytoplasmic ribosomal protein of the large subunit L34.b, *S. cerevisiae*	An07g07430			117	10.0	5.4	5.6	1.31	0.00
TRANSLATION	single-stranded nucleic acid binding protein CBP, *Mus musculus*	An07g07150			360	3.3	4.3	9.7	3.37	2.21
TRANSLATION	cytoplasmic ribosomal protein of the large subunit L23a, *Rattus norvegicus*	An17g02240			154	9.0	6.4	9.3	0.00	0.52
TRANSLATION	translation initiation factor Eif6, *S. cerevisiae*	An17g01815			247	9.1	6.9	6.8	0.32	0.00
TRANSLATION	cytosolic tryptophan--tRNA ligase Wrs1, *S. cerevisiae*	An09g03950			433	0.7	1.5	8.7	7.90	5.73
TRANSLATION	similarity to translation initiation factor eIF-2 α chain EIF2A, *H. sapiens*	An02g09370			332	8.7	6.2	5.1	0.95	0.12
TRANSLATION	cytosolic threonine--tRNA ligase Ths1, *S. cerevisiae*	An01g09500			718	7.6	8.4	5.2	0.43	0.74
TRANSLATION	cytoplasmic ribosomal protein of the small subunit Rps31, *S. cerevisiae*	An01g10720			89	8.4	1.0	1.5	5.40	0.08
TRANSLATION	protein fragment SEQ ID NO:69506 from patent EP1033405-A2, *Zea mays*	An16g02940			267	8.4	5.7	7.3	0.08	0.19
TRANSLATION	cytoplasmic ribosomal protein of the large subunit L23, *S. cerevisiae*	An07g07840			140	5.3	3.2	8.4	0.67	2.36
TRANSLATION	nascent polypeptide-associated complex α chain α-NAC, *Mus musculus*	An15g01700			202	7.9	6.7	7.1	0.05	0.01
TRANSLATION	cytoplasmic ribosomal protein of the large subunit L31, *S. cerevisiae*	An08g10140			123	7.8	0.7	1.1	5.82	0.06
TRANSLATION	cytosolic alanine--tRNA ligase Ala1, *S. cerevisiae*	An16g09320			961	5.2	7.8	4.7	0.02	0.75
TRANSLATION	100 kDa coactivator snd1, *H. sapiens*	An07g03760			883	7.1	7.5	2.8	1.97	2.20
TRANSLATION	cytosolic leucine--tRNA ligase, *N. crassa*	An06g01830			1126	2.9	7.1	0.8	1.29	5.78
TRANSLATION	similarity to brefeldin A resistance protein Bfr1, *S. cerevisiae*	An01g11960			506	7.0	3.0	3.3	1.31	0.02
TRANSLATION	GU4 nucleic-binding protein 1 Arc1, *S. cerevisiae*	An15g06260			448	6.9	5.0	4.9	0.33	0.00
TRANSLATION	translation initiation factor eIF2 γ chain Gcd11, *S. cerevisiae*	An04g01940			513	4.0	5.1	6.8	0.78	0.26
TRANSLATION	eukaryotic initiation factor 3H1 subunit TIF3H1, *A. thaliana*	An08g01790			365	6.7	6.7	5.3	0.16	0.15
TRANSLATION	suppressor of tom1 protein Mpt4, *S. cerevisiae*	An02g06710			303	4.6	6.2	2.1	0.91	2.10
TRANSLATION	cytoplasmic ribosomal protein of the small subunit S19, *S. cerevisiae*	An18g04180			147	3.6	1.8	6.2	0.67	2.48
TRANSLATION	arginine--tRNA ligase Msr1, *S. cerevisiae*	An02g04880			646	6.1	3.5	3.0	1.08	0.03
TRANSLATION	methionyl aminopeptidase Map1, *S. cerevisiae*	An01g11340			379	1.4	1.2	5.8	2.90	3.34

Functional annotation	Protein description	Locus tag	SS	ERRS	PL	NSAF·10^4			G-score	G-score
						M.	X.	S.	M.	X.
TRANSLATION	nuclear pore-associated DEAD-box protein Dbp5, *S. cerevisiae*	An10g00360			482	1.6	1.7	5.7	2.49	2.27
TRANSLATION	polyribosome binding protein Scp160, *S. cerevisiae*	An11g04360			1172	5.2	5.5	2.3	1.12	1.30
TRANSLATION	RNase L inhibitor, *H. sapiens*	An08g02210			782	5.3	5.2	4.2	0.15	0.11
TRANSLATION	asparagine--tRNA ligase ASNS, Thermus aquaticus	An02g14080			574	2.4	3.9	5.2	1.04	0.18
TRANSLATION	similarity to α-complex protein 1 CP-1, *H. sapiens*	An11g04650			421	3.3	4.9	4.6	0.22	0.01
TRANSLATION	glutamine--tRNA ligase, *S. cerevisiae*	An03g01280			625	2.6	4.8	3.1	0.05	0.34
TRANSLATION	valine--tRNA ligase cyt-20, *N. crassa*	An16g08020			1054	2.7	4.7	1.1	0.71	2.39
TRANSLATION	cytosolic glutamate--tRNA ligase, *A. thaliana*	An09g05970	SP		712	2.9	4.4	2.4	0.04	0.63
TRANSLATION	similarity to multifunctional glutamine-proline--tRNA ligase Aats-glupro, D. melanogaster	An15g06360			604	4.4	1.9	1.9	1.00	0.00
TRANSLATION	cytoplasmic tyrosine--tRNA ligase Tyrrs, *S. cerevisiae*	An02g02010			382	2.5	4.0	4.4	0.53	0.02
TRANSLATION	cytoplasmic isoleucine--tRNA ligase Ils1, *S. cerevisiae*	An08g06770			1077	3.3	4.3	2.8	0.04	0.32
TRANSLATION	similarity to mediator of 40S ribosomal subunit assembly gar2p, *S. pombe*	An16g07470			381	3.1	3.5	2.4	0.09	0.23
TRANSLATION	suppressor 2 Sup2, *S. cerevisiae*	An11g04510			727	3.4	2.9	0.9	1.54	1.08
TRANSLATION	ras pathway interacting protein moe1p, *S. pombe*	An15g03780			586	2.4	3.2	2.9	0.05	0.02
TRANSLATION	eukaryotic translation initiation factor 3 subunit p42, *H. sapiens*	An16g05260			288	2.6	2.8	3.2	0.05	0.02
TRANSLATION	exonuclease II SPAC17A5.14, *S. pombe*	An09g05290			1406	2.2	3.1	1.8	0.05	0.40
TRANSLATION	translation initiation factor eIF-4F Tif4631, *S. cerevisiae*	An16g06850			1315	1.4	0.6	3.1	0.65	1.77
TRANSLATION	suppressor of the septation mutant cdc11 sce3p, *S. pombe*	An15g06790			489	2.0	0.9	2.9	0.19	1.09
TRANSLATION	similarity to polyadenylated RNA-binding protein Pub1, *S. cerevisiae*	An08g04280			497	1.9	0.9	2.9	0.18	1.08
TRANSLATION	translation initiation factor IF2, *H. sapiens*	An01g02840			1061	1.5	2.8	2.3	0.17	0.04
TRANSLATION	cytosolic phenylalanine--tRNA ligase β subunit Frs2, *S. cerevisiae*	An07g08140			481	0.2	0.6	2.4	2.15	1.26
TRANSLATION	translation initiation factor eIF3 subunit Tif34, *S. cerevisiae*	An02g12410			337	2.2	2.4	0.4	1.43	1.63
TRANSLATION	RNase III domain protein Afu5g09670, *A. fumigatus*	An07g03190			339	2.2	2.4	1.9	0.02	0.05
TRANSLATION	ATP-dependent RNA helicase ste13p, *S. pombe*	An11g11210			505	1.5	2.3	0.8	0.23	0.81
TRANSLATION	glycine-tRNA ligase Grs1, *S. cerevisiae*	An17g01977			626	1.2	2.2	0.2	0.77	1.88
TRANSLATION	similarity to translation initiation factor 3 complex protein Prt1, *H. sapiens*	An11g10630			591	2.0	1.4	1.5	0.06	0.01
TRANSLATION	cytosolic lysine--tRNA ligase Krs1, *S. cerevisiae*	An11g02400			618	1.6	1.9	0.2	1.16	1.55
TRANSLATION	similarity to cDNA RNA-binding protein TIA-1, *Mus musculus*	An02g14100			833	0.4	1.0	0.5	0.01	0.18
TRANSLATION	translational regulator HsGCN1, *H. sapiens*	An05g00530			2589	0.5	0.9	0.9	0.07	0.00
TRANSLATION	similarity to high density lipoproteinbinding protein HBP, *H. sapiens*	An02g02410			976	0.1	0.6	0.1	0.00	0.37
ROS DEFENCE	Cu Zn superoxide dismutase sodC, *A. fumigatus*	An07g03770			154	13.2	13.5	24.5	3.43	3.24
ROS DEFENCE	similarity to type 2 peroxiredoxin PrxII, Brassica napus	An12g08570			168	15.9	13.4	22.4	1.12	2.29
ROS DEFENCE	acidic Ca2+-independent phospholipase A2 aiPLA2, *Rattus norvegicus*	An04g03360			212	7.6	5.5	12.9	1.39	3.01
ROS DEFENCE	flavohemoglobin Fhp, *Alcaligenes* eutrophus	An14g02460			417	6.4	5.4	10.3	0.91	1.54
ROS DEFENCE	EST an 3344, *A. niger*	An02g12940			253	1.3	1.8	7.7	5.13	3.98
ROS DEFENCE	similarity to serum paraoxonase/arylesterase 2 PON2, Gallus gallus	An11g10790	SP		422	2.3	2.3	6.5	2.09	2.00
ROS DEFENCE	peroxisomal membrane protein PMP20, Candida boidinii	An16g00920			166	3.2	4.9	3.9	0.07	0.11
ROS DEFENCE	similarity to glutaredoxin, Oryza sativa	An08g00600	SA		252	3.0	2.5	4.6	0.37	0.65
ROS DEFENCE	glutathione reductase Glr1, *S. cerevisiae*	An03g03660			472	1.1	2.9	4.1	1.81	0.23

Functional annotation	Protein description	Locus tag	SS	ERRS	PL	NSAF·10^4			G-score	G-score
						M.	X.	S.	M.	X.
ROS DEFENCE	similarity to polyphosphoinositide binding protein Ssh2p, Glycine max	An06g01900			475	2.0	1.7	3.6	0.43	0.66
ROS DEFENCE	thioredoxin reductase TrxB, P. chrysogenum	An01g08570			367	2.0	0.7	3.2	0.25	1.65
ROS DEFENCE	hypothetical protein SPAC8A4.09c, *S. pombe*	An18g02900			372	2.0	0.2	3.1	0.25	2.95
ROS DEFENCE	catalase C catC, *A. nidulans*	An14g07200			490	2.0	1.7	2.4	0.04	0.13
ROS DEFENCE	catalase cta1p, *S. pombe*	An02g02750			501	0.6	0.5	1.8	0.59	0.73
ROS DEFENCE	similarity to HC-toxin non-ribosomal peptide synthase HTS1, Cochliobolus carbonum	An08g02310			6242	0.8	0.7	1.7	0.35	0.41
TRANSLOCATION (ER)	similarity to signal recognition particle receptor β chain Srp102, *S. cerevisiae*	An05g00140	SA		320	17.0	11.5	25.6	1.73	5.43
TRANSLOCATION (ER)	ER protein translocation complex subunit Sbh2, *S. cerevisiae*	An01g03820			127	21.0	7.8	25.6	0.44	9.96
TRANSLOCATION (ER)	ER membrane translocation facilitator Sec61, Y. lipolytica	An03g04340	SA		478	17.2	12.3	22.0	0.59	2.82
TRANSLOCATION (ER)	component of ER protein translocation subcomplex Sec71 from patent WO9949028-A1, *S. cerevisiae*	An16g08830	SP		270	13.8	16.4	19.7	1.03	0.31
TRANSLOCATION (ER)	signal recognition particle receptor Sec63, *S. cerevisiae*	An01g13070			653	11.3	14.8	16.9	1.13	0.14
TRANSLOCATION (ER)	component of the ER protein translocation machinery Sec62, *S. cerevisiae*	An02g01510			465	9.9	9.1	14.2	0.79	1.14
TRANSLOCATION (ER)	endoplasmatic reticulum signal peptidase subunit Spc2, *S. cerevisiae*	An16g07390			209	8.7	9.1	11.8	0.48	0.36
TRANSLOCATION (ER)	signal peptidase subunit Sec11, *S. cerevisiae*	An01g00560			143	9.7	0.6	0.9	8.52	0.05
TRANSLOCATION (ER)	weak similarity to translocation protein Sec72, *S. cerevisiae*	An17g00090			194	3.9	7.9	4.7	0.08	0.83
TRANSPORTERS	hypothetical inorganic phosphate transporter and regulator of Pho81p Pho88, *S. cerevisiae*	An16g01820			203	37.4	44.0	51.8	2.36	0.65
TRANSPORTERS	calcium P-type ATPase nca-1, *N. crassa*	An18g06290			1008	23.4	15.6	27.4	0.32	3.27
TRANSPORTERS	plasma membrane H+-ATPase PmaA, *A. nidulans*	An02g12510			990	25.4	23.0	5.4	14.11	11.81
TRANSPORTERS	vacuolar H+-transporting ATPase subunit Vph1, *S. cerevisiae*	An04g05310			850	16.2	21.9	14.2	0.13	1.67
TRANSPORTERS	hypothetical Ca2+-transporting ATPase Spf1- *S. cerevisiae*	An02g09470			1277	15.6	18.0	17.4	0.09	0.01
TRANSPORTERS	vacuolar H+-transporting ATPase subunit B Vma2, *S. cerevisiae*	An02g02020			507	14.5	13.3	17.2	0.22	0.48
TRANSPORTERS	H+-transporting ATPase vma-1, *N. crassa*	An02g10440			604	14.7	14.2	12.3	0.22	0.14
TRANSPORTERS	vacuolar ATPase subunit E Vma-4, *N. crassa*	An12g08760			231	7.9	10.5	12.9	1.25	0.25
TRANSPORTERS	vanadate resistance protein Van2, *S. cerevisiae*	An17g02140			381	10.9	11.6	9.9	0.05	0.14
TRANSPORTERS	general amino acid permease Gap1, *S. cerevisiae*	An13g00840			585	10.0	10.6	6.4	0.80	1.04
TRANSPORTERS	vacuolar H+-ATPase activator subunit Vma13, *S. cerevisiae*	An08g02770			478	7.8	7.7	10.6	0.42	0.45
TRANSPORTERS	subunit of the vacuolar ATPase Vma6, *S. cerevisiae*	An02g09250			362	6.8	9.7	8.3	0.14	0.12
TRANSPORTERS	bile acid transporter Ybt1, *S. cerevisiae*	An07g03920	SA		1643	5.8	7.3	4.5	0.16	0.67
TRANSPORTERS	cadmium resistance protein Ycf1, *S. cerevisiae*	An03g04060			1541	6.9	6.5	4.8	0.37	0.25
TRANSPORTERS	similarity to phosphate/phosphoenolpyruvate translocator TABPPT8, Nicotiana tabacum	An06g00300			339	6.0	5.6	6.5	0.02	0.07
TRANSPORTERS	bile acid transporter Ybt1, *S. cerevisiae*	An15g05290	SP		1542	4.1	6.5	4.1	0.00	0.53
TRANSPORTERS	H+-transporting ATPase chain C Vma5, *S. cerevisiae*	An08g03000			388	2.5	2.6	6.4	1.76	1.68
TRANSPORTERS	iron and manganese transporter Ccc1, *S. cerevisiae*	An01g08010			303	1.1	6.2	2.1	0.38	2.10
TRANSPORTERS	small oligopeptide transporter, OPT family, A. clavatus NRRL 1	56930			786	5.8	5.6	1.8	2.23	2.04
TRANSPORTERS	similarity to human transmembrane protein HTMPN-73 from patent WO9961471-A2, *H. sapiens*	An03g05000	SP		457	1.6	3.0	4.8	1.65	0.46
TRANSPORTERS	high affinity zinc transport protein Zrt1, *S. cerevisiae*	An12g10320			325	4.3	0.3	0.4	3.75	0.02

Functional annotation	Protein description	Locus tag	SS	ERRS	PL	NSAF·10^4			G-score	G-score
						M.	X.	S.	M.	X.
TRANSPORTERS	voltage-gated potassium channel β subunit Kv β 1, *Rattus norvegicus*-	An01g09590	SP		341	0.3	1.9	4.2	3.97	0.93
TRANSPORTERS	sulfate transport protein shst2, Stylosanthes hamata	An02g09350			730	2.5	2.1	4.1	0.40	0.65
TRANSPORTERS	monosaccharide transporter AmMst-1, Amanita muscaria	An15g03940	SA		527	3.0	3.9	2.2	0.13	0.48
TRANSPORTERS	breast cancer resistance protein 1 BCRP1, *Mus musculus*	An07g09170	SP		1034	2.6	3.6	1.6	0.22	0.74
TRANSPORTERS	water channel protein aquaporin 3 AQP3, *Rattus norvegicus*	An02g13250	SP		285	1.1	3.5	3.2	1.03	0.01
TRANSPORTERS	vacuolar ATPase subunit D Vma-8, *N. crassa*	An18g02470			266	2.0	2.4	3.4	0.37	0.19
TRANSPORTERS	heavy metal ion resistance protein Zrc1, *S. cerevisiae*	An15g03900	SP		431	2.7	2.7	3.3	0.06	0.06
TRANSPORTERS	high-affinity glucose transporter HGT1, K. lactis	An09g02930	SA		527	0.6	2.9	0.7	0.01	1.38
TRANSPORTERS	purine nucleoside permease NUP, C. albicans	An10g00800	SP		407	1.8	0.7	2.9	0.23	1.49
TRANSPORTERS	similarity to amino acid system N transporter SN1, *Rattus norvegicus*	An04g02150			750	1.6	2.8	1.9	0.03	0.16
TRANSPORTERS	peroxisomal transporter Ant1, *S. cerevisiae*	An01g04690	SP		335	1.6	2.4	2.7	0.29	0.02
TRANSPORTERS	similarity to neutral amino acid permease mtr, *N. crassa*	An03g00640			599	2.7	1.7	1.5	0.32	0.01
TRANSPORTERS	secretory pathway Ca2+-ATPase PmrA, *A. niger*	An02g14450			1028	2.6	1.1	2.1	0.04	0.31
TRANSPORTERS	hexose transporter Hxt3, *S. cerevisiae*	An02g03540			560	2.5	0.2	0.2	2.18	0.01
TRANSPORTERS	UDP-galactose transport protein SpUGT, *S. pombe*	An08g10400	SA		410	0.3	2.4	1.0	0.42	0.66
TRANSPORTERS	hypothetical membrane protein YBR287w, *S. cerevisiae*	An01g11100			443	0.7	2.2	0.3	0.19	1.69
TRANSPORTERS	high-affinity inorganic phosphate/H+ symporter Pho84, *S. cerevisiae*	An12g05750			645	1.5	2.1	0.2	1.11	1.82
TRANSPORTERS	nitrate permease crnA, *A. nidulans*	An08g05670	SA		504	1.1	2.0	0.8	0.05	0.54
TRANSPORTERS	GABA permease gabA, *A. nidulans*	An12g10000			532	1.8	0.2	0.2	1.35	0.01
TRANSPORTERS	multidrug transporter bmr3, Bacillus subtilis	An11g06860	SA		550	1.0	1.8	0.7	0.04	0.49
TRANSPORTERS	high affinity hexose transporter Hxt1, *S. cerevisiae*	An01g08780			540	0.6	1.5	1.7	0.54	0.01
TRANSPORTERS	iron transport multicopper oxidase Fet3, C. albicans	An01g08960	SP		613	0.2	1.3	0.2	0.00	0.90
TRANSPORTERS	ATP-binding cassette transporter abc1p, *S. pombe*	An01g10000	SP		1501	1.2	0.4	0.3	0.67	0.04
TRANSPORTERS	ATP-binding cassette transporter PMR1, Penicillium digitatum	An01g12380			1539	1.2	0.4	0.1	1.13	0.23
TRANSPORTERS	plasma membrane ATPase PMA1, K. lactis	An09g05950			1019	1.2	0.3	0.6	0.15	0.16
TRANSPORTERS	hypothetical protein YER036c, *S. cerevisiae*	An17g00240			613	0.2	1.0	1.1	0.71	0.00
TRANSPORTERS	phosphate transport protein Pho90, *S. cerevisiae*	An01g03120			881	0.4	0.9	0.1	0.09	0.62
TRANSPORTERS	Na+-H+ antiporter Nha2, *S. cerevisiae*	An17g01550	SA		707	0.2	0.9	0.9	0.61	0.00
TRANSPORTERS	similarity to hypothetical membrane protein YDR205w, *S. cerevisiae*	An06g01080			899	0.8	0.1	0.1	0.53	0.01
TRANSPORTERS	hypothetical membrane transport protein YGR125w, *S. cerevisiae*	An01g07860			1066	0.3	0.8	0.4	0.01	0.14
VESICULAR TRANSPORT	GTP-binding protein rho1p, *S. pombe*	An18g05980			193	74.7	61.2	33.0	16.62	8.58
VESICULAR TRANSPORT	hypothetical transport protein SPCC830.08c yop1, *S. pombe*	An17g01420	SA		169	32.2	40.0	56.1	6.53	2.71
VESICULAR TRANSPORT	secretion-associated GTP-binding protein SarA, *A. niger*	An01g04040	SP		189	39.0	26.2	39.2	0.00	2.58
VESICULAR TRANSPORT	similarity to BAX-associated fragment SEQ ID NO:242 from patent WO200264766-A2, *S. cerevisiae*	An01g12810	SP		222	24.5	20.7	34.5	1.69	3.49
VESICULAR TRANSPORT	Rab1 GTPase SrgB, *A. niger*	An09g06790			201	27.1	21.1	23.9	0.20	0.18
VESICULAR TRANSPORT	GTP-binding protein rab11, *Rattus norvegicus*	An01g06060			211	19.7	24.3	21.5	0.08	0.17
VESICULAR TRANSPORT	thioredoxin, *A. nidulans*	An01g02500			108	6.9	9.2	22.9	8.98	6.03
VESICULAR TRANSPORT	component of COPII-coated vesicles Erv25, *S. cerevisiae*	An01g08870	SP		211	11.6	22.6	16.6	0.88	0.93

Functional annotation	Protein description	Locus tag	SS	ERRS	PL	NSAF·10^4			G-score	G-score
						M.	X.	S.	M.	X.
VESICULAR TRANSPORT	Rab 6 GTPase SrgC, *A. niger*	An15g05740			209	10.7	15.1	20.5	3.11	0.83
VESICULAR TRANSPORT	hypothetical protein B3E4.60, *N. crassa*	An08g04480			858	15.1	19.9	20.1	0.73	0.00
VESICULAR TRANSPORT	similarity to Golgi membrane protein Emp47, *S. cerevisiae*	An04g08830	SP		415	16.7	19.8	17.8	0.04	0.10
VESICULAR TRANSPORT	v-SNARE Vti1, *S. cerevisiae*	An04g05980			224	14.8	19.7	18.0	0.31	0.08
VESICULAR TRANSPORT	homologue of yeast Erv14 strongly similar to pattern formation protein cni, D. melanogaster-	An07g09160	SP		138	19.4	0.7	0.9	20.52	0.05
VESICULAR TRANSPORT	similarity to protein p58, *Rattus norvegicus*	An02g04250	SP		324	16.8	19.2	18.0	0.04	0.04
VESICULAR TRANSPORT	transport vesicle docking protein Pep12, *S. cerevisiae*	An04g01530			273	19.2	16.8	14.7	0.58	0.14
VESICULAR TRANSPORT	protein RER1, *H. sapiens*	An02g02830	SP		189	18.7	13.8	18.6	0.00	0.69
VESICULAR TRANSPORT	precursor of protein Emp24, *S. cerevisiae*	An08g03590	SP		203	15.3	17.3	12.2	0.35	0.91
VESICULAR TRANSPORT	vesicular transport protein SEC17, Pichia pastoris	An02g01580	SP		294	17.1	15.6	6.6	4.77	3.75
VESICULAR TRANSPORT	COPII vesicle component Yip3, *S. cerevisiae*	An18g06440			173	15.4	16.2	12.8	0.25	0.40
VESICULAR TRANSPORT	hypothetical protein YAR002c-a, *S. cerevisiae*	An04g01780	SP		232	15.2	13.6	10.6	0.81	0.36
VESICULAR TRANSPORT	COPII vesicle coat component protein Erv46, *S. cerevisiae*	An01g04320	SA		406	8.2	14.9	12.5	0.91	0.21
VESICULAR TRANSPORT	hypothetical GTP-binding protein SPAC27E2.03c, *S. pombe*	An08g01610			394	9.5	8.0	14.2	0.93	1.74
VESICULAR TRANSPORT	GTP-binding protein Vps1, *S. cerevisiae*	An02g10450			697	12.1	13.6	9.5	0.31	0.72
VESICULAR TRANSPORT	COP-coated vesicle membrane protein P24 homolog lbrA- Polysphondylium pallidum	An09g05490	SP		239	13.0	12.4	6.0	2.64	2.32
VESICULAR TRANSPORT	hypothetical ER associated protein, *S. pombe*	An08g03960			254	10.5	12.4	9.7	0.03	0.33
VESICULAR TRANSPORT	GTP-binding protein a-ras, *A. nidulans*	An01g02320			212	7.6	12.3	5.5	0.32	2.67
VESICULAR TRANSPORT	similarity to protein cwl1p, *S. pombe*	An08g08600			325	8.2	9.7	11.6	0.58	0.17
VESICULAR TRANSPORT	Erv41, *S. cerevisiae*	An03g04940	SA		399	7.2	11.1	7.5	0.00	0.70
VESICULAR TRANSPORT	small Ras-like GTPase Vps21, *S. cerevisiae*	An02g06400			262	11.0	5.8	2.5	5.83	1.40
VESICULAR TRANSPORT	dynamin-related protein Dnm1, *S. cerevisiae*	An03g06950			798	7.1	6.9	10.3	0.58	0.66
VESICULAR TRANSPORT	α subunit of the coatomer complex Ret1, *S. cerevisiae*	An16g02460			1206	8.1	6.1	9.8	0.17	0.89
VESICULAR TRANSPORT	similarity to Golgi membrane protein Yip1, *S. cerevisiae*	An02g02640			253	9.7	0.4	0.5	10.10	0.03
VESICULAR TRANSPORT	cell division control protein SLY2 homolog YKL196c, *S. cerevisiae*	An04g08480			196	6.0	9.7	8.6	0.47	0.06
VESICULAR TRANSPORT	C2-domain family vesicle protein GLUT4, *Rattus norvegicus*	An12g00800			1520	9.6	9.3	6.9	0.44	0.35
VESICULAR TRANSPORT	coatomer γ subunit 2 copg2, *H. sapiens*	An07g06030			916	1.5	3.1	9.2	6.14	3.25
VESICULAR TRANSPORT	secretory protein Sec23, *S. cerevisiae*	An01g04730			768	4.6	4.1	9.0	1.44	1.85
VESICULAR TRANSPORT	Rab8 GTPase SrgA, *A. niger*	An14g00010			206	8.8	6.6	0.6	8.47	5.70
VESICULAR TRANSPORT	ADP-ribosylation factor 6 ARF6, *H. sapiens*	An02g07780			184	8.7	0.5	0.7	8.04	0.04
VESICULAR TRANSPORT	synaptobrevin Snc2, *S. cerevisiae*	An12g07570			135	8.7	7.3	6.7	0.25	0.03
VESICULAR TRANSPORT	hypothetical protein AFUB 053450, putative Sec12 homologue, *A. fumigatus*	225665			622	5.0	8.0	8.6	0.96	0.02
VESICULAR TRANSPORT	syntaxin-related protein (T-SNARE) Sso2, *S. cerevisiae*	An12g01190			308	3.8	7.9	2.1	0.50	3.57
VESICULAR TRANSPORT	ADP-ribosylation factor arf1, *Ajellomyces capsulatus*	An08g03690			183	7.6	7.4	5.0	0.55	0.48
VESICULAR TRANSPORT	Rab5c GTPase strongly similar to ypt5p, *S. pombe*	An04g02470			218	6.4	7.0	0.6	5.59	6.39
VESICULAR TRANSPORT	β-COP Sec26, *S. cerevisiae*	An08g03270			955	3.5	4.2	6.9	1.18	0.65
VESICULAR TRANSPORT	secretory AAA-ATPase NsfA, *A. niger*	An02g08450			728	6.6	4.3	3.4	1.05	0.12
VESICULAR TRANSPORT	transport protein Sec24, *S. cerevisiae*	An08g10650			919	2.7	6.6	6.4	1.55	0.00

Functional annotation	Protein description	Locus tag	SS	ERRS	PL	NSAF·10^4			G-score	G-score
						M.	X.	S.	M.	X.
VESICULAR TRANSPORT	similarity to VAMP-7 vesicle-associated membrane protein7, *Rattus norvegicus*	An08g07470	SP		269	6.0	6.4	2.4	1.55	1.84
VESICULAR TRANSPORT	similarity to antiviral GTPase Mx1, Oncorhynchus mykiss	An11g00010			802	3.9	4.6	6.3	0.60	0.27
VESICULAR TRANSPORT	hypothetical coiled-coil protein similar to human congenital heart disease protein CAC05252.1, *S. pombe*	An04g00670	SP		196	3.8	4.1	6.0	0.48	0.33
VESICULAR TRANSPORT	coatomer β subunit copB2, *H. sapiens*	An02g05870			873	4.5	5.7	4.0	0.03	0.29
VESICULAR TRANSPORT	similarity to transport protein Bos1, *S. cerevisiae*	An07g02170			244	4.8	5.5	4.8	0.00	0.05
VESICULAR TRANSPORT	ASNA1 product arsenite translocating ATPase, *H. sapiens*	An02g07090			341	5.3	3.4	3.4	0.41	0.00
VESICULAR TRANSPORT	GDP dissociation inhibitor in the secretory pathway Gdi1, *S. cerevisiae*	An02g03120			468	5.3	3.7	1.4	2.40	1.06
VESICULAR TRANSPORT	ε-COP, Cricetulus griseus	An08g06330			324	4.3	4.7	3.6	0.06	0.15
VESICULAR TRANSPORT	ER-Golgi transport protein Sft2, *S. cerevisiae*	An08g01410			217	2.5	2.1	4.2	0.45	0.73
VESICULAR TRANSPORT	luminal ER-protein retention receptor ERD2, Kluyveromyces marxianus	An07g07340	SA		335	2.9	4.0	2.7	0.00	0.26
VESICULAR TRANSPORT	SNARE protein of Golgi compartment Gos1, *S. cerevisiae*	An08g02460			227	1.4	2.0	4.0	1.29	0.69
VESICULAR TRANSPORT	signal peptide-containing protein SIGP from patent WO9933981-A2, *H. sapiens*	An15g01680			355	3.9	2.8	1.8	0.77	0.20
VESICULAR TRANSPORT	casein kinase-1 homolog hhp1p, *S. pombe*	An07g06080			370	2.6	3.7	3.2	0.05	0.04
VESICULAR TRANSPORT	ras-GTPase-activating protein SH3-domain binding protein G3BP, *Mus musculus*	An09g06580			537	2.2	2.2	3.6	0.36	0.36
VESICULAR TRANSPORT	syntaxin Tlg2, *S. cerevisiae*	An04g07020			373	2.0	3.6	3.1	0.25	0.04
VESICULAR TRANSPORT	similarity to hypothetical protein SPAC6F12.04, *S. pombe*	An01g02410			234	3.2	0.4	0.6	2.06	0.03
VESICULAR TRANSPORT	adaptor complex AP-1 medium chain AP47, *Mus musculus*	An07g03200			418	0.8	1.5	2.8	1.23	0.39
VESICULAR TRANSPORT	δ subunit of the coatomer δ-coat protein CopD, Bos taurus	An01g14250			518	1.9	2.3	2.8	0.18	0.05
VESICULAR TRANSPORT	cis-Golgi t-SNARE Sed5, *S. cerevisiae*	An02g12980			343	1.6	0.8	2.7	0.29	1.06
VESICULAR TRANSPORT	β-adaptin BAD1, D. melanogaster-	An16g02490			748	0.4	0.8	2.6	1.73	0.94
VESICULAR TRANSPORT	γ1-adaptin, *H. sapiens*	An01g02600			848	2.4	1.4	2.6	0.01	0.38
VESICULAR TRANSPORT	protein Sly1, *S. cerevisiae*	An09g04170			705	2.6	2.2	1.3	0.44	0.23
VESICULAR TRANSPORT	ARF guanine-nucleotide exchange factor 2 Gea2, *S. cerevisiae*	An18g02490			1554	0.1	0.4	2.3	2.60	1.42
VESICULAR TRANSPORT	transport protein Sec24A, *H. sapiens*	An16g03320			1009	0.1	1.5	2.2	2.32	0.12
VESICULAR TRANSPORT	p150 component of the COPII coat of secretory pathway vesicles Sec31, *S. cerevisiae*	An02g01690	SP		1259	1.1	1.5	0.7	0.08	0.28
VESICULAR TRANSPORT	similarity to hypothetical protein YIL039w, *S. cerevisiae*	An07g07830	SP		564	0.2	1.1	0.7	0.30	0.10
VESICULAR TRANSPORT	weak similarity to Traf2 and NCK interacting kinase (splice variant 8), *H. sapiens*	An06g02180			1053	0.1	0.6	1.1	0.98	0.16
VESICULAR TRANSPORT	protein Sec7, *S. cerevisiae*	An07g02190			1793	0.3	0.6	0.2	0.01	0.15
UNKNOWN/ OTHERS	similarity to hypothetical protein EAA30505.1, *N. crassa*	An18g01000	SA		284	16.9	27.0	14.2	0.24	4.05
UNKNOWN/ OTHERS	lipid phosphoinositide phosphatase Sac1, *S. cerevisiae*	An04g02480			687	23.8	23.2	33.5	1.64	1.86
UNKNOWN/ OTHERS	hypothetical protein EAL85123.1, *A. fumigatus*	An02g08300			164	24.1	15.9	15.0	2.11	0.03
UNKNOWN/ OTHERS	nitrilase NIT1, *A. thaliana*	An12g01260	SP		320	23.7	14.4	9.3	6.46	1.07
UNKNOWN/ OTHERS	glycine-rich RNA-binding protein grrbp2, Euphorbia esula	An02g12270			116	10.1	7.0	23.5	5.47	9.45
UNKNOWN/ OTHERS	methyltransferase family protein, A. flavus NRRL3357	42743			263	22.3	14.7	19.3	0.23	0.60
UNKNOWN/ OTHERS	cytochrome-b5 reductase, *S. cerevisiae*	An02g04860			305	18.6	21.0	14.9	0.40	1.03
UNKNOWN/ OTHERS	polyketide synthase, *A. fumigatus* Af293	211885			2443	20.8	19.0	20.5	0.00	0.05
UNKNOWN/ OTHERS	inorganic pyrophosphatase Ipp1, *S. cerevisiae*	An02g12010			406	20.3	10.4	9.9	3.62	0.01
UNKNOWN/ OTHERS	pyridoxine synthesis component pyroA, *A. nidulans*	An03g04280			309	15.6	19.5	17.2	0.09	0.14

Functional annotation	Protein description	Locus tag	SS	ERRS	PL	NSAF·10^4			G-score	G-score
						M.	X.	S.	M.	X.
UNKNOWN/ OTHERS	weak similarity to phosphoenolpyruvate carboxylase, Escherichia coli	An07g01340			346	18.2	13.8	19.1	0.02	0.87
UNKNOWN/ OTHERS	O-methyltransferase B omtB, A. parasiticus	An07g05520			380	11.5	9.7	16.1	0.75	1.58
UNKNOWN/ OTHERS	weak similarity to hypothetical acetyltransferase MK0549, Methanopyrus kandle	An18g00950			251	10.6	3.9	16.0	1.10	7.84
UNKNOWN/ OTHERS	hypothetical protein H04M03.4, *C. elegans*	An02g08660			510	12.4	12.2	15.0	0.26	0.30
UNKNOWN/ OTHERS	hypothetical single-stranded TG1-3 binding protein tcg, *S. pombe*	An17g00370			361	14.5	12.2	10.4	0.67	0.14
UNKNOWN/ OTHERS	zinc-metalloprotease Ste24, *S. cerevisiae*	An04g01950			456	8.2	14.4	13.4	1.26	0.04
UNKNOWN/ OTHERS	similarity to hypothetical protein AAM35689.1, Xanthomonas axonopodis	An12g05170			295	9.8	14.4	7.5	0.31	2.20
UNKNOWN/ OTHERS	hypothetical pathogenicity protein PATH531, Magnaporthe grisea	An16g06820	SP		323	11.6	8.1	14.1	0.24	1.64
UNKNOWN/ OTHERS	hypothetical precursor of secretory protein Ssp120, *S. cerevisiae*	An18g03100	SP		199	8.1	11.3	13.7	1.49	0.23
UNKNOWN/ OTHERS	nitrite reductase (NADH) niiA, *A. nidulans*	An08g05640			1097	9.3	9.9	13.4	0.76	0.51
UNKNOWN/ OTHERS	zinc binding enoyl reductase, *A. fumigatus* Af293	124807			357	12.9	6.3	5.5	3.08	0.06
UNKNOWN/ OTHERS	hypothetical protein SPBC16H5.12c, *S. pombe*	An11g07970			702	11.1	12.5	8.0	0.52	1.00
UNKNOWN/ OTHERS	Pc24g00650, P. chrysogenum Wisconsin 54-1255	53656			134	12.0	6.1	8.7	0.51	0.49
UNKNOWN/ OTHERS	similarity to hypothetical protein SPBC2G5.01, *S. pombe*	An04g07080			433	7.2	8.5	11.7	1.11	0.50
UNKNOWN/ OTHERS	dipeptidyl peptidase III, *Rattus norvegicus*	An04g00410			707	11.6	10.6	7.5	0.89	0.52
UNKNOWN/ OTHERS	hypothetical protein EAA71297.1, Gibberella zeae	An04g05750	SP		86	11.2	1.0	1.5	8.33	0.08
UNKNOWN/ OTHERS	hypothetical oxidoreductase CAB46711.1, *S. pombe*	An17g00210			360	10.4	7.3	4.7	2.21	0.56
UNKNOWN/ OTHERS	similarity to plasma membrane bound receptor from patent DE19627237-A1, Sus scrofa	An01g10730			213	4.5	5.5	10.4	2.37	1.52
UNKNOWN/ OTHERS	host infection protein cap20, Colletotrichum gloeosporioides	An18g05000			188	0.6	4.3	10.4	10.69	2.57
UNKNOWN/ OTHERS	spermidine synthase Spe3, *S. cerevisiae*	An08g06560			292	9.9	10.2	10.2	0.01	0.00
UNKNOWN/ OTHERS	lysine aminopeptidase ApsA, *A. niger*	An04g03930			881	4.7	8.9	9.9	1.85	0.05
UNKNOWN/ OTHERS	alcohol oxidase AOD1, Candida boidinii	An15g02200			602	8.3	6.1	9.7	0.10	0.81
UNKNOWN/ OTHERS	hypothetical protein	An04g08060			210	9.7	3.9	0.6	9.58	2.62
UNKNOWN/ OTHERS	hypothetical protein EAA57923.1, *A. nidulans*	An12g03990		AEEL	769	3.5	6.9	9.6	3.01	0.45
UNKNOWN/ OTHERS	hypothetical protein mlr2056, Mesorhizobium loti	An03g01320			256	9.6	8.8	6.6	0.56	0.32
UNKNOWN/ OTHERS	hypothetical protein Afu4g11550, *A. fumigatus*	An04g04940			303	9.5	9.2	6.4	0.60	0.50
UNKNOWN/ OTHERS	aminopeptidase METPRO02 from patent EP939131-A2, *H. sapiens*	An02g11940			497	7.5	9.2	1.8	3.72	5.43
UNKNOWN/ OTHERS	similarity to hypothetical protein lin-10, *C. elegans*	An12g05040			99	3.2	0.9	9.2	2.97	7.88
UNKNOWN/ OTHERS	hypothetical protein Afu6g10450, *A. fumigatus*	An11g00890	SA		192	3.9	8.9	2.0	0.60	4.68
UNKNOWN/ OTHERS	weak similarity to hypothetical protein ycnE, Bacillus subtilis	An13g01530			102	7.3	2.7	8.9	0.15	3.58
UNKNOWN/ OTHERS	Casein kinase CK II, *A. thaliana*	An16g08010			335	8.6	8.3	8.1	0.01	0.00
UNKNOWN/ OTHERS	protein sequence 79 from patent WO0129221, *H. sapiens*	An10g00170			330	5.5	8.5	2.0	1.74	4.36
UNKNOWN/ OTHERS	urate oxidase uaz, A. flavus	An02g06030			302	8.1	7.5	7.3	0.04	0.00
UNKNOWN/ OTHERS	similarity to hypothetical protein BAB52928.1, Mesorhizobium loti	An11g07020			260	6.2	8.0	1.5	3.05	4.86
UNKNOWN/ OTHERS	hypothetical protein FG01228.1, Fusarium graminearum	An13g02980			180	7.7	7.5	6.5	0.11	0.07
UNKNOWN/ OTHERS	similarity to peroxisomal membrane protein PMP22, *A. thaliana*	An04g09130			224	4.3	4.4	7.5	0.90	0.82
UNKNOWN/ OTHERS	polypeptide HFIZG53 from patent EP892050-A2, *H. sapiens*	An01g08410			242	7.5	5.6	2.7	2.38	1.04
UNKNOWN/ OTHERS	hypothetical glutathione S-transferase CAA19067.1, *S. pombe*	An18g02720			226	7.1	6.8	7.5	0.01	0.03
UNKNOWN/ OTHERS	dipeptidyl-peptidase V DPP V, *A. fumigatus*	An16g08150			732	1.9	6.5	7.3	3.36	0.04

Functional annotation	Protein description	Locus tag	SS	ERRS	PL	NSAF·10^4			G-score	G-score
						M.	X.	S.	M.	X.
UNKNOWN/ OTHERS	hypothetical protein 2E4.30, *N. crassa*	An07g02800			346	4.0	1.8	7.1	0.88	3.36
UNKNOWN/ OTHERS	similarity to hypothetical proteinase encoded by SCD8A.14c, *Streptomyces coelicolor*	An03g02530			328	4.2	6.9	4.4	0.00	0.57
UNKNOWN/ OTHERS	similarity to hypothetical protein BAE64442.1, A. oryzae	An14g02090			174	6.8	6.7	2.2	2.37	2.36
UNKNOWN/ OTHERS	similarity to secreted protein #70 from patent WO9925825-A2, *H. sapiens*	An12g07510			176	5.5	6.7	5.2	0.01	0.19
UNKNOWN/ OTHERS	similarity to palmitylated serine/threonine kinase PKL12, *Mus musculus*	An16g08180			375	6.6	5.5	1.0	4.46	3.37
UNKNOWN/ OTHERS	similarity to lactone-specific esterase estf1, Pseudomonas fluorescens	An01g05800			296	5.4	6.4	1.3	2.68	3.64
UNKNOWN/ OTHERS	acylaminoacyl-peptidase DPP V, *A. fumigatus*	An09g02830			750	5.8	6.4	2.9	0.97	1.29
UNKNOWN/ OTHERS	leucyl aminopeptidase Ape2, *S. cerevisiae*	An09g06800			882	3.8	6.2	4.0	0.01	0.50
UNKNOWN/ OTHERS	repressor protein qutR, *A. nidulans*	An07g03680			272	2.7	3.6	6.2	1.37	0.67
UNKNOWN/ OTHERS	hypothetical membrane protein Ptm1, *S. cerevisiae*	An14g06830	SP		536	6.2	5.9	2.7	1.43	1.24
UNKNOWN/ OTHERS	linoleate diol synthase, Gaeumannomyces graminis	An04g05880			1080	2.5	6.1	5.7	1.28	0.02
UNKNOWN/ OTHERS	hypothetical protein CAD21419.1, *N. crassa*	An13g00780	SP		286	4.1	5.4	5.9	0.32	0.03
UNKNOWN/ OTHERS	similarity to hypothetical protein F9K20.18, *A. thaliana*	An09g00650			242	2.2	1.9	5.9	1.75	2.21
UNKNOWN/ OTHERS	similarity to hypothetical protein CAD37045.1, *N. crassa*	An07g03660			263	2.0	5.8	5.4	1.61	0.01
UNKNOWN/ OTHERS	hypothetical acid phosphatase CAB58405.1, *S. pombe*	An01g10750			603	1.9	5.5	5.8	2.01	0.01
UNKNOWN/ OTHERS	similarity to β-ketoacyl reductase rhlG, Pseudomonas aeruginosa	An01g09310			262	1.2	1.7	5.5	2.90	2.04
UNKNOWN/ OTHERS	hypothetical cleft lip and palate transmembrane protein 1 CLPTM1, *H. sapiens*	An15g01350			601	2.7	3.4	5.4	0.95	0.43
UNKNOWN/ OTHERS	hypothetical protein SPCC1281.03c, *S. pombe*	An16g04640			186	5.2	5.3	3.5	0.33	0.39
UNKNOWN/ OTHERS	rac-family serine/threonine protein kinase homolog dagA, *Dictyostelium discoideum*	An02g05860			626	1.2	1.0	5.2	2.69	3.09
UNKNOWN/ OTHERS	pyridoxine 4-dehydrogenase PLR, *S. pombe*	An16g02360			329	1.6	3.0	5.1	1.91	0.56
UNKNOWN/ OTHERS	peroxisomal membrane protein Pmp27, *S. cerevisiae*	An11g02590			235	5.0	3.5	3.9	0.14	0.02
UNKNOWN/ OTHERS	hypothetical protein SPCC1450.12, *S. pombe*	An02g11440			919	0.6	0.7	4.9	3.95	3.63
UNKNOWN/ OTHERS	hypothetical protein Afu7g03900, *A. fumigatus*	An13g00320			432	2.7	4.8	2.1	0.08	1.08
UNKNOWN/ OTHERS	prolyl aminopeptidase PapA, *A. niger*	An11g04730			511	2.3	4.8	2.8	0.05	0.52
UNKNOWN/ OTHERS	oxidoreductase for actinorhodin production encoded by Orf11, Streptomyces lividans	An15g04150			293	4.7	1.5	3.1	0.34	0.54
UNKNOWN/ OTHERS	weak similarity to protein CAP59, *Cryptococcus neoformans*	An02g13450			794	4.7	2.4	0.8	3.03	0.80
UNKNOWN/ OTHERS	trifunctional protein of the β-oxidation fox-2, *N. crassa*	An14g00990			901	4.6	3.3	2.5	0.68	0.13
UNKNOWN/ OTHERS	peroxisomal membrane protein Pex14, Hansenula polymorpha	An16g04020	SP		370	2.0	1.7	4.6	1.01	1.35
UNKNOWN/ OTHERS	precursor of linoleate diol synthase, Gaeumannomyces graminis	An02g07930			1110	4.3	4.5	1.8	1.13	1.22
UNKNOWN/ OTHERS	similarity to multifunctional β-oxidation protein, *N. crassa*	An18g05210			322	1.7	3.6	4.4	1.31	0.08
UNKNOWN/ OTHERS	V-ATPase assembly factor strongly similar to Pkr1, *S. cerevisiae*	An11g05260	SA		169	4.4	0.5	0.8	2.85	0.04
UNKNOWN/ OTHERS	hypothetical protein Afu7g04060, *A. fumigatus*	An13g00540			265	2.8	4.4	2.5	0.03	0.57
UNKNOWN/ OTHERS	prolidase, Suberites domuncula	An05g00050			466	4.4	1.7	2.5	0.50	0.14
UNKNOWN/ OTHERS	leukotriene-A4 hydrolase, *Mus musculus*	An05g00070			664	4.3	1.0	1.8	1.13	0.25
UNKNOWN/ OTHERS	hypothetical protein SPAC24C9.05c, *S. pombe*	An18g05820			609	2.6	4.3	4.1	0.30	0.01
UNKNOWN/ OTHERS	nitrate reductase (NADPH) NiaD, *A. niger*	An08g05610			867	3.1	4.3	2.5	0.05	0.44
UNKNOWN/ OTHERS	cytoplasmic metalloproteinase mepB, *A. fumigatus*	An07g01970			716	1.3	4.2	2.4	0.28	0.50
UNKNOWN/ OTHERS	weak similarity to hypothetical protein CAB51071.1, *H. sapiens*	An04g03800			287	4.1	0.3	0.5	3.36	0.03
UNKNOWN/ OTHERS	hypothetical protein SPCC594.04c, *S. pombe*	An07g06990			373	1.4	2.7	3.8	1.13	0.21

Functional annotation	Protein description	Locus tag	SS	ERRS	PL	NSAF·10^4			G-score	G-score
						M.	X.	S.	M.	X.
UNKNOWN/ OTHERS	aldehyde dehydrogenase, A. terreus NIH2624	53357			513	1.5	1.9	3.8	1.08	0.62
UNKNOWN/ OTHERS	acyl-CoA dehydrogenase MCAD, *Rattus norvegicus*-	An17g01150			446	1.2	1.0	3.8	1.41	1.71
UNKNOWN/ OTHERS	similarity to 2-hydroxymuconate-semialdehyde hydrolase phnD, Pseudomonas sp.	An07g09320	SA		408	2.4	3.8	2.9	0.05	0.12
UNKNOWN/ OTHERS	levodione reductase lvr, Corynebacterium aquaticum	An08g07520			314	0.3	1.4	3.7	3.29	1.05
UNKNOWN/ OTHERS	hypothetical protein encoded by An11g10340, *A. niger*	An02g00110			318	2.4	3.1	3.7	0.29	0.05
UNKNOWN/ OTHERS	7-aminocholesterol resistance protein Rta1, *S. cerevisiae*	An05g01070			320	3.7	2.5	1.2	1.29	0.47
UNKNOWN/ OTHERS	similarity to hypothetical protein C01B10.8, *C. elegans*	An07g05160	SP		542	1.4	2.2	3.6	1.02	0.36
UNKNOWN/ OTHERS	weak similarity to predicted protein, A. terreus NIH2624	46101			278	3.5	3.6	1.4	0.90	0.98
UNKNOWN/ OTHERS	hypothetical protein	An07g03080	SP		217	3.4	0.4	0.6	2.22	0.03
UNKNOWN/ OTHERS	protein fragment SEQ ID NO:4306 from patent EP1033405-A2, *A. thaliana*	An04g05490			469	3.4	2.5	3.0	0.02	0.05
UNKNOWN/ OTHERS	cDNA gene trap ankyrin repeat containing protein Gtar, *Mus musculus*	An03g03050			826	0.4	0.5	3.3	2.63	2.19
UNKNOWN/ OTHERS	coproporphyrinogen oxidase III Hem13, *S. cerevisiae*	An07g10040	SA		440	1.7	2.3	3.2	0.49	0.18
UNKNOWN/ OTHERS	uroporphyrinogen decarboxylase from patent WO9925839-A1, Thielavia terrestris-	An01g04250			363	0.3	1.7	3.2	2.85	0.45
UNKNOWN/ OTHERS	hypothetical conserved protein B2F7.100, *N. crassa*	An13g00080			238	3.1	2.7	1.6	0.48	0.24
UNKNOWN/ OTHERS	nonribosomal peptide synthetase; NRPS, Hypocrea virens	55153			5640	3.1	0.6	1.2	0.89	0.20
UNKNOWN/ OTHERS	similarity to hard surface induced protein 3 chip3, Glomerella cingulata	An05g01760			501	2.8	3.1	0.8	1.19	1.45
UNKNOWN/ OTHERS	hypothetical protein encoded by B7F18.130, *N. crassa*	An18g05050	SA		388	3.0	1.2	3.0	0.00	0.85
UNKNOWN/ OTHERS	similarity to retinal short-chain dehydrogenase/reductase retSDR1, *Mus musculus*	An18g05090			387	1.4	3.0	3.0	0.63	0.00
UNKNOWN/ OTHERS	hypothetical protein EAA62682.1, *A. nidulans*	An08g10500			268	0.4	3.0	1.5	0.64	0.56
UNKNOWN/ OTHERS	hypothetical protein Afu6g06700, *A. fumigatus*	An18g06350	SP		209	1.5	3.0	0.6	0.40	1.72
UNKNOWN/ OTHERS	endometrium tumour EST encoded protein 137 from patent DE19817948-A1, *H. sapiens*	An17g00880			483	1.1	1.3	3.0	0.88	0.66
UNKNOWN/ OTHERS	similarity to transsulphurylation protein hxB, *A. nidulans*	An11g01960	SP		345	0.9	2.9	0.4	0.24	2.17
UNKNOWN/ OTHERS	cell wall antigen 6C5 from patent WO200048620-A1, C. albicans	An04g05380			348	1.5	2.8	2.6	0.28	0.01
UNKNOWN/ OTHERS	mitogen-activated protein kinase FsMAPK, Fusarium solani	An08g10670			354	2.1	2.8	2.6	0.04	0.01
UNKNOWN/ OTHERS	regulator subunit of the protein phosphatase 2A PR65, Xenopus laevis	An18g03290			616	2.6	2.8	2.7	0.00	0.00
UNKNOWN/ OTHERS	aberrant X segregation Axs, D. melanogaster	An14g01960			734	2.8	2.1	2.7	0.00	0.07
UNKNOWN/ OTHERS	similarity to monoglyceride lipase mgll, *Mus musculus*	An11g03380			301	1.8	2.7	2.2	0.04	0.06
UNKNOWN/ OTHERS	polyketide synthase PKS1, Cochliobolus heterostrophus	An15g04140			2565	2.3	2.4	2.6	0.02	0.00
UNKNOWN/ OTHERS	hypothetical protein YBR096w, *S. cerevisiae*	An06g00280	SP		297	2.5	0.3	0.4	1.62	0.02
UNKNOWN/ OTHERS	hypothetical protein F12K21.21, *A. thaliana*	An01g14290			471	2.5	0.2	0.3	2.05	0.02
UNKNOWN/ OTHERS	UV excision repair protein (RadW), putative, A. clavatus NRRL 1	204514			369	2.0	1.7	2.5	0.04	0.14
UNKNOWN/ OTHERS	hypothetical protein Afu3g04020, *A. fumigatus*	An03g03650			332	1.0	2.4	1.2	0.02	0.46
UNKNOWN/ OTHERS	protease involved in a-factor processing Ste23, *S. cerevisiae*	An16g01860			1167	1.2	2.2	1.4	0.03	0.17
UNKNOWN/ OTHERS	hypothetical protein encoded by An01g01140, *A. niger*	An11g03480			434	2.2	0.6	2.1	0.00	0.84
UNKNOWN/ OTHERS	peroxisomal acetyl-CoA C-acyltransferase POT1, Y. lipolytica	An08g05400			418	0.8	0.2	2.2	0.70	1.87
UNKNOWN/ OTHERS	protein fragment SEQ ID NO:17753 from patent EP1033405-A2, *A. thaliana*	An17g00680	SA		548	2.1	0.2	0.2	1.76	0.01
UNKNOWN/ OTHERS	similarity to phosphatidylinositol phosphate phosphatase Inp52, *S. cerevisiae*	An15g02810			441	0.7	1.4	2.1	0.67	0.11
UNKNOWN/ OTHERS	similarity to hypothetical protein, Magnaporthe grisea	An11g01260			492	0.7	2.0	1.3	0.23	0.15
UNKNOWN/ OTHERS	FAD binding domain protein, A. clavatus NRRL 1	208521			581	0.9	0.8	2.0	0.42	0.57

Functional annotation	Protein description	Locus tag	SS	ERRS	PL	NSAF·10^4			G-score	G-score
						M.	X.	S.	M.	X.
UNKNOWN/ OTHERS	weak similarity to 75 kDa invariant surface glycoprotein ISG75, Trypanosoma brucei	An07g08740			314	0.3	2.0	1.2	0.55	0.18
UNKNOWN/ OTHERS	fatty-acyl coenzyme A oxidase (Pox1), putative, *A. fumigatus* A1163	181397			694	2.0	1.4	0.6	0.86	0.39
UNKNOWN/ OTHERS	similarity to hypothetical protein MLD14.3, *A. thaliana*	An04g07160	SP		375	2.0	0.2	0.3	1.28	0.02
UNKNOWN/ OTHERS	hypothetical protein related to host-specific AK-toxin Akt2 B23L21.350- *N. crassa*	An05g01890			461	0.7	0.2	2.0	0.64	1.69
UNKNOWN/ OTHERS	similarity to serine/threonine protein kinase Yak1, *S. cerevisiae*	An14g01050			895	0.1	0.5	1.9	1.88	0.85
UNKNOWN/ OTHERS	chromosome segregation protein cut14p, *S. pombe*	An02g03010			1179	0.8	1.0	1.9	0.43	0.27
UNKNOWN/ OTHERS	similarity to secreted protein SEQ ID NO:58 from patent WO9957132-A1, *H. sapiens*	An14g03020			737	1.0	1.8	1.2	0.02	0.12
UNKNOWN/ OTHERS	hypothetical protein	An12g03320			762	1.8	0.1	0.2	1.60	0.01
UNKNOWN/ OTHERS	hypothetical protein SPAC32A11.02c, *S. pombe*	An05g00900			748	0.7	1.8	0.5	0.03	0.75
UNKNOWN/ OTHERS	similarity to β-lactamase from patent FR2792651-A1, Pyrococcus abyssi	An06g00710			1084	0.1	0.7	1.8	1.85	0.45
UNKNOWN/ OTHERS	hypothetical β-lactamase XF1621, Xylella fastidiosa	An16g02560			506	1.1	0.9	1.8	0.19	0.31
UNKNOWN/ OTHERS	peroxisomal acetyl-CoA C-acyltransferase POT1, Y. lipolytica	An04g05720			419	1.8	0.2	0.3	1.15	0.02
UNKNOWN/ OTHERS	similarity to Topoisomerase I TopoI, Filobasidiella neoformans-	An18g04030			514	0.6	0.9	1.8	0.57	0.31
UNKNOWN/ OTHERS	hypothetical protein YKR018c, *S. cerevisiae*	An08g02280			692	0.2	0.4	1.7	1.49	0.87
UNKNOWN/ OTHERS	hypothetical protein SPCC4G3.11, *S. pombe*	An02g03290	SA		444	1.7	0.2	0.3	1.08	0.02
UNKNOWN/ OTHERS	similarity to Not2p, *H. sapiens*	An02g03090			523	0.6	1.6	0.2	0.16	1.05
UNKNOWN/ OTHERS	guanine deaminase Gda, *Mus musculus*	An14g01140			531	0.6	1.5	0.2	0.16	1.03
UNKNOWN/ OTHERS	hypothetical protein AN2579.2, *A. nidulans*	An05g01350			419	0.8	1.5	0.3	0.20	0.86
UNKNOWN/ OTHERS	transcription regulator protein Cdc39, *S. cerevisiae*	An16g04100			2361	0.6	0.9	1.5	0.40	0.16
UNKNOWN/ OTHERS	hypothetical conserved protein 12F11.50, *N. crassa*	An02g11810			551	1.0	1.5	0.2	0.48	1.00
UNKNOWN/ OTHERS	similarity to erythrocyte splice form 1 of ankyrin ANK1, *H. sapiens*	An11g05660			1254	1.4	0.1	0.1	1.39	0.01
UNKNOWN/ OTHERS	similarity to hypothetical membrane protein YIL067c, *S. cerevisiae*	An09g02540			681	0.2	1.2	1.0	0.64	0.03
UNKNOWN/ OTHERS	hypothetical protein SPCC622.11, *S. pombe*	An18g04730	SP		687	0.8	1.2	0.2	0.38	0.80
UNKNOWN/ OTHERS	weak similarity to β transducin-like protein het-e1, P. anserina	An02g01260			1404	1.0	1.0	0.8	0.01	0.01
UNKNOWN/ OTHERS	similarity to hypothetical protein CAC28841.2, *N. crassa*	An15g05840	SP		844	0.9	0.1	0.2	0.57	0.01
UNKNOWN/ OTHERS	hypothetical membrane protein YDR326c, *S. cerevisiae*	An17g00320			1252	0.1	0.8	0.1	0.00	0.60
UNKNOWN/ OTHERS	PX domain protein, *A. fumigatus* Af293	211733			1024	0.1	0.6	0.6	0.42	0.00
UNKNOWN/ OTHERS	similarity to hypothetical protein T21J18.40, *A. thaliana*	An18g02760			1689	0.3	0.4	0.1	0.16	0.21

Supplementary Table S2. Proteins from non-secretory organelles. NSAF: normalised spectral abundance factor; SpC: spectral counts, XYL: D-xylose addition; SORB: D-sorbitol addition; grey box: significantly more abundant on D-xylose; white box: significantly more abundant on D-sorbitol.

A. niger locus	Protein description	SpC		NSAF.10^4	
		X.	S.	X.	S.
NUCLEAR					
An06g01440	similarity to heterogeneous nuclear ribonucleoprotein (hnRNP) Tom34, *S. cerevisiae*	27	29	14.8	22.9
An11g11310	histone H2B, *A. nidulans*	11	9	14.7	17.5
An03g06670	weak similarity to myosin-like protein Mlp1, *S. cerevisiae*	248	122	21.6	15.3
An07g05820	hypothetical transmembrane protein usgS, *A. nidulans*	26	14	13.1	10.3
An15g06440	karyopherin alpha Srp1, *S. cerevisiae*	17	21	5.8	10.2
An16g01870	mRNA cleavage factor I 25 kDa subunit CFIM25, *H. sapiens*	7	8	4.9	8.0
An08g10060	small G-protein Gsp1, *C. albicans*	10	6	8.9	7.9
An15g00170	protein kinase skp1p, *S. pombe*	11	11	5.3	7.6
An08g06940	histone H4.1, *A. nidulans*	3	2	6.1	6.3
An07g02990	similarity to RNA-binding protein AUF1, *H. sapiens*	13	7	7.7	6.2
An14g04940	mRNA turnover 4 protein Mrt4, *S. cerevisiae*	8	5	6.6	6.1
An11g11140	nuclear pore membrane protein Pom152, *S. cerevisiae*	48	28	7.0	5.9
An12g07790	transcription factor btf3p, *S. pombe*-	2	3	2.9	5.9
An12g08030	NADH oxidoreductase complex I subunit Sub2, *S. cerevisiae*	12	9	5.1	5.6
An07g02690	similarity to hypothetical regulational protein PBK1, *H. sapiens*-	4	8	2.0	5.4
An01g12230	nucleolar protein Nop1, *S. cerevisiae*	18	6	10.7	5.4
An14g00100	nucleoporin-interacting protein Nic96, *S. cerevisiae*	10	20	1.9	5.4
56745	pre-mRNA splicing factor (Srp1), putative [*Neosartorya fischeri* NRRL 181]	7	4	6.1	5.3
An07g01520	nucleoporin Nup170, *S. cerevisiae*	11	25	1.5	4.9
An12g00410	RNA binding protein 47 RBP47, *Nicotiana plumbaginifolia*	6	7	2.9	4.9
An01g06040	hypothetical membrane protein YOL077c, *S. cerevisiae*	6	6	3.3	4.7
An16g01810	histone H2A variant pht1p, *S. pombe*-	1	2	2.0	4.7
An14g02360	U2 snRNA-specific protein A, *H. sapiens*	4	4	3.2	4.6
An01g14070	karyopherin β Kap95, *S. cerevisiae*-	19	15	4.0	4.6
An04g01520	similarity to nuclear envelope protein cut11p, *S. pombe*	6	9	2.1	4.4
An09g00500	weak similarity to transcription factor Arg81, *S. cerevisiae*	16	13	3.4	4.0
An02g08100	translin-like protein TRAX, *Gallus gallus*-	2	3	1.9	3.9
An02g09260	nucleolar protein Nop5, *S. cerevisiae*	11	8	3.6	3.8
An15g00140	similarity to transcription repressor Tup1, *S. cerevisiae*-	4	8	1.4	3.8
An08g00520	protein sonA, *A. nidulans*	4	4	2.3	3.3
An16g03090	small nucleolar RNP component Nop56, *S. cerevisiae*	9	6	3.3	3.3
An07g03430	hypothetical protein CAD70902.1, *N. crassa*	4	3	2.8	3.1
An17g02170	centromere/microtubule-binding protein Cbf5, *S. cerevisiae*	11	5	4.3	3.0
An15g00160	transcription regulator CaGCR3, *C. albicans*-	17	8	3.7	2.6
An02g03860	hypothetical protein B1D1.160, *N. crassa*-	9	12	1.4	2.6
An07g06730	cut3p, *S. pombe*-	3	12	0.5	2.5
An11g01510	similarity to the protein involved in sister chromatid segregation Src1, *S. cerevisiae*	3	6	0.9	2.3
An07g09830	hypothetical protein encoded by B19C19.110, *N. crassa*	5	4	1.9	2.3
An18g01170	poly(ADP-ribose) polymerase NAP protein from patent WO200004173-A1, *Zea mays*-	0	5	0.1	2.2
An02g12640	RNA-binding protein 30, *Nicotiana plumbaginifolia*-	7	4	2.5	2.2
An08g09010	spliceosomal protein SAP130, *H. sapiens*	14	9	2.2	2.0
An02g03940	glucose repression mediator protein Ssn6, *S. cerevisiae*-	1	6	0.3	2.0
An02g14750	actin-related protein, *H. sapiens*	3	3	1.3	1.9
An16g05050	similarity to importin RanBP7, *H. sapiens*	6	7	1.1	1.9
An04g02130	similarity to U1 and U2 snRNPs component SmB, *H. sapiens*	4	1	3.7	1.8
An02g03520	G protein-binding protein CRFG, *H. sapiens*	9	3	2.6	1.4
An01g00150	nuclear protein Enp1, *S. cerevisiae*	5	2	2.0	1.3
An08g07050	189 kD subunit of DNA-directed RNA polymerase I rpa190p, *S. pombe*	10	8	1.1	1.3
An15g01240	protein required for accurate mitotic chromosome segregation Cse1, *S. cerevisiae*	23	4	4.4	1.2
An16g09200	U5 snRNP-specific protein U5-116kD, *Mus musculus*	9	4	1.7	1.2

A. niger locus	Protein description	SpC		NSAF.10^4	
		X.	S.	X.	S.
An07g07420	splicing factor PRP8, *H. sapiens*	15	10	1.2	1.1
An18g02480	DNA repair protein XAB2, *H. sapiens*-	1	3	0.3	1.1
An11g04870	ribonucleoprotein autoantigen Sm-D, *H. sapiens*	4	0	6.7	1.1
An14g06530	similarity to nucleoporin Nup192, *S. cerevisiae*-	3	5	0.4	0.8
An02g05400	146D nuclear protein, *Xenopus laevis*	5	3	0.8	0.8
An04g05870	E3 ubiquitin ligase Tom1, *S. cerevisiae*	17	11	0.8	0.7
An04g05630	similarity to nuclear pore complex subunit Nup100, *S. cerevisiae*-	1	5	0.1	0.7
An04g02640	protein pescadillo, *H. sapiens*	11	1	3.1	0.6
An15g06390	ribosomal RNA processing protein Rrp5, *S. cerevisiae*	13	3	1.3	0.5
An07g10400	cell division control protein Cdc68, *S. cerevisiae*	5	1	1.0	0.4
An02g10200	protein TRRAP, *H. sapiens*	4	3	0.2	0.2
An08g06090	similarity to nucleoporin nup184p, *S. pombe*	6	1	0.6	0.2
An11g01770	135 kD subunit of DNA-directed RNA polymerase I, *N. crassa*	8	0	1.3	0.1
An12g00720	138 kD subunit of DNA-dependent RNA polymerase II rpb2p, *S. pombe*	4	0	0.6	0.1
An16g07120	regulator protein Sin3, *S. cerevisiae*	3	0	0.4	0.1
An17g00540	similarity to suppressor of S.cerevisiae sin4 mutation Rlr1, *S. cerevisiae*	5	0	0.4	0.1
Mitochondrial					
An18g04220	mitochondrial ADP/ATP carrier anc1p, *S. pombe*	207	114	117.3	93.4
An14g04180	H+-transporting ATP synthase β chain, *N. crassa* [truncated ORF]	219	141	95.0	88.3
An01g13600	mitochondrial phosphate transport protein Mir1, *S. cerevisiae*	116	56	66.9	46.8
An09g06650	core protein II of ubiquinol--cyt c reductase CAA42214.1, *Bos primigenius taurus*	103	80	40.8	45.7
An04g04060	cytochrome-c peroxidase precursor Ccp1, *S. cerevisiae*	67	63	33.5	45.4
An07g06840	precursor of dihydrolipoamide dehydrogenase Lpd1, *S. cerevisiae*	84	67	29.7	34.2
An16g07410	mitochondrial F1-ATPase alpha-subunit Atp1, *S. cerevisiae*	136	68	44.3	32.1
An09g05870	nucleoside-diphosphate kinase NDK-1, *N. crassa*	25	18	30.1	31.5
An02g01830	cytochrome c cyc, *A. niger*	16	13	26.6	31.4
203715	outer mitochondrial membrane protein porin [*A.clavatus* NRRL 1]	76	41	39.4	30.9
An07g02180	dihydrolipoamide acetyltransferase Lat1, *S. cerevisiae*	58	78	15.6	30.3
An12g04940	mitochondrial heat shock protein Hsp60, *S. cerevisiae*	146	60	45.0	26.8
An02g11910	similarity to mitochondrial pyruvate DH complex protein Pdx1, *S. cerevisiae*	22	28	14.0	25.7
An14g04400	succinate dehydrogenase iron-sulfur protein subunit Sdh2, *S. cerevisiae*	40	27	24.4	23.9
An01g00100	pyruvate dehydrogenase β chain precursor Pdb1, *S. cerevisiae*	32	32	15.7	22.6
An02g12770	succinate dehydrogenase Sdh1, *S. cerevisiae*	123	54	34.5	22.0
An07g02160	mitochondrial malate dehydrogenase Mdh1, *S. cerevisiae*	55	28	29.4	21.8
An15g01710	F1Fo-ATP synthase subunit 7 ATP7, *K. lactis*	38	14	40.1	21.8
An09g06680	citrate synthase citA, *A. niger*	57	38	21.9	21.1
An08g07360	mitochondrial import receptor TOM20, *N. crassa*	15	13	16.7	21.0
An02g09930	subunit VI of cytochrome c oxidase Cox6, *S. cerevisiae*	16	12	18.8	20.6
An09g03940	ketol-acid reductoisomerase ilv-2, *N. crassa*	46	31	20.9	20.4
An16g07290	F1Fo-ATP synthase subunit 4 ATP4, *K. lactis*	40	17	29.9	18.7
An01g06180	cytochrome c1 of ubiquinol--cytochrome c reductase CYT-1, *N. crassa*	64	22	36.8	18.5
An16g08550	ATP synthase coupling factor (F0) subunit e Tim11, *S. cerevisiae*	11	6	22.5	18.4
An11g09390	21 kD subunit of NADH:ubiquinone reductase nuo-21, *N. crassa*	33	14	27.6	17.2
An09g06850	78 kD subunit of NADH:ubiquinone reductase NDUFS1, *Bos taurus*	132	48	32.4	17.1
An14g04080	iron-sulfur subunit of ubiquinol--cytochrome c reductase rip1p, *S. pombe*	44	15	33.7	16.9
An01g03570	cytochrome-b5 reductase Mcr1, *S. cerevisiae*	64	20	36.1	16.6
An15g00190	mitochondrial import receptor MOM38, *N. crassa*	47	22	24.2	16.5
An11g10200	subunit VIa of cytochrome c oxidase Cox13, *S. cerevisiae*	13	8	17.3	15.7
An08g10690	40 kD subunit of NADH-ubiquinone reductase NUO-40, *N. crassa*	54	21	26.4	15.0
An08g00210	glycerol-3-phosphate dehydrogenase gdm1, *Mus musculus*	82	40	21.1	15.0
An02g05470	49 kD subunit of NADH:ubiquinone reductase, *N. crassa*	56	26	21.4	14.5
An08g04070	mitochondrial receptor complex chain MOM22, *N. crassa*	8	8	10.0	14.5
An01g12210	core protein I of ubiquinol--cytochrome-c reductase β-MPP, *N. crassa*	98	25	37.1	13.9
An14g04170	cytochrome c oxidase subunit V cox5, *A. niger*	26	10	24.1	13.8
An15g00690	14.8 kD subunit of NADH:ubiquinone reductase, *N. crassa*	11	6	16.9	13.8

A. niger locus	Protein description	SpC		NSAF.10^4	
		X.	S.	X.	S.
An02g05900	similarity to hypothetical protein AA57718.1, *A. nidulans*	9	6	13.8	13.6
An14g00220	hypothetical protein SPAC17C9.06, *S. pombe*	44	26	15.6	13.4
An08g05580	precursor of isocitrate dehydrogenase (NAD+) chain Idh2, *S. cerevisiae*	22	22	9.3	13.4
An06g01390	21.3 kD subunit of NADH:ubiquinone reductase, *N. crassa*	26	9	24.5	12.7
An16g05090	endonuclease SceI 75 kDa subunit Ens1, *S. cerevisiae*	39	30	10.7	11.9
An08g06540	antiproliferative protein prohibitin Phb1, *S. cerevisiae*	36	12	23.6	11.7
An11g06200	31 kD subunit of NADH:ubiquinone reductase, *N. crassa*	30	12	19.6	11.6
An02g05880	29.9 kD subunit of NADH:ubiquinone reductase, *N. crassa*	25	10	19.4	11.5
An07g09530	alpha subunit E1 of the pyruvate dehydrogenase complex Pda1, *S. cerevisiae*	14	17	6.5	11.3
An12g04750	prohibitin Phb2, *S. cerevisiae*	33	12	19.7	10.6
An14g00060	20.9 kD subunit of NADH:ubiquinone reductase, *N. crassa*	19	7	18.7	10.4
An04g05220	subunit 6 of ubiquinol--cytochrome-c reductase Qcr6, *S. cerevisiae*	9	6	10.3	10.1
An07g07390	subunit IV of cytochrome c oxidase Cox4, *S. cerevisiae*	29	7	27.4	10.1
An02g04520	H+-transporting ATP synthase delta chain precursor Atp5, *S. cerevisiae*	20	8	16.2	9.7
An03g03900	similarity to single-stranded DNA-binding protein Rim1, *S. cerevisiae*	5	5	6.7	9.7
An01g03480	sorbitol dehydrogenase gutB, *Bacillus subtilis*	18	12	9.8	9.6
An07g03070	mitochondrial carrier protein ARALAR2, *H. sapiens*	96	25	25.0	9.5
An12g00220	hypothetical protein EAA61911.1, *A. nidulans*	6	5	7.6	9.3
An03g04790	mitochondrial outer membrane protein Tom70, *Podospora anserina*	63	21	18.2	8.9
An08g04470	mitochondrial elongation factor Tu, *Arabidopsis thaliana*	16	14	6.8	8.6
An01g10880	similarity to F1F0-ATP synthase subunit g homolog Atp20, *S. cerevisiae*	18	6	16.9	8.5
An17g01110	17.2 kD subunit of NADH:ubiquinone reductase b17.2, *Bos taurus*	6	4	8.4	8.4
An17g01670	succinyl coenzyme A synthase alpha subunit SYRTSA, *Rattus norvegicus*	9	10	5.2	8.2
An07g10010	mitochondrial carrier protein Yhm1, *S. cerevisiae*	37	9	21.9	8.0
An14g02250	flavocytochrome b2 L-lactate dehydrogenase CYB2, *Pichia anomala*	8	14	3.1	7.5
An18g01590	carnitine O-acetyltransferase cat2, *Candida tropicalis*	10	18	2.9	7.5
An12g04780	24 kD subunit of NADH:ubiquinone reductase Nuo24, *N. crassa*	18	7	12.4	7.3
An08g01370	Oxodicarboxylate carrier Odc2, *S. cerevisiae*	24	8	14.5	7.3
An15g01780	2-methylcitrate dehydratase PrpD, *Salmonella typhimurium*	9	13	3.4	7.0
An04g02460	heart muscle protein mitofilin HMP, *H. sapiens*	59	16	17.0	6.8
An13g00670	mitochondrial protein Mia1, *S. cerevisiae*-	2	3	3.3	6.7
An18g05890	similarity to pyruvate dehydrogenase phosphatase 1 PDP1, *Rattus norvegicus*	24	15	7.3	6.7
An04g05640	mitochondrial proton-pumping NADH:ubiquinone reductase nuo51, *A. niger*	67	12	24.5	6.6
An07g09920	NADH-dependent glutamate synthase NADH-GOGAT, *Medicago sativa*	76	50	6.5	6.2
An04g04750	oxoglutarate dehydrogenase (lipoamide) Kgd1, *S. cerevisiae*	71	24	12.2	6.0
An02g12430	precursor of mitochondrial isocitrate dehydrogenase icdA, *A. niger*	10	9	4.6	6.0
An15g01920	methylcitrate synthase mcsA, *A. nidulans*	6	10	2.5	5.9
An08g04910	22 kD subunit NADH:ubiquinone reductase, *N. crassa*	5	3	6.2	5.7
An03g03640	mitochondrial sulfide dehydrogenase (coenzyme Q2) SPBC2G5.06c, *S. pombe*	27	11	9.4	5.7
An09g06670	suppressor gene of mitochondrial histone Yhm2, *S. cerevisiae*	30	6	17.4	5.4
An01g09840	hypothetical protein AN0630.2, *A. nidulans*	5	1	13.4	5.3
An18g05670	23 kD subunit of NADH:ubiquinone reductase, Bos taurus	14	4	11.7	5.2
An04g00110	21/29 kD subunit of NADH:ubiquinone reductase, *N. crassa*	17	5	11.3	5.1
An03g04660	weak similarity to hypothetical protein YGR165w, *S. cerevisiae*-	11	7	5.4	5.0
An01g04630	gamma chain precursor of the H+-transporting ATP synthase Atp3, *S. cerevisiae*	14	5	8.8	4.8
An02g07320	AU-specific RNA-binding protein / enoyl-CoA hydratase AUH, *H. sapiens*-	3	5	2.1	4.7
An11g11280	dihydrolipoamide succinyltransferase kgd2, *A. fumigatus*	19	8	7.5	4.7
An11g05700	similarity to hypothetical membrane protein YGR235c, *S. cerevisiae*	11	4	8.2	4.6
An18g02990	similarity to mitochondrial ribosomal protein Mrp20, *S. cerevisiae*-	3	3	3.2	4.6
An16g07110	acetyl-CoA hydrolase Ach1, *S. cerevisiae*	9	8	3.3	4.2
An08g01590	similarity to membrane associated protein SLP-2, *H. sapiens*	24	6	10.1	3.9
An08g05500	mitochondrial ribosomal protein of the large subunit Yml3, *S. cerevisiae*	5	5	2.7	3.9
An02g07600	succinate dehydrogenase Sdh1, *S. cerevisiae*	11	9	3.2	3.8
An03g03360	carnitine/acyl carnitine carrier acuH, *A. nidulans*	16	4	9.2	3.6
An16g02130	similarity to novel cell death-regulatory protein GRIM19, *Mus musculus*	12	1	20.7	3.6
An12g04110	precursor of mitochondrial nuclease Nuc1, *S. cerevisiae*	14	4	7.8	3.5

A. niger locus	Protein description	SpC		NSAF.10^4	
		X.	S.	X.	S.
An08g04880	hypothetical protein CAD27304.1, *A. fumigatus*	9	3	6.5	3.5
An04g01200	14 kD subunit of ubiquinol--cytochrome c reductase Qcr7, *S. cerevisiae*	5	1	8.1	3.2
An08g10530	mitochondrial aconitate hydratase Aco1, *S. cerevisiae*	56	9	13.1	3.2
An02g11200	similarity to 13 kD subunit of NADH:ubiquinone reductase, Bos taurus	7	3	4.6	3.1
An18g06760	NAD(+)-isocitrate dehydrogenase subunit I idh1, Ajellomyces capsulatus	4	4	2.1	3.0
An13g03940	long-chain-acyl-CoA dehydrogenase precursor LCAD, Rattus norvegicus	5	4	2.4	2.8
An01g03110	similarity to ribosomal protein of the small subunit Rsm7, *S. cerevisiae*-	1	4	0.6	2.8
An07g07880	similarity to ORFX ORF2689 polypeptide sequence SEQ ID NO:5378, patent WO200058473-A2, *H. sapiens*	12	5	4.4	2.8
An02g01750	chaperone involved in mitochondrial protein import Mge1, *S. cerevisiae*	10	2	7.9	2.7
An17g01530	alcohol-dehydrogenase adhA from patent WO8704464-A, *A. niger*-	1	3	0.8	2.6
An08g04240	alternative NADH:ubiquinone reductase NDH2, Yarrowia lipolytica	33	5	10.7	2.5
An07g07000	mitochondrial m-AAA protease subunit Yta12, *S. cerevisiae*	27	8	5.5	2.5
An07g02770	hypothetical protein YKL195w, *S. cerevisiae*	5	2	3.7	2.4
An16g08740	17.8 kD subunit of NADH:ubiquinone reductase Nuo-17.8, *N. crassa*	7	1	7.9	2.3
An04g00220	methionine-N-acetyltransferase Nat2, *S. cerevisiae*	4	2	2.8	2.3
An07g09550	mitochondrial ribosomal protein Nam9, *S. cerevisiae*	5	3	2.3	2.1
An06g01730	mtRNA splice defect-suppressing mitochondrial carrier Mrs3, *S. cerevisiae*	4	2	2.5	2.0
An04g09030	mitochondrial succinate-fumarate transporter Sfc1, *S. cerevisiae*	8	2	4.7	2.0
An02g06530	protein required for dispersion of mitochondria cluA, Dictyostelium discoideum	20	9	3.0	2.0
53140	mitochondrial cytochrome b2, putative [Aspergillus flavus NRRL3357]	4	3	1.7	1.9
An07g09110	similarity to monooxygenase VioC, Chromobacterium violaceum	4	3	1.6	1.8
An01g13930	similarity to succinate dehydrogenase, *S. cerevisiae*	7	1	6.1	1.8
An12g00130	mRNA processing protein of cytochrome c oxidase Mss51, *S. cerevisiae*	6	3	2.2	1.7
An16g04170	acetolactate synthase protein from patent EP257993-A, *S. cerevisiae*-	5	4	1.4	1.7
An04g00060	19.3 kD subunit of NADH:ubiquinone reductase, *N. crassa*	6	1	5.1	1.7
An05g00110	hypothetical protein YNR020c, *S. cerevisiae*	8	1	6.5	1.6
An01g06370	hypothetical protein YKR065c, *S. cerevisiae*	5	1	4.0	1.6
An04g04970	Yta11, *S. cerevisiae*	28	4	6.4	1.5
An15g00980	maintaining mitochondrial morphology protein MMM1, *N. crassa*	4	2	1.7	1.3
An07g03130	mitochondrial cation transporter Mmt1, *S. cerevisiae*	10	2	3.9	1.3
An18g05590	mitochondrial carrier protein Ymc1, *S. cerevisiae*	6	1	3.9	1.3
An08g04250	dynamin-related protein msp1p, *S. pombe*	7	4	1.5	1.3
An11g10070	hypothetical protein Afu3g06270, *A. fumigatus*	5	1	3.1	1.2
An01g10190	similarity to mitochondrial tricarboxylate carrier, Rattus sp.	7	1	3.7	1.1
An12g07580	acetylglutamate kinase/N-acetyl-γ-glutamyl-P reductase arg-6, *N. crassa*-	5	3	1.1	1.0
An11g09350	mitochondrial NADH dehydrogenase ndh64, *N. crassa*	9	2	2.4	0.9
An04g08800	mitochondrial carrier Leu5, *S. cerevisiae*	3	1	1.5	0.9
An02g04000	pyruvate dehydrogenase kinase isoform 2, Zea mays	3	1	1.4	0.9
An04g07060	peptide ABC transporter protein Mdl1, *S. cerevisiae*	6	1	1.5	0.5
An11g11230	citrate transport protein Ctp1, *S. cerevisiae*	7	0	4.6	0.4
An14g00810	hypothetical protein EAA61688.1, *A. nidulans*	3	0	1.8	0.4
An15g02490	similarity to 3-isopropylmalate dehydrogenase leuB, Sulfolobus sp.	3	0	1.7	0.4
An01g06960	hypothetical phosphatidyl synthase SPAC22A12.08c, *S. pombe*	5	0	2.7	0.4
An02g12070	mitochondrial phosphate transport protein G7, Glycine max	7	0	3.6	0.3
An01g07190	component of the translocase of mitochondrial inner membrane Tim54, *S. cerevisiae*	3	0	1.4	0.3
An01g07200	similarity to N-acetylglucosaminyltransferases chain p110, Rattus norvegicus	19	0	4.2	0.2

Supplementary Table S3. **Proteins involved in quality control and glycosylation.** NSAF: normalised spectral abundance factor; SpC: spectral counts, XYL: D-xylose addition; SORB: D-sorbitol addition Boldface: higher sequence similarity to mammalian proteins.

A. niger	Yeast	% Identity (E value)	*H. sapiens*	% Identity (E value)	Description	NSAF.10^4	
						XYL	SORB
An05g00140	(Srp102)	46 (7e-12)	(SRPB)	41 (2e-04)	SRP receptor β subunit	11.6	25.6
An01g03820	Sbh2	68 (7e-22)	SEC61B	60 (6e-10)	Translocation to the ER (GEF)	7.8	25.6
An03g04340	**Sec61**	**79 (0.0)**	**SEC61A1**	**82 (0.0)**	**Targeting to ER**	**12.3**	**22.1**
An01g13070	Sec63	46 (5e-53)	SEC63	45 (5e-38)	Targeting and import to the ER	14.8	16.9
An02g01510	Sec62	55 (8e-31)	SEC62	48 (5e-18)	Targeting and import to the ER	9.1	14.3
An16g08830	(Sec66)	50 (2e-16)	no hits	no hits	Targeting and import to the ER	16.4	19.8
An17g00090	(Sec72)	41 (1e-05)	(LONRF3)	44 (4e-04)	Targeting and import to the ER	7.9	4.7
An16g07390	(Spc2)	47 (2e-11)	(SPC2)	43 (0.065)	Signal peptidase protein	9.1	11.8
An02g14800	Pdi1	56 (4e-90)	PDIA3	54 (2e-75)	Protein disulfide isomerase PdiA	59	75.6
An18g02020	**(Pdi1)**	**60 (2e-18)**	**(PDIA6)**	**53 (7e-40)**	**Protein disulfide isomerase TigA**	**25.9**	**33**
An01g04600	(Mpd1)	54 (5e-33)	(PDIA6)	58 (7e-24)	Protein disulfide isomerase PrpA	26.2	26.6
An02g05890	**(Mpd1)**	**58 (3e-14)**	**(TXNDC5)**	**45 (5e-29)**	**Protein disulfide isomerase**	**28.5**	**17.6**
An16g07620	(Ero1)	49 (2e-74)	(ERO1LB)	50 (1e-59)	Thiol-oxidase EroA	5.6	5.0
An04g02020	**Cpr1**	**79 (1e-59)**	**PPIB**	**79 (2e-67)**	**PPIase cyclophilin CypB**	**41.3**	**37.4**
An01g06670	**Fpr2**	**64 (4e-28)**	**FKBP2**	**60 (9e-29)**	**PPIase FK506 binding protein**	**4.7**	**4.8**
An11g04180	Kar2	84 (0.0)	HSPA5	83 (0.0)	DnaK chaperone ATPase BipA	52.7	71.8
An01g08420	**Cne1**	**48 (2e-56)**	**CANX**	**66 (3e-116)**	**Glycoprotein chaperone ClxA**	**46.4**	**42.4**
An12g10590	(Ecm10)	50 (0.030)	(HSPA5)	52 (0.39)	Unknown ER DnaK protein	2.4	2.4
An05g00880	Scj1	55 (2e-69)	DNAJA4	53 (8e-57)	ER DnaJ co-chaperone	7.6	9.1
An12g00580	(Scj1)	58 (3e-07)	(DNAJB5)	57 (3e-07)	ER DnaJ co-chaperone	3.2	6.8
An18g06470	(Erj5)	46 (5e-15)	(DNAJC1)	41 (1e-10)	DnaJ-domain protein	2.5	6.2
An01g13220	**(Lhs1)**	**52 (2e-50)**	**(HYOU1)**	**48 (2e-80)**	**Nucleotide exchange factor LhsA**	**22.1**	**20.2**
An04g07440	Shr3	49 (1e-17)	no hits	no hits	ER packaging chaperone	15.5	26.4
54765	**no hits**	**no hits**	**TTC35**	**55 (5e-19)**	**TTC35 protein**	**5.7**	**6.5**
An08g10400	**no hits**	**no hits**	**SLC35A3**	**59 (1e-45)**	**UDP-GlcNAc/UDP-Gal transporter**	**2.4**	**1.0**
An17g02140	Vrg4	74 (1e-102)	(SLC35D2)	44 (9e-11)	GDP-Mannose transporter	11.6	9.9
An14g03820	Gal10	72 (2e-122)	GALE	64 (6e-99)	UDP-Glc 4-epimerase	9.5	9.5
An08g04450	Gda1	67 (2e-126)	ENTPD6	47 (4e-45)	Guanosine-diphosphatase	13.3	9.0
An18g06820	Gfa1	78 (0.0)	GFPT2	72 (0.0)	Gln-Fru-6-P amidotransferase	7.4	12.9
An04g04990	Psa1	84 (7e-156)	GMPPB	79 (2e-130)	Mannose-1-P guanyltransferase	1.7	3.2
An18g05170	**Pcm1**	**57 (5e-39)**	**PGM3**	**63 (9e-53)**	**Phosphoglucomutase**	**2.8**	**3.1**
An12g00820	Ugp1	79 (0.0)	UGP2	70 (1e-147)	UGPase	26.5	23.2
An02g02980	Die2	42 (2e-36)	ALG10B	44 (6e-29)	α-1,2-Glucosyltransferase	2.1	3.9
An04g03130	**no hits**	**no hits**	**MPDU1**	**54 (1e-33)**	**Man-P-Dol utilization protein**	**4.5**	**2.2**
An16g04330	**Dpm1**	**50 (2e-24)**	**DPM1**	**80 (7e-92)**	**Dol-P β-D-mannosyltransferase**	**23.9**	**26**
An08g07020	**Alg9**	**50 (1e-83)**	**ALG9**	**52 (1e-89)**	**α-1,2-Mannosyltransferase**	**2.8**	**3.7**
An18g05910	**Alg11**	**56 (8e-68)**	**ALG11**	**59 (2e-94)**	**α-1,2-Mannosyltransferase**	**1.8**	**1.2**
An04g08820	Alg8	61 (2e-114)	ALG8	58 (7e-102)	α-1,3-Glucosyltransferase	1.7	0.7
An02g14560	**(Ost1)**	**48 (2e-45)**	**(RPN1)**	**47 (0.0)**	**OT α subunit OstA**	**35.7**	**41.1**
An07g04190	**(Wbp1)**	**49 (4e-47)**	**(DDOST)**	**52 (2e-50)**	**OT β subunit**	**38**	**42.3**
An02g14930	**(Ost3)**	**42 (4e-19)**	**(TUSC3)**	**46 (4e-21)**	**OT γ subunit**	**15.3**	**8.2**
An04g03495	**(Swp1)**	**47 (2e-11)**	**RPN2**	**52 (9e-14)**	**OT δ subunit**	**21.7**	**16.8**
An16g08570	Stt3	78 (0.0)	STT3B	71 (0.0)	OT catalytic subunit	15.7	11.4
An15g01420	Cwh41	55 (9e-146)	MOGS	46 (5e-107)	Processing α-glucosidase I	21	13.8
An09g05880	**Rot2**	**56 (0.0)**	**GANAB**	**56 (0.0)**	**Glucosidase II α subunit**	**28.9**	**27.6**
An13g00620	(Gtb1)	43 (7e-17)	(PRKCSH)	43 (2e-15)	Glucosidase II β subunit	12.9	16.7
An07g06430	**(Kre5)**	**40 (3e-26)**	**UGGT1**	**51 (0.0)**	**UDP-Glc glucosyltransferase**	**10**	**9.1**
An06g01510	(Ylr057w)	42 (4e-42)	MAN1B1	55 (1e-26)	α-1,2-Mannosidase	10.3	5.5
An18g06220	Mns1	59 (2e-119)	MAN1B1	60 (2e-103)	α-1,2-Mannosidase	3.4	2.9
An07g10350	Pmt2	67 (0.0)	(POMT2)	53 (2e-128)	O-Mannosyltransferase PmtA	12.5	9.3
An11g09890	Pmt1	60 (0.0)	(POMT2)	54 (1e-119)	O-Mannosyltransferase	4.9	7.6
An16g08490	Pmt4	64 (0.0)	(POMT1)	52 (3e-99)	O-Mannosyltransferase	6.0	4.9
An03g01090	(Hoc1)	42 (1e-15)	no hits	no hits	α-1,6-Mannosyltransferase	3.3	2.2
An05g02320	(Hoc1)	44 (9e-12)	no hits	no hits	α-1,6-Mannosyltransferase	5.6	1.6
An07g04940	Hoc1	55 (2e-64)	no hits	no hits	α-1,6-Mannosyltransferase	2.7	1.1
An12g07020	(Hoc1)	48 (3e-23)	no hits	no hits	α-1,6-Mannosyltransferase	4.9	2.2
An03g05010	Mnn9	64 (3e-98)	no hits	no hits	MTC complex subunit	4.8	4.3
An04g01260	Anp1	65 (2e-82)	no hits	no hits	MTC complex subunit	21.7	15.5
An15g06230	Anp1	69 (2e-136)	no hits	no hits	MTC complex subunit	4.2	3.4
An03g02990	(Gnt1)	58 (1e-17)	no hits	no hits	GlcNAc-transferase	2.4	1.0
An11g10260	Gnt1	60 (4e-25)	(GYG1)	46 (0.072)	GlcNAc-transferase	4.4	2.6
An18g02170	Ktr5	57 (8e-104)	no hits	no hits	α-1,2-Mannosyltransferase	16.4	8.0
An02g09940	Ktr1	64 (3e-85)	no hits	no hits	α-1,2-Mannosyltransferase	13.4	12.1
An14g03910	Ktr1	70 (2e-124)	no hits	no hits	α-1,2-Mannosyltransferase	11.7	11
An02g11720	Ams1	63 (0.0)	MAN2C1	60 (0.0)	α-Mannosidase Msd2/MsdB	1.2	1.1

Supplementary Table S4. Proteins involved in protein sorting, vesicular transport and membrane fusion. NSAF: normalised spectral abundance factor; SpC: spectral counts, XYL: D-xylose addition; SORB: D-sorbitol addition Boldface: higher sequence similarity to mammalian proteins.

A. niger	Yeast	% Identity (E-value)	*H. sapiens*	% Identity (E-value)	Description	NSAF 10^4	
						XYL	SORB
An14g00900	Mcd4	60 (0.0)	PIGN	57 (0.0)	GPI anchor assembly	2.1	4.1
An05g02300	**(Gpi12)**	**46 (2e-17)**	**(PIGL)**	**45 (6e-24)**	**GPI anchor assembly**	**14**	**2.2**
An17g00780	(Pbn1)	44 (3e-11)	no hits	no hits	GPI Man-transferase subunit	2.3	1.8
An10g00480	(Gpi11)	38 (0.002)	no hits	no hits	Man-EthNH P-transferase	2.4	2.5
An01g13530	Gpi8	82 (4e-116)	PIGK	75 (1e-95)	GPI-transamidase complex	0.7	2.3
An07g09270	(Gpi17)	43 (3e-34)	(PIGS)	42 (9e-32)	GPI-transamidase complex	1.4	1.1
An11g06770	Gpi16	59 (9e-114)	PIGT	46 (3e-77)	GPI-transamidase complex	1.7	2
An18g05180	(Per1)	50 (2e-42)	(PGAP3)	51 (2e-33)	Assists GPI-phospholipase	2.7	1.7
An16g03370	Cwh43	60 (0.0)	CWH43	46 (5e-84)	Addition of ceramides to GPI	8.4	9.6
An04g02500	Nmt1	67 (2e-121)	NMT2	64 (8e-109)	N-myristoyl transferase	2.4	2.4
An05g00200	(Akr1)	49 (1e-93)	(ZDHHC17)	46 (1e-52)	Palmitoyl transferase	7.5	4.8
An03g03570	(Tor2)	52 (0.017)	no hits	no hits	C-methylation of prenylCys.	2.6	0.3
An02g08450	Sec18	71 (0.0)	NSF	69 (0.0)	NsfA for release of Sec17	4.3	3.4
An02g01580	Sec17	60 (4e-44)	NAPB	62 (4e-43)	SNAP for NSF binding	15.6	6.6
An12g04710	Vtc4	65 (0.0)	(XPR1)	47 (2e-08)	VTC subunit	6.8	7.9
An07g09800	Vtc3	52 (5e-133)	(XPR1)	42 (3e-05)	VTC subunit	9.2	10.3
An09g04170	Sly1	57 (1e-126)	SCFD1	55 (6e-119)	SM protein, binds Sed5	2.2	1.3
An02g12980	Sed5	54 (3e-49)	STX5	53 (2e-47)	Qa.II type SNARE	0.8	2.7
An08g01410	Sft2	60 (3e-37)	SFT2D3	53 (9e-05)	Qa type SNARE (putative)	2.1	4.2
An04g07020	Tlg2	52 (4e-34)	STX16	51 (63-33)	Qa.III.a type SNARE	3.6	3.1
An04g01530	**(Pep12)**	**49 (2e-20)**	**(STX12)**	**54 (2e-20)**	**Qa.III.b type SNARE**	**16.8**	**14.8**
An12g01190	(Sso2)	50 (5e-20)	(STX2)	51 (3e-10)	Qa.IV type SNARE	7.9	2.1
An07g02170	(Bos1)	47 (2e-14)	(GOSR2)	59 (2e-10)	Qb.II type SNARE	5.5	4.8
An04g05980	Vti1	59 (2e-26)	VTI1A	56 (5e-26)	Qb.III.b type SNARE	19.7	18
An08g02460	Gos1	58 (1e-33)	GOSR1	51 (1e-24)	Qb.II type SNARE	2.0	4.0
An12g07570	Snc2	72 (3E-28)	VAMP4	68 (5e-11)	R.IV type SNARE	7.3	6.7
An08g07470	**(Nyv1)**	**60 (1e-11)**	**(VAMP7)**	**50 (2e-20)**	**R.III type SNARE**	**6.4**	**2.4**
An04g08480	Ykt6	72 (9e-60)	YKT6	66 (2e-45)	R.II tye SNARE	9.7	8.6
An12g00800	Tcb1	50 (8e-157)	no hits	no hits	Tricalbin	9.3	6.9
An03g04940	(Erv41)	47 (4e-36)	(PTX1)	44 (4e-33)	Erv41/46 complex	11.1	7.5
An01g04320	Erv46	56 (5e-79)	ERGIC3	56 (3e-76)	Erv41/46 complex	14.9	12.5
An15g01680	**(Yif1)**	**47 (1e-30)**	**(YIF1A)**	**54 (2e-34)**	**COPII/Golgi fusion**	**2.8**	**1.8**
An01g04730	**Sec23**	**69 (0.0)**	**SEC23A**	**71 (0.0)**	**Activator of GTPase**	**4.1**	**9.0**
An08g10650	Sec24	60 (0.0)	SEC24B	59 (1e-150)	Sec23/24 complex	6.6	6.4
225665	Sed4	37 (0.062)	no hits	no hits	Regulator of SarA	8.0	8.6
An02g01690	Sec31	46 (9e-152)	SEC31A	51 (1e-116)	COPII coat	1.5	0.7
An08g03960	Erv29	67 (5e-55)	SURF4	61 (3e-44)	Vesicle transport	12.4	9.7
An04g08830	(Emp47)	52 (1e-17)	(LMAN1L)	40 (2e-09)	Vesicle transport	19.8	17.9
An01g08870	Erv25	69 (2e-53)	TMED10	59 (1e-28)	Erv25 p24 family	22.7	16.7
An04g01780	Erp1	60 (1e-44)	TMED9	56 (1e-33)	Erp1 p24 family	13.6	10.7
An09g05490	Erp3	52 (7e-26)	TMED2	50 (4e-21)	p24 family	12.5	6
An08g03590	Emp24	62 (6e-47)	TMED2	55 (4e-29)	Erv25/Erp1/Emp24	17.3	12.2
An07g07830	(Ted1)	42 (1e-50)	no hits	no hits	Cargo exit from ER	1.1	0.7
An16g03320	**Sfb3**	**48 (7e-111)**	**SEC24C**	**53 (3e-130)**	**Sorting of PmaA**	**1.5**	**2.2**
An07g07340	**Erd2**	**55 (2e-28)**	**KDELR3**	**59 (4e-31)**	**(K/H)DEL binding**	**4.0**	**2.7**
An04g00670	**(Get1)**	**46 (3e-05)**	**(WRB)**	**51 (4e-08)**	**GET subunit**	**4.1**	**6**
An02g07090	**Get3**	**70 (1e-93)**	**ASNA1**	**72 (1e-95)**	**GET subunit**	**3.4**	**3.4**
An02g04250	**(Uip5)**	**43 (5e-11)**	**LMAN2L**	**56 (1e-40)**	**ER export receptor**	**19.2**	**18.1**
An02g02830	**Rer1**	**70 (1e-50)**	**RER1**	**79 (1e-57)**	**Retrieves ER membrane proteins**	**13.8**	**18.6**
An07g06080	**Hrr25**	**87 (2e-134)**	**CSNK1E**	**78 (3e-143)**	**Ser/Thr kinase**	**3.7**	**3.2**
An01g02500	Trx1	34 (1e-23)	TXN	57 (1e-17)	Thioredoxin	9.2	22.9
An16g02460	Cop1	69 (0.0)	COPA	67 (0.0)	COPI α subunit	6.1	9.8
An08g03270	**Sec26**	**69 (0.0)**	**COPB1**	**69 (0.0)**	**COPI β subunit**	**4.3**	**6.9**
An02g05870	**Sec27**	**72 (0.0)**	**COPB2**	**75 (0.0)**	**COPI β' subunit**	**5.7**	**4**
An07g06030	Sec21	63 (0.0)	COPG2	61 (0.0)	COPI γ subunit protein	3.1	9.2
An01g14250	**Ret2**	**56 (5e-78)**	**ARCN1**	**57 (1e-96)**	**COPI δ subunit**	**2.3**	**2.8**
An08g06330	**(Sec28)**	**43 (3e-05)**	**(COPE)**	**51 (2e-28)**	**COPI ε subunit**	**4.7**	**3.6**
An01g04040	Sar1	82 (1e-76)	SAR1A	75 (1e-66)	ARF GTPase SarA	26.2	39.2
An08g03690	**Arf2**	**89 (3e-81)**	**ARF1**	**90 (2e-84)**	**ARF GTPase**	**7.4**	**5**
An08g04480	Sey1	53 (5e-127)	no hits	no hits	Dynamin GTPase	19.9	20.2
An03g06950	Dnm1	69 (0.0)	DNM1	61 (0.0)	Dynamin GTPase	6.9	10.3
An02g10450	Vps1	77 (0.0)	DNM1L	64 (3e-167)	Dynamin GTPase	13.6	9.5
An11g00010	**(Vps1)**	**44 (2e-19)**	**(MX2)**	**48 (3e-29)**	**Dynamin GTPase**	**4.6**	**6.3**
An14g00010	**Sec4**	**81 (7e-65)**	**RAB8A**	**79 (6e-72)**	**Rab8 GTPase SrgA**	**6.6**	**0.6**
An01g06060	**Ypt31**	**85 (7e-74)**	**RAB11A**	**84 (1e-89)**	**Rab11 GTPase**	**24.4**	**21.6**
An09g06790	**Ypt1**	**82 (1e-82)**	**RAB1A**	**87 (2e-92)**	**Rab1 GTPase SrgB**	**21.1**	**24**
An15g05740	**Ypt6**	**75 (7e-66)**	**RAB6A**	**85 (2e-87)**	**Rab6 GTPase SrgC**	**15.1**	**20.5**
An04g02470	**Vps21**	**69 (2e-58)**	**RAB5C**	**73 (6e-67)**	**Rab5 GTPase**	**7.0**	**0.6**
An02g06400	Vps21	62 (8e-67)	RAB5B	59 (1e-53)	Rab5 GTPase	5.9	2.5

A. niger	Yeast	% Identity (E-value)	*H. sapiens*	% Identity (E-value)	Description	NSAF 10⁴	
						XYL	SORB
An06g02180	**no hits**	**no hits**	**(C8orf80)**	**48 (0.001)**	**Ras GTPase**	**0.6**	**1.1**
An01g02320	Ras2	82 (2e-65)	KRAS	81 (6e-59)	Ras GTPase RasA	12.3	5.5
An18g05980	Rho1	90 (6e-85)	RHOA	81 (8e-79)	Ras GTPase RhoA	61.2	33
An18g02490	(Gea2)	49 (1e-149)	GBF1	54 (5e-74)	GEF for ARFs	0.4	2.3
An07g02190	Sec7	57 (0.0)	ARGEF2	52 (0.0)	GEF HypB for ARFs	0.6	0.2
An18g06440	Yip3	73 (4e-43)	RABAC1	54 (6e-13)	Interacts with Rab GTPases	16.2	12.8
An04g09250	Mvp1	54 (2e-58)	SNX8	49 (3e-29)	PtdIns-3-P binding protein	7.6	2.6
An03g06880	Pep1	51 (7e-175)	no hits	no hits	Receptor vacuolar hydrolases	7.9	2.6
An18g03490	(Mrl1)	53 (2e-18)	(M6PR)	42 (3e-09)	Receptor vacuolar hydrolases	2.5	2
An18g03980	Vps70	49 (3e-104)	FOLH1	52 (1e-95)	Vacuolar protein sorting	1.8	1.5
An14g05020	Vac8	79 (0.0)	no hits	no hits	Cytoplasm to vacuole targeting	2.3	3.4
An16g04270	**Vps35**	**76 (5e-90)**	**VPS35**	**59 (3e-92)**	**Retromer coat**	**9.5**	**11.3**
An01g07320	**Pep8**	**55 (1e-76)**	**VPS26B**	**75 (4e-109)**	**Retromer coat**	**4.4**	**9.2**
An08g01030	**Vps29**	**61 (4e-31)**	**VPS29**	**64 (2e-46)**	**Retromer coat**	**5.1**	**10**
An01g08400	Vps5	51 (1e-65)	SNX1	54 (2e-58)	Retromer coat	0.5	2.5
An12g04500	Drs2	71 (0.0)	ATP8A1	66 (0.0)	Flippase	0.7	0.1
An15g01510	Neo1	67 (2e-96)	OSBPL9	45 (1e-36)	Flippase	1.7	0.5
An02g07570	Kes1	72 (0.0)	ATP9B	66 (0.0)	Oxysterol binding protein	2.0	4.1
An04g02070	**Chc1**	**73 (0.0)**	**CLTC**	**75 (0.0)**	**Clathrin heavy chain**	**15**	**31.4**
An16g02490	**Apl2**	**58 (1e-146)**	**AP2B1**	**69 (0.0)**	**β-Adaptin: AP-1 complex**	**0.8**	**2.6**
An01g02600	**Apl4**	**54 (4e-113)**	**AP1G1**	**63 (0.0)**	**γ-Adaptin: AP-1 complex**	**1.4**	**2.6**
An07g03200	**Apm1**	**72 (6e-154)**	**AP1M1**	**83 (5e-176)**	**μ-Like subunit: AP-1 complex**	**1.5**	**2.8**
An07g08220	Ent3	75 (4e-61)	CLINT1	68 (8E-41)	Epsin-like domain protein	0.5	2.2
An02g08820	(Bud7)	46 (5e-69)	no hits	no hits	Golgi cargo export	1.7	5.7
An02g03120	Gdi1	75 (2e-154)	GDI1	70 (8e-132)	GDP dissociation inhibitor	3.7	1.4
An01g08590	(Tvp38)	57 (1e-29)	(TMEM64)	45 (8e-08)	Asymetric localization of Kar9	3.4	2.7
An17g01420	Yop1	56 (7e-27)	REEP5	55 (2e-21)	ER tubular morphology	40	56.2
An08g08600	No Hits	no hits	no hits	no hits	Reticulon-like protein	9.7	11.6
An08g01610	Ola1	80 (6e-154)	OLA1	67 (6e-108)	P-loop ATPase	8.0	14.2
An02g05210	**no hits**	**no hits**	**(ANXA7)**	**50 (1e-48)**	**Annexin AnxC3.1**	**1.4**	**1.4**
An01g12810	(Yet3)	52 (4e-19)	no hits	no hits	Invertase secretion in yeast	20.7	34.6
An01g13390	(Atg27)	46 (0.087)	no hits	no hits	Autophagy	3.1	0.3
An09g06580	**(Bre5)**	**45 (1e-08)**	**(G3BP1)**	**42 (3e-23)**	**Ras-GTPase-activating protein**	**2.2**	**3.6**
An14g00900	Mcd4	60 (0.0)	PIGN	57 (0.0)	GPI anchor assembly	2.1	4.1
An05g02300	**(Gpi12)**	**46 (2e-17)**	**(PIGL)**	**45 (6e-24)**	**GPI anchor assembly**	**14**	**2.2**
An17g00780	(Pbn1)	44 (3e-11)	no hits	no hits	GPI Man-transferase subunit	2.3	1.8
An10g00480	(Gpi11)	38 (0.002)	no hits	no hits	Man-EthNH P-transferase	2.4	2.5

Supplementary Table S5. Proteins involved in cytoskeleton integrity, intracellular motility, protein folding in the cytoplasm, polarised growth, and cytokinesis. NSAF: normalised spectral abundance factor; SpC: spectral counts, XYL: D-xylose addition; SOR: D-sorbitol addition Boldface: higher sequence similarity to mammalian proteins.

A. niger	Yeast	% Identity (E-value)	*H. sapiens*	% Identity (E-value)	Description	NSAF.10^4	
						XYL	SOR
An07g10420	Cdc50	67 (3e-97)	TMEM30B	50 (1e-47)	Endosomal protein: actin patch	4.7	2.9
An17g01945	Rvs161	73 (1e-84)	(AMPH)	46 (3e-18)	Amphiphysin protein: actin polarization	3.8	7.5
An14g04160	Cof1	61 (5e-26)	CFL1	51 (6e-12)	Cofilin: actin filament depolarization	2.9	5.9
An11g10320	Sla2	71 (5e-88)	(HIP1R)	45 (6e-68)	Actin linking to clathrin	2.2	1.2
202202	Sac6	80 (0.0)	PLS3	60 (2e-126)	Actin-bundling protein	5.5	14.3
An18g03200	Arp3	81 (0.0)	ACTR3	71 (2e-142)	Arp2/3 complex	3.9	4.4
An08g06400	Arp2	86 (9e-151)	ACTR2	82 (1e-136)	Arp2/3 complex	2.4	1.1
An01g05510	**Arc35**	**60 (5e-59)**	**ARPC2**	**64 (1e-74)**	**Structural, ARP2/3 complex**	**5.9**	**5.3**
An16g01570	Arc18	63 (6e-45)	ARPC3	60 (1e-39)	Structural, ARP2/3 complex	6.2	6.2
An04g01830	**(Mdm20)**	**43 (2e-06)**	**(C12orf30)**	**38 (8e-21)**	**N-terminal acetyltransferase**	**2.4**	**1.2**
An02g02230	Lsb6	52 (2e-94)	PI4K2B	54 (2e-70)	PtdIns 4-kinase: actin polymerization	5.0	1.6
An15g00560	Act1	97 (0.0)	ACTG1	96 (0.0)	Actin ActA: cell polarity	42.1	53.8
An07g01640	**Mlc1**	**59 (3e-23)**	**CALML3**	**63 (5e-28)**	**Myosin light chain**	**3.2**	**10**
An17g02290	Myo2	64 (0.0)	MYO5A	61 (0.0)	Myosin motor	0.5	0.4
An08g06130	**Gpa2**	**63 (2e-80)**	**GNAI1**	**70 (5e-113)**	**FadA: proliferation**	**4.3**	**1.1**
An01g09520	Slt2	81 (6e-152)	MAPK7	63 (2e-93)	MAP kinase: polarized growth	2.8	4.0
An18g06270	Bmh2	85 (7e-102)	YWHAE	84 (3e-101)	Similar to ArtA: exocytosis	28.8	30.1
An07g07760	Bmh1	82 (3e-109)	YWHAE	89 (2e-106)	Similar to ArtA: exocytosis	29.5	30.5
An06g01200	Emp70	61 (6E-157)	TM9SF2	60 (3e-141)	Endosomal: filamentous growth	2.7	0.6
An18g06050	Yck2	81 (7e-137)	CSNK1G2	70 (9e-108)	Ser/Thr kinase: septin assembly	2.4	2.1
An08g00310	Cdc10	79 (1e-108)	SEPT9	73 (8e-93)	Septin family protein AspD	9.1	7.1
An07g05110	Cdc11	65 (1e-99)	SEPT7	63 (6e-69)	Septin ring protein AspA	7.9	4.5
An09g05260	Cdc12	72 (1e-120)	SEPT7	58 (2e-77)	Septin ring protein	4.0	3.1
An02g07690	Bim1	55 (4e-51)	MAPRE1	57 (3e-46)	Structural: cortical microtubule capture	7.7	10.1
An08g10490	**Stu2**	**45 (8e-62)**	**CKAP5**	**54 (8e-83)**	**Structural: microtule dynamics**	**0.9**	**0.4**
An01g05650	**Tub3**	**86 (0.0)**	**TUBA1C**	**89 (0.0)**	**α-Tubulin TubA**	**15.5**	**18.9**
An08g03190	**Tub2**	**90 (0.0)**	**TUBB2B**	**94 (0.0)**	**β-Tubulin TubB**	**29.3**	**34.1**
An01g06480	Cct2	86 (0.0)	CCT2	82 (0.0)	Cct ring complex subunit β	1.2	1.2
An02g12750	**Cct4**	**83 (0.0)**	**CCT4**	**83 (0.0)**	**Cct ring complex subunit δ**	**1.2**	**2.2**
An18g05770	Cct7	79 (0.0)	CCT7	77 (0.0)	Cct ring complex subunit η	1.0	0.2
An09g06590	Hsc82	87 (0.0)	HSP90AA1	80 (0.0)	Hsp90 chaperone SspB	38.7	46.9
An08g05300	Sse2	68 (0.0)	HSPA4	59 (2e-158)	Hsp90 chaperone complex	12.3	6.4
An07g09990	Ssa4	90 (0.0)	HSPA8	89 (0.0)	Hsp70 protein: SRP-dependent targeting	40.1	72.5
An16g09260	Ssb2	89 (0.0)	HSPA2	74 (0.0)	Hsp70 protein HscA	11.3	11.2
An04g05270	Aha1	56 (2e-63)	AHSA1	48 (3e-43)	Co-chaperone: activator of Hsp82	4.7	8.4
An12g00790	Sti1	67 (2e-163)	STIP1	57 (3e-109)	Hsp90 co-chaperone	1.9	2.3
An14g01560	Zuo1	63 (1e-79)	DNAJC2	60 (1e-61)	DnaJ protein	3.8	1.5
An07g08300	**Cpr1**	**71 (7e-52)**	**PPIA**	**70 (5e-53)**	**PPIase cyclophilin CypA**	**32.7**	**65.1**
An07g05920	**Cpr6**	**59 (2e-80)**	**PPID**	**62 (5e-89)**	**PPIase cyclophilin CypD**	**3.6**	**6.6**
An08g01640	Sgt2	55 (6e-48)	SGTA	49 (8e-32)	TTC protein	0.8	2.7
An07g04570	(Hyp2)	51 (8e-11)	(EIF5A2)	53 (3e-08)	HexA protein: Woronin body	28	50
An13g01220	Ynl320w	49 (4e-30)	ABHD13	53 (4e-29)	Supressor of Bud 5	5.9	6.7

Supplementary Table S6. Proteins involved in the unfolded protein response (UPR) and the ER-associated degradation (ERAD).of proteins. NSAF: normalised spectral abundance factor; SpC: spectral counts, XYL: D-xylose addition; SOR: D-sorbitol addition. Boldface: higher sequence similarity to mammalian proteins.

A. niger	Yeast	% Identity (E-value)	*H. sapiens*	% Identity (E-value)	Description	NSAF 10^4	
						XYL	SOR
An08g00830	Ptc2	67 (2e-81)	PPM1A	55 (2e-50)	Ser/Thr phospatase	2.8	2.1
An03g02770	Dcr2	55 (3e-62)	no hits	no hits	Phosphoesterase: UPR downregulation	1.8	1.7
An08g01480	Trl1	55 (9e-145)	no hits	no hits	tRNA ligase required for tRNA splicing	1.2	0.2
An04g01720	**Hlj1**	**52 (1e-26)**	**DNAJB12**	**48 (2e-39)**	**ERAD of membrane substrates**	**8.4**	**7**
An01g04280	Ydj1	69 (2e-120)	DNAJA1	62 (7e-94)	Chaperone for protein translocation	2.8	4.1
An16g08470	**(Yos9)**	**48 (1e-10)**	**OS9**	**40 (9e-17)**	**HRD ligase**	**3.4**	**5.4**
An01g12720	**(Hrd3)**	**43 (3e-39)**	**SEL1L2**	**52 (3e-75)**	**HRD complex subunit**	**2.2**	**3.2**
An04g09170	Cdc48	88 (0.0)	VCP	87 (0.0)	Retrotranslocation of Ub-proteins	21	1.4
An01g02880	Rpl40a	100 (4e-69)	UBA52	93 (6e-63)	Fusion protein, precursor of Ub	12	7.1
An02g07010	**Rps31**	**91 (1e-57)**	**RPS27A**	**86 (7e-63)**	**Fusion protein, precursor of Ub**	**5.3**	**0.8**
An09g05480	Ubp15	50 (4e-174)	USP7	53 (2e-165)	Ub-specific protease	3.7	3.5
An15g06020	Uba1	77 (0.0)	UBA1	72 (0.0)	Ub activating enzyme	5.1	3.6
An04g01730	Ufd2	52 (3e-134)	UBE4B	49 (2e-103)	Ub-Ub ligase	1.8	4.5
An02g06300	**Vps70**	**47 (5e-53)**	**FOLH1**	**50 (1e-85)**	**Proteolysis**	**0.9**	**0.1**
An11g03970	**(Yta12)**	**44 (5e-06)**	**(SPG7)**	**47 (2e-07)**	**Proteolysis**	**4.1**	**5**
An11g11250	**Jem1**	**53 (7e-14)**	**DNAJC3**	**50 (7e-61)**	**Degradation of substrates (putative)**	**5.2**	**5.9**
An14g00180	Rpt6	88 (4e-179)	PSMC5	87 (8e-168)	19S RP proteasome ATPase	3	2.3
An18g06230	Rpt4	85 (3e-170)	PSMC6	88 (1e-169)	19S RP proteasome ATPase	2.5	3.6
An18g05230	Rpt5	88 (0.0)	PSMC3	86 (4e-179)	19S RP proteasome ATPase	2.1	2.5
An07g10110	Rpn8	77 (8e-108)	PSMD7	74 (2e-90)	19S RP proteasome ATPase	5.3	4
An11g09690	**Rpn5**	**66 (1e-109)**	**PSMD12**	**64 (4e-115)**	**19S RP proteasome ATPase**	**5**	**8.3**
An11g10380	**Rpn3**	**57 (4e-85)**	**PSMD3**	**65 (5e-114)**	**19S RP proteasome ATPase**	**1.3**	**3**
An08g10710	Rpn9	56 (1e-64)	PSMD13	56 (3e-60)	19S RP proteasome ATPase	2.1	3.8
An18g05070	**Rpn6**	**69 (8e-102)**	**PSMD11**	**69 (3e-110)**	**19S RP proteasome ATPase**	**7**	**11.4**
An16g02210	Rpn12	52 (7e-32)	PSMD8	53 (5e-28)	19S RP proteasome ATPase	2.9	5.1
An18g03010	**Rpn1**	**64 (3e-146)**	**PSMD2**	**71 (0.0)**	**19S RP proteasome ATPase**	**7.3**	**7.9**
An04g03270	**Rpn2**	**59 (7e-178)**	**PSMD1**	**59 (0.0)**	**19S RP proteasome ATPase**	**2.3**	**1.5**
An02g07040	Scl1	75 (4e-81)	PSMA6	76 (2e-79)	20S CP proteasomal α subunit	12.2	1.6
An07g02010	Pre8	76 (1e-99)	PSMA2	63 (5e-71)	20S CP proteasomal α subunit	15.2	3.3
An11g06720	Pre9	80 (2e-93)	PSMA4	77 (1e-82)	20S CP proteasomal α subunit	9.6	0.5
An02g10790	Pre6	86 (8e-102)	PSMA7	82 (3e-83)	20S CP proteasomal α subunit	11	0.5
An02g03400	Pup2	83 (7e-101)	PSMA5	78 (3e-87)	20S CP proteasomal α subunit	7.7	0.5
An15g00510	**Pre5**	**72 (2e-73)**	**PSMA1**	**67 (3e-77)**	**20S CP proteasomal α subunit**	**14.8**	**0.5**
An18g06800	Pre10	77 (3e-89)	PSMA3	72 (5e-79)	20S CP proteasomal α subunit	15.5	3.3
An13g01210	Pre3	87 (5e-80)	PSMB6	76 (1e-65)	20S CP proteasomal β subunit	10.4	4.6
An11g04620	Pup1	79 (1e-96)	PSMB7	74 (2e-84)	20S CP proteasomal β subunit	3.6	0.5
An04g01800	Pup3	84 (2e-87)	PSMB3	74 (7e-66)	20S CP proteasomal β subunit	6.6	3.2
An04g01870	Pre1	79 (2e-67)	PSMB2	66 (1e-40)	20S CP proteasomal β subunit	4.9	0.6
An11g01760	Pre2	75 (1e-92)	PSMB5	70 (7e-59)	20S CP proteasomal β subunit	4.5	1
An18g06700	Pre7	71 (2e-77)	PSMB1	61 (5e-51)	20S CP proteasomal β subunit	21.9	0.5
An18g06680	Pre4	62 (2e-64)	PSMB4	65 (3e-53)	20S CP proteasomal β subunit	5.9	2.5
An04g05320	Blm10	40 (6e-90)	PSME4	42 (5e-65)	Proteasome regulator	1.8	0.5
An07g01470	**Ddi1**	**55 (2e-56)**	**DDI1**	**68 (5e-60)**	**Ub-dependent protein catabolism**	**0.8**	**4.4**
An17g02180	**Dfm1**	**47 (1e-07)**	**DERL1**	**48 (2e-17)**	**Derlin-like protein**	**6**	**3.6**
An01g12370	(Ubx3)	53 (7e-35)	(FAF2)	52 (4e-28)	Ub activator domain protein	5.3	5.2

Supplementary Table S7. Proteins of predicted intracellular localisation identified from culture filtrates. SP: signal peptide; TMD: transmembrane domains; MAL.: maltose; XYL.: xylose; SORB.: sorbitol; BR: biological replicate; NSAF: normalised spectral abundance factor.

Locus tag	Protein description	Signal sequence	TMD	NSAF 10^3		
				MAL	XYL	SORB
An01g02500	thioredoxin, *A. nidulans*		0	24.2	11.5	5.7
An02g10150	similarity to hypothetical dehydratase/racemase, *Rhodococcus erythropolis*		0	1.5	1.3	4.8
An16g07410	mitochondrial F1-ATPase α-subunit Atp1, *S. cerevisiae*	SP	0	3.7	3.1	1.9
An12g04940	mitochondrial heat shock protein Hsp60, *S. cerevisiae*		0	8.4	5.5	1.8
An11g04180	dnaK-type molecular chaperone BipA, *A. niger*	SP	1	3.0	1.1	0.3
An16g05420	glucose-6-phosphate isomerase PgiA strongly similar to Pgi1, *S. cerevisiae*		0	3.7	0.4	0.4
An18g04220	mitochondrial ADP/ATP carrier anc1p, *S. pombe*		4	19.1	5.4	3.2
203715	outer mitochondrial membrane protein porin, *A. clavatus* NRRL 1		0	9.1	2.1	1.8
40895	hypothetical protein AN0516.2, *A. nidulans* FGSC A4		0	4.8	1.9	4.6
An16g04350	hypothetical protein		1	2.0	1.7	2.0

Supplementary Table S8. Secreted proteins identified from culture filtrates. SP: signal peptide; TMD: transmembrane domain. Black box: significantly more abundant on D-maltose; grey box: significantly more abundant on D-xylose; white box: significantly less abundant on D-maltose or D-xylose compared to D-sorbitol; MAL: D-maltose addition; XYL: D-xylose addition; SORB: D-sorbitol addition.

Predicted classification EC number	Protein description	Locus tag		TMD	NSAF · 10^3			G-score	
					MAL	XYL	SORB	MAL	XYL
Oxidoreductase 1.-.-.-	sulphydryl oxidase Sox (SoxA) from patent EP565172-A1, *A niger*	An09g05940	SP	0	20.0	24.7	25.8	0.73	0.02
Oxidoreductase 1.1.3.-	glucooligosaccharide oxidase strongly similar to carbohydrate oxidase from patent WO9931990-A1, *Microdochium nivale*	An01g14520	SP	0	4.1	5.5	2.9	0.20	0.82
Oxidoreductase 1.1.3.-; 1.5.3.6	similarity to carbohydrate oxidase from patent WO9931990-A1, *Microdochium nivale*	An10g00190	SP	0	6.8	5.8	6.3	0.02	0.02
Oxidoreductase 1.1.1.-	isoamyl alcohol oxidase mreA, *A. oryzae*	An11g03740	SP	0	6.6	4.8	9.8	0.61	1.74
Oxidoreductase 1.1.1.-	isoamyl alcohol oxidase mreA, *A. oryzae*	An03g06270	SP	0	7.7	6.6	8.4	0.03	0.22
Oxidoreductase 1.1.1.-	FAD/FMN-containing isoamyl alcohol oxidase MreA, *A. fumigatus*	208521	SP	1	1.5	3.0	4.6	1.66	0.35
Oxidoreductase 1.5.3.6	similarity to 6-hydroxy-D-nicotine oxidase, *Arthrobacter oxidans*	An07g02360	SP	0	23.7	21.2	22.8	0.02	0.06
Oxidoreductase 1.5.3.6	6-hydroxy-D-nicotine oxidase, *Arthrobacter oxidans*	An03g00460	SP	0	9.9	7.4	8.7	0.08	0.09
Oxidoreductase 1.5.3.14	polyamine oxidase PAO, *Zea mays*	An13g02480	SP	0	3.9	6.1	4.3	0.02	0.32
Oxidoreductase 1.8.4.8	thioredoxin, *A. nidulans*	An01g02500		0	24.2	11.5	5.7	12.27	1.96
Oxidoreductase 1.11.1.6	catalase R CatR, *A niger*	An01g01820	SP	0	9.2	6.5	10.4	0.09	0.95
Oxidoreductase 1.11.1.10	similarity to chloroperoxidase CPO, *Caldariomyces fumago*	An06g00720	SP	0	27.4	27.1	25.7	0.06	0.04
Oxidoreductase 1.14.18.1	weak similarity to tyrosinase melC2, *Streptomyces lincolnensis*	An01g09220	SP	0	19.3	16.5	16.8	0.18	0.00
Transferase 2.-.-.-	weak similarity to cDNA for 59-kDa readthrough protein RT, Sorghum chlorotic spot virus	An11g00040	SP	1	22.9	15.2	16.3	1.14	0.03
Transferase 2.4.1.-	β-1,6-N-acetylglucosaminyltransferase strongly similar to GPI anchored protein, putative, *A. flavus* NRRL3357	55058	SP	0	11.6	7.7	8.2	0.58	0.02
Transferase 2.4.1.25	4-α-glucanotransferase AgtB, *A niger*	An12g02460	SP	1	1.6	1.4	2.6	0.26	0.41
Transferase 2.7.10.1	EcmA strongly similar to GPI-anchored cell wall organization protein ECM33, *S. pombe*	An04g01230	SP	0	12.3	14.2	23.1	3.36	2.15
Transferase 2.8.3.16	similarity to hypothetical dehydratase/racemase, *Rhodococcus*	An02g10150		0	1.5	1.3	4.8	1.72	2.06
Hydrolase 3.-.-.-	hypothetical protein BAC47708.1, *Bradyrhizobium japonicum*	An18g02752	SP	0	5.1	5.7	2.6	0.85	1.15
Hydrolase 3.1.1.3	triacylglycerol lipase Lip5, Candida rugosa	An11g00100	SP	0	5.5	6.4	8.2	0.52	0.21
Hydrolase 3.1.1.5; 3.1.4.3	phospholipase B from patent US6146869-A, *A. oryzae*	An16g03700	SP	0	5.6	2.7	7.5	0.28	2.41
Hydrolase 3.1.3.-	phytase phyA3, *A. fumigatus*	An12g01910	SP	0	7.6	14.5	10.4	0.43	0.68
Hydrolase 3.1.3.2	acid phosphatase AphA, *A niger*	An13g01750	SP	0	6.1	5.3	5.7	0.02	0.02
Hydrolase 3.1.4.3	similarity to enantiomer-selective amidase amdA, Rhodococcus	An02g00190	SP	0	10.5	7.2	9.5	0.04	0.32
Hydrolase 3.1.27.1	ribonuclease T2 precursor rntB, *A. oryzae*	An01g10580	SP	0	14.4	6.6	27.4	4.16	13.70
Hydrolase 3.1.27.3	extracellular guanyl-specific ribonuclease RntA, *A. fumigatus*	42238	SP	0	15.1	5.5	19.9	0.66	8.61

Predicted classification EC number	Protein description	Locus tag		TMD	NSAF · 10^3			G-score	
					MAL	XYL	SORB	MAL	XYL
Hydrolase 3.2.1.-	glycosyl hydrolase strongly similar to allergen Asp F7-like, *A. fumigatus*	128537	SP	0	31.2	24.8	32.8	0.04	1.12
Hydrolase 3.2.1.-	glycosyl hydrolase strongly similar to allergen rAsp f 4, *A. fumigatus*	An07g08400	SP	0	11.5	8.3	16.9	1.05	3.01
Hydrolase 3.2.1.-	cell wall antigen MP1, *Penicillium marneffei*	An14g02100	SP	0	7.1	7.7	5.0	0.35	0.59
Hydrolase 3.2.1.-	glycosyl hydrolase strongly similar to hypothetical allergen rAsp f 4 from patent WO9828624-A1, *A. fumigatus*	An03g00770	SP	0	3.9	6.0	3.9	0.00	0.46
Hydrolase 3.2.1.1	acid α-amylase AamA- *A niger*	An11g03340	SP	0	10.9	7.4	2.9	5.04	2.06
Hydrolase 3.2.1.3	glucan 1,4-α-glucosidase (glucoamylase) GlaA, *A niger*	An03g06550	SP	0	50.4	30.6	35.1	2.74	0.31
Hydrolase 3.2.1.4	cell wall remodelling protein strongly similar to protein from patent WO9931255-A2, *Emericella desertoru*	An03g05530	SP	0	15.2	9.0	9.1	1.53	0.00
Hydrolase 3.2.1.4	endoglucanase EglB (An07g08950), *A niger*	An16g06800	SP	0	7.7	11.3	9.4	0.18	0.18
Hydrolase 3.2.1.4	endoglucanase A EglA, *A niger*	An14g02760	SP	0	1.2	9.3	0.9	0.06	8.23
Hydrolase 3.2.1.4	hypothetical endoglucanase IV, *T. reesei*	An08g05230	SP	0	2.2	6.8	3.6	0.35	1.00
Hydrolase 3.2.1.4	similarity to cellulase #2 from patent US2003036176-A1, *Xanthomonas campestris*	An03g04190	SP	0	2.8	5.2	5.9	1.16	0.04
Hydrolase 3.2.1.4; 3.2.1.-	endoglucanase IV egl4, *T. reesei*	An14g02670	SP	0	0.8	3.6	5.3	3.65	0.35
Hydrolase 3.2.1.6	cell wall protein CrhB strongly similar to Utr2, *S. cerevisiae*	An07g07530	SP	0	10.3	6.4	10.2	0.00	0.86
Hydrolase 3.2.1.6	cell wall protein CrhD strongly similar to Crh1, *S. cerevisiae*	An01g11010	SP	0	8.1	5.6	7.8	0.00	0.35
Hydrolase 3.2.1.6	cell wall protein CrhA strongly similar to Crh1, *S. cerevisiae*	An11g01540	SP	0	7.5	5.0	3.0	2.04	0.52
Hydrolase 3.2.1.8	endo-1,4-β-xylanase A precursor XynA, *A niger*	An03g00940	SP	0	0.9	20.5	0.6	0.04	23.59
Hydrolase 3.2.1.14	chitinase ChiF/CtcA strongly similar to chiA, *A. nidulans*	An09g06400	SP	0	0.7	0.2	2.1	0.77	1.88
Hydrolase 3.2.1.20	extracellular α-glucosidase AgdA, *A niger*	An04g06920	SP	0	11.5	5.8	5.2	2.41	0.03
Hydrolase 3.2.1.20	α-glucosidase AgdB strongly similar to enzyme with sugar transferase activity from patent JP11009276-A, Acremonium sp.	An01g10930	SP	0	3.7	6.0	5.5	0.35	0.03
Hydrolase 3.2.1.21	β-glucosidase BglA/ bgl1, *A niger*	An18g03570	SP	0	7.1	18.2	10.3	0.60	2.20
Hydrolase 3.2.1.22	α-galactosidase AglB, *A niger*	An02g11150	SP	0	8.5	9.5	8.8	0.01	0.02
Hydrolase 3.2.1.23	β-galactosidase LacA, *A niger*	An01g12150	SP	0	0.3	3.7	0.2	0.01	3.80
Hydrolase 3.2.1.28	α,α-trehalase TreA strongly similar to treA, *A. nidulans*	An01g01540	SP	0	0.8	2.1	4.0	2.34	0.64
Hydrolase 3.2.1.37	β-xylosidase XlnD, *A niger*	An01g09960	SP	0	0.4	17.0	0.8	0.15	18.25
Hydrolase 3.2.1.37	xylan 1,4-β-xylosidase, *Butyrivibrio fibrisolvens*	An08g01900	SP	0	0.5	5.0	0.3	0.02	4.97
Hydrolase 3.2.1.55	1,4-β-D-arabinoxylan arabinofuranohydrolase AxhA, *A niger*	An03g00960	SP	0	0.9	17.2	0.6	0.04	19.29
Hydrolase 3.2.1.55	arabinofuranosidase B AbfB, *A niger*	An15g02300	SP	0	0.6	16.4	4.5	3.48	7.13
Hydrolase 3.2.1.55	α-L-arabinofuranosidase a precursor AbfA, *A niger*	An01g00330	SP	0	0.5	2.8	0.3	0.02	2.19
Hydrolase 3.2.1.58	BgtB similar to glucan 1,3-β-glucosidase Bgl2, *S. cerevisiae*	An03g05290	SP	0	25.7	35.8	23.5	0.09	2.55

Predicted classification EC number	Protein description	Locus tag		TMD	NSAF · 10^3			G-score	
					MAL	XYL	SORB	MAL	XYL
Hydrolase 3.2.1.58	1,3-β-glucanosyltransferase GelA strongly similar to gel1, *A. fumigatus*	An10g00400	SP	1	23.5	22.2	34.7	2.17	2.75
Hydrolase 3.2.1.58	BgtA strongly similar to 1,3-β-glucanosyltransferase bgt1, *A. fumigatus*	An08g03580	SP	0	14.5	14.0	19.9	0.85	1.02
Hydrolase 3.2.1.58	related to β-1,3-glucanosyltransferase; pH-responsive protein 2 precursor, A. terreus	53033	SP	0	10.3	10.6	8.8	0.11	0.17
Hydrolase 3.2.1.58	1,3-β-glucanosyltransferase GelD strongly similar to gel3, *A. fumigatus*	An09g00670	SP	1	9.1	7.8	9.5	0.01	0.17
Hydrolase 3.2.1.58	1,3-β-glucanosyltransferase GelB strongly similar to Gas1, *S. cerevisiae*	An08g07350	SP	0	7.8	6.6	8.9	0.08	0.33
Hydrolase 3.2.1.58	BxgA strongly similar to hypothetical glucan β-1,3 exoglucanase exgS, A. phoenicis	An01g12450	SP	0	1.5	2.4	0.7	0.37	1.03
Hydrolase 3.2.1.75	acidic β-1,6-glucanase NegA strongly similar to protein SEQ ID NO:10 from patent WO200018931-A1, *A. fumigatus*	An03g00500	SP	0	8.9	12.7	13.9	1.11	0.06
Hydrolase 3.2.1.99	putative endoarabinanase AbnC strongly similar to AbnA (An09g01190), *A niger*	An02g10550	SP	0	10.0	3.9	1.9	5.99	0.67
Hydrolase 3.2.1.113	mannosyl-oligosaccharide 1,2-α-mannosidase msdS, *A. saitoi*	An01g12550	SP	0	13.0	15.0	9.2	0.64	1.37
Hydrolase 3.4.14.2	dipeptidyl peptidase II DPPII, *Rattus norvegicus*	An12g05960	SP	0	18.9	13.5	13.4	0.94	0.00
Hydrolase 3.4.14.9	lysosomal pepstatin insensitive protease CLN2, *H. sapiens*	An06g00190	SP	0	11.2	11.3	13.5	0.21	0.21
Hydrolase 3.4.14.9	similarity to lysosomal protease CLN2, Rattus norvegicus	An01g01750	SP	0	5.8	6.5	7.3	0.17	0.05
Hydrolase 3.4.14.9	lysosomal pepstatin insensitive protease CLN2, *H. sapiens*	An03g01010	SP	0	4.8	4.1	4.0	0.07	0.00
Hydrolase 3.4.14.9	ProtB strongly similar to hypothetical lysosomal pepstatin insensitive protease CLN2, *Canis lupus*	An08g04640	SP	0	4.5	4.7	3.9	0.04	0.07
Hydrolase 3.4.16.-	endoprotease ProtA/ Endo-Pro, *A niger*	An08g04490	SP	0	11.6	8.0	5.9	1.91	0.33
Hydrolase 3.4.16.-	serine-type carboxypeptidase I CpdA strongly similar to cpdS, *A. saitoi*	An02g04690	SP	0	7.2	5.2	9.0	0.21	1.05
Hydrolase 3.4.16.-; 3.4.16.6	carboxypeptidase ProtF strongly similar to carboxypeptidase S1, *Penicillium janthinellum*	An03g05200	SP	0	18.0	14.5	12.7	0.89	0.11
Hydrolase 3.4.21.-	serine endopeptidase strongly similar to protein PRO304 from patent WO200104311-A1, *H. sapiens*	An14g02470	SP	0	11.9	9.3	7.1	1.23	0.31
Hydrolase 3.4.23.-	ProtG strongly similar to aspartic protease pr1, *Phaffia rhodozyma*	An12g03300	SP	0	3.2	2.7	5.0	0.40	0.68
Hydrolase 3.4.23.18; 3.4.23.1	aspartic proteinase aspergillopepsin I PepA, *A niger*	An14g04710	SP	0	49.4	56.0	46.6	0.08	0.87
Hydrolase 3.4.23.35; 3.4.23.1	extracellular protease precursor Bar1, *S. cerevisiae*	An18g01320	SP	0	3.2	3.8	4.1	0.11	0.01
Hydrolase 3.5.1.2	glutaminase A gtaA, *A. oryzae*	An02g13750	SP	0	3.8	4.7	5.1	0.19	0.02
Hydrolase 3.6.3.14	mitochondrial F1-ATPase α-subunit Atp1, *S. cerevisiae*	An16g07410	SP	0	3.7	3.1	1.9	0.60	0.33
Hydrolase 3.6.4.9	mitochondrial heat shock protein Hsp60, *S. cerevisiae*	An12g04940		0	8.4	5.5	1.8	4.74	2.02
Hydrolase 3.6.4.10	dnaK-type molecular chaperone BipA, *A niger*	An11g04180	SP	1	3.0	1.1	0.3	2.57	0.48
Isomerase 5.1.3.3	mutarotase enzyme from patent JP07039380-A, *Sus scrofa*	An02g09090	SP	0	6.5	6.8	4.6	0.32	0.41
Isomerase 5.3.1.9	glucose-6-phosphate isomerase PgiA strongly similar to Pgi1, *S. cerevisiae*	An16g05420		0	3.7	0.4	0.4	3.13	0.01
Isomerase 5.4.2.1	similarity to hypothetical protein mlr2143, *Mesorhizobium loti*	An15g07520	SP	0	14.9	9.9	17.7	0.23	2.21
Isomerase 5.4.2.1	similarity to trehalose metabolism factor Pmu1, *S. cerevisiae*	An08g02590	SP	0	0.8	4.8	1.7	0.34	1.54

Predicted classification EC number	Protein description	Locus tag		TMD	NSAF · 10^3			G-score	
					MAL	XYL	SORB	MAL	XYL
Isomerase 5.5.1.1	similarity to cis,cis-muconate lactonizing enzyme I TcMLE, *Trichosporon cutaneum*	An01g14730	SP	0	24.5	27.3	23.7	0.01	0.25
Ligase 6.3.5.	hypothetical amidase Z37509, *S. cerevisiae*	An05g01860	SP	1	0.5	3.5	4.9	4.26	0.22
	antifungal protein AnAFP strongly similar to antifungal protein precursor paf, *P. chrysogenum*	An07g01320	SP	0	34.7	45.8	60.5	7.06	2.03
	hypothetical protein	An13g01520	SP	0	22.3	19.1	15.9	1.11	0.30
	weak similarity to hypothetical protein Ta0309, *Thermoplasma acidophilum*	An09g03650	SP	0	14.5	16.8	21.5	1.37	0.56
	mitochondrial ADP/ATP carrier anc1p, *S. pombe*	An18g04220		4	19.1	5.4	3.2	12.52	0.57
	purine nucleoside permease NUP, *C. albicans*	An10g00800	SP	0	13.6	5.5	7.6	1.70	0.34
	cell wall protein PhiA strongly similar to hypothetical protein binB, *A. nidulans*	An14g01820	SP	0	7.9	12.1	3.4	1.88	5.27
	hypothetical protein	37529	SP	0	1.9	8.1	12.0	8.27	0.80
	protein required for cell wall integrity Wsc1/Slg1, *S. cerevisiae*	An03g00250	SP	0	3.8	3.3	11.8	4.24	5.10
	hypothetical protein EAA64623.1, *A. nidulans*	An16g07920	SP	0	10.8	9.2	9.9	0.04	0.02
	hypothetical conserved protein SPAC12B10.16c, *S. pombe*	An04g08730	SP	0	8.1	9.7	10.4	0.28	0.02
	outer mitochondrial membrane protein porin, *A. clavatus*	203715		0	9.1	2.1	1.8	5.45	0.03
	SUN family protein Psu1p, *S. pombe*	An07g02730	SP	0	3.1	2.6	7.4	1.84	2.37
	similarity to hypothetical protein EAA64430.1, *A. nidulans*	An07g05660	SP	0	5.5	3.9	6.1	0.02	0.49
	hypothetical protein AN0516.2, *A. nidulans*	40895		0	4.8	1.9	4.6	0.00	1.23
	hypothetical protein	An07g00170	SP	0	3.8	3.2	2.7	0.19	0.05
	hypothetical protein	An16g04350		1	2.0	1.7	2.0	0.00	0.02

Supplementary Table S9. Non-validated secreted proteins found from culture filtrates (< 2 unique peptides in one BR and 1 unique peptide in the other BR). ERRS: ER retention sequence; SA: signal anchor; SP: signal peptide; TMD: transmembrane domains; MAL: maltose; XYL: xylose; SOR: sorbitol; BR: biological replicate; NSAF: normalised spectral abundance factor.

Locus tag	Protein description	Signal	TM	ERRS	Spectral counts					
					MAL		XYL		SOR	
			D		BR1	BR2	BR1	BR2	BR1	BR2
An03g03300	PgnN similar to N-glycosidase from patent EP676473-A2	SP	0		1	1	0	2	0	2
An10g00210	hypothetical protein	SP	0		1	1	1	1	1	1
An01g01550	catalase cat1 - *A. fumigatus*	SP	0		1	0	1	0	1	0
An07g03880	serine proteinase pepC - *A. niger*	SP	0		0	1	0	1	0	0
An13g02060	cytochrome P450 monooxygenase TRI4 - *Fusarium sporotrichioides*	SP	1		0	1	0	1	0	0
45472	hypothetical Pc21g11200 - *P. chrysogenum* Wisconsin 54-1,255	SP	1		1	0	1	0	0	0
44921	predicted protein - *A. terreus* NIH2624	SP	0		0	1	0	1	0	0
An02g04060	hypothetical protein	SP	0		0	6	0	1	0	0
40197	hypothetical protein	SP	0		0	2	0	0	0	0
An12g08720	hexosyltransferase similar to AAG27909.1 - *A. thaliana*	SA	0		0	1	0	0	0	0
An02g00850	hypothetical mixed-linked glucanase related MLG1 - *N. crassa*	SP	0		1	0	0	0	0	0
An13g00620	glucosidase II β subunit strongly similar to G19P1 - *H. sapiens*	SP	0	KDEL	0	1	0	0	0	0
An09g05880	α-glucosidase AgdE similar to ModA - *Dictyostelium discoideum*	SP	1		0	1	0	0	0	0
An14g00800	cell surface regulatory component of β-1,3-glucan synthesis HkrA	SP	1		1	0	0	0	0	0
An01g08430	methylmalonate-semialdehyde dehydrogenase MMSDH - *Rattus norvegicus*	SP	0		0	1	0	0	0	0
An09g03940	ketol-acid reductoisomerase ilv-2 - *N. crassa*	SP	0		0	1	0	0	0	0
An04g02020	cyclophilin CypB	SP	2	HEEL	1	0	0	0	0	0
An18g02020	disulfide isomerase TigA	SP	0	KDEL	1	0	0	0	0	0
An10g00150	cytochrome P450 monooxygenase TRI4 - Myrothecium roridum	SP	2		1	0	0	0	0	0
An15g01950	cephalosporin C from patent JP06038763-A – *A. chrysogenum*	SP	0		1	0	0	0	0	0
An15g03900	heavy metal ion resistance protein Zrc1 - *S. cerevisiae*	SP	5		0	1	0	0	0	0
An09g03120	similarity to hypothetical serine-rich protein - *S. pombe*	SP	2		1	0	0	0	0	0
An16g01780	similarity to protein CAP22 - Colletotrichum gloeosporioides	SP	0		0	1	0	0	0	0
An09g03100	4-α-glucanotransferase AgtA strongly similar to α-amylase precursor amy - *A. niger*	SP	0		1	1	0	1	1	1
An02g01550	secreted serine protease 19 kDa CS antigen CS-Ag – *C. immitis*	SP	0		1	1	0	1	1	1
An07g03930	hypothetical protein	SP	0		0	1	0	0	0	1
An09g00260	α-galactosidase aglC - *A. niger*	SP	0		1	0	0	0	1	0
An11g06540	β-mannosidase mndA - *A. niger*	SP	0		1	0	0	0	0	1
An12g08280	exo-inulinase InuE/ inu1 - *A. niger*	SP	0		1	0	0	0	1	0
An02g03310	hypothetical Ptdglycerol/PtdIns transfer protein pltpao - *A. oryzae*	SP	0		0	1	0	0	1	0
An15g07790	similarity to hypothetical protein encoded by An11g02730 - *A. niger*	SP	0		0	1	0	0	0	1
An01g00780	endo-1,4-xylanase xynB - *A. niger*	SP	0		0	0	1	1	0	0
An15g04550	xylanase A xynA from patent WO200068396-A2 - *A. niger*	SP	0		0	0	1	1	0	0
An07g00440	secretory lipase LIP2 - *C. albicans*	SP	0		0	0	0	2	0	0
An08g10780	hypothetical protein T16K5.230 - *A. thaliana*	SP	0		0	0	0	2	0	0
An09g00120	ferulic acid esterase A FaeA protein	SP	0		0	0	1	0	0	0
An12g05010	acetyl xylan esterase AxeA protein	SP	0		0	0	0	1	0	0
An09g03300	AxlA α-xylosidase similar α-xylosidase XylS - *Sulfolobus solfataricus*	SP	0		0	0	1	0	0	0
An03g01050	similarity to endo-β-1,4-glucanase - *Bacillus polymyxa*	SP	0		0	0	1	0	0	0
An14g04200	rhamnogalacturonase RhgB protein	SP	0		0	0	0	1	0	0
An01g06500	GPI-anchored endomannanase DfgD	SP	1		0	0	0	1	0	0
An01g11520	polygalacturonase Pgal protein	SP	0		0	0	0	1	0	0
An03g01620	high affinity glucose transporter HGT1 - *K. lactis*	SA	12		0	0	1	0	0	0
An01g12240	hypothetical protein CAC28784.2 - *N. crassa*	SP	0		0	0	1	0	0	0
An08g04630	hypothetical protein	SP	0		0	0	0	1	0	0
An15g07560	similarity to hypothetical protein dag11 - *A. bisporus*	SP	0		0	0	1	0	0	0

Locus tag	Protein description	Signal	TMD	ERRS	Spectral counts					
					MAL		XYL		SOR	
					BR1	BR2	BR1	BR2	BR1	BR2
An01g00490	isoamyl alcohol oxidase mreA - *A. oryzae*	SP	0		0	0	0	1	0	0
An16g04820	NAD dependent epimerase/dehydratase	SP	0		0	0	1	0	0	0
An12g05310	5' nucleotidase and UDP-sugar hydrolase UshaA	SP	0		0	0	1	0	0	0
An02g12350	similarity to neuronal long splice form of ankyrin ANK2 - *H. sapiens*	SP	5		0	0	0	1	0	0
An01g10000	ATP-binding cassette transporter abc1p - *S. pombe*	SP	14		0	0	0	1	0	0
An15g04570	endoglucanase IV - *T. reesei*	SP	0		1	0	1	1	1	0
An09g05170	similarity to hypothetical protein 15E11.110 - *N. crassa*	SP	0		0	0	0	3	1	1
An16g02440	hypothetical mlr1518 - Mesorhizobium loti	SP	0		0	0	0	3	1	1
An01g14940	similarity to phospholipase C -PLC - Burkholderia pseudomallei	SP	0		1	0	0	2	0	1
An16g03330	extracellular thaumatin domain protein weakly similar to endo-1,4-β-xylanase CAA93120.1 - Ascochyta pisi	SP	0		0	1	1	1	1	1
An06g00180	hypothetical protein	SP	0		0	0	1	1	1	1
An08g11030	acid phosphatase aph 3-phytase phyB - *A. niger*	SP	0		0	0	0	2	1	1
An04g09690	pectin methylesterase PmeB strongly similar to pme1 – A. aculeatus	SP	0		0	0	0	1	1	0
An06g00360	filamentous growth DfgF strongly similar to Dfg5 - *S. cerevisiae*	SP	0		0	0	0	1	1	0
An05g02390	similarity to 6-hydroxy-D-nicotine oxidase 6-HDNO - Arthrobacter oxidans	SP	0		0	0	1	0	1	0
An11g01110	lysosomal pepstatin insensitive protease CLN2 - *H. sapiens*	SP	0		0	0	0	1	1	0
An14g02150	serine-type carboxypeptidase precursor cpdS - A. phoenicis	SP	0		0	0	1	0	1	0
An01g01630	hypothetical protein encoded by An09g00510 - *A. niger*	SP	0		0	0	0	0	1	1
An04g07160	similarity to hypothetical protein MLD14.3 - *A. thaliana*	SP	0		0	0	0	0	1	1
An07g00510	similarity to hypothetical lipoprotein SC4A2.13c – S. coelicolor	SP	0		0	0	0	0	3	0
An01g01430	similarity to hydroquinone oxidase mcrA - Streptomyces lavendulae	SP	0		0	0	0	0	2	0
An02g14290	cephalosporin esterase - Rhodosporidium toruloides	SP	0		0	0	0	0	0	2
An12g10810	EST an_2678 - *A. niger*	SP	0		0	0	0	0	2	0
An08g09420	cell wall galactomannoprotein	SP	0		0	0	0	0	0	1
An13g02530	similarity to α-carbonic anhydrase CAH - Neisseria gonorrhoeae	SP	0		0	0	0	0	1	0
An02g00740	similarity to 6-hydroxy-D-nicotine oxidase 6-HDNO - Arthrobacter oxidans	SP	0		0	0	0	0	1	0
An03g00830	weak similarity to intestinal mucin MUC2 - *H. sapiens*	SP	0		0	0	0	0	1	0
An02g13650	hypothetical protein	SP	0		0	0	0	0	1	0
An08g01180	hypothetical protein SC4G1.04c - Streptomyces coelicolor	SP	0		0	0	0	0	0	1
An02g11390	extracellular serine-rich protein	SP	0		0	0	0	0	1	0
An02g13220	lysophospholipase phospholipase B - Penicillium notatum	SP	0		0	0	0	0	0	1
An09g02180	phospholipase A1 from patent JP10155493-A - *A. oryzae*	SP	0		0	0	0	0	1	0
An08g09840	putative cysteine proteinase	SP	0		0	0	0	0	0	1
An14g02070	weak similarity to endo-1,4-β-glucanase celE – C. thermocellum	SP	0		0	0	0	0	1	0
An16g06990	endo-polygalacturonase A PgaA protein [putative frameshift]	SP	0		0	0	0	0	1	0
An18g04100	exo-β-1,3-glucanase strongly similar to 43 kDa secreted glycoprotein precursor gp43 - Paracoccidioides brasiliensis	SP	0		0	0	0	0	1	0
An11g01660	similarity to hypothetical protein B24P11.210 - *N. crassa*	SP	0		0	1	0	1	1	1
An14g01068	EST an_2307 - *A. niger*	SP	0		0	1	0	1	1	1
An14g06730	adenine-repressible gene rds1p - *S. pombe*	SP	0		0	1	0	1	1	1
An06g01000	hypothetical protein	SP	0		0	1	0	1	1	1
An08g07090	similarity to protein Sim1 - *S. cerevisiae*	SP	0		0	1	0	1	1	1
An04g01440	precursor of pepsin A3 - *H. sapiens*	SP	0		1	0	1	0	1	1
An01g06280	IgE-binding protein - *A. fumigatus*	SP	0		0	1	0	1	0	2
An02g04900	endopolygalacturonase pgaB - *A. niger*	SP	0		0	1	0	1	0	2
An18g00410	similarity to hypothetical protein T22K18.2 - *A. thaliana*	SP	0		0	1	0	2	0	3
An06g00170	α-galactosidase aglA - *A. niger*	SP	0		0	2	0	2	3	0
An09g06650	core protein II of ubiquinol--cytochrome c reductase CAA42214.1 - Bos primigenius taurus		0		0	2	0	2	0	2
An02g05880	29.9 kD subunit of NADH:ubiquinone reductase - *N. crassa*		0		0	1	0	1	0	1

Locus tag	Protein description	Signal	TM D	ERRS	Spectral counts MAL BR1	MAL BR2	XYL BR1	XYL BR2	SOR BR1	SOR BR2
An15g06280	aspartic proteinase aspergillopepsin I pepA - *A. niger*		0		0	1	0	1	0	1
An01g05650	tubulin α-1 chain tubA - A. nidulans		0		0	1	0	1	0	1
An04g05220	subunit 6 of ubiquinol--cytochrome-c reductase Qcr6 - *S. cerevisiae*		0		0	1	0	1	0	0
An01g13600	mitochondrial phosphate transport protein Mir1 - *S. cerevisiae*		0		0	1	1	0	0	0
An04g04750	oxoglutarate dehydrogenase (lipoamide) Kgd1 - *S. cerevisiae*		0		0	1	0	1	0	0
An07g06840	precursor of dihydrolipoamide dehydrogenase Lpd1 - *S. cerevisiae*		0		0	1	0	1	0	0
An16g05340	similarity to trans-2-enoyl-ACP reductase II fabK – S. pneumoniae		0		0	1	0	1	0	0
An07g10100	adenylate kinase Adk1 - *S. cerevisiae*		0		0	1	0	1	0	0
An08g03430	cytoplasmic ribosomal protein of the large subunit L6 - *S. cerevisiae*		0		1	0	1	0	0	0
An08g03910	cytoplasmic ribosomal protein of the large subunit L10a - *Rattus norvegicus*		0		1	0	1	0	0	0
An04g00870	similarity to insertion and deletion mismatch repair protein Mlh3 - *S. cerevisiae*		0		1	0	1	0	0	0
An07g09990	heat shock protein 70 hsp70 - Ajellomyces capsulatus		0		0	1	1	0	0	0
An02g03590	UDP-glucose-hexose-1-P uridylyltransferase Gal7 - *S. cerevisiae*		0		0	1	0	1	0	0
An14g03820	UDP-glucose 4-epimerase Gal10 - *S. cerevisiae*		0		1	0	1	0	0	0
An11g02040	phosphogluconate dehydrogenase Gnd1 - *S. cerevisiae*		0		1	0	1	0	0	0
An18g00910	similarity to alkyl salicylate esterase salE - Acinetobacter sp.		0		1	0	1	0	0	0
An01g10050	IgE-dependent histamine-releasing factor - *H. sapiens*		0		1	0	1	0	0	0
An17g01825	huntingtin interacting protein 1 HIF-1 - *H. sapiens*		0		1	0	1	0	0	0
An04g09130	similarity to peroxisomal membrane protein PMP22 - *A. thaliana*		3		0	1	0	1	0	0
An09g02940	hypothetical protein		0		1	0	1	0	0	0
An10g00820	oxaloacetate acetyl hydrolase OahA - *A. niger*		0		1	1	0	0	0	0
An17g00370	hypothetical single-stranded TG1-3 binding protein tcg - *S. pombe*		0		1	1	0	0	0	0
An02g00660	similarity to hypothetical protein CAC18275.2 - *N. crassa*		5		1	1	0	0	0	0
An07g05630	hypothetical coiled-coil protein - *S. pombe*		0		1	1	0	0	0	0
An18g04840	translation elongation factor 1 α - P. anserina		0		0	16	0	1	0	2
An14g04180	H+-transporting ATP synthase β chain - *N. crassa*		0		0	8	0	2	0	1
An07g08300	cyclophilin-like peptidyl prolyl cis-trans isomerase cypA - *A. niger*		0		0	3	0	0	0	0
An02g05700	translation elongation factor eEF-2 - Cricetulus griseus		0		3	0	1	0	0	0
An01g12210	core protein I of ubiquinol:cytochrome-c reductase β - *N. crassa*		0		0	2	0	0	0	0
An02g02170	tryptophan synthase Trp5 - *S. cerevisiae*		0		2	0	0	0	0	0
An08g10480	cytoplasmic ribosomal protein of the large subunit L7 - *S. pombe*		0		2	0	0	0	0	0
An11g04360	polyribosome binding protein Scp160 - *S. cerevisiae*		0		2	0	0	0	0	0
An12g07580	acetylglutamate kinase/N-acetyl-γ-glutamyl-phosphate reductase precursor arg-6 - *N. crassa*		0		2	0	0	0	0	0
An18g06250	phosphopyruvate hydratase ENO1 - *C. albicans*		0		2	0	0	0	0	0
An11g00530	cytoplasmic ATP citrate lyase - *H. sapiens*		0		1	1	1	0	0	0
An09g06350	protein snaD - A. nidulans		0		1	1	0	1	0	0
An02g08300	hypothetical protein encoded by An11g06450 - *A. niger*		0		1	1	0	0	0	1
An02g13180	β-1,3-exoglucanase lam1.3 - Trichoderma atroviride		0		1	0	0	0	0	0
An07g00240	α-L-rhamnosidase ramA - Clostridium stercorarium		0		1	0	0	0	0	0
An02g07650	phosphoglucomutase pgmB - A. nidulans		0		1	0	0	0	0	0
An08g05790	glycogen phosphorylase Gph1 - *S. cerevisiae*		0		0	1	0	0	0	0
An04g00410	dipeptidyl peptidase III - *Rattus norvegicus*		0		0	1	0	0	0	0
An07g02010	proteasome 20S subunit Pre8 - *S. cerevisiae*		0		1	0	0	0	0	0
An07g07780	similarity to mitochondrial H^+-transporting ATP synthase inhibitor precursor Inh1 - *S. cerevisiae*		0		0	1	0	0	0	0
An03g04790	mitochondrial outer membrane protein Tom70 - P. anserina		1		0	1	0	0	0	0
An06g01390	21.3 kD subunit of NADH:ubiquinone reductase - *N. crassa*		3		0	1	0	0	0	0
An07g07000	mitochondrial m-AAA protease subunit Yta12 - *S. cerevisiae*		0		0	1	0	0	0	0
An08g04470	mitochondrial elongation factor Tu - *A. thaliana*		0		0	1	0	0	0	0
An02g11040	mitochondrial aconitate hydratase Aco1 - *S. cerevisiae*		0		0	1	0	0	0	0

Locus tag	Protein description	Signal	TMD	ERRS	Spectral counts					
					MAL		XYL		SOR	
					BR1	BR2	BR1	BR2	BR1	BR2
An01g09760	cytochrome P450 4F2 CYP4F2 - *H. sapiens*		1		1	0	0	0	0	0
An02g04860	microsomal NADH-cytochrome-b5 reductase - *S. cerevisiae*		0		0	1	0	0	0	0
An14g01590	sterol transmethylase ERG6 - *C. albicans*		0		0	1	0	0	0	0
An01g00060	fatty acid synthase α subunit fas2p - *S. pombe*		0		1	0	0	0	0	0
An04g05720	peroxisomal acetyl-CoA C-acyltransferase POT1 - Y. lipolytica		0		0	1	0	0	0	0
An16g03640	similarity to PtdCho-sterol O-acyltransferase Lcat - Mus musculus		1		0	1	0	0	0	0
An18g05120	subunit of succinyl-CoA:benzylsuccinate CoA-transferase bbsF - Thauera aromatica		0		0	1	0	0	0	0
An11g10310	similarity to gentisate 1,2-dioxygenase GDO - Pseudomonas alcaligenes		0		1	0	0	0	0	0
An01g02900	translation initiation factor Eif-5a.2 - *S. cerevisiae*		0		0	1	0	0	0	0
An15g00760	translation elongation factor eEF-1 γ chain - Artemia sp.		0		1	0	0	0	0	0
An02g03950	cytoplasmic ribosomal protein of the large subunit L3 - *S. cerevisiae*		0		1	0	0	0	0	0
An07g08850	cytoplasmic ribosomal protein of the small subunit Rps11b - *S. cerevisiae*		0		0	1	0	0	0	0
An09g05180	cytoplasmic ribosomal protein of the large subunit L4 - *S. cerevisiae*		0		1	0	0	0	0	0
An12g00510	cytoplasmic ribosomal protein of the small subunit S24.e - *S. cerevisiae*		0		0	1	0	0	0	0
An06g01780	(β)-transducin like protein TBL1 - *H. sapiens*		0		1	0	0	0	0	0
An02g01260	weak similarity to β transducin-like protein het-e1 - P. anserina		0		0	1	0	0	0	0
An02g07890	transcription factor pacC - *A. niger*		0		1	0	0	0	0	0
An04g06950	similarity to homeobox transcription factor hth - D. melanogaster		0		1	0	0	0	0	0
An07g02690	similarity to hypothetical regulational protein PBK1 - *H. sapiens*		0		1	0	0	0	0	0
An01g10870	DEAD box RNA helicase CHR1 - *C. albicans*		0		1	0	0	0	0	0
An12g08110	intracellular signalling protein INTRA31 from patent WO200077040-A2 - *H. sapiens*		0		0	1	0	0	0	0
An12g09980	weak similarity to zinc-binding protein Rar1 - Toxoplasma gondii		0		0	1	0	0	0	0
An01g06060	GTP-binding protein rab11 - *Rattus norvegicus*		0		0	1	0	0	0	0
An03g04910	clathrin coat assembly protein AP19 - Camptotheca acuminata		0		0	1	0	0	0	0
An16g05370	similarity to zinc-finger protein Glo3 -*S. cerevisiae*		0		0	1	0	0	0	0
An10g00890	ankyrin Ank3 - Mus musculus		0		1	0	0	0	0	0
An08g06560	spermidine synthase Spe3 - *S. cerevisiae*		0		0	1	0	0	0	0
An04g09530	melanin polyketide synthase PKS - Nodulisporium sp.		0		0	1	0	0	0	0
An08g06570	transketolase Tkl1 - *S. cerevisiae*		0		1	0	0	0	0	0
An09g02700	branched-chain α-keto acid dehydrogenase E1 α subunit BCHEL1 -*H. sapiens*		0		1	0	0	0	0	0
An17g00910	4-aminobutyrate transaminase gatA - A. nidulans		0		0	1	0	0	0	0
An13g00440	uridine-monophosphate kinase Ura6 - *S. cerevisiae*		0		1	0	0	0	0	0
An01g12430	hypothetical protein CAF32157.1 - *N. crassa*		0		1	0	0	0	0	0
An02g02500	conserved hypothetical protein - *A. clavatus* NRRL 1		0		0	1	0	0	0	0
An02g14760	conserved hypothetical protein - Neosartorya fischeri NRRL 181		0		1	0	0	0	0	0
An03g04360	hypothetical protein EAA61234.1 - A. nidulans		0		1	0	0	0	0	0
An11g09310	hypothetical protein SPBC337.17c - *S. pombe*		0		0	1	0	0	0	0
An12g04820	hypothetical conserved protein SPCC132.01c - *S. pombe*		0		1	0	0	0	0	0
An13g00520	similarity to EST an_3235 - *A. niger*		0		1	0	0	0	0	0
An14g01685	conserved hypothetical protein - *A. fumigatus* Af293		0		0	1	0	0	0	0
An16g05930	hypothetical protein encoded by An08g06890 - *A. niger*		0		1	0	0	0	0	0
123664	conserved hypothetical protein - *A. fumigatus* A1163		0		0	1	0	0	0	0
An04g07080	similarity to hypothetical protein SPBC2G5.01 - *S. pombe*		1		0	1	0	0	0	0
An15g03150	hypothetical protein SPCC1183.11 - *S. pombe*		4		1	0	0	0	0	0
An16g05280	hypothetical protein		0		0	1	0	0	0	0
An17g00920	hypothetical protein		0		1	0	0	0	0	0
An07g04570	hex1 - A. nidulans		0		0	6	0	3	0	4

Locus tag	Protein description	Signal	TM D	ERRS	Spectral counts MAL BR1	MAL BR2	XYL BR1	XYL BR2	SOR BR1	SOR BR2
An18g05640	hypothetical mold-specific protein MS8 - Ajellomyces capsulatus		0		0	4	0	3	0	3
An04g06380	mitochondrial aspartate aminotransferase mAspAT - Mus musculus		0		0	1	0	0	0	1
An02g13210	similarity to RNA-binding tumour suppressor LUCA15 - *H. sapiens*		0		0	1	0	0	1	0
An08g05640	nitrite reductase (NADH) niiA - A. nidulans		0		0	1	0	0	0	1
An18g02690	dihydrogeodin oxidase DHGO - *A. terreus*		0		0	1	0	0	1	0
An07g03660	similarity to hypothetical protein CAD37045.1 - *N. crassa*		0		0	2	0	1	0	1
An06g02570	similarity to N assimilation regulatory protein nit-4 - *N. crassa*		1		0	0	1	1	0	0
An09g04120	spindle checkpoint protein Mad2 - *S. cerevisiae*		0		0	0	0	2	0	0
An19g00150	similarity to formyl-CoA transferase from patent WO9816632-A1 - Oxalobacter formigenes		0		0	0	1	1	0	1
An12g10440	hypothetical protein CAD70539.1 - *N. crassa*		12		0	0	1	1	0	1
An01g05070	hypothetical protein SPBC776.06c - *S. pombe*		0		0	1	1	1	0	0
An08g04060	hypothetical transcription factor IIIc-like protein CAE47909.1 - *A. fumigatus*		0		0	1	1	1	0	0
An01g01830	catalase/peroxidase cpeB - Streptomyces reticuli		0		0	1	0	2	0	0
An18g03600	similarity to erythromycin esterase type II ereB - Escherichia coli		0		0	0	0	1	0	0
An02g04520	H+-transporting ATP synthase δ chain precursor Atp5 - *S. cerevisiae*		0		0	0	0	1	0	0
An11g04550	pyruvate dehydrogenase α subunit E1 α Pda1 - *S. cerevisiae*		0		0	0	0	1	0	0
An01g01290	squalene-hopene cyclase SHC - Alicyclobacillus acidocaldarius		0		0	0	1	0	0	0
An08g10860	fatty acid synthase β subunit fasB - A. nidulans		0		0	0	1	0	0	0
An11g05960	lovastatin diketide synthase lovF - *A. terreus*		0		0	0	1	0	0	0
An01g11620	similarity to transcription activator of lysine pathway Lys14 - *S. cerevisiae*		0		0	0	0	1	0	0
An02g12040	helicase Fun30 -*S. cerevisiae*		0		0	0	1	0	0	0
An09g05290	exonuclease II SPAC17A5.14 - *S. pombe*		0		0	0	0	1	0	0
An04g01210	similarity to DNA-3-methyladenine glycosidase I mag1p - *S. pombe*		0		0	0	1	0	0	0
An07g03150	nuclear tRNA export receptor exportin-t - *H. sapiens*		0		0	0	1	0	0	0
An02g14690	heterogeneous nuclear ribonucleoprotein Hrp1 - *S. cerevisiae*		0		0	0	1	0	0	0
An16g07890	similarity to transcription factor pro1 -Sordaria macrospora		0		0	0	0	1	0	0
An07g06030	coatomer γ subunit 2 copg2 - *H. sapiens*		0		0	0	0	1	0	0
An15g00560	actin γ -A. nidulans		0		0	0	0	1	0	0
An18g02440	tubulin-folding cofactor D - Bos taurus		0		0	0	0	1	0	0
An14g00230	ubiquitin conjugating enzyme Ubc6 - *S. cerevisiae*		1		0	0	0	1	0	0
An04g02840	flavocytochrome b2 L-lactate dehydrogenase CYB2 - Pichia anomala		0		0	0	0	1	0	0
An11g06160	proline oxidase prnD -A. nidulans		0		0	0	1	0	0	0
An11g09790	sulfate adenylyltransferase sC- A. nidulans		0		0	0	1	0	0	0
An17g00130	weak similarity to cercosporin resistance protein crg1 - Cercospora nicotianae		0		0	0	0	1	0	0
An01g04300	strong similarity fragment SEQ ID NO:54638 from patent EP1033405-A2 - *A. thaliana*		0		0	0	1	0	0	0
An06g01520	similarity to hypothetical protein SPBC24C6.10c - *S. pombe*		0		0	0	0	1	0	0
An07g07770	weak similarity to hypothetical protein P0034C11.5 - Oryza sativa		0		0	0	1	0	0	0
An09g02230	similarity to hypothetical protein BAA10688.1 - Synechocystis sp.		0		0	0	0	1	0	0
An12g07250	similarity to hypothetical conserved protein - Thermotoga maritima		0		0	0	0	1	0	0
An15g04170	similarity to conserved hypothetical protein - A. flavus NRRL3357		0		0	0	0	1	0	0
An03g00470	hypothetical protein EAA48619.1 - Magnaporthe grisea		4		0	0	0	1	0	0
An03g04440	hypothetical protein		0		0	0	1	0	0	0
An04g07280	hypothetical protein		0		0	0	1	0	0	0
An16g03680	hypothetical protein		0		0	0	1	0	0	0
46152	predicted protein - *A. terreus* NIH2624		0		0	0	1	0	1	0
An04g03270	proteasome 19S regulatory particle subunit Rpn2 - *S. cerevisiae*		0		0	0	0	1	0	1
An08g06430	similarity to allantoate permease Dal5 - *S. cerevisiae*		9		0	0	0	1	1	0
An11g05660	similarity to erythrocyte splice form 1 of ankyrin ANK1 - *H. sapiens*		0		0	1	0	2	1	1

Supplementary table S9

Locus tag	Protein description	Signal	TMD	ERRS	Spectral counts					
					MAL		XYL		SOR	
					BR1	BR2	BR1	BR2	BR1	BR2
An07g09920	NADH-dependent glutamate synthase NADH-GOGAT - Medicago sativa		0		0	0	0	0	1	1
An12g05220	similarity to transcription factor nft1p - *S. pombe*		0		0	0	0	0	1	1
An03g03500	hypothetical protein CAD36989.1 - *N. crassa*		1		0	0	0	0	1	1
An07g04650	similarity to glucan 1,3-β-glucosidase Bgl2 - *S. cerevisiae*		1		0	0	0	0	1	0
An06g00540	similarity to sterigmatocystin biosynthetic gene stcQ - A. nidulans		0		0	0	0	0	1	0
An14g04590	transcription factor Kcs1 - *S. cerevisiae*		0		0	0	0	0	0	1
An09g03490	protein involved in DNA repair SNM1 - Mus musculus		0		0	0	0	0	1	0
An02g04840	chromosome scaffold protein sudA - A. nidulans		0		0	0	0	0	0	1
An12g07590	similarity to meiotic cohesin rec8p -*S. pombe*		0		0	0	0	0	1	0
An04g07020	syntaxin Tlg2 -*S. cerevisiae*		0		0	0	0	0	1	0
An16g03020	similarity to myosin heavy chain - Pecten maximus		0		0	0	0	0	0	1
An18g02940	ciliary dynein β heavy chain - Anthocidaris crassispina		0		0	0	0	0	1	0
An11g00550	chaperonin Hsp10 -*S. cerevisiae*		0		0	0	0	0	0	1
An12g05650	ankyrin 3 Ank3 - Mus musculus		0		0	0	0	0	1	0
209924	inosine and guanosine-specific phosphorylase I- *A. fumigatus* Af293		0		0	0	0	0	1	0
An08g01960	adenosylhomocysteinase - *H. sapiens*		0		0	0	0	0	0	1
An01g00070	N2,N2-dimethylguanosine tRNA methyltransferase trm1p - *S. pombe*		0		0	0	0	0	1	0
An07g00300	fluconazole resistance transporter Flr1 - *S. cerevisiae*		11		0	0	0	0	1	0
An04g09720	pathogenicity gene PEP2 - Nectria haematococca		0		0	0	0	0	0	1
An05g00180	similarity to hypothetical protein B13M15.020 - *N. crassa*		0		0	0	0	0	1	0
An16g04680	similarity to hypothetical protein SPAC23A1.16c - *S. pombe*		0		0	0	0	0	1	0
An16g06980	hypothetical protein		0		0	0	0	0	0	1
An07g01890	hypothetical protein		0		0	0	0	0	0	1
An02g08620	transcription factor involved in acriflavine resistance acr-2 - *N. crassa*		0		0	1	0	1	1	1

NEDERLANDSE SAMENVATTING

Filamenteuze schimmels komen bijna overal in de wereld voor. De wijde verspreiding van de filamenteuze schimmels is mede te danken aan hun veelzijdige metabolisme. Dit stelt ze in staat om groeien op simpele substraten zoals nitraat, acetaat, ethanol en ammonia. Daarnaast kunnen ze gebruik maken van complexe substraten zoals biopolymeren van plantaardig of dierlijk materiaal. Om op deze complexe biopolymeren (bijv. polysacchariden uit celwanden van planten) te kunnen groeien moeten schimmels hydrolyserende en modificerende enzymen uitscheiden. Deze enzymen zorgen voor de polysaccharide afbraak, en vervolgens voor de opname van de gegenereerde eenvoudigere moleculen, zoals suiker monomeren.

De filamenteuze schimmel *Aspergillus niger* was het onderwerp van uitgebreid onderzoek in de afgelopen decennia. Dit organisme is de belangrijkste producent van citroenzuur in de wereld. Daarnaast produceert *A. niger* grote hoeveelheden enzymen die belangrijk zijn voor de biotechnologische industrie. Dit betreft enzymen voor de voedsel en diervoeding bereiding, of enzymen voor de omzetting van cellulose naar bioethanol. Het onderzoek naar de secretie van extracellulaire enzymen in *A. niger* was tot dusverre voornamelijk gebaseerd op vergelijking van de genen met die in andere organismen, maar ook op de analyse van de transcriptie. Er is tot dusverre in *A. niger* weinig direct onderzoek gedaan naar de rol en functie van de bij de secretie betrokken eiwitten, in verschillende hoofdstukken van dit proefschrift wordt een aanzet tot dit functionele onderzoek beschreven.

Het doel van het onderzoek in deze proefschrift wordt beschreven was om via functioneel onderzoek genen en eiwitten te identificeren die betrokken zijn bij de eiwit secretie in *A. niger*. Een onderdeel daarvan was de dynamische veranderingen van het secretie proteome onder hoge secretie condities te onderzoeken. Hiervoor is een combinatie van gen expressie profiling gecombineerd met shotgun proteomics van de secretie organellen.

Hoofdstuk 2 beschrijft een methode voor gen silencing in filamenteuze schimmels met RNA interference. Deze methode maakt gebruik van vectoren die lange hairpin RNAs tot expressie brengen. In *A. niger* waren tot voor kort gen knock-out strategieën de

voornaamste methode om te bepalen welke functie een gen had. Maar een gen knock-down strategie zoals beschreven in hoofdstuk 2, kan ook belangrijk zijn voor het onderzoek naar gen functie. Dit om twee redenen: a) essentiële genen kunnen worden bestudeerd omdat RNAi niet altijd leidt tot een totaal verlies van de gen functie. En b) meerdere gen kopieën of paraloge genen kunnen worden beïnvloed met één enkel construct. In het hier beschreven werk werd het gen dat codeert voor de transcriptie activator XlnR down gereguleerd. XlnR is een transcriptie factor die verantwoordelijk is voor de expressie van cellulases en hemicellulases in *A. niger* Dit resulteerde in verschillende niveau's van verlaging van de cellulase en hemicellulase productie in de verschillende transformanten.

In hoofdstuk 3 wordt het onderzoek naar het effect van D-xylose op de gen expressie in *A. niger* beschreven. De inducer van (hemi)cellulases, D-xylose, was toegevoegd aan culturen van *A. niger* die groeide op het niet-inducerende sorbitol. Genen die differentieel tot expressie kwamen op D-xylose werden geïdentificeerd als kandidaat genen betrokken bij een reactie op deze suiker. Deze studie bevestigde dat D-xylose genen activeert die betrokken zijn bij xylan afbraak en D-xylose metabolisme. Bovendien activeert D-xylose ook genen verantwoordelijk voor de opname van andere monomeren die vrijkomen bij de afbraak van arabinoxylan and cellulose. Statistische analyse is gebruikt om van iedere externe factor vast te stellen wat het effect was op de gen expressie. Deze analyse was belangrijk voor een reproduceerbare monster behandeling voor microarray analyse.

Hoofdstuk 4 beschrijft de *A. niger* secretie pathway eiwitten die betrokken zijn bij de productie van (hemi)cellulases na de inductie met D-xylose. Hiervoor was *A. niger* gegroeid onder dezelfde condities als die beschreven zijn in hoofdstuk 3. Na de isolatie van microsomen, zijn de bijbehorende eiwitten geanalyseerd m.b.v. shotgun proteomics. De inductie met D-xylose was gerelateerd aan de toename in eiwitten die betrokken zijn bij eiwit secretie. Deze waren voornamelijk kleine GTPases voor het vesicle transport and gepolariseerde groei. Het meest belangrijke was dat na de inductie met D-xylose het complex voor eiwit afbraak, 20S proteasome, geassocieerd bleek te zijn met de microsomen. Deze resultaten geven aan dat er een nieuwe manier van regulatie bestaat waarbij de proteasome wordt gerekruteerd door secretie organellen na de inductie van extracellulaire enzymen.

In hoofdstuk 5 wordt de analyse van secretie eiwitten beschreven zoals in hoofdstuk 4 maar nu toegepast op een systeem met D-maltose als inducer voor zetmeel afbrekende

enzymen. Dit hoofdstuk bevat ook de vergelijkende studie van uitgescheiden eiwitten na inductie met D-maltose of D-xylose. Na het toevoegen van D-maltose werden drie zetmeel hydrolyserende eiwitten verhoogd waargenomen. Terwijl na toevoeging van D-xylose werden verscheidene andere eiwitten verhoogd waargenomen, deze eiwitten werden voornamelijk geassocieerd met de arabinoxylan en cellulose degradatie. De effecten van D-maltose op het microsomale proteome waren hetzelfde als die van D-xylose. De inductie met D-maltose en met D-xylose resulteerde in beide gevallen in verhoogde hoeveelheden van mitochondriale eiwitten. De 20S proteasome opbouw is een ATP afhankelijk proces. Om deze reden wordt de hypothese gesteld dat de opbouw en associatie van het 20S proteasome na de inductie gerelateerd is aan een toename van de ATP productie in de buurt van de secretie organellen.

ACKNOWLEDGEMENTS

Completing a PhD project is never an individual task, and for this reason I would like to express my gratitude to the many people who were directly or indirectly involved in the project.

In the first place I would like to thank the supervisor of this thesis Prof. John van der Oost. Dear John, you were invited at a very late stage to become supervisor of the project. I can imagine that this is not an easy situation. Still your constructive criticism was determinant for the success of the project. Next, I would like to thank my co-supervisor Dr. Leo de Graaff. Leo, my gratitude goes without saying. A bit more than a year after the unfortunate illness of my former co-supervisor Dr. Ling Qing, you took the initiative to propose a new path to the project and this proved to be a good one. Also, you have taught me to be a more confident and direct researcher and this is something I will take to my future path as a scientist. I am especially grateful for the support that you gave me in my last period of the project, when this was in fact what I most needed both for professional and for personal reasons.

Besides my supervisor and my co-supervisor, I would like to thank all the staff of our old group "Fungal Genomics". Peter, you have supported this project beyond reasonable expectations. Your input was important not only as a co-author of two manuscripts, but also as my temporary co-supervisor together with Leo, after Ling's illness. And of course I cannot forget the huge computer screen that you have lent me for the shotgun proteomics analysis of data! Douwe, your contribution was also fundamental for this project. First, your suggestion to expand the project to proteomics was priceless. Also, your rigorous experimental settings for fungal cultivation and gene expression analysis during induction by xylose were fundamental for the subsequent proteomic experiments. And of course it was an honour for me to be one of your "paranymfs". René and Jorg, besides the fact that you were great colleagues, I am grateful for your support during my first two years of PhD, including the organisation of practical courses and Problem-Based Learning classes. I also thank you both for the support during the Kluyver Centre symposiums. Bas, thank you for the all the support, especially during the last period of this project. Thank you for accepting being one of my paranymfs. I am also grateful for the help that you and Willy provided in setting up bioreactors and for the tips on the protein work. Next, I would like to thank Elena and Henk-Jan for their involvement as post-doctoral fellows in the project of protein secretion. Some of their insights were also helpful in chosing a shotgun proteomic approach and not a more specific approach. On the bioinformatic side of the project, apart from Peter I would like to thank Said Basmagi for the COG database developed (which I have used countless times) and Remko Kuipers for his patience sorting some of the comma-separated data. I would also like to thank some of my former colleagues who have participated in the daily lab life: Kelly Chan, Luísa Trindade, Christina Geerts-Dimitriadou, Aytaç Kocabaş, Jing Wang, Katsuichi Saito, Rob Joosten, Cozmina Vrabie, Betül and Alper Söyler, Harrie Kools, Geja Krooshof, Hans Visser. Thank you Hans also for believing in my work when I was still a fellow researcher there, this was actually what allowed me to come to

the Netherlands for research in the first place. I would also like to thank the BSc and MSc students whom I supervised or helped supervise: Virginie Dehouck, Sonja Bobic, Kyle McPherson, Lorenzo Fanchi, Djawad Radjabzadeh, Niels Zondervan, Sedef Dinçer, Marloes Vernooij, Marieke Lammers. Each of them helped the project in his or her own way. Special thanks to Virginie for developing a general RNAi destination vector that dispenses co-transformation and to Niels Zondervan for his bioinformatic analyses on the mitochondria-associated membrane in *A. niger*. I also thank Mark van Passel for his input as a co-author in two of the manuscripts presented in this thesis.

Apart from the people from the old group of Fungal Genomics, I would like to thank some of the technical staff from the Microbiology group, especially Wim Roelofsen, who is one of the best problem-solvers that I have ever had the priviledge to know. I also have good memories from all the people that helped co-organise the PhD trip to California: thank you Mark, Marco, Bart, Rob, Filipe and Arno! I extend my thanks to all the people from the Microbiology department and to the head of the group Prof. Willem de Vos, who is the responsible for such an extraordinary group of people.

Additionally, I would like to thank Sjef Boeren from the Biochemistry department (Wageningen University) and also from the company Biqualys for his support on sample processing for LC-MS/MS. I would also like to thank Miguel Peñalva and Eduardo Espeso from the Aspergillus Molecular Genetics Unit (Centro de Investigaciones Biológicas, Madrid) for their helpful suggestions on how to explore the full potential of the proteomic data.

Also, I would like to thank all my friends, including some of the people that I have mentioned previously and other people whom I have met in the Netherlands. Special thanks to Daniela and Sjors who helped me to come to the Netherlands and made me feel welcome there. Also special thanks to Ana, Nardy and Lan (aka Cara) for their concern and enduring friendship. Ana, thank you for accepting being my paranymf, together with Bas. Also many thanks to Alex, Qiao-Qiao, Vera, Bjarne, Sashka, Gesuino, Miao-Miao, Tim, Erik “0”, Ben, Lidia, Fabrizio, Francesco, Randy, Marjon, Víctor and Jing. We have had many good times in Wageningen and Nijmegen, and hopefully we can meet up soon!

Finally, I would like to say thank you to my siblings Margarida, Ana, João, Pedro, to Tiago who has had infinite patience during this last period of the project and above all to my parents.

ABOUT THE AUTHOR

José Miguel Pimenta Ferreira de Oliveira was born on the 7th of March 1978, in the city of Porto, Portugal. He completed his secondary education in 1996 and in September of this year, he started his licentiate studies in Biochemistry at the University of Porto (Faculty of Sciences). During the last year of his studies, he conducted research on the analysis of mutations on the Complement C4 gene in patients with systemic lupus erythematosus, after which period he specialised in Applied Biochemistry. On November 2000, he was granted the licenciate degree.

From January 2001 to January 2004 he was a fellow researcher at the Hospital Geral de Santo António (Saint Anthony's General Hospital) in Porto, at the Hematology department, Molecular Biology Unit. His main research was focused on the study of specific mutations or polymorphisms associated with trombophilia and analysis of CAG-repeat polymorphisms of the androgen receptor in patients with unilateral and bilateral cryptorchidism. This work resulted in two publications, one for each topic.

In February 2004, he received an EU grant to conduct research in the area of genomics and gene expression, at the Fungal Genomics group, University of Wageningen (The Netherlands). The research topic was the influence of oxidative stress on the expression of carotenogenic genes and genes related to defence against ROS in *Xanthophyllomyces dendrorhous*. Simultaneously, a protocol for quantitative RT-PCR using an external reference gene was developed.

In January 2005, he initiated his PhD project entitled "Functional genomics analysis of the secretory pathway in *Aspergillus niger*", the results of which are summarised in this thesis. The project took place at the Fungal Genomics group (Wageningen University), under the supervision of Prof. John van der Oost and Dr. Leo de Graaff.

OVERVIEW OF COMPLETED TRAINING ACTIVITIES

Discipline-specific activities	Year
Safe handling of radio-active materials and sources 5B, Wageningen	2008
2nd International Advanced Course on Proteomics, Wageningen	2008
2nd Kluyver Centre Symposium, Noordwijkerhout (poster)	2005
Annual Dutch Meeting on Molecular and Cellular Biophysics, Lunteren (poster)	2005
3rd Kluyver Centre Symposium, Noordwijkerhout (poster)	2006
8th European Conference on Fungal Genetics, Vienna, Austria	2006
4th Kluyver Centre Symposium, Noordwijkerhout (poster+presentation)	2007
5th Kluyver Centre Symposium, Noordwijkerhout (poster)	2008
9th European Conference on Fungal Genetics, Edinburgh, UK (poster)	2008
6th Kluyver Centre Symposium, Noordwijkerhout	2009

General courses	
VLAG introduction week, Bilthoven	2005
Techniques for Writing and Presenting a Scientific Paper, Wageningen (presentation)	2006
Communication in Interdisciplinary Research, Wageningen (presentation)	2008

Optional activities	
Preparation of PhD research proposal	2005
Group meetings (Fungal Genomics), Wageningen	2005-9
PhD/Postdoc meetings Laboratory of Microbiology, Wageningen	2005-9
Organization of PhD study trip to California, United States of America	2005-6
PhD study trip to California, United States of America	2006

The research described in this thesis was financially supported by the Kluyver Centre for Genomics of Industrial Fermentation, which is supported by the Netherlands Genomics Initiative.

Financial support from Wageningen University for printing this thesis is gratefully acknowledged.

Design and layout: Miguel Oliveira

Printed by: GVO drukkers & vormgevers B.V. | Ponsen & Looijen